Final Technical Report
Research Project Agreement No. T9233, Task 41
Seismic Vulnerability of the Alaskan Way Viaduct Phase II

SEISMIC VULNERABILITY OF THE ALASKAN WAY VIADUCT: GEOTECHNICAL ENGINEERING ASPECTS

by

Steve Kramer
Assistant Professor
Department of Civil Engineering
University of Washington

Nadarajah Sivaneswaran
Research Associate
University of Washington

Katherine Tucker
Research Assistant
University of Washington

Washington State Transportation Center (TRAC)
University of Washington
University District Building
1107 NE 45th Street, Suite 535
Box 354802
Seattle, Washington 98105-4631

Washington State Department of Transportation
Technical Monitor
Edward H. Henley Jr.
Special Project Engineer

Prepared for

Washington State Transportation Commission
Department of Transportation
and in cooperation with
U.S. Department of Transportation
Federal Highway Administration

July 1995

TECHNICAL REPORT STANDARD TITLE PAGE

1. REPORT NO.	2. GOVERNMENT ACCESSION NO.	3. RECIPIENT'S CATALOG NO.
WA-RD 363.2		

4. TITLE AND SUBTITLE	5. REPORT DATE
SEISMIC VULNERABILITY OF THE ALASKAN WAY VIADUCT — GEOTECHNICAL ENGINEERING ASPECTS	July 1995
	6. PERFORMING ORGANIZATION CODE
7. AUTHOR(S) Steven L. Kramer, Nadarajah Sivaneswaran, Kathryn M. Tucker	8. PERFORMING ORGANIZATION REPORT NO.
9. PERFORMING ORGANIZATION NAME AND ADDRESS Washington State Transportation Center (TRAC) University of Washington University District Building; 1107 NE 45th Street, Suite 535 Box 354802 Seattle, Washington 98105-4631	10. WORK UNIT NO.
	11. CONTRACT OR GRANT NO. Agreement T9233, Task 41
12. SPONSORING AGENCY NAME AND ADDRESS Washington State Department of Transportation Transportation Building, MS 7370 Olympia, Washington 98504-7370	13. TYPE OF REPORT AND PERIOD COVERED Final Technical Report
	14. SPONSORING AGENCY CODE

15. SUPPLEMENTARY NOTES

This study was conducted in cooperation with the U.S. Department of Transportation, Federal Highway Administration.

16. ABSTRACT

This report describes the geotechnical engineering aspects of a seismic vulnerability analysis of the Alaskan Way Viaduct in Seattle, Washington. The Alaskan Way Viaduct is an approximately 40-year-old, two-level, reinforced concrete structures that carries some 86,000 vehicles per day along the Seattle waterfront.

Subsurface data from previous investigations for construction of the Alaskan Way Viaduct and other structures in the general area were collected and interpreted. The existing subsurface data was supplemented by additional borings, cone penetration test soundings, shear wave velocity tests, and laboratory tests. The existing and supplemental subsurface data was then combined to form a model of the subsurface conditions along the length of the Viaduct.

A probabilistic seismic hazard analysis was performed to develop design-level ground motions for use in the seismic vulnerability analysis. These ground motions were used as input for site-specific ground response analyses that predicted the nature of ground shaking along the length of the Viaduct. The ground response analyses also predicted cyclic loading levels that were used in subsequent liquefaction analyses.

Foundation stiffness and damping characteristics of the existing foundations were analyzed for use in analyses of the dynamic response of the Alaskan Way Viaduct superstructure.

The subsurface investigations revealed evidence of potentially liquefiable soils along the majority of the length of the Alaskan Way Viaduct. Review of historical documents verified that the soils were deposited in a manner that has produced liquefiable soils in other parts of the U.S. and the world, and that liquefaction has been observed near the Alaskan Way Viaduct in past earthquakes. A detailed liquefaction hazard evaluation that considered issues of susceptibility, initiation, and effects was conducted. The evaluation indicated that widespread liquefaction would be caused by the design-level ground motions. This liquefaction could cause bearing failure of the pile foundations that support the Viaduct. It could also produce significant post-earthquake settlement and lateral movement that could cause severe damage or collapse of the Viaduct.

17. KEY WORDS	18. DISTRIBUTION STATEMENT
liquefaction, seismic hazard analysis, foundation stiffness, foundation damping, lateral spreading	No restrictions. This document is available to the public through the National Technical Information Service, Springfield, VA 22616

19. SECURITY CLASSIF. (of this report)	20. SECURITY CLASSIF. (of this page)	21. NO. OF PAGES	22. PRICE
None	None	289	

DISCLAIMER

The contents of this report reflect the views of the authors, who are responsible for the facts and the accuracy of the data presented herein. The contents do not necessarily reflect the official views or policies of the Washington State Transportation Commission, Department of Transportation, or the Federal Highway Administration. This report does not constitute a standard, specification, or regulation.

TABLE OF CONTENTS

Section		Page
Chapter 1	**Introduction**	**1**
1.1	Background	1
1.2	The Alaskan Way Viaduct	2
1.3	Scope of Report	2
1.4	Organization of Report	3
Chapter 2	**Subsurface Conditions**	**7**
2.1	Geology and History of Site Development	7
2.2	Review of Previous Subsurface Data	9
2.3	Supplemental Subsurface Investigation	11
	SPT	12
	CPT	13
	Shear Wave Velocity	13
2.4	Laboratory Testing	14
2.5	Characterization of Subsurface Conditions	14
	Waterfront Fill	15
	Tideflat Deposit	16
	Till	17
	Discussion	17
Chapter 3	**Foundation Conditions**	**39**
3.1	Foundation Types and Configurations	39
	Types of Piles	39
	Pile Group Configurations	40
	Footing Dimensions	41
3.2	Pile Driving Records	45
	Pile Lengths	45
	Final Driving Resistance	45
3.3	Summary	46
Chapter 4	**Ground Motions**	**47**
4.1	Probabilistic Seismic Hazard Analysis	47
	Identification of Earthquake Sources	48
	Seismicity of Earthquake Sources	49
	Prediction of Ground Motion	50
	Probability Computations	51
	Results of PSHA	52
4.2	Development of Site-Specific Ground Motions	53
	Generation of Synthetic Stiff Soil Motions	53
	Development of Consistent Bedrock Motions	55
	Ground Response Analyses	56
	Results of Ground Response Analyses	57
4.3	Summary	59

TABLE OF CONTENTS (Continued)

Section		Page
Chapter 5	**Foundation Response Characteristics**	**83**
5.1	Modes of Deformation	83
5.2	Method of Analysis	84
	Sources of Stiffness and Damping	84
	Effects of Ground Motion Frequency	86
	Pile Group Interaction	86
	Effects of Soil Nonlinearity	87
5.3	Results of Analyses	87
5.4	Summary	88
Chapter 6	**Liquefaction Hazards**	**99**
6.1	Historical Evidence of Liquefaction	100
6.2	Previous Investigations of Liquefaction Potential	101
6.3	Site-Specific Evaluation of Liquefaction Potential	102
	Liquefaction Susceptibility	103
	Initiation of Liquefaction	105
	Effects of Liquefaction	112
	Vertical Foundation Movements	115
6.4	Summary	126
Chapter 7	**Summary and Conclusions**	**161**
	Summary	161
	Conclusions	163
Acknowledgments		**171**
References		**173**
Appendix A.	**Supplementary Subsurface Investigation: Boring Logs**	
Appendix B.	**Supplementary Subsurface Investigation: Cone Penetration Test Soundings**	
Appendix C.	**Supplementary Subsurface Investigation: Shear Wave Velocity Test Results**	

LIST OF FIGURES

Figure		Page
1.1	Site Plan of the Alaskan Way Viaduct	3
1.2	Typical Configuration of the Elevated Portion of the Alaskan Way Viaduct (WSDOT Section)	4
2.1	Seattle Waterfront In 1884	18
2.2	Hydraulic Filing Operation During Tideflat Reclamation	19
2.3	Profile and Plan Views of a Typical Section of the Railroad Avenue Seawall	20
2.4	Locations of Available Boring Logs in the Vicinity of the Alaskan Way Viaduct	21
2.5	Longitudinal Profile along the Length of the Alaskan Way Viaduct	23
2.6	Soil Profile at Pike/Union Cross-Section	25
2.7	Soil Profile at Columbia Street Cross-Section	26
2.8	Soil Profile at Washington Street Cross-Section	27
2.9	Soil Profile at Jackson/King Cross-Section	28
2.10	Locations of Boring and Insitu Tests in Supplemental Subsurface Investigations	29
2.11	Uncorrected Standard Penetration Resistances from Previous Investigations and Supplemental Subsurface Investigation	30
2.12	Uncorrected Tip Resistances from Cone Penetration Tests Conducted in Supplemental Subsurface Investigation	30
2.13	Uncorrected Shear Wave Velocities from Cone Penetration Tests Conducted in Supplemental Subsurface Investigation	31
2.14	Soil Profile along the Length of the Alaskan Way Viaduct as Inferred from Results of Previous and Supplemental Subsurface Investigations	33
2.15	Comparison of Measured CPT Resistances with CPT Resistance Required to Resist Liquefaction for 50 Ft of Soft Soil	35
2.16	Corrected Standard Penetration Resistances for Waterfront Fill from Standard Penetration Tests Conducted in Supplemental Subsurface Investigation	35
2.17	Corrected Tip Resistances for Waterfront Fill from Cone Penetration Tests Conducted in Supplemental Subsurface Investigation	36
2.18	Corrected Shear Wave Velocities for Tideflat Deposit from Seismic Cone Tests Conducted in Supplemental Subsurface Investigation	36
2.19	Corrected Standard Penetration Resistances for Tideflat Deposit from Standard Penetration Tests Conducted in Supplemental Subsurface Investigation	37
2.20	Corrected Tip Resistances for Tideflat Deposit from Cone Penetration Tests Conducted in Supplemental Subsurface Investigation	37
2.21	Variation of Measured Shear Wave Velocity in Till from Previous and Supplemental Subsurface Investigations	38

LIST OF FIGURES (Continued)

Figure		Page
3.1	Concrete Piles	42
3.2	Typical Interior Column Pile Group in Seattle Section	43
3.3	Typical Exterior Column Pile Group in Seattle Section	43
3.4	Typical Interior Column Pile Group in WSDOT Section	44
3.5	Typical Exterior Column Pile Group in WSDOT Section	44
4.1	Geometry of Tectonic Plates in the Pacific Northwest	60
4.2	Hypocenters of Small Earthquakes between 1982 and 1986	61
4.3	Bedrock Outcrop Motions from PSHA And Deconvolution Analyses	62
4.4	Response Spectra (5% damping) for Bedrock Outcrop Motions: (a) Individual Motions, and (b) Average of Individual Motions	63
4.5	Ground Surface Response Spectra and accelerograms for Soft Soil Thickness of 0 Ft	64
4.6	Ground Surface Response Spectra and accelerograms for Soft Soil Thickness of 10 Ft	65
4.7	Ground Surface Response Spectra and accelerograms for Soft Soil Thickness of 20 Ft	66
4.8	Ground Surface Response Spectra and accelerograms for Soft Soil Thickness of 30 Ft	67
4.9	Ground Surface Response Spectra and accelerograms for Soft Soil Thickness of 40 Ft	68
4.10	Ground Surface Response Spectra and accelerograms for Soft Soil Thickness of 50 Ft	69
4.11	Ground Surface Response Spectra and accelerograms for Soft Soil Thickness of 60 Ft	70
4.12	Ground Surface Response Spectra and accelerograms for Soft Soil Thickness of 80 Ft	71
4.13	Ground Surface Response Spectra and accelerograms for Soft Soil Thickness of 100 Ft	72
4.14	Ground Surface Response Spectra and accelerograms for Soft Soil Thickness of 120 Ft	73
4.15	Ground Surface Response Spectra and accelerograms for Soft Soil Thickness of 140 Ft	74
4.16	Ground Surface Response Spectra and accelerograms for Soft Soil Thickness of 170 Ft	75
4.17	Variation of Computed Peak Ground Surface Acceleration along the Length of the Alaskan Way Viaduct	77
4.18	Variation of Computed Spectral Acceleration for T = 1.0 Sec and T = 2.0 Sec along the Length of the Alaskan Way Viaduct	79
4.19	Variation of Computed Average Maximum Cyclic Shear Stress with Depth for Various Soft Soil Thicknesses	81
5.1	Foundation and Soil Profile Used for Foundation Stiffness and Damping Analyses	85

LIST OF FIGURES (Continued)

Figure		Page
6.1	Map of Lateral Spreading Displacement Hazard for the Seattle South Quadrangle. (Displacements indicated By Legend Represent Maximum Expected Lateral Spreading Displacements (After Mabey and Youd, 1991))	126
6.2	Corrected SPT Resistances Used for Liquefaction Analyses of Saturated Soils	127
6.3	Corrected CPT Tip Resistances Used for Liquefaction Analyses of Saturated Soils	127
6.4	Corrected Shear Wave Velocities Used for Liquefaction Analyses of Saturated Soils	128
6.5	Comparison of Measured SPT Resistances with SPT Resistance Required To Resist Liquefaction for 20 Ft Soft Soil	128
6.6	Comparison of Measured SPT Resistances with SPT Resistance Required To Resist Liquefaction for 30 Ft Soft Soil	129
6.7	Comparison of Measured SPT Resistances with SPT Resistance Required To Resist Liquefaction for 40 Ft Soft Soil	129
6.8	Comparison of Measured SPT Resistances with SPT Resistance Required To Resist Liquefaction for 50 Ft Soft Soil	130
6.9	Comparison of Measured SPT Resistances with SPT Resistance Required To Resist Liquefaction for 60 Ft Soft Soil	130
6.10	Comparison of Measured SPT Resistances with SPT Resistance Required To Resist Liquefaction for 70 Ft Soft Soil	131
6.11	Variation of average Factor of Safety Against Liquefaction with Depth for Design-Level Ground Motions	132
6.12	Comparison of Measured CPT Resistances with CPT Resistance Required To Resist Liquefaction for 20 Ft Soft Soil	133
6.13	Comparison of Measured CPT Resistances with CPT Resistance Required To Resist Liquefaction for 30 Ft Soft Soil	133
6.14	Comparison of Measured CPT Resistances with CPT Resistance Required To Resist Liquefaction for 40 Ft Soft Soil	134
6.15	Comparison of Measured CPT Resistances with CPT Resistance Required To Resist Liquefaction for 50 Ft Soft Soil	134
6.16	Comparison of Measured CPT Resistances with CPT Resistance Required To Resist Liquefaction for 26 Ft Soft Soil	135
6.17	Comparison of Measured CPT Resistances with CPT Resistance Required To Resist Liquefaction for 70 Ft Soft Soil	135
6.18	Comparison of Measured Shear Wave Velocities with Shear Wave Velocities Required To Resist Liquefaction for 20 Ft Soft Soil	136
6.19	Comparison of Measured Shear Wave Velocities with Shear Wave Velocities Required To Resist Liquefaction for 30 Ft Soft Soil	136
6.20	Comparison of Measured Shear Wave Velocities with Shear Wave Velocities Required To Resist Liquefaction for 40 Ft Soft Soil	137

LIST OF FIGURES (Continued)

Figure		Page
6.21	Comparison of Measured Shear Wave Velocities with Shear Wave Velocities Required To Resist Liquefaction for 50 Ft Soft Soil	137
6.22	Comparison of Measured Shear Wave Velocities with Shear Wave Velocities Required To Resist Liquefaction for 60 Ft Soft Soil	138
6.23	Comparison of Measured Shear Wave Velocities with Shear Wave Velocities Required To Resist Liquefaction for 70 Ft Soft Soil	138
6.24	Comparison of Measured SPT Resistances with SPT Resistance Required To Resist Liquefaction for 20 Ft Soft Soil for the 1965 Seattle Earthquake Motion	139
6.25	Comparison of Measured SPT Resistances with SPT Resistance Required To Resist Liquefaction for 30 Ft Soft Soil for the 1965 Seattle Earthquake Motion	139
6.26	Comparison of Measured SPT Resistances with SPT Resistance Required To Resist Liquefaction for 40 Ft Soft Soil for the 1965 Seattle Earthquake Motion	140
6.27	Comparison of Measured SPT Resistances with SPT Resistance Required To Resist Liquefaction for 50 Ft Soft Soil for the 1965 Seattle Earthquake Motion	140
6.28	Comparison of Measured SPT Resistances with SPT Resistance Required To Resist Liquefaction for 60 Ft Soft Soil for the 1965 Seattle Earthquake Motion	141
6.29	Comparison of Measured SPT Resistances with SPT Resistance Required To Resist Liquefaction for 70 Ft Soft Soil for the 1965 Seattle Earthquake Motion	141
6.30	Variation of Average Factor of Safety Against Liquefaction with Depth for the 1965 Seattle Earthquake Motion	142
6.31	Variation of Average Peak Pore Pressure Ratio with Depth for 20 Ft Soft Soil	142
6.32	Variation of Average Peak Pore Pressure Ratio with Depth for 30 Ft Soft Soil	143
6.33	Variation of Average Peak Pore Pressure Ratio with Depth for 40 Ft Soft Soil	143
6.34	Variation of Average Peak Pore Pressure Ratio with Depth for 50 Ft Soft Soil	144
6.35	Variation of Average Peak Pore Pressure Ratio with Depth for 60 Ft Soft Soil	144
6.36	Variation of Average Peak Pore Pressure Ratio with Depth for 70 Ft Soft Soil	145
6.37	(a) Variation of Pore Pressure Ratio with Depth at Different Times after the Beginning of Earthquake Shaking for 20 Ft Soft Soil, and (B) Variation of Pore Pressure Ratio with Time in the Vicinity of the Tips of the Existing Pile Foundations (2.5 Ft Below Top of Till)	146

LIST OF FIGURES (Continued)

Figure		Page
6.38	(a) Variation of Pore Pressure Ratio with Depth at Different Times after the Beginning of Earthquake Shaking for 30 Ft Soft Soil, and (B) Variation of Pore Pressure Ratio with Time in the Vicinity of the Tips of the Existing Pile Foundations (2.5 Ft Below Top of Till)	147
6.39	(a) Variation of Pore Pressure Ratio with Depth at Different Times after the Beginning of Earthquake Shaking for 40 Ft Soft Soil, and (B) Variation of Pore Pressure Ratio with Time in the Vicinity of the Tips of the Existing Pile Foundations (2.5 Ft Below Top of Till)	148
6.40	(a) Variation of Pore Pressure Ratio with Depth at Different Times after the Beginning of Earthquake Shaking for 50 Ft Soft Soil, and (B) Variation of Pore Pressure Ratio with Time in the Vicinity of the Tips of the Existing Pile Foundations (2.5 Ft Below Top of Till)	149
6.41	(a) Variation of Pore Pressure Ratio with Depth at Different Times after the Beginning of Earthquake Shaking for 60 Ft Soft Soil, and (B) Variation of Pore Pressure Ratio with Time in the Vicinity of the Tips of the Existing Pile Foundations (2.5 Ft Below Top of Till)	150
6.42	(a) Variation of Pore Pressure Ratio with Depth at Different Times after the Beginning of Earthquake Shaking for 70 Ft Soft Soil, and (B) Variation of Pore Pressure Ratio with Time in the Vicinity of the Tips of the Existing Pile Foundations (2.5 Ft Below Top of Till)	151
6.43	Idealized Soil Profile at Columbia Street Cross-Section with Computed Factors of Safety for Various Potential Failure Surfaces.	152
6.44	Original and Final Configurations of the Columbia Street Cross-Section as Estimated By Byrne et al. (1991) Approach	153
6.45	Displaced Shape of Fixed Head Pile with EI = 5 x 10^{10} lb-in^2 due to 6-inch Lateral Spreading Displacement	154
6.46	Computed Pile Bending Moments in Fixed Head Pile with EI = 5 x 10^{10} lb-in^2 due to 6-inch Lateral Spreading Displacement	155
6.47	Computed Shear in Fixed Head Pile with EI = 5 x 10^{10} lb-in^2 due to 6-inch Lateral Spreading Displacement	156
6.48	Computed Unit Soil Resistance for Fixed Head Pile with EI = 5 x 10^{10} lb-in^2 due to 6-inch Lateral Spreading Displacement	157
6.49	Computed Maximum Bending Moments for Piles of Various Flexural Stiffnesses—Pinned Head Conditions	158
6.50	Computed Maximum Bending Moments for Piles of Various Flexural Stiffnesses—Fixed Head Conditions	159

LIST OF TABLES

Table		Page
4.1	Brune Spectrum Parameters for Initial Fourier Amplitude Spectrum	54
4.2	Combination of Waterfront Fill and Tide flat Deposit Thickness used in Ground Response Analyses	57
5.1	Stiffness and Damping Coefficients for the East Column of Bent 106	90
5.2	Stiffness and Damping Coefficients for the West Column of Bent 106	91
5.3	Stiffness and Damping Coefficients for the East Column of Bent 107	92
5.4	Stiffness and Damping Coefficients for the West Column of Bents 107 and 108	93
5.5	Stiffness and Damping Coefficients for the East Column of Bent 109	94
5.6	Stiffness and Damping Coefficients for the West Column of Bent 109	95
5.7	Stiffness and Damping Coefficients for the East and West Columns of Bent 151	96
5.8	Stiffness and Damping Coefficients for the East and West Columns of Bent 152 and 153	97
5.9	Stiffness and Damping Coefficients for the East and West Columns of Bent 154	98
6.1	Percentage of SPT Resistance Values Lower than the Minimum Values Required to Resist Liquefaction	109
6.2	Percentage of CPT Resistance Values Lower than the Minimum Values Required to Resist Liquefaction	110
6.3	Percentage of Shear Wave Velocity Values Lower than the Minimum Values Required to Resist Liquefaction	110
6.4	Percentage of SPT Resistance Values Lower than the Minimum Values Required to Resist Liquefaction for the 1965 Seattle-Tacoma Earthquake Motion	111
6.5	Computed Settlements Due to Seismic Compaction of Fill Above Water Table	114
6.6	Computed Settlements of Saturated Waterfront Fill and Tideflat Deposits Following Design-Level Earthquake	115

CHAPTER 1
INTRODUCTION

The Alaskan Way Viaduct is one of a number of major highway bridges that the Washington State Department of Transportation (WSDOT) has determined requires detailed evaluation of seismic vulnerability. The 2.2-mile (3.5 km) long reinforced concrete structure was designed and constructed in the late 1940s and early 1950s, before earthquake effects had been recognized in bridge design codes and before modern principles of earthquake-resistant design were developed. The Viaduct is an extremely important link in the Washington State highway system, carrying some 86,000 vehicles per day on one of only two north-south freeways through downtown Seattle.

1.1 BACKGROUND

In the 1989 Loma Prieta earthquake, the Cypress Viaduct in Oakland, California, collapsed, and several elevated viaducts in San Francisco were severely damaged. These viaducts were about the same age as the Alaskan Way Viaduct; consequently, they were designed and constructed with similar knowledge of earthquake design forces and earthquake-resistant design. Immediately after the Loma Prieta earthquake, engineers from the WSDOT Bridge and Structures office conducted an in-house, preliminary investigation of the seismic vulnerability of the Alaskan Way Viaduct (Dodson et al., 1990). Shortly thereafter, WSDOT authorized an independent, preliminary investigation by researchers from the University of Washington. Both investigations concentrated on the seismic response and vulnerability of the Alaskan Way Viaduct superstructure and concluded that more detailed analyses, particularly of the structural details, were warranted. Both investigations also concluded that additional information on the existing subsurface conditions and on the anticipated soil behavior was needed.

In September, 1992, WSDOT authorized a detailed investigation of the seismic vulnerability of the Alaskan Way Viaduct. The detailed investigation was to include both

structural and geotechnical aspects of the seismic hazards that could impact the Viaduct. The investigation was performed by a team of geotechnical and structural engineering researchers from the University of Washington. This report and companion reports by Eberhard et al. (1995a; 1995b), constitute the final report of the seismic vulnerability investigation.

1.2 THE ALASKAN WAY VIADUCT

The Alaskan Way Viaduct carries traffic on Highway 99 along the waterfront immediately west of downtown Seattle (Figure 1.1). The 3.5 km Viaduct runs from near the south end of the Battery Street tunnel south to approximately Holgate Street; approximately 1.7 miles of its 2.2-mile length (2.7 of 3.5 km) is in the double-deck configuration shown in Figure 1.2. Near the north and south ends, the Viaduct changes to two parallel, single-deck structures that bring Highway 99 back to grade.

The Alaskan Way Viaduct was constructed in two main sections. The first, which extended from the current north end of the Viaduct south to approximately Dearborn Street, was designed by the City of Seattle in the late 1940s and construction in 1950. The second section, which runs from the southern end of the first section to the current southern end of the Viaduct, was designed by WSDOT in the early 1950s and constructed in 1956. These two parts of the Viaduct are often referred to as the Seattle section and the WSDOT section.

Previous preliminary investigation, as well as the structural vulnerability portion of this investigation, have focused on typical portions of the Seattle and WSDOT sections of the Viaduct. Therefore, geotechnical input for the structural vulnerability analyses concentrated, on the conditions at these typical sections, although results for the entire Viaduct are also presented.

1.3 SCOPE OF REPORT

This report describes the geotechnical earthquake engineering investigation of the seismic vulnerability of the Alaskan Way Viaduct. The investigation included characterization of subsurface soil conditions, evaluation of site-specific ground motions, identification of existing

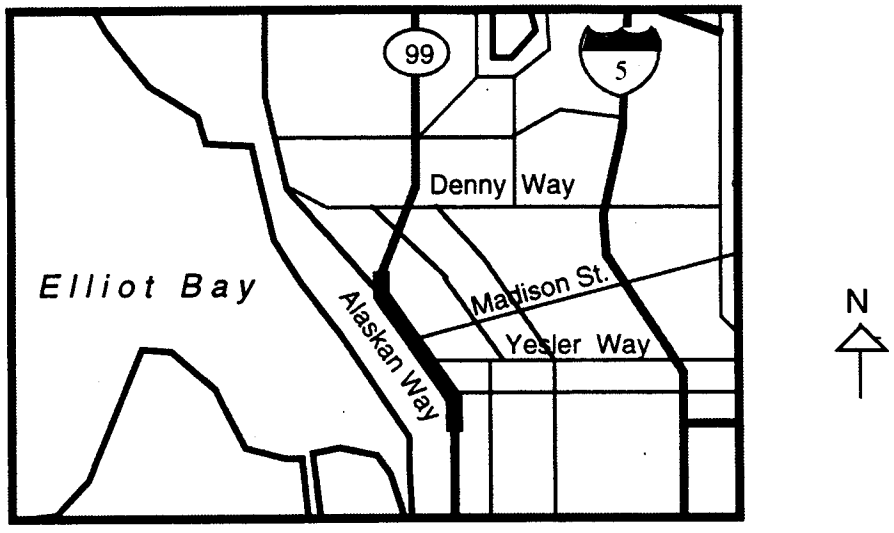

Figure 1.1. Site Plan Of The Alaskan Way Viaduct

foundation conditions, evaluation of dynamic foundation response characteristics, and evaluation of liquefaction hazards. The results of several of these aspects of the investigation were used as input to a series of structural analyses of the seismic vulnerability of the Viaduct. The results of the structural vulnerability evaluation are presented in companion reports by Eberhard et al. (1995a; 1995b). An additional report (Eberhard and Kramer, 1995) summarizes the results of the geotechnical and structural investigations and the overall seismic vulnerability of the Viaduct.

1.4 ORGANIZATION OF REPORT

This report presents the methods and results of a number of geotechnical earthquake engineering analyses relating to the seismic vulnerability of the Alaskan Way Viaduct. Chapter 2 presents the results of a comprehensive investigation of the subsurface soil conditions around the Viaduct. Historical factors, existing subsurface data, and the results of a supplemental subsurface investigation are described and interpreted. The existing foundation conditions, determined from a review of historical information from the archives of the Seattle Engineering

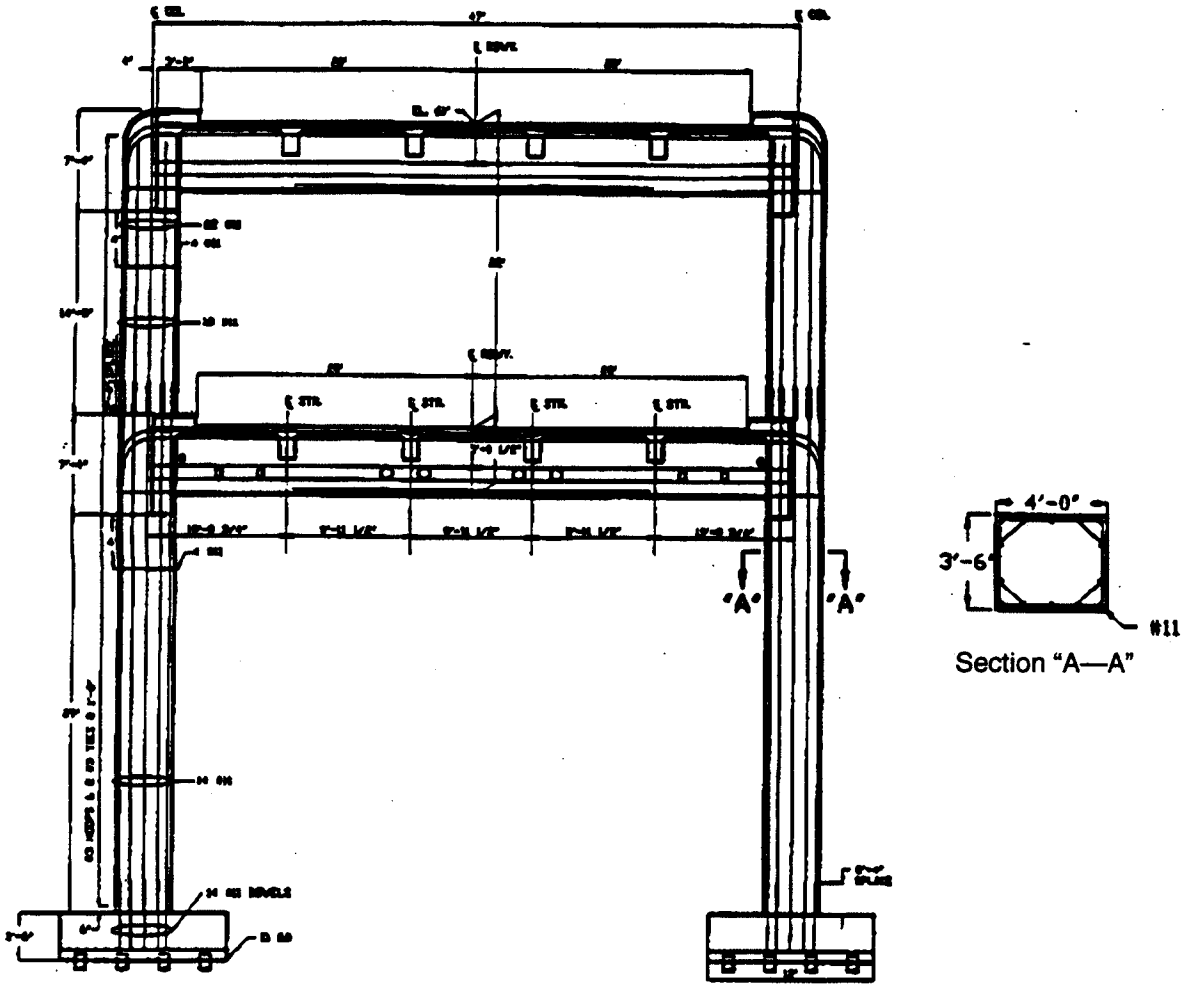

Transverse Elevation of Interior Bent

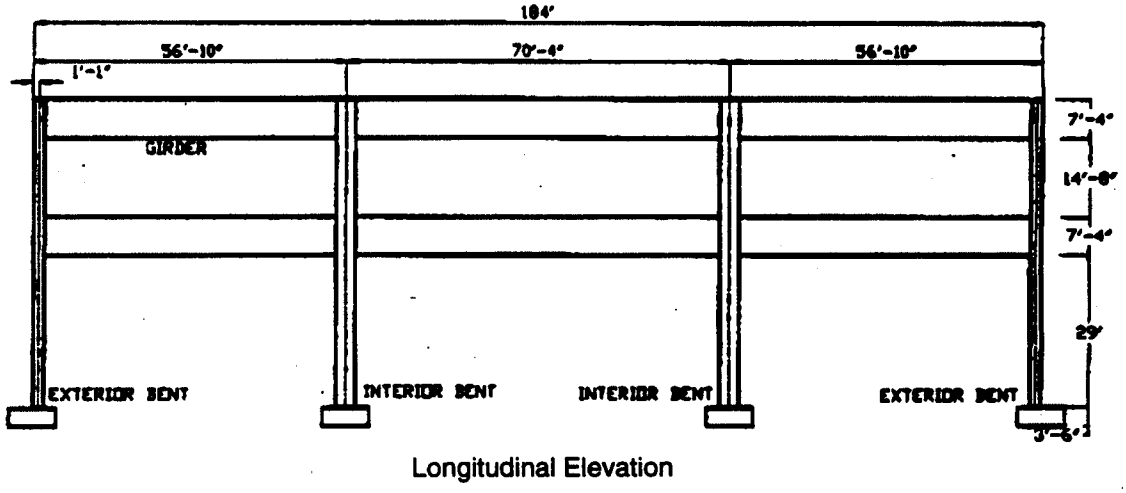

Longitudinal Elevation

Figure 1.2. Typical Configuration of the Elevated Portion of the Alaskan Way Viaduct (WSDOT Section)

Department and WSDOT, are presented in Chapter 3. Chapter 4 presents the results of site-specific analyses of anticipated earthquake ground motions along the length of the Viaduct.

These analyses were performed to provide input for structural analyses of the Viaduct, and for subsequent geotechnical earthquake engineering analyses. The dynamic response characteristics of the existing foundations that support the Viaduct are described in Chapter 5. This information was developed to provide input for structural analyses of the Viaduct. Chapter 6 describes the techniques and results of a detailed series of liquefaction hazards analyses. Finally, the conclusions of the geotechnical earthquake engineering investigations are described in Chapter 7.

CHAPTER 2
SUBSURFACE CONDITIONS

Subsurface conditions along the Alaskan Way Viaduct are relatively complex and are dominated by a sporadic and unevenly documented sequence of filling operations that took place in the late 1800s and early 1900s. To evaluate the seismic vulnerability of the Viaduct, a comprehensive subsurface investigation was undertaken. The investigation included review of historical data on earthwork activities near the Viaduct, review of available data from previous subsurface investigations, and the performance of additional subsurface investigations, which included field and laboratory tests.

The following sections describe the various aspects of the subsurface investigation in the order described above. The results of the investigation are then interpreted to identify and characterize the engineering properties of the major subsurface soil units.

2.1 GEOLOGY AND HISTORY OF SITE DEVELOPMENT

Seattle lies near the center of the Puget Sound Basin, a physiographic region whose geology and geography are dominated by scour and deposition during Pleistocene glaciation. Pleistocene continental ice moved in a generally southward direction from British Columbia into the Puget Sound Basin, eventually extending as far as 50 (80.5 km) south of Seattle. A series of at least five major advances produced a complex sequence of lacustrine deposits, advance outwash, glaciomarine drift, till, and recessional outwash (Galster and Laprade, 1991). As the most recent ice retreated, it left behind a series of north-south trending ridges separated by glacially scoured troughs. The deepest of these troughs are now occupied by major bodies of water such as Puget Sound, Lake Washington, and Lake Sammamish. Other troughs have been alluviated by rivers or naturally filled as tidelands.

Within the area now occupied by the Seattle central business district, settlers encountered a series of north-south trending hills bounded on the south by a large tideflat of Elliot Bay that extended eastward to the base of Beacon Hill. North of the tideflat, the eastern edge of Elliot

Bay was approximately at the current location of First Avenue, though several pile-supported docks had extended into the Bay. An 1884 view of the waterfront area, including the northern portion of the tideflat, is shown in Figure 2.1. In 1887, the Seattle Lakeshore and Eastern Railroad constructed a single rail line on a pile-supported trestle along an alignment approximately coincident with the northern portion of the current Alaskan Way Viaduct. By 1900, 16 rail lines ran along the waterfront, and the trestle that supported them above Elliot Bay became known as Railroad Avenue.

Expansion of the city as a center of commerce required regrading the hills and valleys of the business district so that slopes would not be steeper than could be climbed by the teams of horses that were used to move goods to and from the waterfront. These regrading activities are responsible for much of the current topography of the central business district and for the creation of the industrial district immediately to the south. The regrading also provided the soil used to fill most of the existing waterfront over which the Alaskan Way Viaduct now passes.

There is little record of the sources of fill material placed or the sequence in which it was placed beneath Railroad Avenue north of the tideflat. Much of the fill was washed or dumped under the Railroad Avenue trestles, apparently in relatively small volumes that included broken concrete and sawmill refuse as well as soil. Records do reveal that the fill was deposited by pluviation through the water of Elliot Bay. Much of the fill in the tideflat area came from the Jackson Street and Dearborn Street regrades. Additional fill came from an eventually abandoned attempt to connect Lake Washington to Elliot Bay by cutting through Beacon Hill, and from dredging operations in the Duwamish River. This fill was placed hydraulically to depths of up to 40 feet (12.2 m); the slurry consisted of 7 percent to 16 percent solids (Dorpat, 1984; Morse, 1989) as it left the discharge pipes (Figure 2.2). Most of the former tideflat area is now used for industrial purposes; the Kingdome is the most prominent structure in this area.

Railroad Avenue eventually reached a width of 150 ft (45.7 m) and provided for both rail and vehicular traffic, which traveled on asphalt-paved portions of the trestle. As early as 1911, maintenance problems caused city engineers to consider placing a retained fill along the

waterfront. Difficulties in obtaining financing and developing a suitable design delayed construction of the seawall for some 20 years. Construction finally commenced in 1934. To eliminate excessive loading on the previously placed, loose saturated fills, the seawall was designed with a relieving platform, as illustrated in Figure 2.3. The relieving platform was approximately 13 ft (4.0 m) below grade and was supported by vertical and batter piles. These timber piles were driven through the existing fill and into the dense underlying soil. The timber relieving platform was then constructed and attached to precast concrete seawall sections. Alternate planks were omitted from the relieving platform to facilitate placement of additional fill below the platform. This fill was dumped and then worked into place by sluicing jets operating through holes in the platform and precast panels (Engineering News-Record, 1934). The soil beneath the precast section was retained by steel sheet piling.

Thus, the historical record indicates that the present alignment of the Alaskan Way Viaduct (with the exception of the portion north of approximately Massachusetts Street) was in Elliot Bay a century ago. The earthwork operations that produced the current waterfront area were completed prior to construction of the Viaduct. Further, the historical record shows that the majority of the fill along the length of the Viaduct was placed by pluviation through water and without the benefit of compaction. Fills placed in this manner are known to be loose and compressible, and they have been associated with geotechnical and structural failures during earthquakes in other parts of the United States and the world.

2.2 REVIEW OF PREVIOUS SUBSURFACE DATA

Design of the original portion of the Alaskan Way Viaduct began in the late 1940s, and a series of test borings were drilled in 1948 to provide information for design of its foundations. Approximately 50 shallow borings (less than 20 feet (6.1 m) deep) were drilled at that time by the Seattle Engineering Department. In the mid-1950s, a series of 17 borings (some penetrating to depths greater than 100 feet (30.5 m)) were drilled to provide information for design of the southern portion of the Viaduct. The boring logs from these subsurface investigations were obtained from the archives of the Seattle Engineering Department and the Washington State

Department of Transportation (WSDOT) and were incorporated into a database of subsurface conditions developed for this project. Because these borings provided a limited view of the subsurface conditions beneath the Viaduct, the database was supplemented with data available from other borings drilled in conjunction with various construction projects located near the Viaduct. Those borings from the resulting database that provided the most comprehensive information and that could be located accurately are shown in Fig. 2.4. Subsurface conditions from borings aligned roughly perpendicular to the Viaduct were compiled at four locations: Columbia Street, the vicinity of Jackson and King Streets, the vicinity of Union and Pike Streets, and Washington Street. The locations of these transverse sections are also shown in Figure 2.4.

Initial characterization of the soil conditions beneath the Alaskan Way Viaduct was based on all available borings in the database located within 100 feet (30.5 m) of the centerline of the Viaduct. Because the borings were performed by different agencies and firms at different times and for different purposes, the logs revealed considerable diversity in the type and amount of subsurface information reported. All of the boring logs included visual classification of soil samples, although descriptive detail ranged from short and vague to lengthy and convoluted. SPT data, moisture content, unit weight, plasticity information, depth to water table, and USCS classification were included with some borings but not with others.

The existing borings provided considerable insight into the subsurface conditions along the length of the Alaskan Way Viaduct. The subsurface conditions inferred from these borings are consistent with the known history of soil deposition along the Seattle waterfront. The boring logs indicated that the Viaduct was underlain by 0 to 55 feet (0 to 16.8 m) of loose waterfront fill north of approximately Yesler Street. The waterfront fill consisted predominantly of clean to silty sand with intermittent (and apparently discontinuous) layers of sandy silt and occasional debris. The portions of the waterfront fill described in the boring logs as "silty sand" appeared to contain approximately 5 percent nonplastic fines. In this area, the waterfront fill was underlain by dense glacial till, generally described in the boring logs as "dense sand and gravel." The groundwater level was somewhat variable but averaged about 10 feet (3.0 m) below the ground

surface. South of Yesler Street, similar waterfront fills were encountered from the ground surface to depths of 10 to 70 feet (3 to 21.3 m). In this area, however, the waterfront fills were underlain by a soft, loose, natural tideflat deposit. The thickness of the tideflat deposit varied from about 0 to 20 feet (0 to 6.1 m) between Yesler Street and about Dearborn Street, but increased rapidly south of Dearborn Street to a maximum thickness of approximately 100 feet (30.5 m) near the southern end of the Viaduct. The tideflat deposit was also described as clean to silty fine sand and sandy silt. The tideflat deposit appeared, from the descriptions given in the boring logs, to be somewhat siltier but otherwise similar to the waterfront fills. A subsurface profile showing the locations and the measured SPT-values of the borings used for subsurface characterization along the alignment of the Alaskan Way Viaduct is shown in Figure 2.5. The transverse sections are shown in Figures 2.6-2.9.

Although the borings revealed a great deal about the subsurface conditions, spatial gaps in subsurface information along the length of the Viaduct and uncertainty regarding possible temporal changes in soil conditions and properties due to consolidation, subsequent shaking, or other phenomena prompted the initiation of a supplemental subsurface investigation.

2.3 SUPPLEMENTAL SUBSURFACE INVESTIGATION

From approximately June through October 1993, WSDOT conducted a supplemental subsurface investigation to furnish data for gaps in the longitudinal soil profile between Pike Street and University Street, Washington Street and Jackson Street, and King Street and Dearborn Street. New data were also collected in other locations so that researchers could evaluate the current applicability of soil properties measured in previous subsurface investigations.

A number of methods are available for obtaining such data from the field. In the supplemental subsurface investigation, three in-situ tests were conducted for subsurface soil characterization. Each test provided different information about the soil that was tested. Two of these field tests, the Standard Penetration Test (SPT) and the Cone Penetrometer Test (CPT),

induced large strains in the soil, while the third, the Downhole Shear Wave Velocity Test, provided information on low-strain soil properties.

In the supplemental subsurface investigation, WSDOT crews drilled eight borings in which SPT resistances were measured. They also performed cone penetration tests at 16 locations along the length of the Viaduct; shear wave velocities were measured at 15 of those locations. Later, in December 1993 and January 1994, two deep borings were drilled, and PVC casing was subsequently installed, to allow measurement of shear wave velocities in the upper portion of the till. These borings extended to depths of 221.5 and 250 feet (67.5 and 76.2 m). The locations of the borings and soundings for the supplemental subsurface investigation are shown in Figure 2.10.

SPT

The SPT provides a useful, empirical measure of the density of cohesionless sands, and, because of its long history of widespread use, SPT resistance is often used to characterize the sands' engineering behavior. Figure 2.11 presents measured SPT values from the waterfront fill and tideflat deposits obtained during the supplemental subsurface investigation; boring logs from these tests are presented in Appendix A. Figure 2.11 clearly shows that although the SPT resistances were highly variable, the average SPT resistance was quite low. At some locations, anomalously high SPT resistances were measured in the waterfront fill and tideflat deposits; these values are thought to have been influenced by gravel, debris, or other obstructions embedded in the soil. The generally low measured SPT resistances indicate that the soils of the waterfront fill and tideflat deposits are loose, an observation that is consistent with the known depositional history of these soils.

The SPT resistances measured in the supplemental subsurface investigation were carefully compared with those from the database of existing subsurface data. Because some of the existing data included SPT resistances measured some 45 years before the supplemental subsurface investigation, this comparison was required to determine the current validity of the older data. Comparison between SPT results from borings drilled as close as possible to

previous borings and comparison of overall SPT results showed no significant trends or differences that could raise questions about the current validity of the older SPT data. As a result, the SPT resistances from the database of existing subsurface data and from the supplementary subsurface investigation were combined and weighted equally in all subsequent analyses.

CPT

In recent years, use of the Cone Penetration Test (CPT) in geotechnical engineering practice has rapidly increased in the United States. The absolute and relative magnitudes of the tip resistance and sleeve resistance can be correlated to many of the same properties as the SPT, and also to soil type. The CPT provides a continuous profile of penetration resistance that can detect the presence of thin layers or seams that can easily be missed in the SPT testing. Figure 2.12 presents measured CPT tip resistances from all cone soundings from the waterfront fill and tide flat deposits. Raw data for the CPT tests conducted in this investigation are presented in Appendix B. Tip resistances in the waterfront fill and tideflats deposits were typically less than 50 tsf (4800 kN/m); higher values probably represented isolated seams and/or layers of denser sand and silt, gravel particles, debris, or other obstructions. The low CPT tip resistances measured in these tests provided additional evidence that the waterfront fill and tideflat deposits are predominantly soft and loose.

Shear Wave Velocity

The use of shear wave velocity to characterize the engineering behavior of soil is a fairly recent development in the United States. The shear wave velocity is related to the low-strain stiffness of the soil. Measured shear wave velocities from the WSDOT subsurface investigation are presented in Figure 2.13. Raw data from these tests are presented in Appendix C. Shear wave velocities in the waterfront fill and tideflat deposit ranged from 250 to 700 ft/sec (76.2 to 213.4 m/sec), although some higher values were measured in some denser layers. When compared to the results of the SPT and CPT investigations, the shear wave velocity results

further corroborated the conclusions discussed previously concerning the soft, loose nature of the waterfront fill and tideflat deposit.

2.4 LABORATORY TESTING

The in-situ field tests described in the previous section provided no information on such important soil characteristics as grain-size distribution, Atterberg limits, fines content, and permeability. To further characterize the subsurface soils, laboratory tests were performed at the WSDOT Materials Laboratory on samples from three borings from the supplemental subsurface investigation. The borings were located near Massachusetts Street, between Dearborn and Connecticut streets, and near Seneca Street. The laboratory tests included measurements of unit weight, moisture content, fines content, Atterberg limits, USCS classification, permeability, and strength.

A comparison of the laboratory test results with corresponding soil descriptions in the borings logs indicated that the term "silty" generally corresponded to 5-10 percent fines and the term "silt" corresponded to a range of 79-100 percent fines. In all cases, however, the fines appeared to be nonplastic, even at depths of 145 feet (44.2 m) below the surface.

2.5 CHARACTERIZATION OF SUBSURFACE CONDITIONS

All available data, from previous investigations and the supplemental subsurface investigation performed as part of this project, confirmed that the soils beneath the Alaskan Way Viaduct can be divided into three basic units: the waterfront fill, the tideflat deposit, and the glacial till. The locations of these units, as interpreted from the available subsurface data, are shown in Figure 2.14. Prediction of seismic ground response, foundation stiffness and damping behavior, and evaluation of liquefaction hazards required the characterization of the engineering behavior of each soil unit. Characterization was based on visual examination and description, in situ test results, and laboratory test results. The most important of these properties were the unit weight, stiffness, permeability, and liquefaction resistance of the soils.

Waterfront Fill

The unit weight of the waterfront fill was measured in 11 laboratory tests on samples from 0 to 45 feet (13.7 m). These tests indicated an average saturated unit weight of 109 pcf (1746 kg/m^3). This unit weight, while quite low, is consistent with the low penetration resistances measured in the in-situ tests.

The stiffness of the waterfront fill was characterized in terms of shear wave velocity. Shear wave velocity profiles were measured at 15 locations with seismic cone penetration equipment, and at two other locations with geophysical downhole test equipment. For many engineering analyses, measured shear wave velocities are customarily corrected to a standard effective overburden pressure of 1 tsf (96 kPa) by the following relationship

$$v_{s1} = v_s \sigma'_v{}^{-1/n} \qquad \text{Equation 2.1}$$

where v_s is the measured shear wave velocity, σ'_v is in tsf, and n is assumed to be 3 (Tokimatsu et al., 1991) or 4 (Finn, 1991; Kayen et al., 1992). For this investigation, n was 3.5. Figure 2.15 presents corrected shear wave velocity data for the waterfront fill.

Liquefaction resistance was characterized by the three in-situ test parameters: SPT resistance, CPT resistance, and shear wave velocity. For liquefaction analysis, measured SPT resistances are corrected to a standard effective overburden pressure of 1 tsf (96 kPa) and a standard energy of 60 percent of the free-fall energy of the SPT system. The corrected SPT resistances were calculated from the following relationship:

$$(N1)_{60} = NC_N(E_m/0.6E_{ff}) \qquad \text{Equation 2.2}$$

where N is the measured SPT resistance and C_N is the overburden correction factor, which is $C_N = \sqrt{\sigma'_v}$, where σ'_v is in tsf, E_m is the delivered energy, and E_{ff} is the free-fall energy. Though actual hammer energies were not measured, the WSDOT Materials Laboratory indicated that the

energy delivered by the WSDOT drill rig was approximately 60 percent of the free-fall energy (Al Kilian, personal communication, 1993). Corrected SPT resistances for the waterfront fill are presented in Figure 2.16. For liquefaction analyses, CPT resistances also require correction for overburden effects. The measured CPT resistances were corrected to a standard effective overburden pressure at 1 tsf (96 kPa) by the following relationship

$$q_{c1} = q_c(1.8/0.8+s'_v) \qquad \text{Equation 2.3}$$

where q_c is the measured CPT resistance and σ'_v is the effective overburden pressure in tsf. The corrected CPT resistances for the waterfront fill are shown in Figure 2.17.

Liquefaction resistance is also influenced by fines content. Grain size distribution curves from samples of the waterfront fill indicated that the portions of the fill described as "silty sand" had an average fines content of about 5 percent. Atterberg limits tests of these fines and of the fines from samples described as "silt" or "sandy silt" consistently indicated that they were nonplastic. The effects of liquefaction are influenced by the permeability of the liquefied soil. Permeability tests conducted on samples of the waterfront fill at a depth of approximately 36 ft (11 m) from one of the borings obtained during the supplemental subsurface investigation resulted in an average $k = 10 \times 10^{-4}$ cm/sec.

Tideflat Deposit

The unit weight of the tideflat deposit was measured in 10 laboratory tests on samples from depths of 20 to 140 feet (6.1 to 42.7 m). The tests indicated an average saturated unit weight of 110 pcf (1762 kg/m^3), which was consistent with the low penetration resistances measured in the in-situ tests and nearly identical to the average saturated unit weight of the waterfront fill.

Corrected shear wave velocities, SPT resistances, and CPT resistances for the tideflat deposit are presented in Figures 2.18, 2.19, and 2.20, respectively. A comparison of these results to those shown in Figures 2.15, 2.16, and 2.17, presented in the previous section on the

waterfront fill, revealed a consistent similarity in the behavior of these two deposits during these tests. Permeability tests conducted on samples of the tideflat deposit at a depth of 70 ft (21.3 m) produced an average $k = 3 \times 10^{-4}$ cm/sec, a value very close to that of the fill.

Till

Measurement of the unit weight of the till was complicated by the relatively high gravel content. The saturated unit weight of the till was calculated as 140 pcf (2242 kg/m^3) by using water content data from a previous boring installed in the till by the Department of Natural Resources, Geology Division. This boring was located at the Federal Building. This saturated unit weight is typical for this type of material and was used for the till throughout the profile.

The stiffness of the till was characterized from the results of the two deep borings in which geophysical downhole shear wave tests were performed. Shear wave velocities from both borings are shown in Figure 2.21. Combining the results of these tests with those from the previous test at the Federal Building site produced an average shear wave velocity for the till of 1250 ft/sec (381 m/sec) in the first 25 feet (7.6 m) below the waterfront fill/tideflat deposit, as 1700 ft/sec (518 m/sec) for the next 175 feet (53.4 m), and as 2,500 ft/sec (762 m/sec) deeper than 200 ft (61 m) below the bottom of the waterfront fill/tideflat deposit.

Discussion

Careful examination of the engineering properties of the waterfront fill and tideflat deposits revealed no discernible differences that would significantly influence many aspects of their engineering behavior. Because their average unit weights were virtually identical and because no significant differences in their stiffnesses could be identified, they were treated as a single "soft soil" layer in many of the analyses described in subsequent sections of this report. Given that the geologic sources of the two deposits were the same and that both were deposited by pluviation through water (albeit at very different rates of deposition), the observed similarity is not surprising.

Figure 2.1. Seattle Waterfront In 1884

Figure 2.2. Hydraulic Filling Operation During Tideflat Reclamation

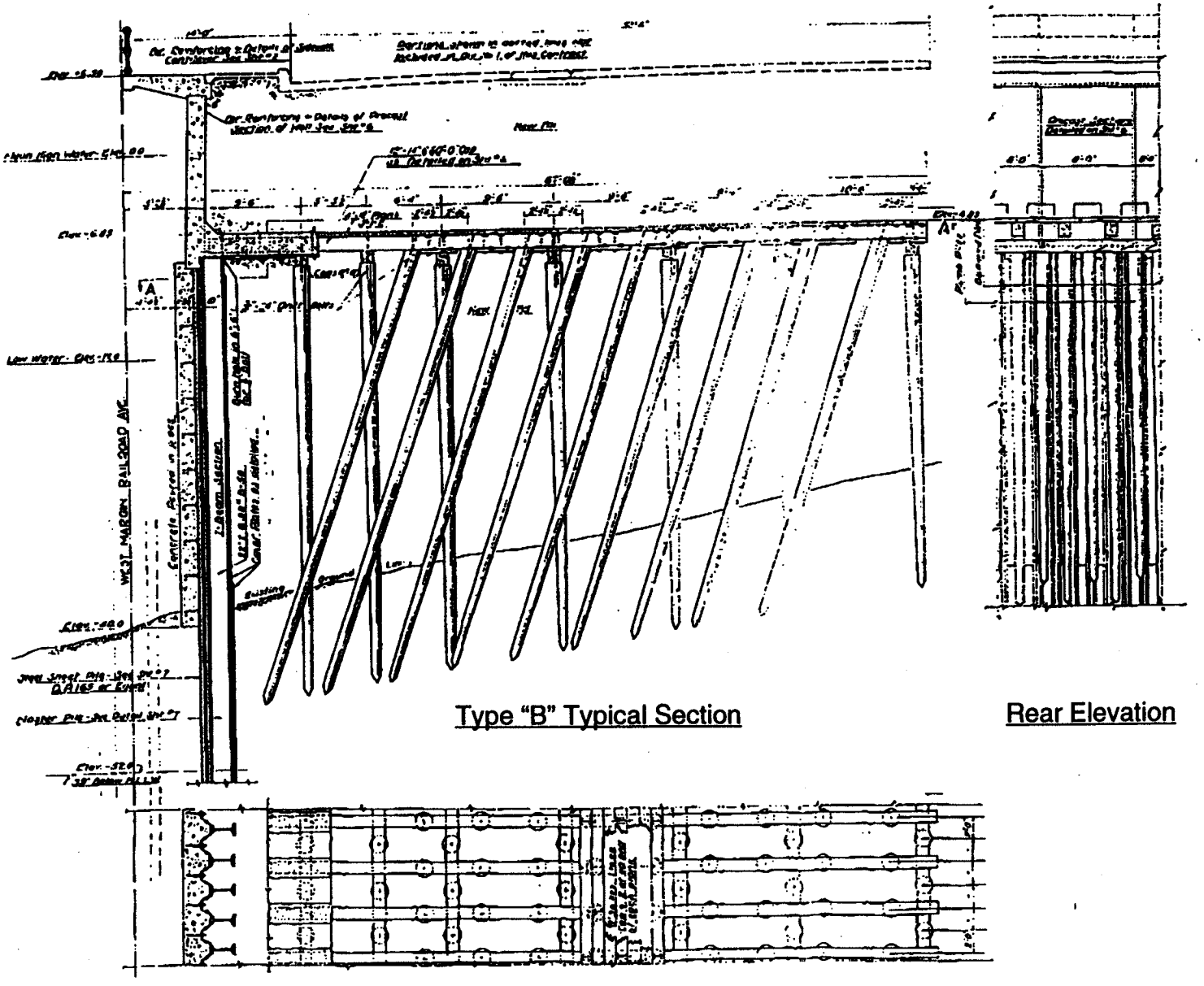

Figure 2.3. Profile and Plan Views of a Typical Section of the Railroad Avenue Seawall

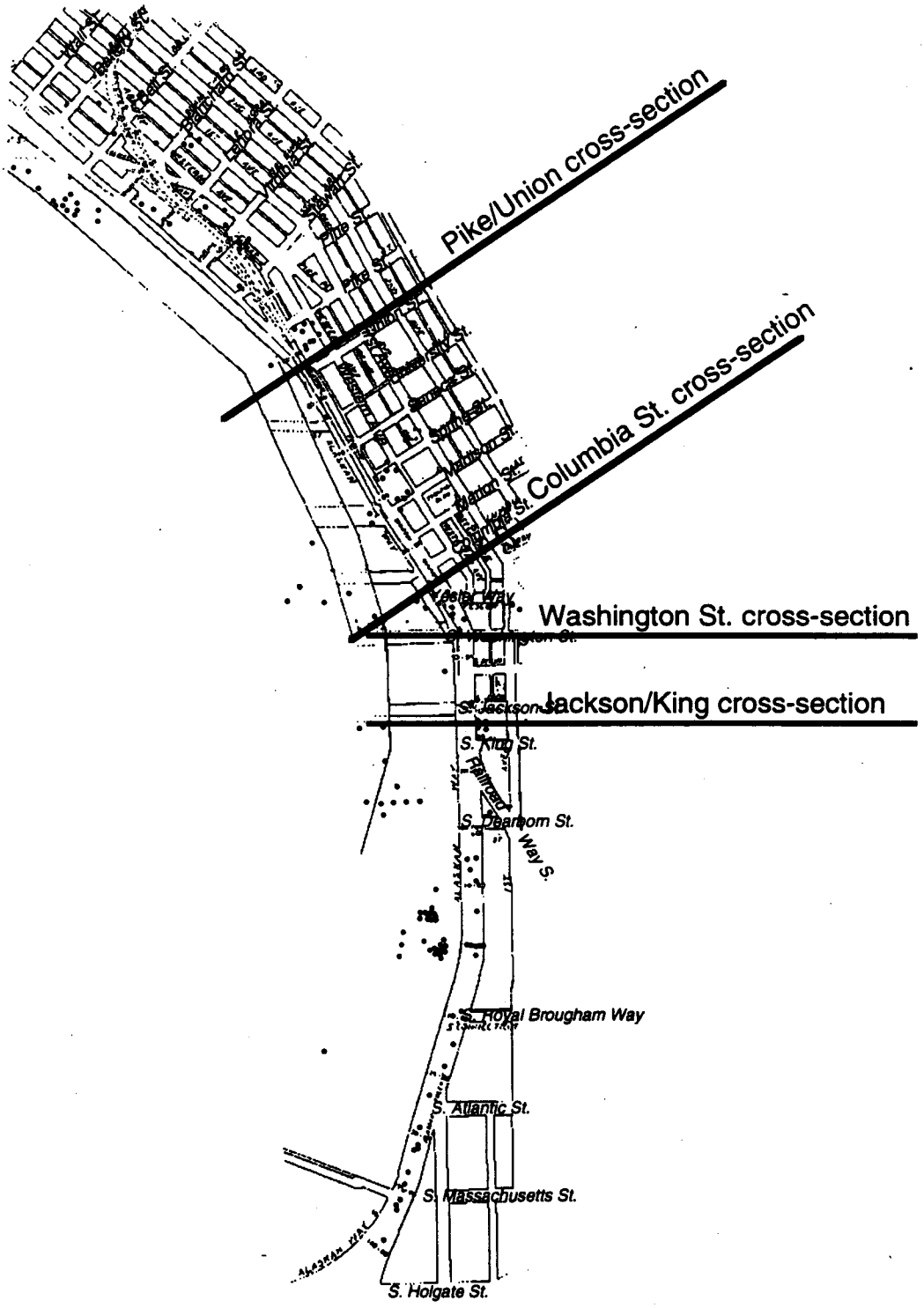

Figure 2.4. Locations of Available Boring Logs in the Vicinity of the Alaskan Way Viaduct

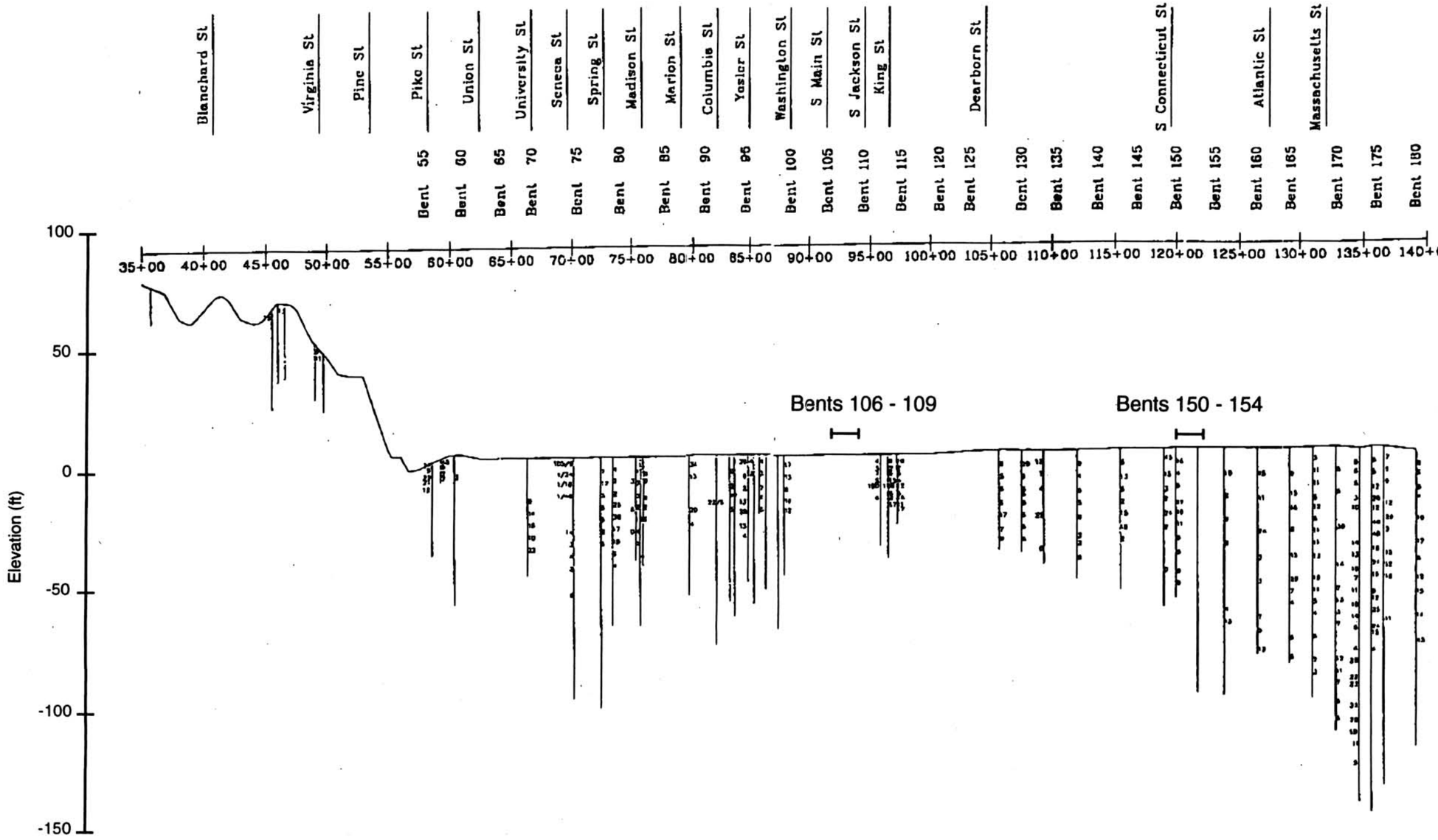

Figure 2.5. Longitudinal profile along the centerline of the Alaskan Way Viaduct. Locations are indicated by cross streets, bent numbers, and station numbers. Standard penetration resistances are indicated adjacent to borings, where available.

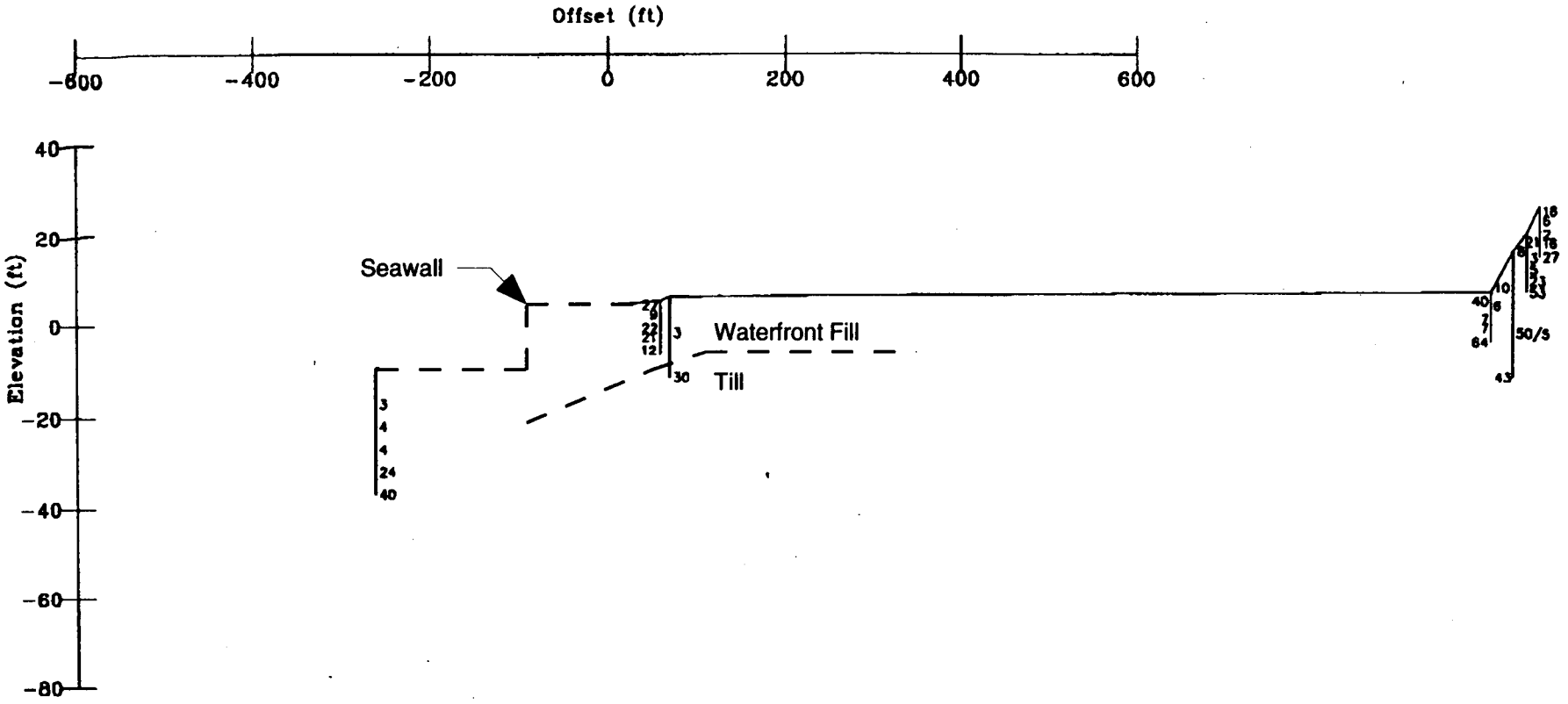

Figure 2.6. Soil Profile at Pike/Union Cross-Section. Standard penetration resistances are indicated adjacent to borings, where available. Offset is measured from approximate centerline of Alaskan Way Viaduct.

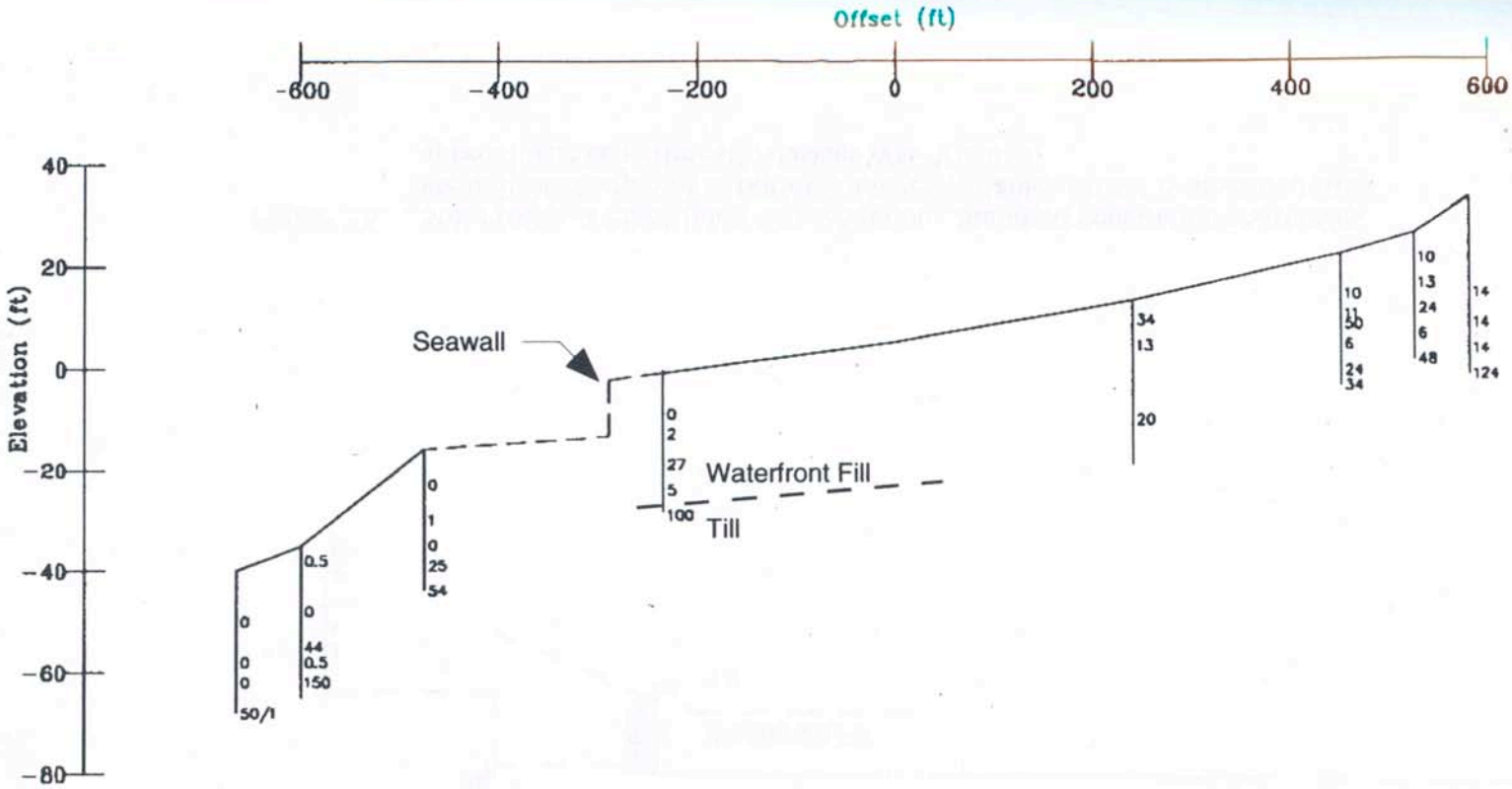

Figure 2.7. Soil Profile at Columbia Street Cross-Section. Standard penetration resistances are indicated adjacent to borings, where available. Offset is measured from approximate centerline of Alaskan Way Viaduct.

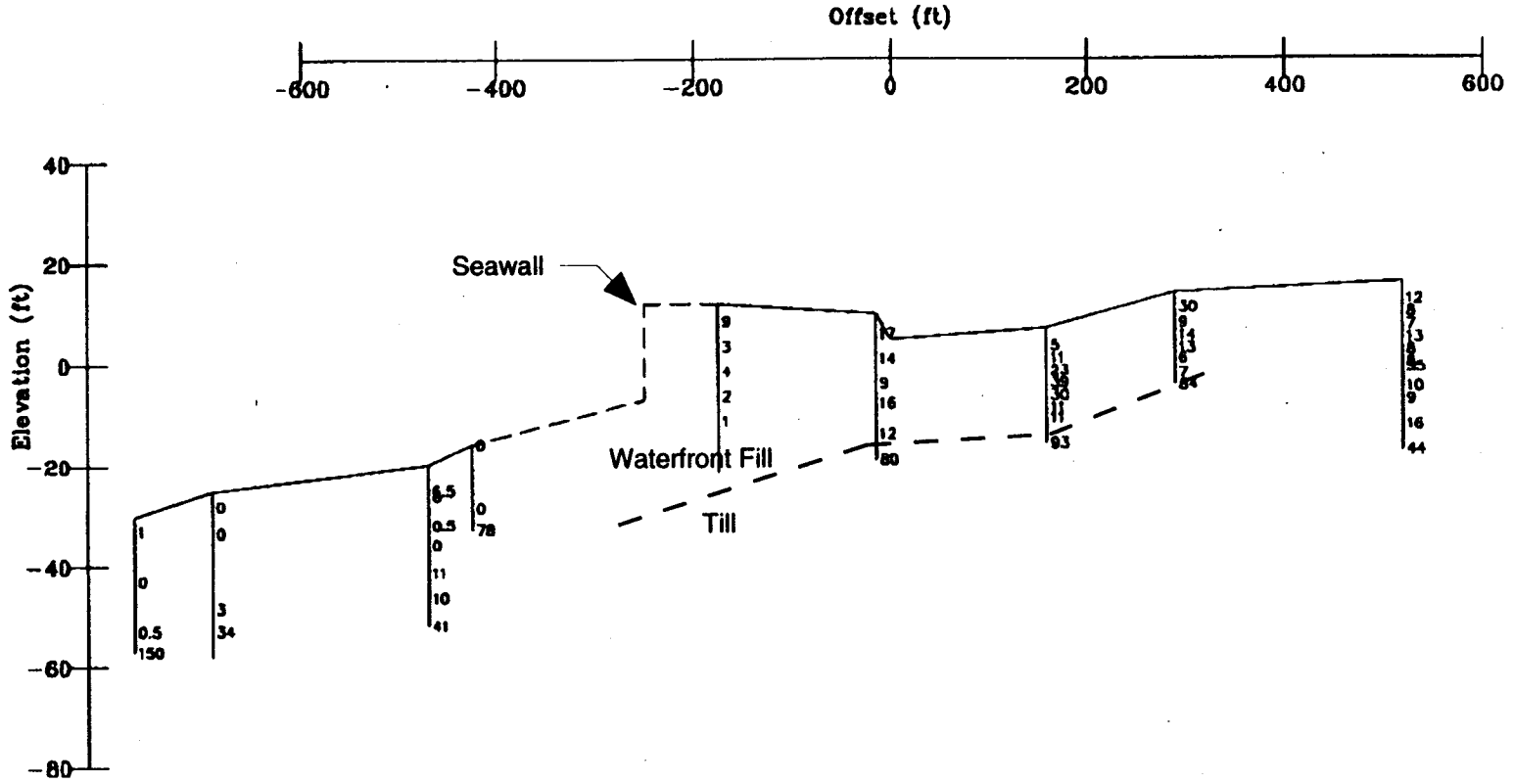

Figure 2.8. Soil Profile at Washington Street Cross-Section. Standard penetration resistances are indicated adjacent to borings, where available. Offset is measured from approximate centerline of Alaskan Way Viaduct.

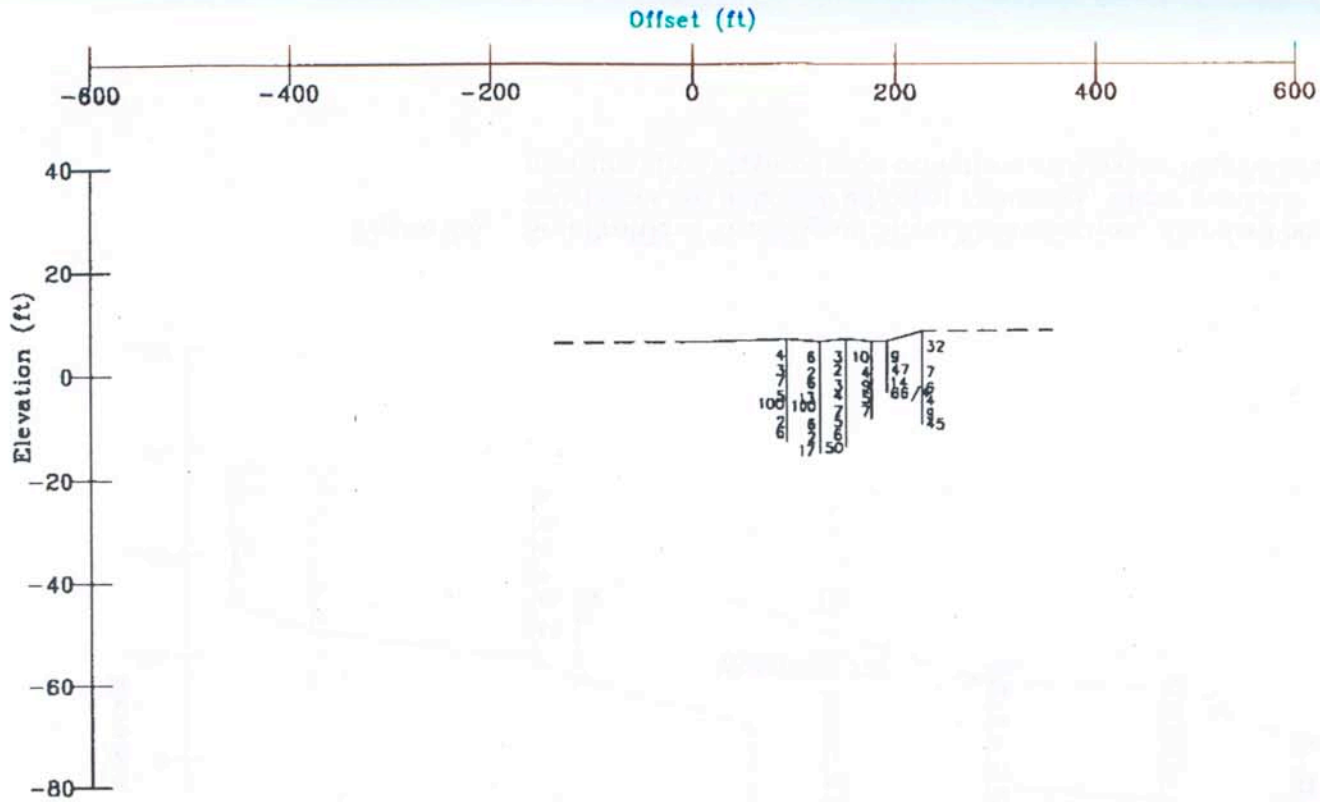

Figure 2.9. Soil Profile at Jackson/King Cross-Section. Standard penetration resistances are indicated adjacent to borings, where available. Offset is measured from approximate centerline of Alaskan Way Viaduct.

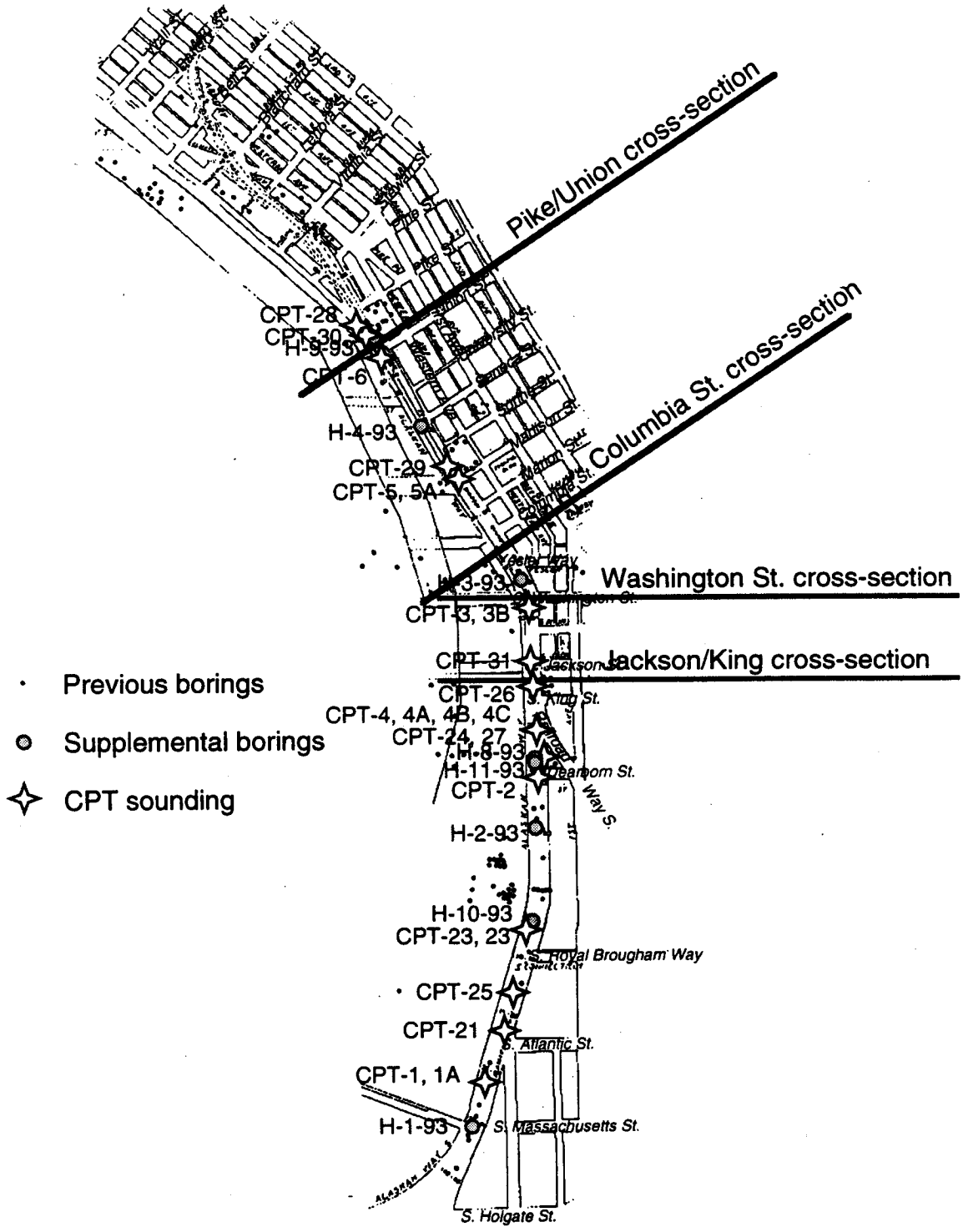

Figure 2.10. Locations of Boring and Insitu Tests in Supplemental Subsurface Investigations. Downhole shear wave velocity tests were conducted in Borings H-9-93 and H-10-93. Seismic cone surveys were conducted in all CPT soundings except CPT-23.

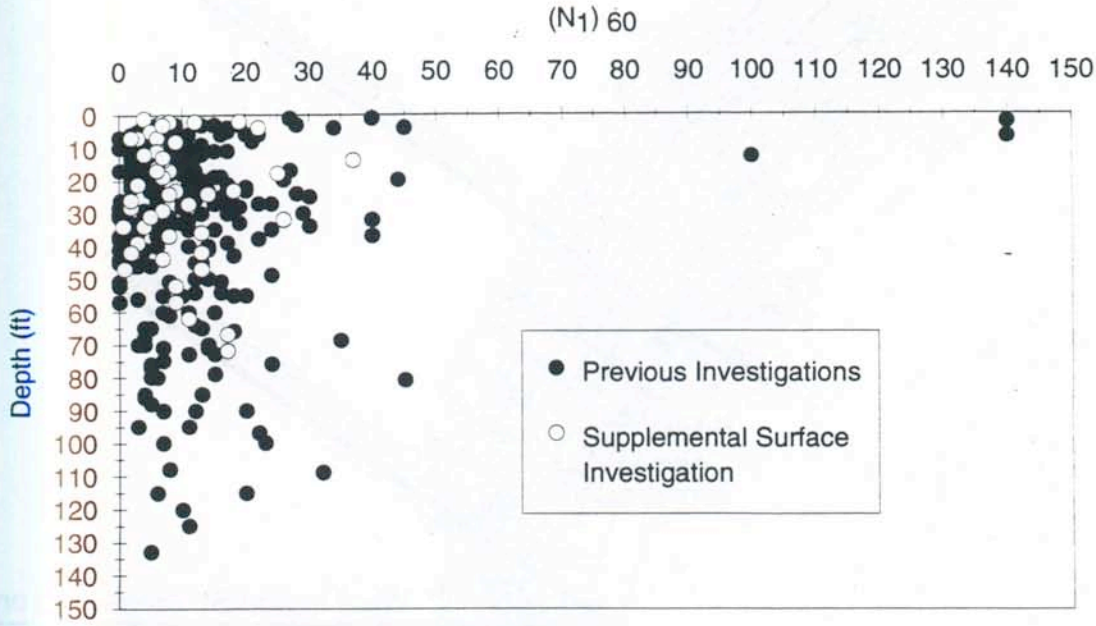

Figure 2.11. Uncorrected Standard Penetration Resistances from Previous Investigations and Supplemental Subsurface Investigation

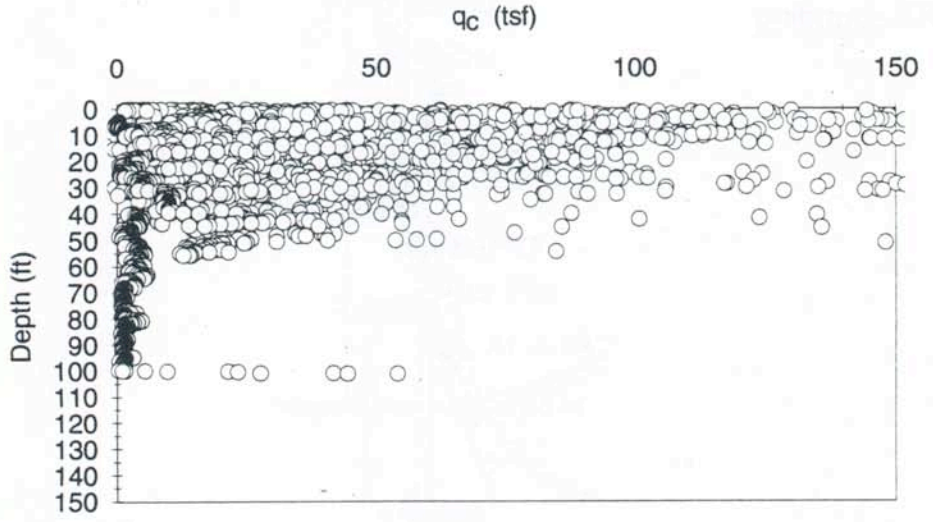

Figure 2.12. Uncorrected Tip Resistances from Cone Penetration Tests Conducted in Supplemental Subsurface Investigation

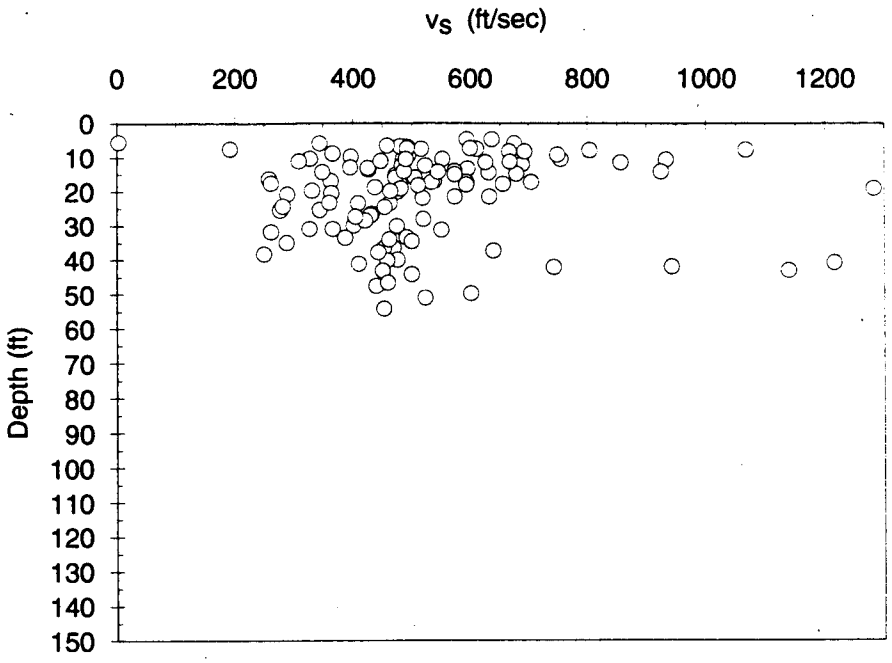

Figure 2.13. Uncorrected Shear Wave Velocities from Cone Penetration Tests Conducted in Supplemental Subsurface Investigation

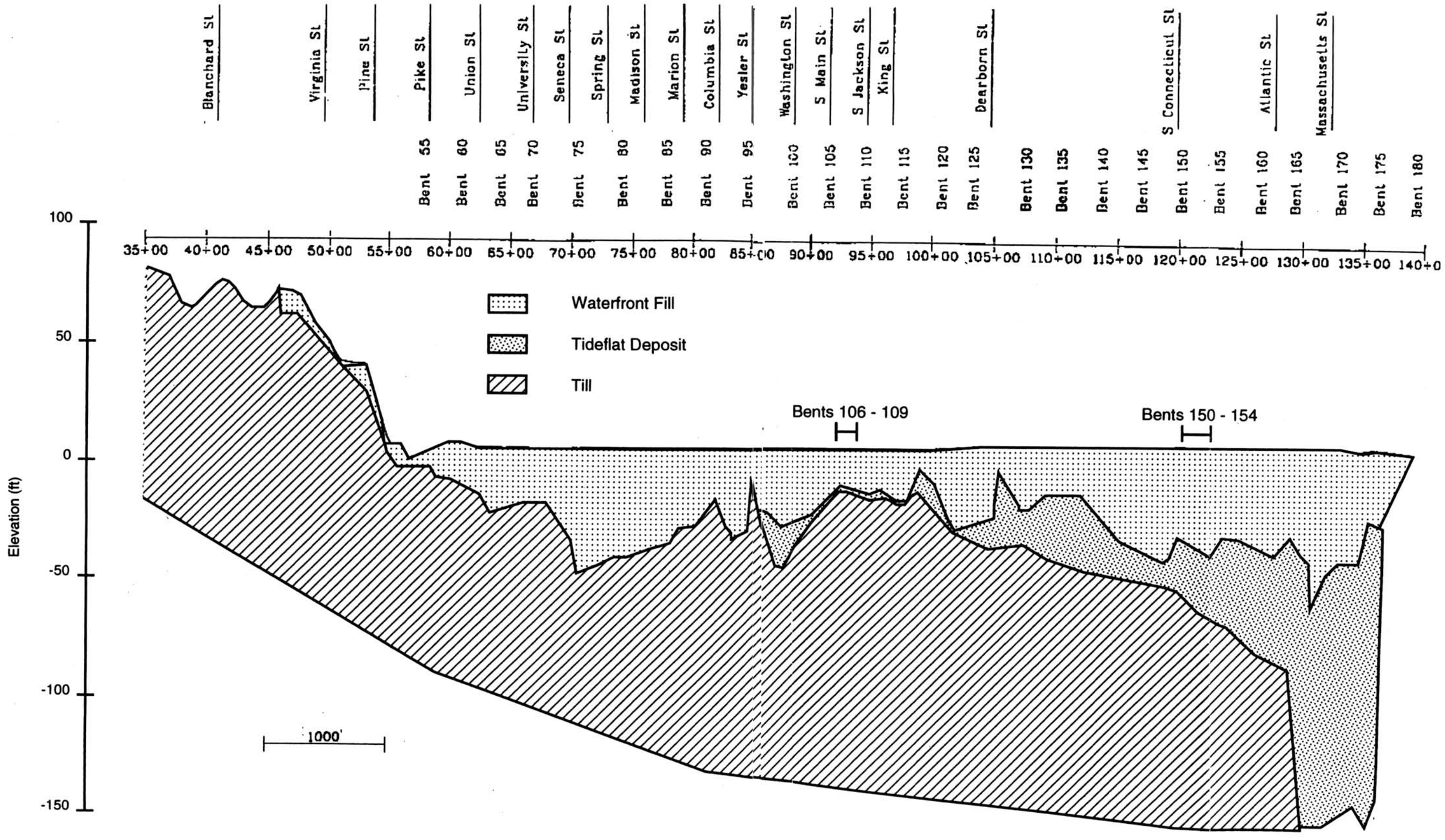

Figure 2.14. Soil Profile along the Length of the Alaskan Way Viaduct as Inferred from Results of Previous and Supplemental Subsurface Investigations

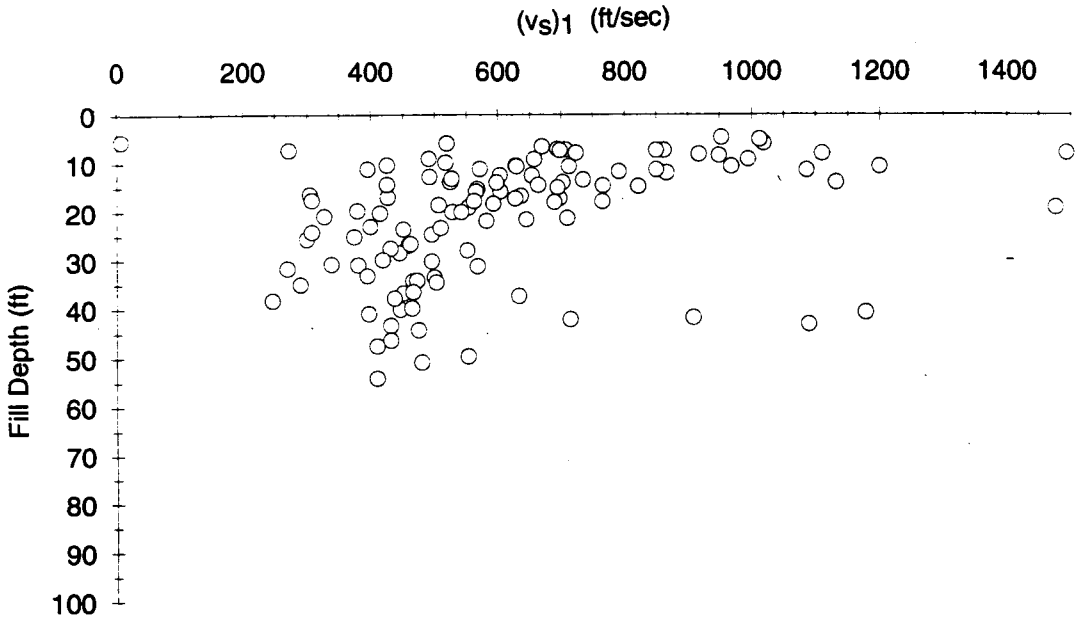

Figure 2.15. Comparison of Measured CPT Resistances with CPT Resistance Required to Resist Liquefaction for 50 Ft Soft Soil

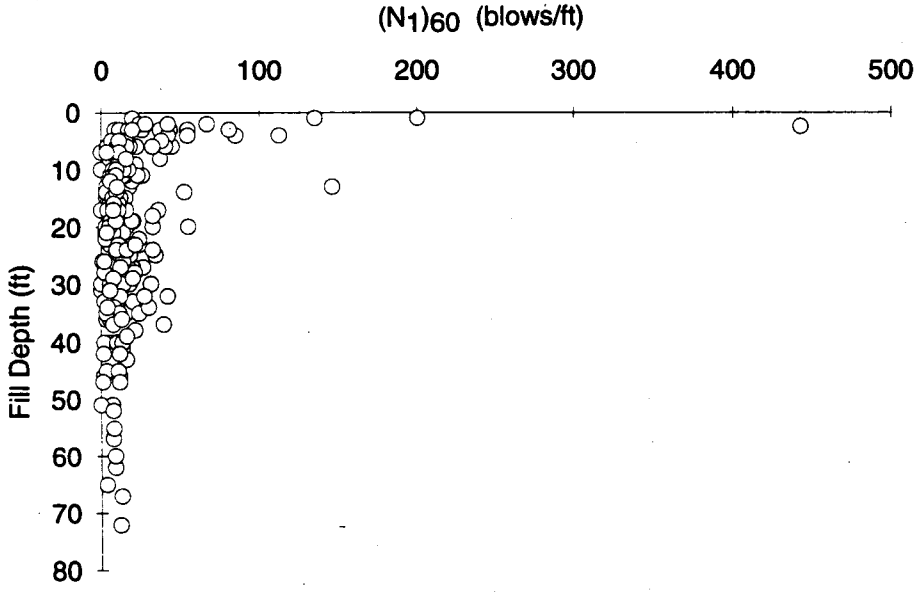

Figure 2.16. Corrected Standard Penetration Resistances for Waterfront Fill from Standard Penetration Tests Conducted in Supplemental Subsurface Investigation

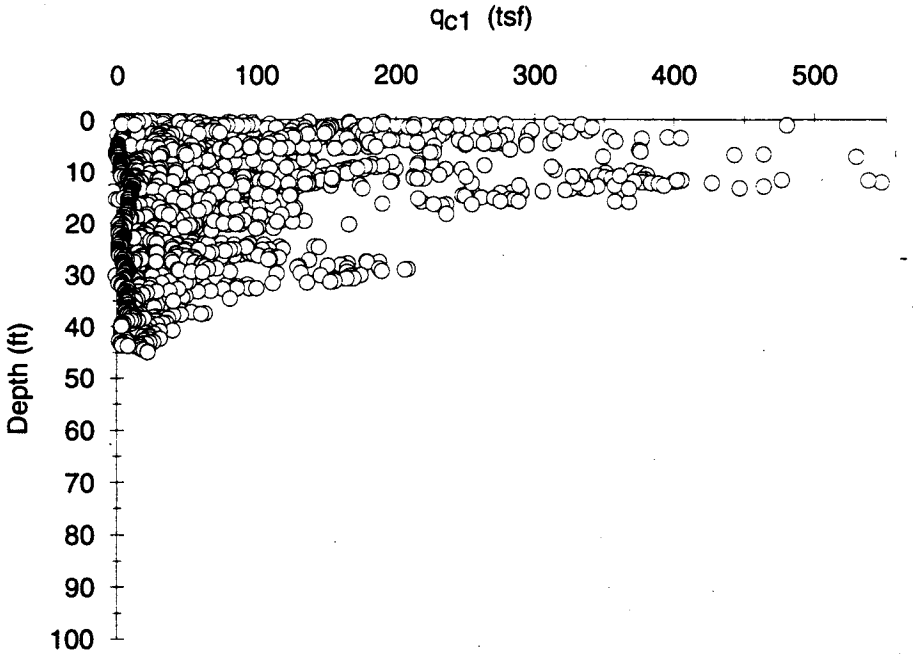

Figure 2.17. Corrected Tip Resistances for Waterfront Fill from Cone Penetration Tests Conducted in Supplemental Subsurface Investigation

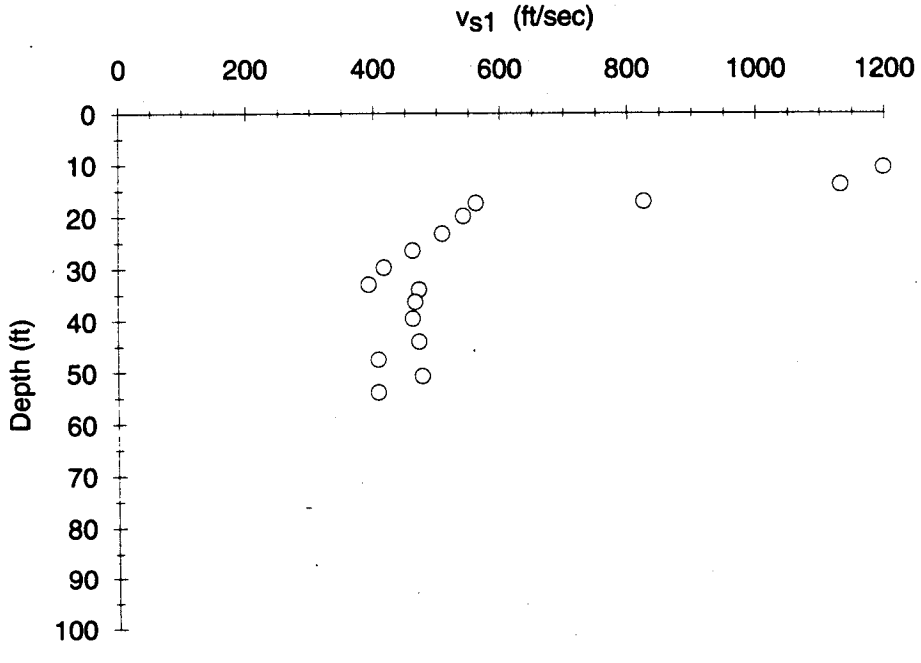

Figure 2.18. Corrected Shear Wave Velocities for Tideflat Deposit from Seismic Cone Tests Conducted in Supplemental Subsurface Investigation

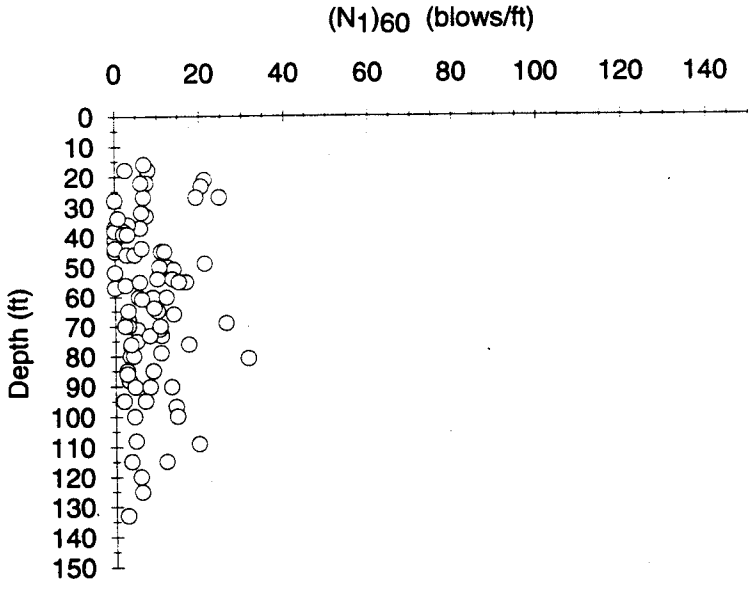

Figure 2.19. Corrected Standard Penetration Resistances for Tideflat Deposit from Standard Penetration Tests Conducted in Supplemental Subsurface Investigation

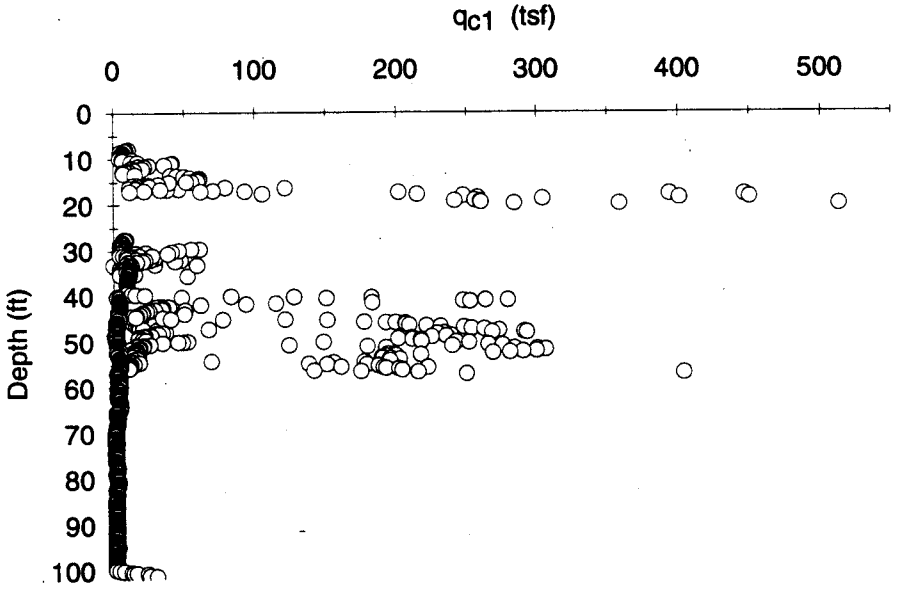

Figure 2.20. Corrected Tip Resistances for Tideflat Deposit from Cone Penetration Tests Conducted in Supplemental Subsurface Investigation

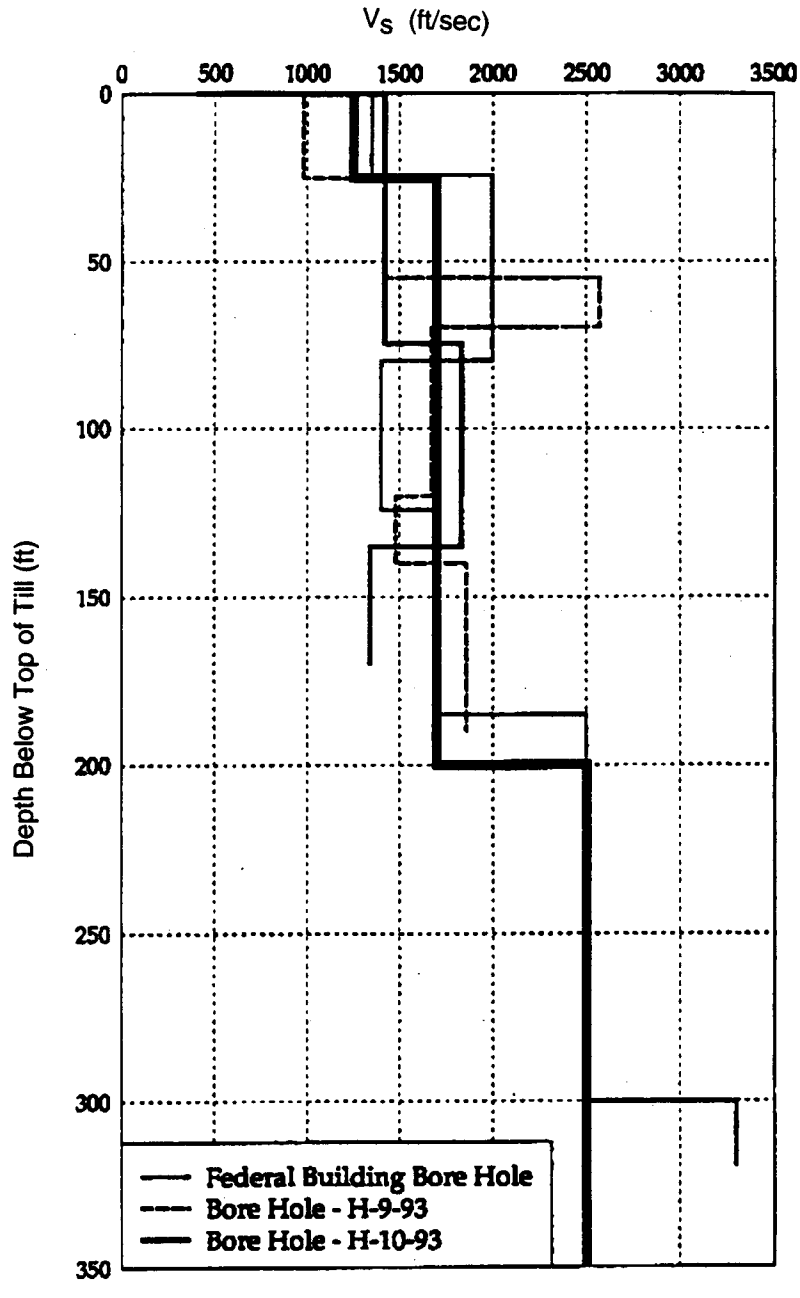

Figure 2.21. Variation of Measured Shear Wave Velocity in Till from Previous and Supplemental Subsurface Investigations (Thick solid line represents average shear wave velocity profile used in analyses.)

CHAPTER 3
FOUNDATION CONDITIONS

The foundations that support the Alaskan Way Viaduct strongly influence its vulnerability to seismic loading. During an earthquake, the foundations will simultaneously transmit ground motions to the structure and interact with the surrounding soil to provide restraint to lateral movement of the Viaduct. Furthermore, the foundations must support the weight of the Viaduct without significant deformations during and after earthquake shaking. Evaluation of the seismic vulnerability of the Viaduct required that the existing foundation conditions be identified.

3.1 FOUNDATION TYPES AND CONFIGURATIONS

Available records indicate that the foundations for both the Seattle section (Bents 1-121) and the WSDOT section (Bents 121-183) of the Viaduct are supported on pile foundations, except for Bents 1-6 and 24-31 at the northern end, where shallow foundations were used. The pile foundations consist of groups of piles that extend through the waterfront fill and tideflat deposits, and support the footings on which the Viaduct columns rest. The shallow foundations are found where glacial till is at the ground surface and where the north- and southbound sections of the viaduct diverge into two separate structures.

Types of Piles

According to available records, foundations for the Seattle section used cast-in-place (CIP), precast concrete, and steel H-piles. CIP piles were constructed with self-supporting driven shells or mandrel-driven shells. CIP and precast piles were required to be installed at sufficient depths to develop a minimum load bearing capacity of 40 tons (36.3×10^3 kg), while the H-piles were required to be driven to develop a minimum load bearing capacity of 48 tons (43.5×10^3 kg). The piles were originally intended to be H-piles; however, the project history states that "... at the contractor's request and because of the slow rate of delivery on 'H' beam piles, the Bridge Department agreed to use cast-in-place piles in lieu of 'H' beams wherever possible." The final

pile driving records indicate that both CIP and H-piles were used, and in some cases, a combination of both were used in the same pile group. Details of the CIP and precast concrete piles are shown in Figure 3.1.

The WSDOT section is supported on composite piles and steel H-piles. Detailed descriptions or drawings of the composite piles were not available. They were apparently constructed by first augering through the upper portion of the fill and driving a timber pile of about 13-inch (33 cm) tip diameter with a follower so that its butt end was typically at depths of 6 to 12 feet (1.8 to 3.7 m) below the bottom of the pile caps. The timber pile was then spliced to a CIP section that extended up to the bottom of the pile cap. The splice was apparently accomplished by trimming the butt of the timber pile to allow the placement of a 3-foot (91 cm) long, 12-inch (30.5 cm) diameter steel pipe over its end and securing the pipe with four spikes driven through holes in its side, before filling the CIP section with concrete. According to the final driving records, the composite piles were most commonly used in the WSDOT section, although some foundations used combinations of composite and H-piles. Records do not reveal whether the timber piles were treated with creosote or other preservatives. Considering the relative depths of the timber piles and the groundwater surface, it is likely that untreated timber piles were used and installed at such depths with the intent that they remain below the groundwater level.

Pile Group Configurations

Because of differences in the loads they were required to support, the pile groups supporting external columns had different sizes and configurations than those supporting internal columns. For the most part, the foundations for exterior columns in the Seattle section used 14 piles in each group arranged in three rows of five, four, and five piles. The interior column foundations generally used 20 piles in each group, arranged in four rows of five piles each. In the WSDOT section, the exterior foundations typically used 11 piles in each pile group arranged in three rows of four, three, and four piles, and the interior bents had 16 piles in each group arranged in four rows of four piles each. The piles were installed 3.5 feet and 3 feet (1.1 m and

91 cm) center to center in the Seattle and WSDOT sections, respectively. The main pile group configurations used in the Seattle section are shown in Figures 3.2 and 3.3, and those used in the WSDOT section are shown in Figures 3.4 and 3.5.

In addition to these typical configurations, a number of other configurations were used in both the Seattle and WSDOT sections, with the number of piles and arrangements differing substantially among them. The total number of piles in individual foundations varied from as few as four to as many as 44 in the Seattle section and from five to 34 in the WSDOT section. Some of the foundations were constructed with unconventional configurations that appear to have been selected during pile installation to allow the required number of piles to be driven within the restricted space available for the pile cap.

Footing Dimensions

Most of the footings in the Seattle section had a stepped shape consisting of a small rectangular block over a larger rectangular block (Figure 3.4). In the WSDOT section, the footings were single, rectangular blocks. The footings in both the Seattle and WSDOT sections were constructed monolithically. Typically, the Seattle section footings had external plan dimensions of 17 feet by 10 feet (5.2 m by 3.5 m) for the foundations supporting exterior columns and 17 feet by 13.5 feet (5.2 m by 4.1 m) for the foundations supporting the interior columns. The WSDOT section had footings of 12 feet by 8.5 feet (3.7 m by 2.6 m) at the base for the foundations at the exterior columns and 12 feet by 12 feet (3.7 m by 3.7 m) for the foundations of interior columns. The bases of the footings were embedded to depths of about 4.5 feet and 7 feet (1.4 m and 5.2 m) in the Seattle and WSDOT sections, respectively.

In addition to these typical dimensions, the footing dimensions varied in a number of locations to accommodate additional piles in both the Seattle and WSDOT sections. The footing base dimensions varied from 5.5 feet by 5.5 feet (1.7 m by 1.7 m) to 27.5 feet by 20.5 feet (8.4 m by 6.3 m) and, in cases where combined foundations were used, to 35.5 feet by 12 feet (10.8 m by 3.7 m) in the Seattle section. In the WSDOT section, they varied from 6.5 feet by 6.5 feet (2.0 m by 2.0 m) to 18 feet by 17 feet (5.5 m by 5.2 m).

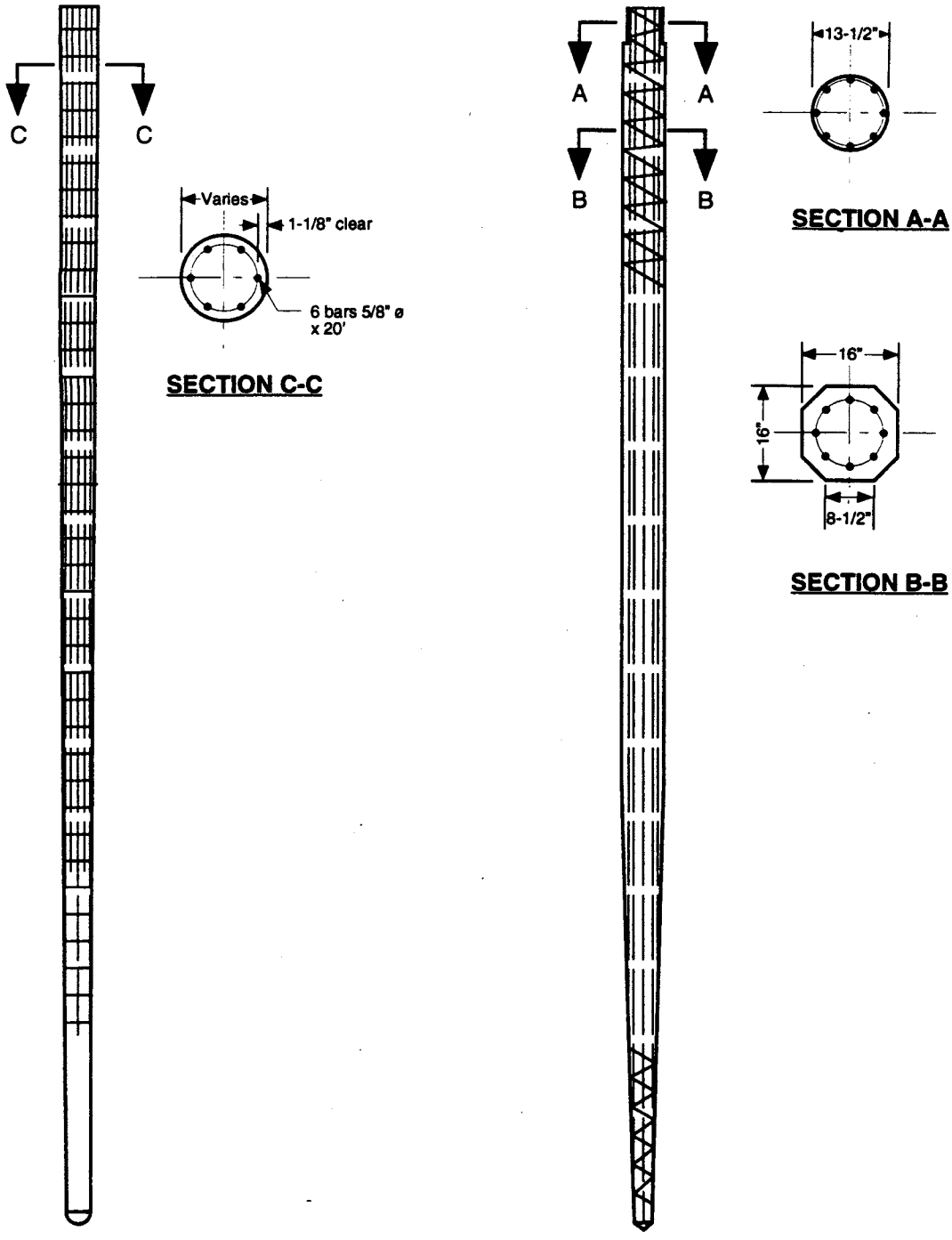

Figure 3.1. Concrete Piles

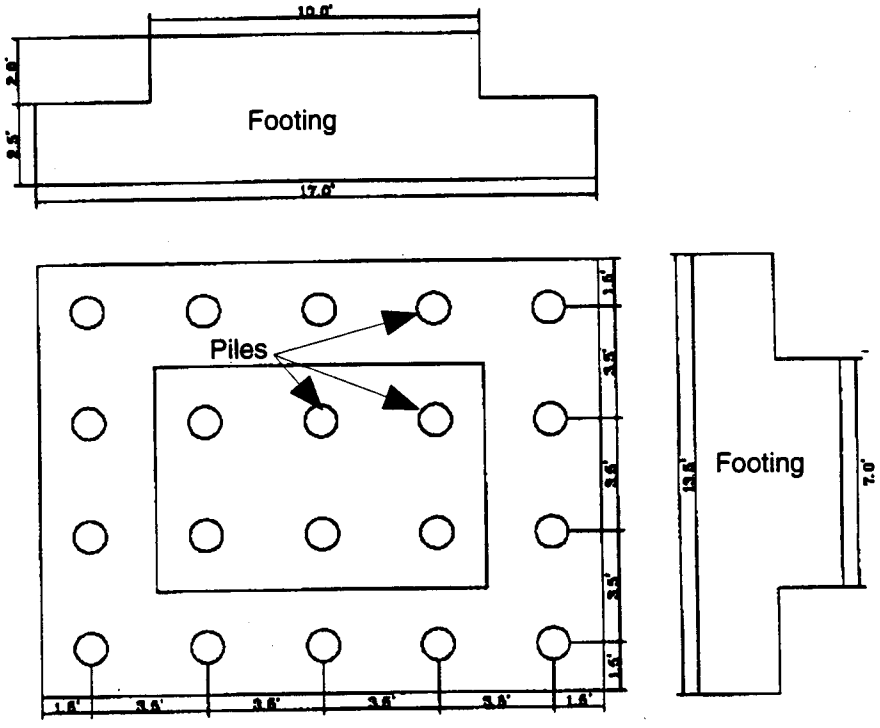

Figure 3.2. Typical Interior Column Pile Group in Seattle Section

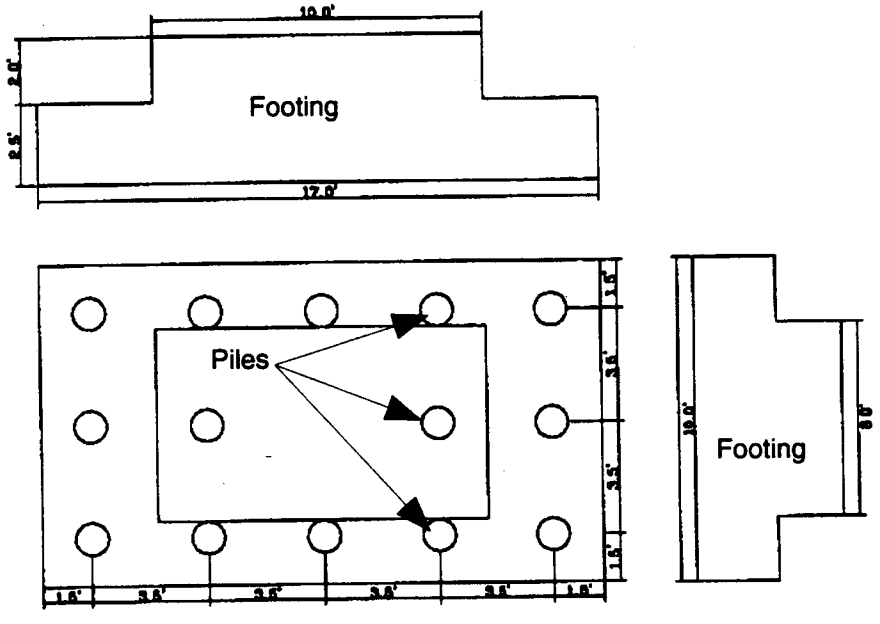

Figure 3.3. Typical Exterior Column Pile Group in Seattle Section

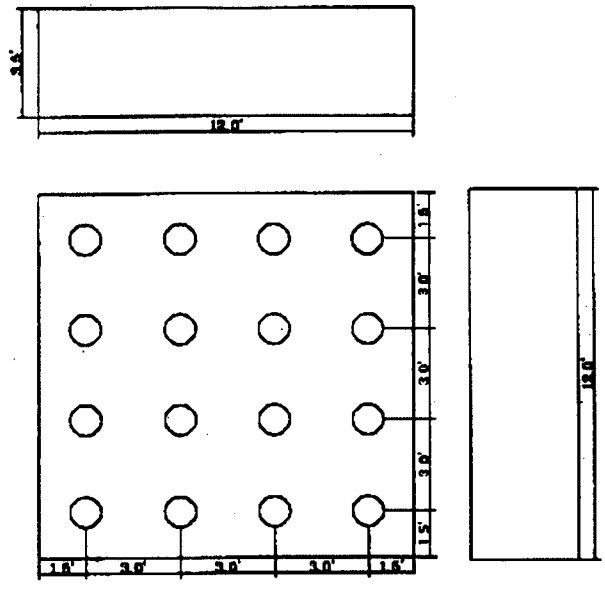

Figure 3.4. Typical Interior Column Pile Group in WSDOT Section

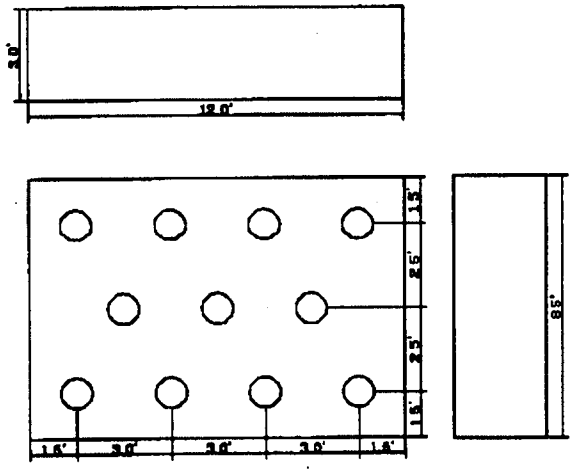

Figure 3.5. Typical Exterior Column Pile Group in WSDOT Section

3.2 PILE DRIVING RECORDS

The archives of the Seattle Engineering Department, the WSDOT Bridge and Structures Office, and the WSDOT Materials Laboratory were searched for information on pile driving characteristics. Pile driving records were only available for Bents 54-115 in the Seattle section and Bents 137-157 in the WSDOT section. However, driving characteristics at these locations, were expected to be representative of those encountered at other locations along the length of the Viaduct.

Pile Lengths

The design records specified that the piles were to be driven to depths sufficient to develop the minimum load bearing capacity required in the design. The available pile driving records indicated that the average pile length in each pile group varied from 8 feet to 62 feet (2.4 m to 18.9 m) in the Seattle section and from 52 to 81 feet (15.9 to 24.7 m) in the WSDOT section. Available test pile driving records indicated easy driving through the waterfront fill and tideflat deposits, with sharp increases in driving resistance within the first few feet of penetration into the underlying glacial till. This behavior is consistent with the characteristics of the soils observed in the subsurface investigation. Given the driving records from a number of test piles, and comparison of pile lengths with subsurface conditions, the piles appear to penetrate about 2 to 5 feet (0.6 m to 1.5 m) into the glacial till.

Final Driving Resistance

Available pile driving records indicated that the average final bearing value at each foundation varied from 55 to 84 tons (49.9 to 76.2 x 10^3 kg) with most values falling around 65 tons (59 x 10^3 kg) in the Seattle section. Pile driving records for the WSDOT section listed only the final blow counts in the last foot of penetration. The average final driving resistance at each foundation varied from 34 to 45 blows/ft, with most of them falling around 40 blows/ft. The average blow count in the Seattle section varied from 48 to 88 blows per foot, with most near 60 blows per foot.

3.3 SUMMARY

Information available in WSDOT and Seattle Engineering Department records, though not complete, allowed the foundation conditions along the length of the Alaskan Way Viaduct to be characterized with reasonable accuracy. In those portions of the Viaduct that are of greatest interest from the standpoint of seismic vulnerability, interior and exterior columns are supported by pile groups connected by common footings. The size, pattern, and number of piles in each group vary with soil, loading, and construction conditions. Records indicated that the piles were driven until a minimum driving resistance was obtained, at which point they were considered capable of adequately supporting the design loads. Because of the high strength and density of the glacial till, the minimum driving resistance was apparently obtained with very little penetration at those locations where the piles were driven into the till. At the very southern end of the Viaduct, the pile resistance is developed primarily in friction. Therefore, most of the piles appear to be acting as end-bearing piles that derive most of their capacity from the upper several feet of the dense glacial till.

CHAPTER 4
GROUND MOTIONS

The seismic response of the Alaskan Way Viaduct depends on the nature of ground shaking transmitted to its foundations by the underlying soils. Evaluation of the seismic vulnerability of the Viaduct requires that its performance be analyzed with respect to a certain reference-level ground motion. The reference-level ground motion used for the design of new structures is referred to as a "design-level" ground motion, as the structure is required to perform satisfactorily when subjected to that motion. Though the Alaskan Way Viaduct is an existing structure, the reference-level ground motion for which its seismic vulnerability was evaluated is referred to in this report as the design-level ground motion. An investigation of the characteristics of design-level ground motions along the length of the Alaskan Way Viaduct was performed. This investigation included a probabilistic seismic hazard analysis and site-specific ground response analyses.

4.1 PROBABILISTIC SEISMIC HAZARD ANALYSIS

In the past 25 years, the use of probabilistic concepts has allowed uncertainties in the size, location, and recurrence rate of earthquakes, and in the variation of ground motion characteristics with earthquake size and location, to be explicitly considered in the evaluation of ground motion characteristics. Probabilistic seismic hazard analysis (PSHA) provides a framework in which these uncertainties can be identified, quantified, and combined in a rational manner to determine the likelihood of various levels of ground shaking from all sources.

In a PSHA, all earthquake sources capable of producing significant ground motions at the site are identified, and their geometries are characterized. The probability distribution of potential rupture locations within each source is also characterized. Next, the seismicity, or temporal distribution of earthquake recurrence, is characterized by a recurrence relationship, which specifies the average rate at which an earthquake of some size will be exceeded. The ground motions produced at the site by earthquakes of any possible size occurring at any possible

point in each source zone are then determined with the use of predictive relationships. The uncertainty inherent in the predictive relationships is also considered in the PSHA. Finally, the uncertainties in earthquake location, earthquake size, and ground motion parameter prediction are combined to obtain the probability that a specific value of the ground motion parameter will be exceeded during a particular time period.

Identification of Earthquake Sources

Tectonic activity in the Pacific Northwest is dominated by the interaction of the Juan de Fuca plate with the North American plate. The Juan de Fuca plate is known to be subducting beneath the Juan de Fuca plate along the Cascadia subduction zone (Figure 4.1) at a rate of about 1.25-1.6 inches/year (3-4 cm/yr) (Chase et al., 1975; Adams, 1984; Nishimura et al., 1984). This process of subduction is thought to control, directly or indirectly, most of the observed earthquake activity in western Washington.

McCrumb et al. (1989) identified five tectonic domains produced by interaction of the Juan de Fuca and North American plates. They are, from west to east, the Juan de Fuca plate, the continental margin, the fore-arc, the volcanic arc, and the back-arc. The Puget Sound basin is part of the fore-arc. Though similar tectonic conditions exist within each of these domains, insufficient information is available at present to characterize each as individual seismic source zones of known seismicity.

Instead, seismic source zones are typically obtained by aggregating observed seismicity into different spatial zones. It is well established that most earthquake activity in western Washington originates in one of two zones: a shallow zone (less than about 15.6 miles (25 km) deep) and a deep zone (sloping downward to the east at depths of 22 to 50 miles (35 to 80 km)). The hypocenters of small earthquakes along an east-west section through Washington State between 1982 and 1986 clearly illustrates the shallow and deep zones (Figure 4.2).

For the seismic hazard analysis used in this investigation, relatively simple seismic source zones similar to those of Ihnen and Hadley (1987) were employed. These source zones were

developed from a corrected catalog of earthquake activity between latitudes 46° N and 49° N and longitudes 121° W and 124° W (Crosson, 1983). The seismic source zones were as follows:

Zone I. A zone of shallow background seismicity that covered the entire 3° by 3° area. All seismicity in this zone was projected to an average depth of 9.4-10 miles (15-16 km).

Zone II. A composite zone that reflected seismicity near the dipping Juan de Fuca plate. The depth of the Zone II source varied from 18.8 to 33.5 miles (30 to 110 km).

Two additional seismic source zones were used for the Alaskan Way Viaduct seismic hazard analysis to investigate the effects of postulated long return-period events on the relatively short-term hazards of interest for this project.

Zone III. A source zone that represented subduction earthquakes produced by the Cascadia subduction zone. This zone was conservatively assigned the same geometry as source Zone II; the actual locations of subduction zone earthquakes may be concentrated farther to the west of the site. The actual locations of subduction earthquakes were intended to be refined if the contribution of Zone III was found to be significant.

Zone IV. A source zone that represented the recently postulated (Bucknam et al., 1992) Seattle fault. This zone was initially assigned a very simple, approximate geometry to determine whether its contribution to the seismic hazard of interest was significant. The geometry was intended to be refined later if the contribution of Zone IV was found to be significant.

Seismicity of Earthquake Sources

Recurrence relationships describing seismicity in Zones I and II were taken from Ihnen and Hadley (1987) on the basis of the findings of Crosson (1983). These recurrence relationships were described by the Gutenberg-Richter law as follows:

Zone I: $\log l_m = 4.98 - 1.02\ M$ Equation 4.1

Zone II: $\log l_m = 3.67 - 0.73\ M$ Equation 4.2

The maximum magnitude earthquake that can be produced by some of the source zones is a matter of scientific debate. In this PSHA, a logic tree approach was used to assign different probabilities to different maximum magnitudes. For the Source Zone I, the maximum magnitude was assumed to be 6.75 (with a weighting factor of 0.25) and 7.0 (with a weighting factor of

0.75). Source Zone II was assigned a maximum magnitude of 7.5, a value for which general agreement exists in the seismology and earthquake engineering communities.

To evaluate the effects of postulated events from the Cascadia subduction zone (Zone III) and the Seattle fault (Zone IV), simple characteristic earthquake models were assigned. Zone III was assumed capable of generating only M = 8.0 (weighting factor of 0.25), M = 8.5 (weighting factor of 0.50), and M = 9.0 (weighting factor of 0.25) earthquakes, with a 600-year return period. Though this return period is consistent with the possible rate of recurrence suggested by recent paleoseismic investigations, it must be regarded as a crude approximation of the actual seismicity. For Zone IV, seismicity was characterized by M = 7.0 (weighting factor 0f 0.25), M = 7.25 (weighting fatter 0f 0.25), and M = 7.5 (weighting fatter 0f 0.50) earthquakes, with a return period of 1,500 years. This return period is simply the midpoint of the 1,000- to 2,000-year range implied by recent studies (Bucknam et al., 1992) and must also be regarded as a crude estimate. For the purpose of a preliminary evaluation of whether Zone III and IV would significantly influence seismic hazards with relatively short return periods, these approximations were considered reasonable.

Prediction of Ground Motion

The effects of strong ground motions on soils and structures is strongly influenced by the amplitude, frequency content, and duration of the motion. Consequently, design-level ground motions for the Alaskan Way Viaduct site were characterized in three ways: by peak horizontal acceleration (PHA), by spectral response ordinates, and by strong motion duration. Different predictive relationships were used for the shallow and deep seismic source zones.

Peak Horizontal Acceleration

Ground motion amplitudes at relatively high frequencies are well characterized by peak accelerations. For the shallow source zones (I and IV), peak horizontal accelerations were predicted by the attenuation relationship of Joyner and Boore (1981). This relationship is based on ground motions measured at sites within 230 miles (370 km) of shallow, magnitude 5.0 to 7.7 earthquakes in western North America. For the deep zones (II and III), the predictive

relationship of Crouse (1991), which includes results from earthquakes in western Washington, was used. This relationship was developed for the Pacific Northwest on the basis of ground motion measurements from sites subjected to deep earthquakes in subduction zone environments in the United States, Japan, Chile, Peru, and Mexico. Because the database for subduction-type earthquakes is much smaller than those for shallower earthquakes, the standard error for this attenuation relationship is relatively large. The effects of this large standard error are significant, as discussed in the presentation of results.

Response Spectrum Ordinates

For the shallow source zones (I and IV), spectral velocity ordinates for 5 percent damping were predicted by the relationship of Joyner and Boore (1982). This relationship was also based on ground motions measured at sites within 230 miles (370 km) of shallow, magnitude 5.0 to 7.7 earthquakes in western North America. Spectral velocity ordinates at 5 percent damping were predicted for the deeper zones (II and III) by the expression of Crouse (1991). This relationship was based on the same data that were used to develop the previously described peak acceleration attenuation relationship. Again, the standard errors in this attenuation relationship are relatively large, since the database for subduction-type events is much smaller than that for other types of earthquakes.

Duration

Strong motion duration was described by the bracketed duration approach of Bolt (1969) using 0.05 g as a threshold acceleration level. The predictive relationship of Chang and Krinitzsky (1977) was used to predict duration as a function of magnitude and distance. Standard errors are not available for the Chang and Krinitzsky predictive relationship.

Probability Computations

Identification and geometric representation of the source zones allow probability distributions of the source-site distance to be computed for each source. Definition of the recurrence relationships allows probability distributions of the earthquake magnitude generated by each source zone to be computed. Definition of the appropriate predictive relationships

allows evaluation of the probability of exceeding a particular value of the ground motion parameter, given specific values of source-site distances and magnitude. Combining all of this information, the average rate of exceedance of a ground motion parameter, y*, will be given by the following:

$$l_{y*} = \sum_{i=1}^{N_S} n_i \int\int P[Y > y^* \mid m, r] f_{Mi}(m) f_{Ri}(r) \, dm \, dr \qquad \text{Equation 4.3}$$

where $\nu_i = 10^{(a_i - b_i m_o)}$, m_o is the minimum magnitude of interest, and N_s is the number of seismic source zones, and $f_{Mi}(m)$ and $f_{Ri}(r)$ are the probability density functions for magnitude and distance, respectively.

The individual components of this equation are, for virtually all realistic PSHAs, sufficiently complicated that the integrals of the preceding expression cannot be evaluated analytically. Consequently, the average exceedance rates were computed by numerical integration. The computed average exceedance rates can be used to compute exceedance probabilities for finite time intervals. Using the Poisson model, the probability of exceeding the ground motion parameter, y*, in a period of time, T, is as follows:

$$P[Y > y^*] = 1 - \exp[-l_y * T] \qquad \text{Equation 4.4}$$

Results of PSHA

The PSHA was used to predict design-level ground motion parameters with 10 percent probabilities of being exceeded in a 50-year period. This level of exceedance, which corresponds to a 475-year return period, is consistent with that specified by current building codes and standards (UBC, NEHRP, AASHTO) and used by WSDOT for the design of new bridge structures.

The PSHA clearly showed that the deep seismic source zone (Zone II) dominates the seismic hazard at the Alaska Way Viaduct site. Primarily because their return periods are much longer than the 50-year design period, the Cascadia Subduction Zone (Zone III) and Seattle Fault

Zone (Zone IV) contribute negligibly to the total seismic hazard. For that reason, refinement of the sources' geometric and recurrence characteristics assumed in the preliminary analyses was not considered to be warranted. The shallow seismic source zone (Zone I) contributes to the seismic hazard, but much less than the deep source zone.

All ground motion parameters were computed for stiff soil outcrop conditions. Therefore, the ground motion amplitude parameters, e.g., peak acceleration and spectral accelerations, were larger than those that would have been computed at the level of the underlying bedrock. The effects of the soil conditions inherent in the PSHA were considered in the subsequent computation of site-specific design-level ground motions.

4.2 DEVELOPMENT OF SITE-SPECIFIC GROUND MOTIONS

The ground motion, parameters obtained from the PSHA were developed from attenuation relationships based on measured response at stiff soil sites. To evaluate the seismic vulnerability of the Alaskan Way Viaduct, it was necessary to develop ground motions that were consistent with this spectrum and the design duration but that applied to the actual subsurface conditions along the length of the Viaduct. Because these soil conditions differed from those in the databases of the attenuation relationships, a multi-step procedure was used to develop site-specific, design-level ground motions.

Generation of Synthetic Stiff Soil Motions

The design-level response spectrum and design-level duration were based on predictive relationships for stiff soil conditions; consequently, they provided parameters from which synthetic stiff soil motions could be generated. These ground motions were generated by the following process.

1. An initial Fourier amplitude spectrum (FAS) with a frequency content similar to that expected of the stiff soil design-level ground motion was developed. The initial FAS was modeled by a Brune spectrum (Brune, 1970; 1971), i.e.,

$$FAS(\omega) = \left[\frac{R_{\theta\phi} F V}{4\pi\rho v_s^3} M_o \frac{\omega^2}{1 - (\omega/\omega_c)^2} \frac{1}{\sqrt{1 + (\omega/\omega_{max})^8}} \right] \left[\frac{e^{-\omega R/2Q(\omega)v_s}}{R} \right] \quad \text{Equation 4.5}$$

where R_{qf} accounts for the radiation pattern, F accounts for the free surface effect, r and v_S are respectively the density and shear wave velocity of the rock, M_O is the seismic moment, w_C and w_{max} are the lower and upper corner frequencies, R is the source-site distance, and Q is the quality factor of the rock. The lower corner frequency w_C, was obtained from the following:

$$\omega_c = \frac{4.9 \times 10^6 v_s}{2\pi} \left(\frac{\Delta\sigma}{M_o}\right)^{1/3} \qquad \text{Equation 4.6}$$

where v_S is in km/sec, M_O is in dyne-in, and Ds is the stress drop. The seismic moment was obtained from the moment magnitude using the relationship

$$M_o = 10^{1.5\,(M_w + 10.7)} \qquad \text{Equation 4.7}$$

Values of the estimated Brune spectrum parameters used to develop the initial FAS are given in Table 4-1.

Table 4-1. Brune spectrum parameters for initial Fourier amplitude spectrum

Parameter	Value	Parameter	Value
R_{qf}	0.55	w_{max}	10 Hz
F	2	R	20 km
r	2.7 g/cc	Q	300
v_S	2.438 km/sec	M_W	7.5
Ds	100 bars		

2. A Fourier phase spectrum (FPS) consistent with the typical shape of earthquake accelerograms and with the design-level duration was developed. In contrast to amplitude spectra, phase spectra have no well-defined structure, so the FPS were obtained by

   a. generating a time history of white noise using a simple random number generator

   b. multiplying the white noise signal by a shaping function consistent with the typical shape of earthquake accelerograms; for these motions the shaping function of Saragoni and Hart (1974) was used

   c. computing the FPS of the shaped white noise acceleragram.

This process was repeated three times, each with a different seed value for the random number generator. Therefore, three different Fourier phase spectra were produced.

3. The FAS and the three FPS developed in the previous steps were combined to produce three initial accelerograms. The response spectra for these accelerograms were then computed.

4. Each computed response spectrum was compared with the design-level stiff soil response spectrum obtained from the PSHA. To improve agreement between the computed and design-level stiff soil spectra, the ordinates of the FAS were multiplied by the ratio of the corresponding design-level spectral ordinate to the computed spectral ordinates.

5. The modified FAS was then combined with the original FPS, and steps 3 and 4 were repeated until the computed motion produced a response spectrum that agreed well with the design-level stiff soil response spectrum. The iterative nature of this approach renders the computed motion relatively insensitive to the initial Brune spectrum parameters (W. Silva, personal communication, 1995). Therefore, the estimated Brune spectrum parameters listed in Table 4-1 are considered reasonable.

The analyses described in steps 4 and 5 were performed with the computer program RASCAL (Silva, 1987). This process produced three accelerograms, each of which was consistent with the design-level stiff soil response spectrum and the design-level duration. Because the design-level stiff soil response spectrum was smooth (a consequence of the PSHA process), the accelerograms had a relatively smoothly varying frequency content. While actual, individual earthquake motions do not exhibit such smooth response spectra and frequency contents, the average values of several actual motions will produce smooth spectra and frequency contents. Therefore, the responses generated by these motions are expected to envelope the range of responses produced by individual actual earthquake motions.

Development of Consistent Bedrock Motions

The stiff soil motions described in the previous section corresponded to the types of stiff soil sites from which the attenuation relationship databases were developed. A review of the literature and discussions with the developer of the attenuation relationship that most strongly influenced the results of the PSHA (C.B. Crouse, personal communication, 1993) showed clearly that the loose, saturated fills along the Alaskan Way Viaduct were significantly different from the soil conditions at the sites from which the attenuation relationships were developed. Thus, to

predict the levels of ground shaking along the Alaska Way Viaduct, it was necessary to develop bedrock motions that were consistent with the design-level stiff soil motions.

Bedrock outcrop motions were obtained by deconvolving the three synthetic stiff soil accelerograms through three different stiff soil profiles intended to represent a range of typical soil conditions similar to those that existed in the attenuation relationship database. The three soil profiles consisted of 20 ft, 30 ft, and 40 ft of stiff clay (PI = 30, v_S = 1200 ft/sec) overlying a semi-infinite bedrock halfspace (v_S = 2500 ft/sec). The one-dimensional ground response analysis program SHAKE (Schnabel, et al., 1972) was used to perform the deconvolution. The resulting motions at the surface of the bedrock are shown in Figures 4.3 and 4.4. Because of the large standard error in the Crouse (1991) attenutation relationship used for Source Zone II in the PSHA, these motions were relatively strong. While a smaller design-level motion could have been produced with different attenuation relationships, the Crouse relationships are considered to be the most accurate available for sites in the Pacific Northwest. No attempt to justify reduction of the standard error was made, the analysis was completed in a straightforward, objective manner. In view of the surprisingly large ground motions recently measured in the Northridge, California, earthquake, and the life safety consequences of a potential failure of the Alaska Way Viaduct, the conservative approach used in this investigation appeared to be appropriate.

Ground Response Analyses

To account for the influence of the variable soil conditions along the alignment of the Viaduct, a series of ground response analyses were performed. The ground response analyses were conducted with the computer program SHAKE (Schnabel et al., 1972). By dividing the subsurface soils into three basic units—waterfront fill, tideflat deposits, and glacial till—and examining the subsurface profile (Figure 2.14), all possible combinations of waterfront fill and tideflat deposit thickness along the Viaduct were identified. Individual ground response analyses for each of these combinations, illustrated in Table 4-2, were performed. For each profile, the waterfront fill and/or tideflat deposit was assumed to be underlain by 200 feet (61 m) of till and

then by bedrock. Each of the 41 combinations shown in Table 4-2 was subjected to all three bedrock motions.

Table 4-2. Combinations of waterfront fill and tideflat deposit thickness used in ground response analyses.

Fill Thickness	Tideflat Deposit Thickness (in feet)										
(feet)	0	10	20	30	40	50	60	70	80	90	100
0											
10	x	x	x	x							
20	x	x	x	x							
30	x	x	x	x							
40	x	x	x	x	x	x					
50	x	x	x		x		x	x	x	x	x
60					x	x	x	x	x	x	x
70					x	x	x	x	x	x	x

The ground response analyses were repeated using the nonlinear ground response analysis program DESRA (Lee and Finn, 1978). Although the soil model parameters for the DESRA program had to be estimated, reasonable agreement with the results of the SHAKE analyses was observed.

Results of Ground Response Analyses

The similarity of the stiffness and damping characteristics of the waterfront fill and tideflat deposits made differences in ground motions for profiles with equally soft soil thicknesses difficult to distinguish. For that reason, the computed ground motions were interpreted in terms of the total thickness of waterfront fill plus tideflat deposit, which is referred

to hereafter as the soft soil thickness. Figures 4.5-4.16 illustrate site-specific, design-level ground surface motions for soft soil thicknesses ranging from 0 to 170 feet (51.9 m).

Examination of Figures 4.5-4.16 illustrates the significant effect of the waterfront fill and tideflat deposits on the amplitude and frequency content of ground surface motions. Because the stiffnesses of these soils are much lower than that of the till, they tend to attenuate high-frequency components of the bedrock motion and amplify low-frequency components.

Peak Horizontal Acceleration

The effect of local soil conditions on peak horizontal acceleration, a parameter commonly associated with the higher frequency components of a ground motion, are illustrated in Figure 4.17. The peak acceleration decreased with increasing soft soil thickness; it ranged from as high as 0.5 g with about 10 ft (3.1 m) of fill (north of Spring Street) to as low as 0.07 g near Massachusetts Street, where the soft soils are quite thick.

Spectral Accelerations

The sizes and shapes of ground surface response spectra are also strongly influenced by local soil conditions. Figure 4.18 shows the variation of average spectral acceleration (5 percent damping) at structural periods of 1.0 and 2.0 sec over the length of the Viaduct. Structural analyses (Eberhard et al., 1995a; 1995b) indicated that the fundamental periods of typical Alaskan Way Viaduct sections are about 1.0 second. Consequently, the largest structural response would be expected near University and Dearborn streets. The spectral acceleration at T = 2.0 sec corresponded to lower frequency components of the ground motion than that at T = 1.0 sec. As a result, the spectral acceleration at T = 2.0 sec generally showed greater amplification at those points along the Viaduct underlain by greater soil thickness.

Shear Stress

The shear stress and shear strain induced in the waterfront fill and tideflat deposits strongly influences their liquefaction potential. Profiles of average cyclic shear stress for various soft soil thicknesses are shown in Figure 4.19. The shear stresses increased with depth moderately in the soft soils, and much more quickly with depth in the underlying till. These

shear stresses were used, as subsequently described in Chapter 6, to characterize seismic loading for the purpose of liquefaction hazard evaluation.

4.3 SUMMARY

Evaluation of the seismic vulnerability of the Alaskan Way Viaduct was based on design-level ground motions that had a 10 percent probability of being exceeded in a 50-year period. On the basis of historical seismicity of the Puget Sound area, the design-level motions represented strong shaking at the site of the Viaduct. The design-level motions were considerably stronger than any motions that the Viaduct has been subjected to since it was constructed.

Site-specific ground response analyses showed that the nature of ground shaking depends strongly on the total thickness of the soft soils that overly the dense glacial till. Because this thickness varies over the length of the Viaduct, ground motion characteristics will vary significantly over the length of the Viaduct.

The ground response analyses also indicated that significant shear stresses and shear strains will be induced in the waterfront fill and tideflat deposits. The level of cyclic shear stresses and strains strongly influences the generation of excess porewater pressures in cohesionless soils, a phenomenon that is considered in detail in Chapter 6.

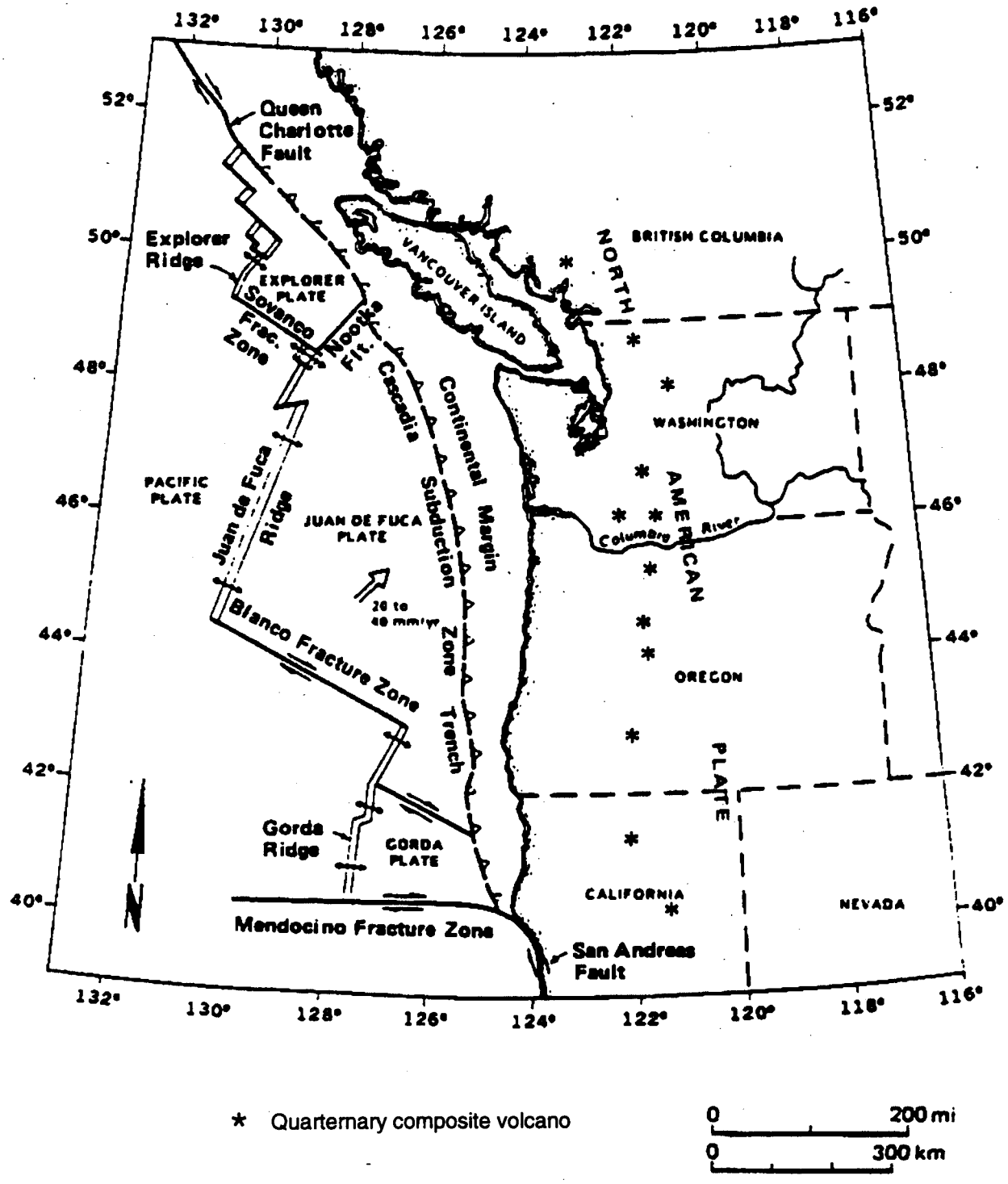

Figure 4.1. Geometry of Tectonic Plates in the Pacific Northwest (The Juan De Fuca Plate is subducting beneath the North American Plate beneath the coasts of Washington and Oregon) (after McCrumb et al., 1989)

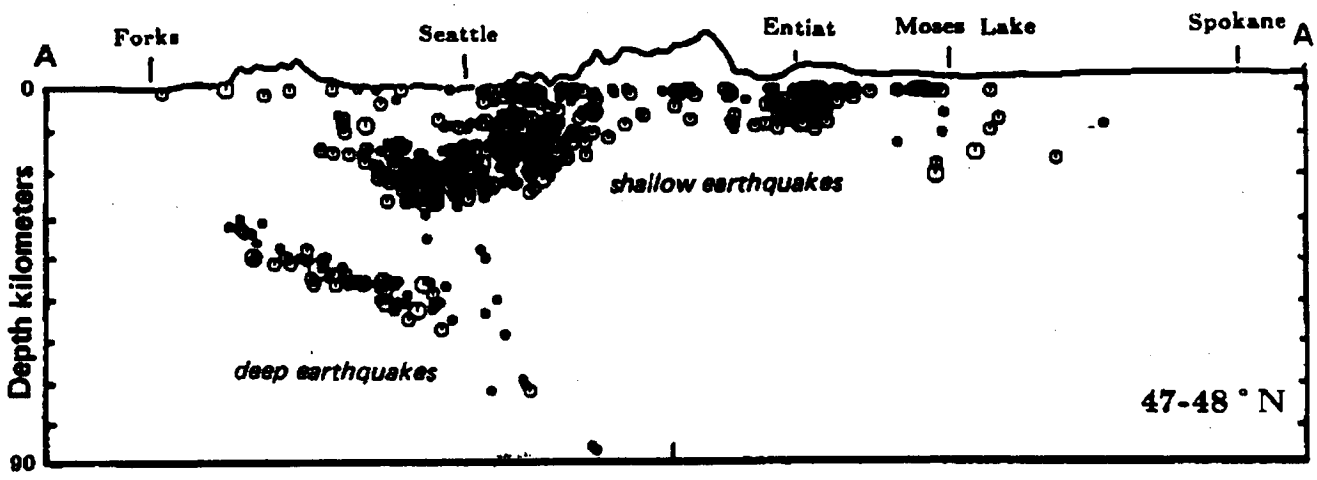

Figure 4.2. Hypocenters of Small Earthquakes between 1982 and 1986 (After Noson et al., 1988)

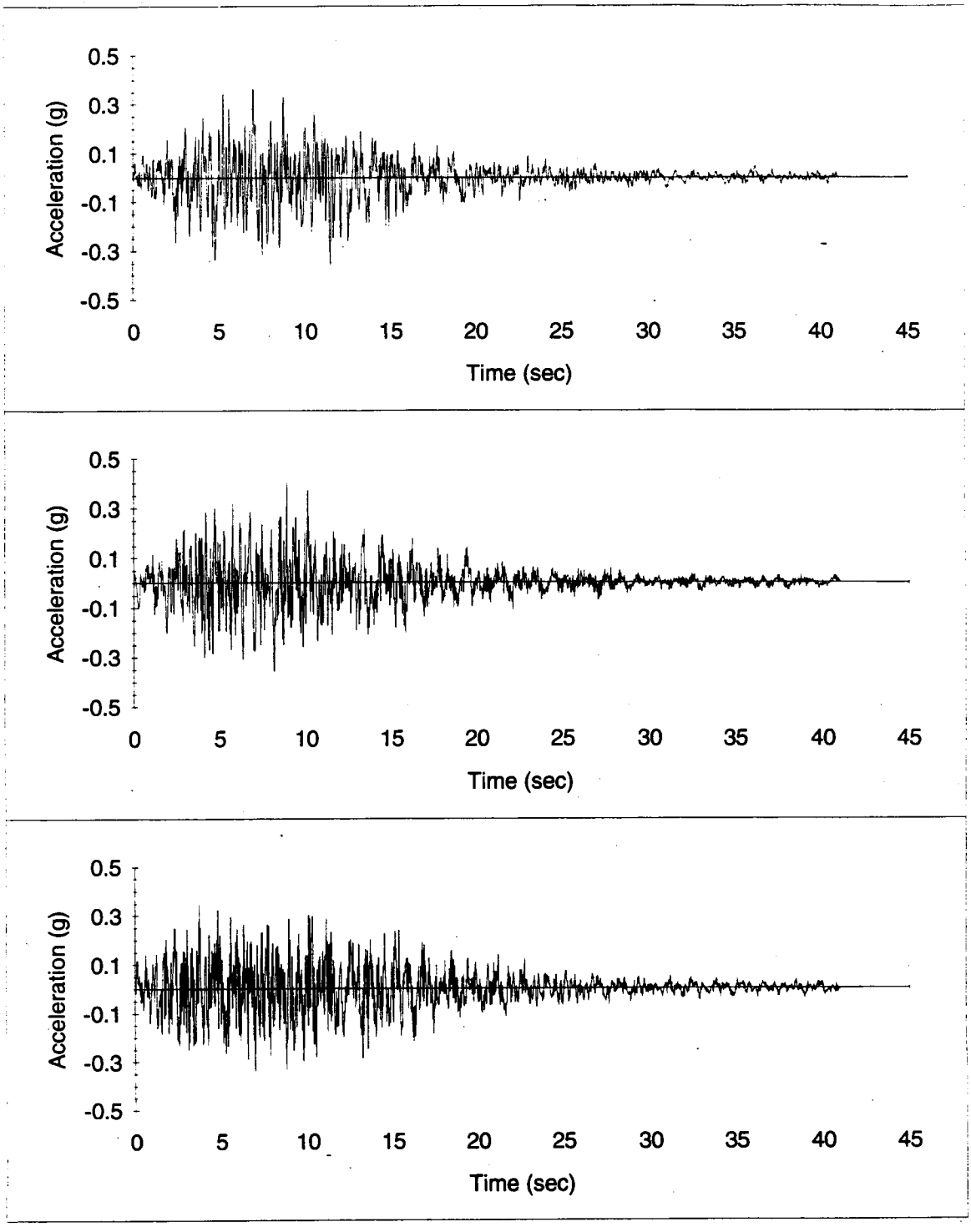

Figure 4.3. Bedrock Outcrop Motions from PSHA and Deconvolution Analyses

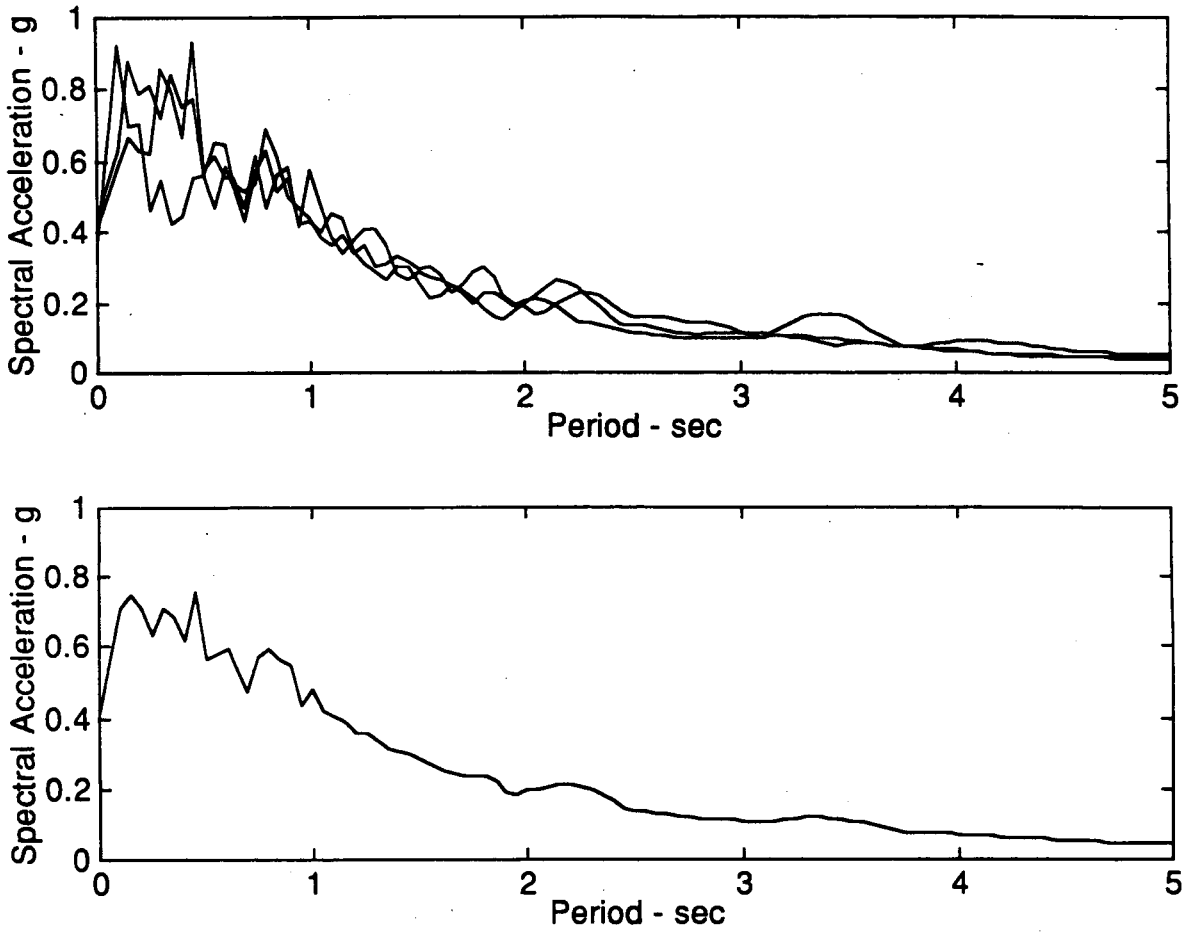

Figure 4.4. Response Spectra (5% damping) for Bedrock Outcrop Motions: (a) Individual Motions, and (b) Average of Individual Motions.

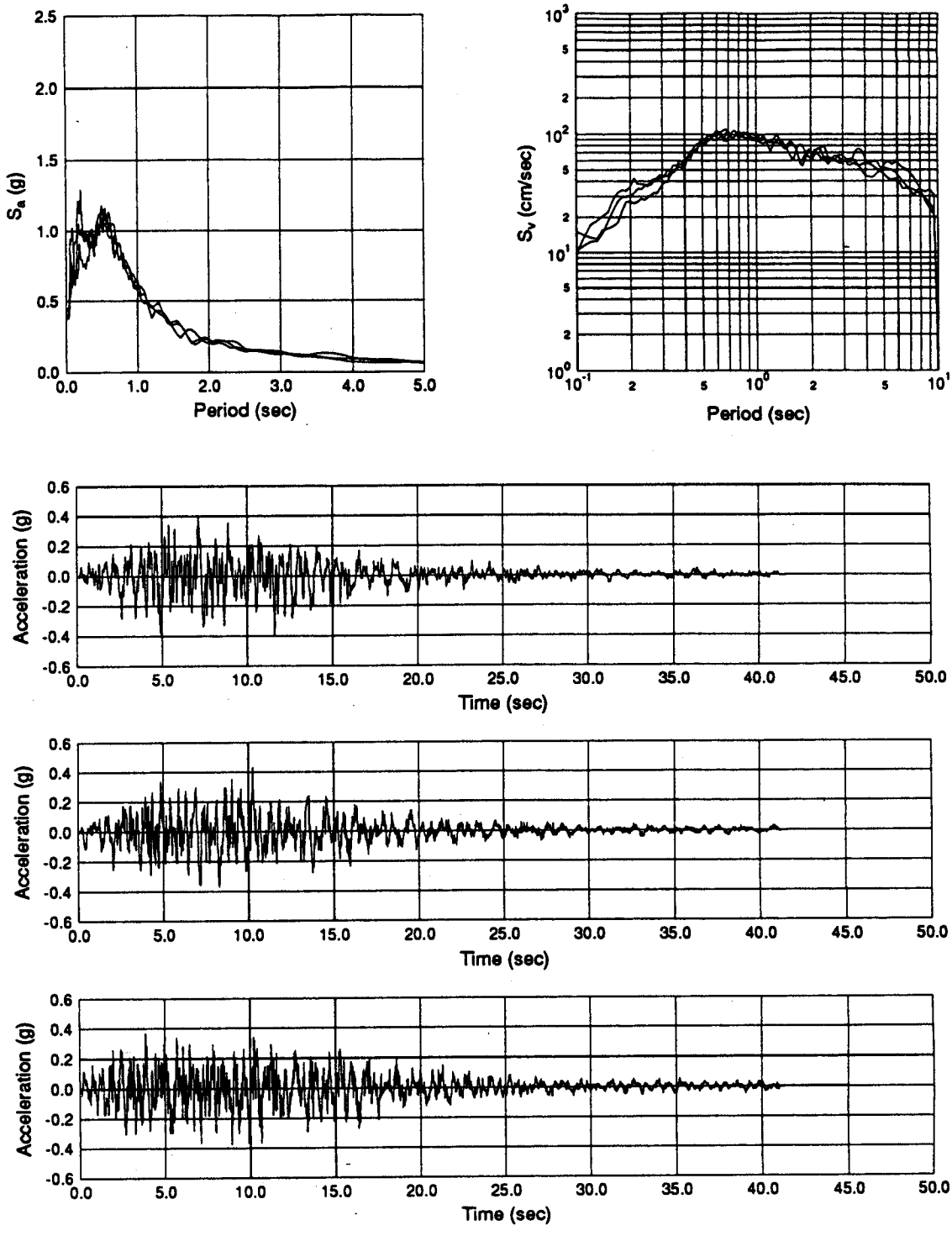

Figure 4.5. Ground Surface Response Spectra and accelerograms for Soft Soil Thickness of 0 Ft.

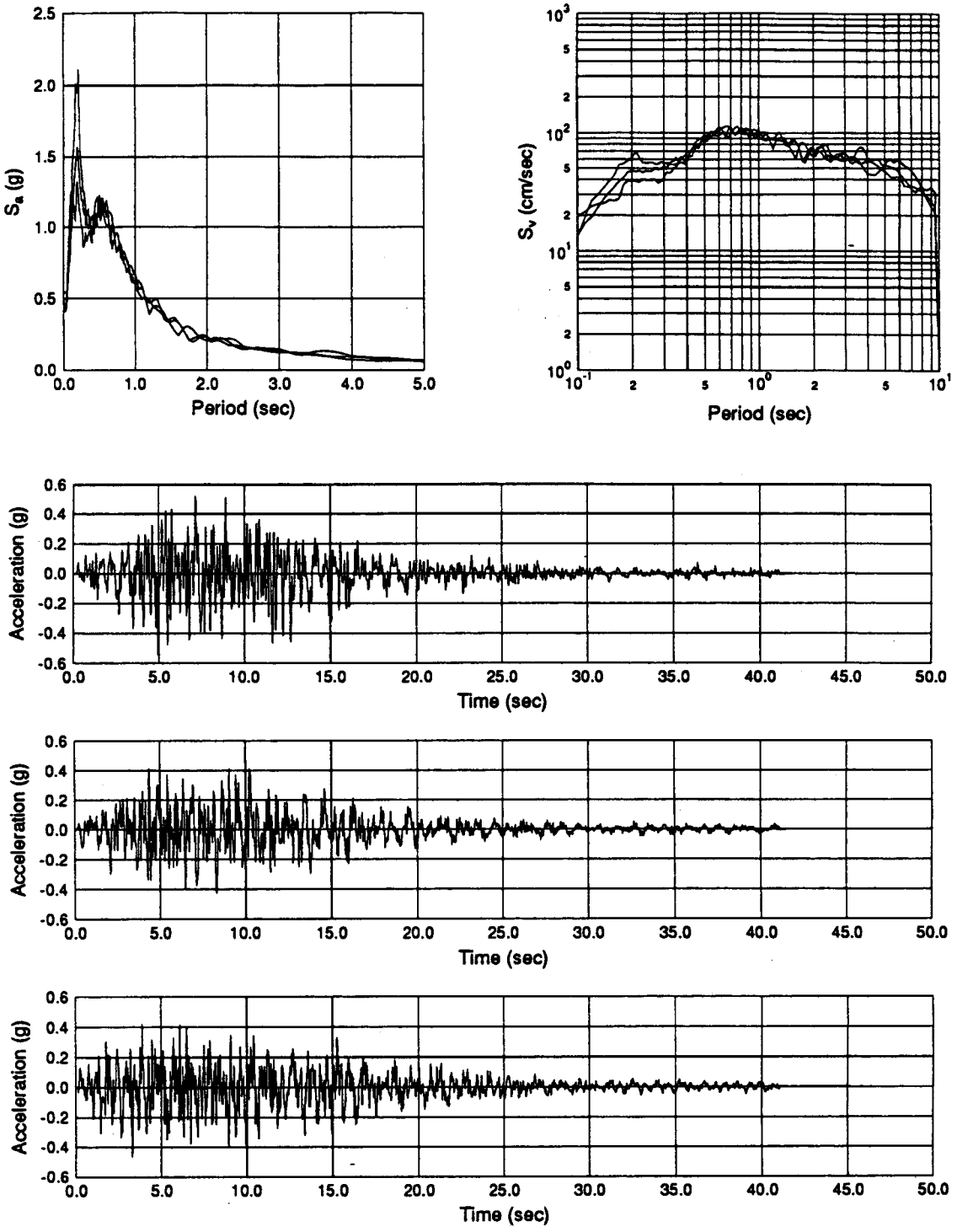

Figure 4.6. Ground Surface Response Spectra and accelerograms for Soft Soil Thickness of 10 Ft.

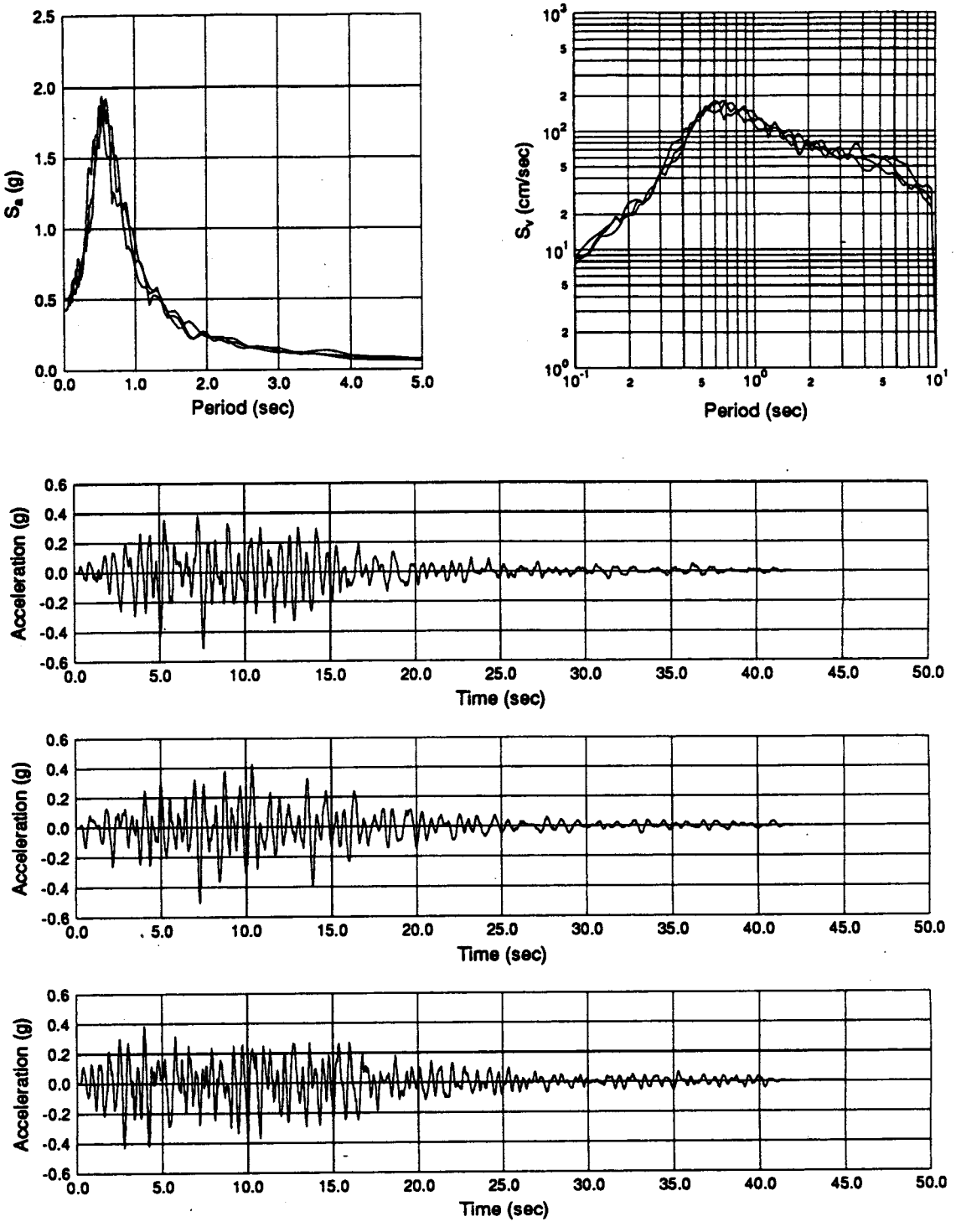

Figure 4.7. Ground Surface Response Spectra and accelerograms for Soft Soil Thickness of 20 Ft.

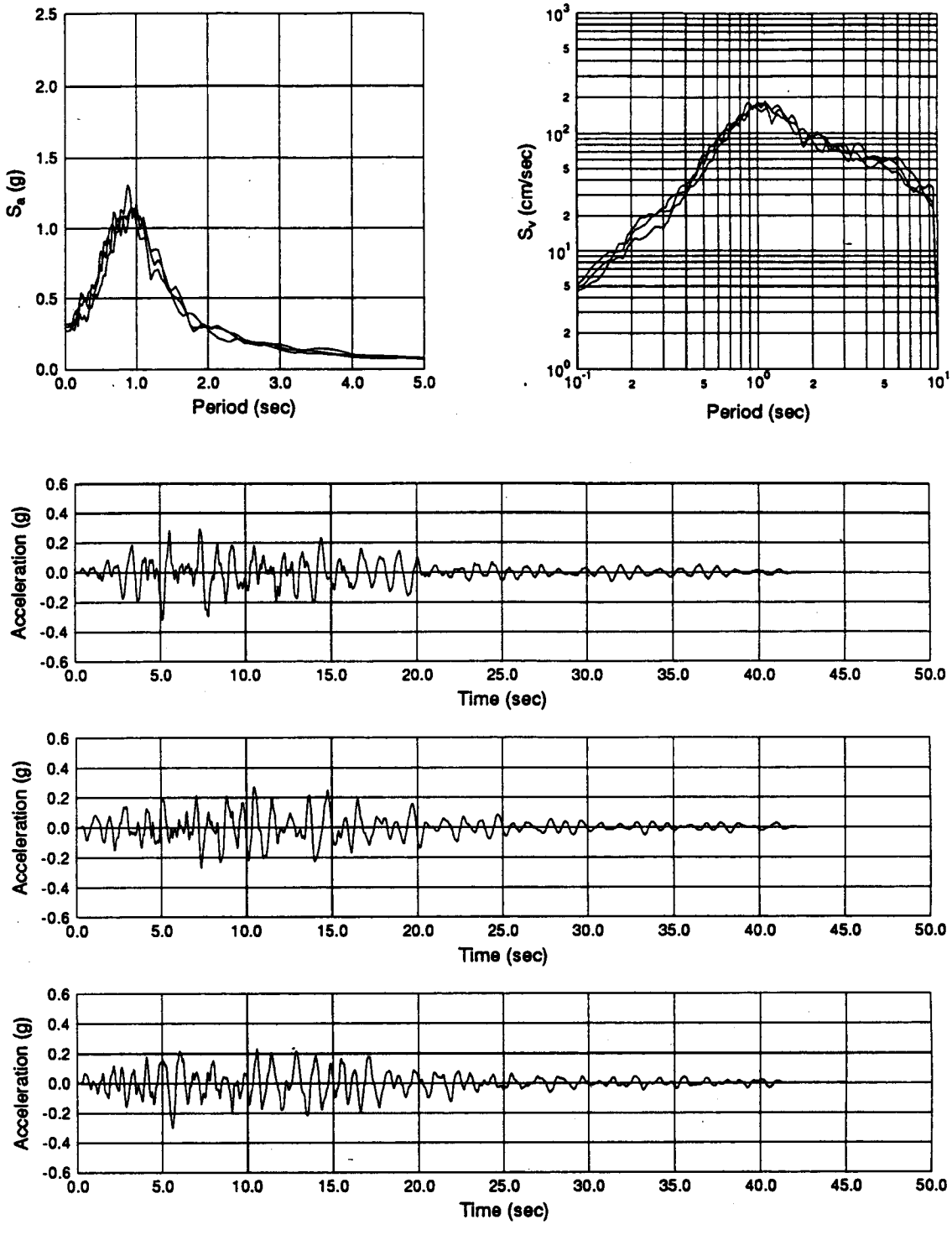

Figure 4.8. Ground Surface Response Spectra and accelerograms for Soft Soil Thickness of 30 Ft.

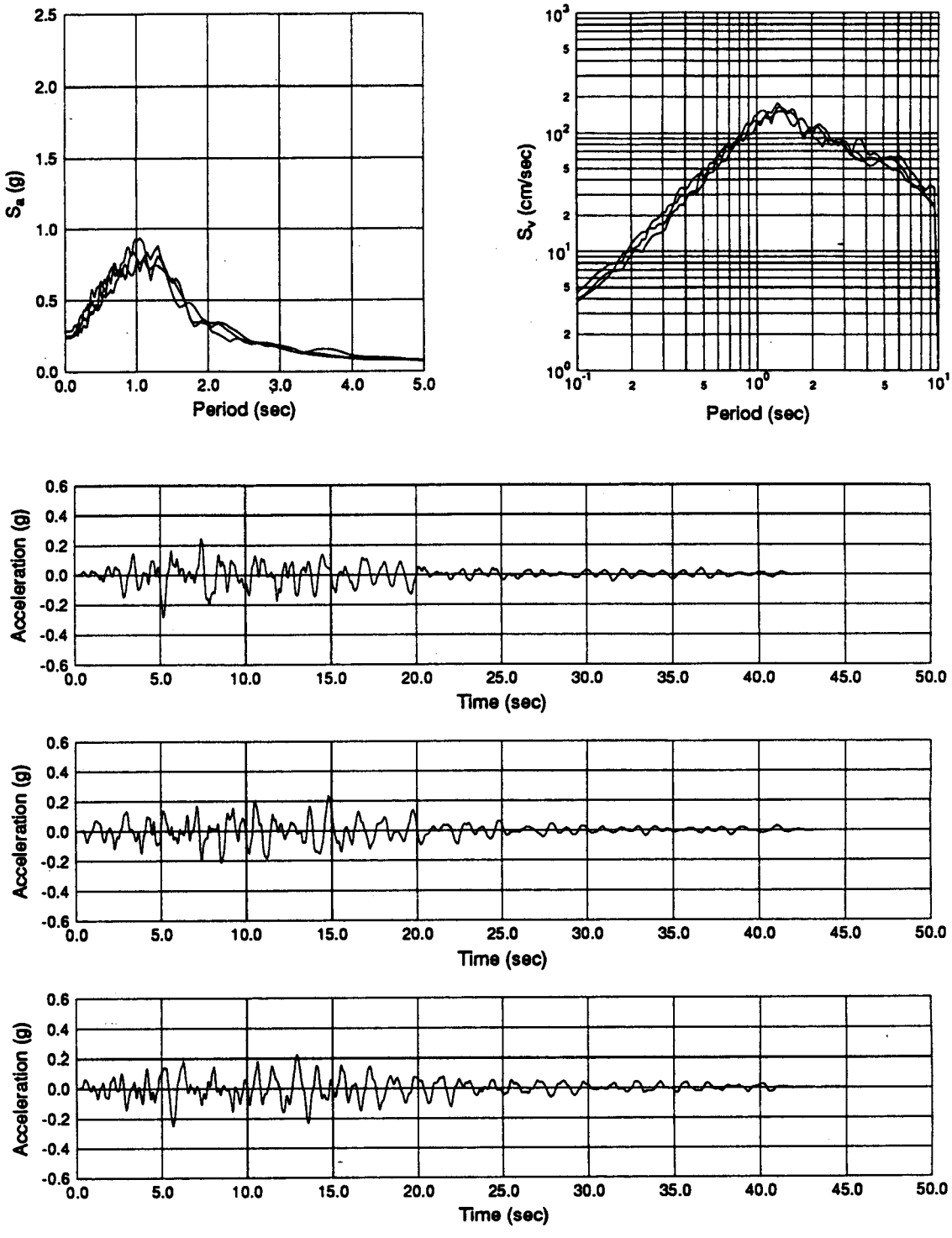

Figure 4.9. Ground Surface Response Spectra and accelerograms for Soft Soil Thickness of 40 Ft.

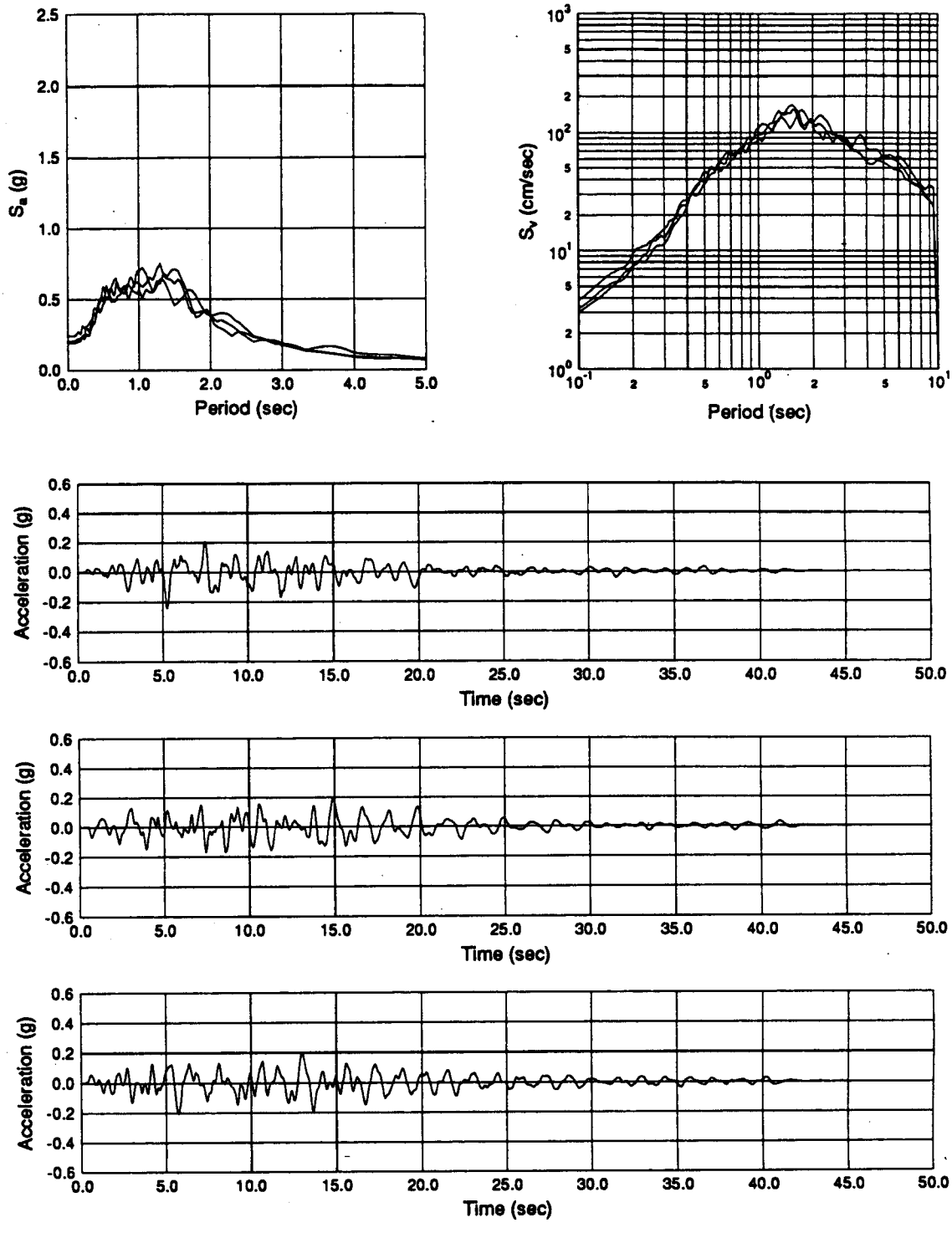

Figure 4.10. Ground Surface Response Spectra and accelerograms for Soft Soil Thickness of 50 Ft.

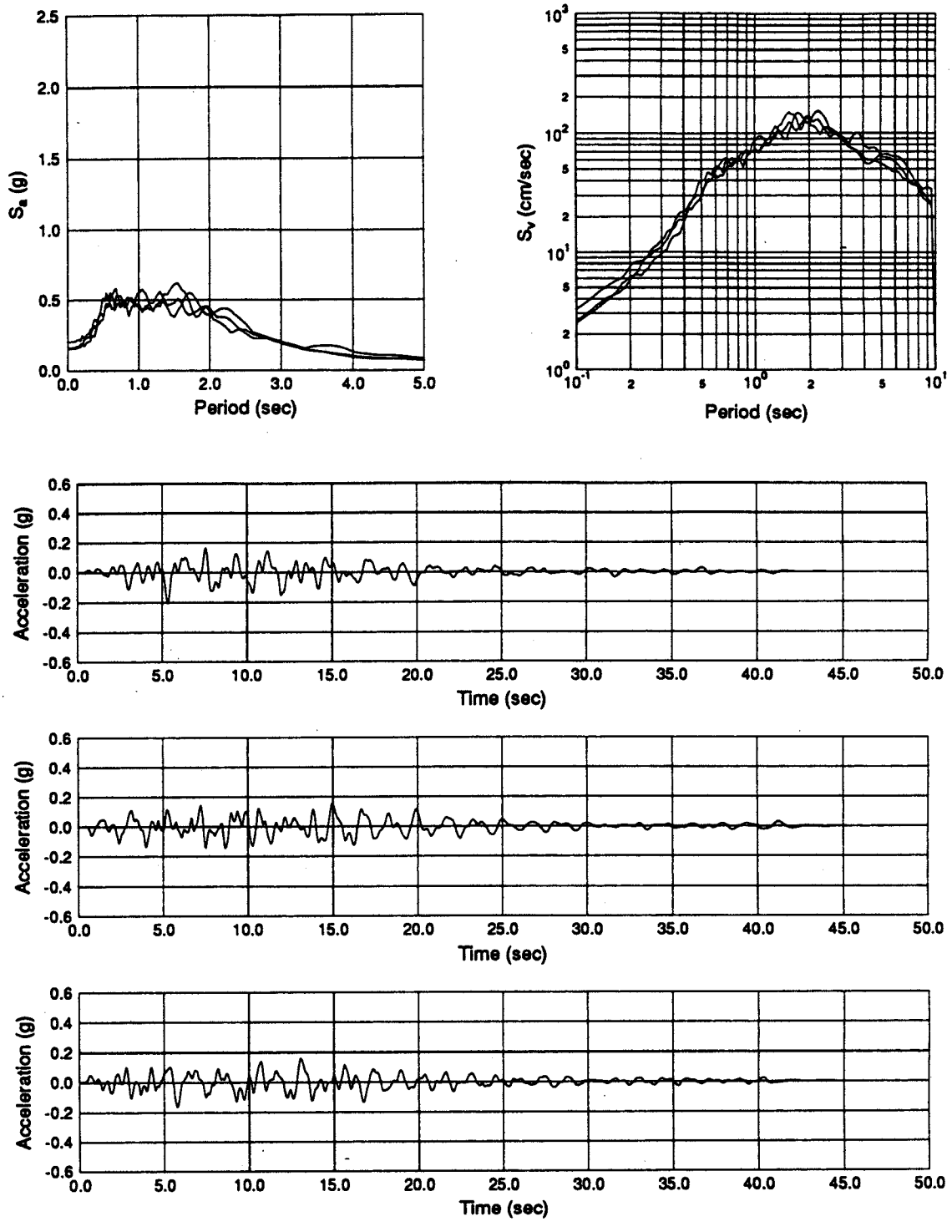

Figure 4.11. Ground Surface Response Spectra and accelerograms for Soft Soil Thickness of 60 Ft.

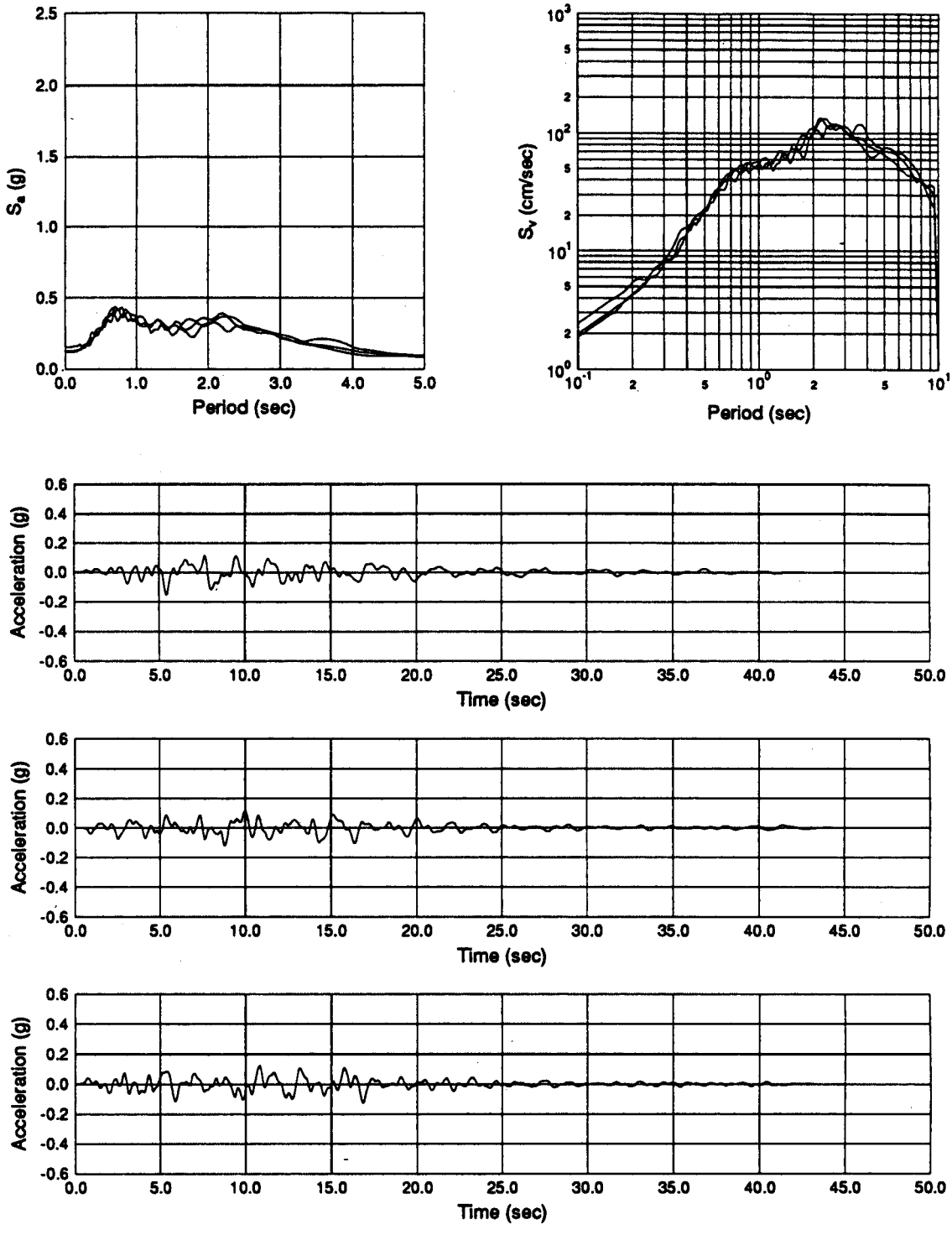

Figure 4.12. Ground Surface Response Spectra and accelerograms for Soft Soil Thickness of 80 Ft.

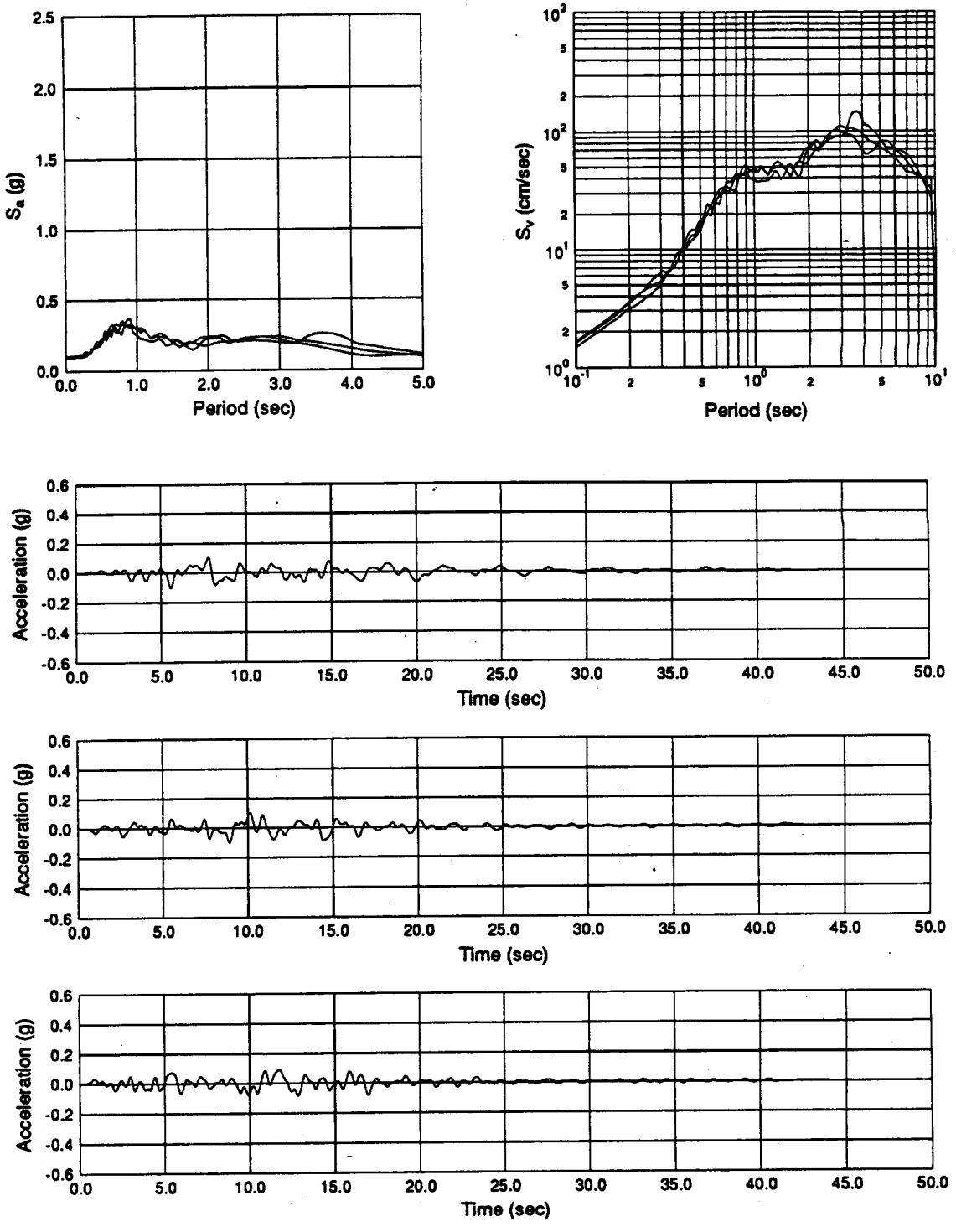

Figure 4.13. Ground Surface Response Spectra and accelerograms for Soft Soil Thickness of 100 Ft.

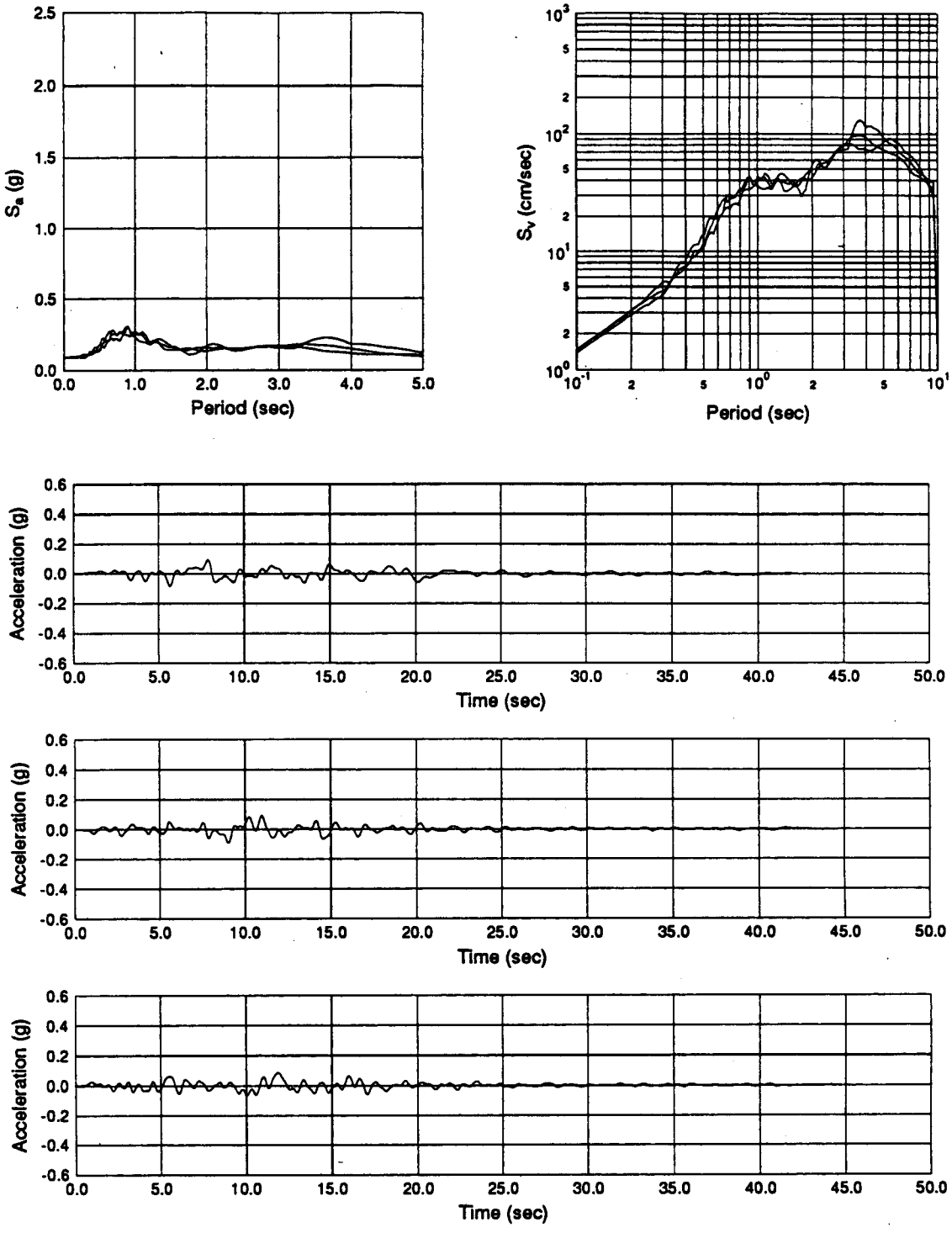

Figure 4.14. Ground Surface Response Spectra and accelerograms for Soft Soil Thickness of 120 Ft.

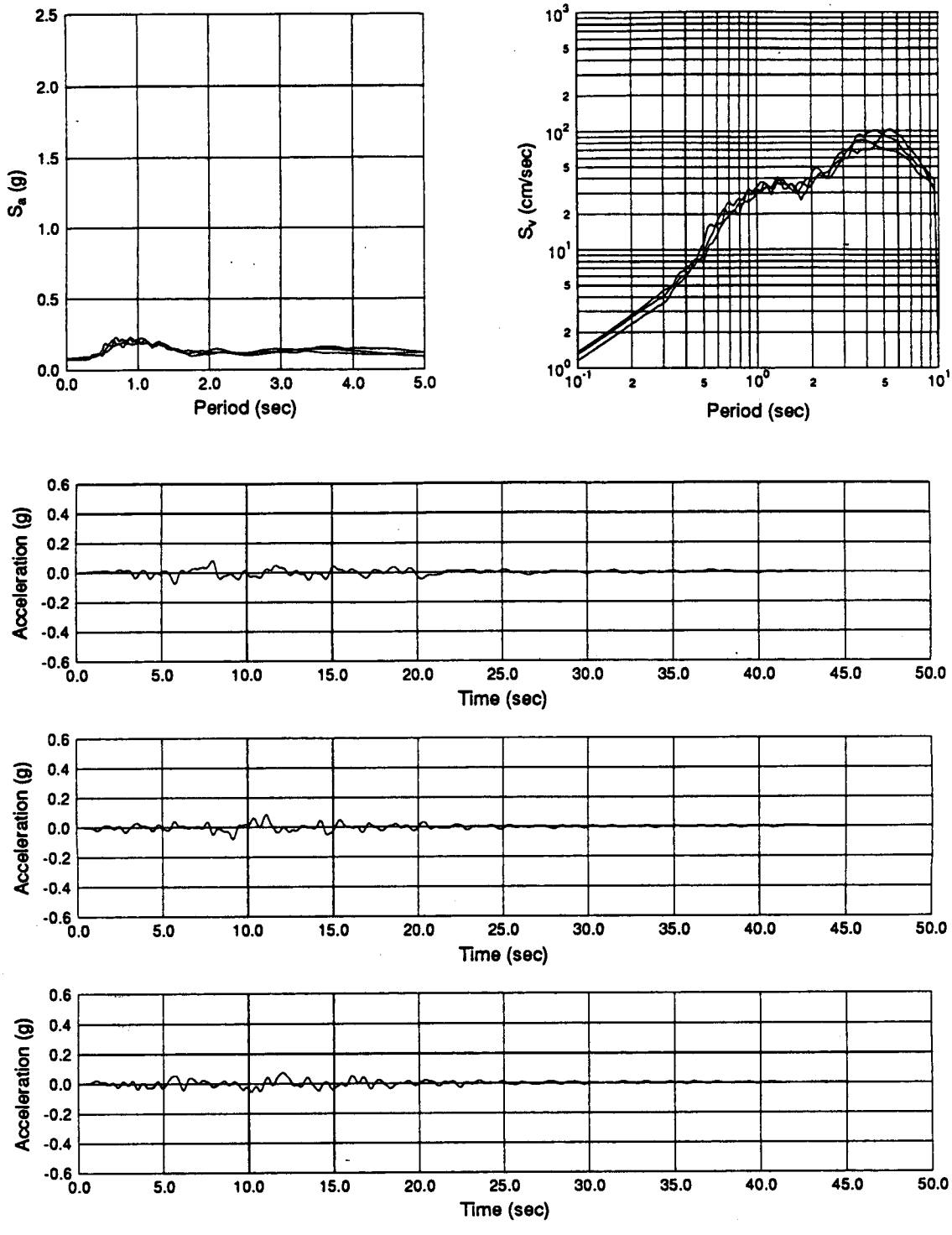

Figure 4.15. Ground Surface Response Spectra and accelerograms for Soft Soil Thickness of 140 Ft.

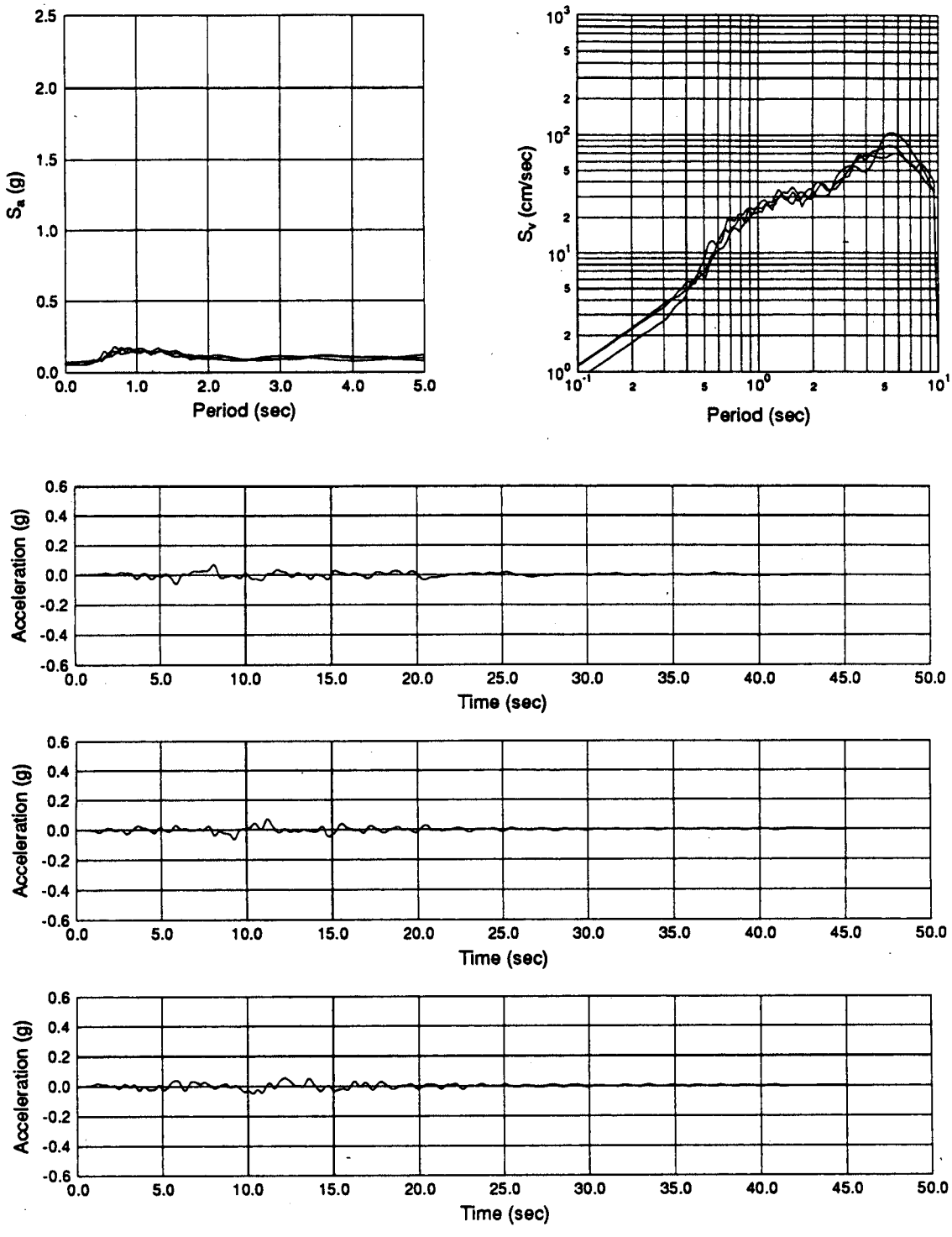

Figure 4.16. Ground Surface Response Spectra and accelerograms for Soft Soil Thickness of 170 Ft.

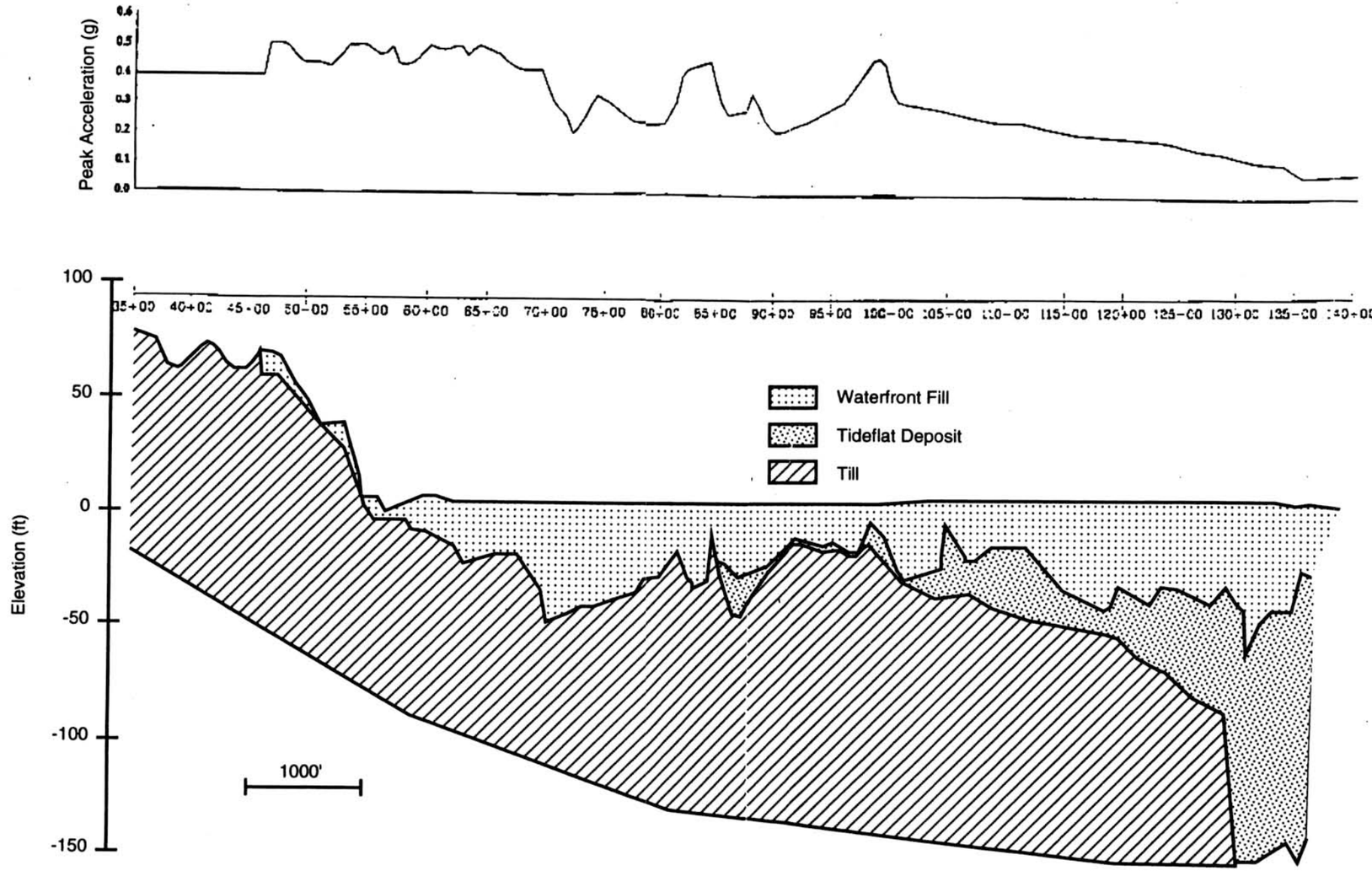

Figure 4.17. Variation of Computed Peak Ground Surface Acceleration along the Length of the Alaskan Way Viaduct

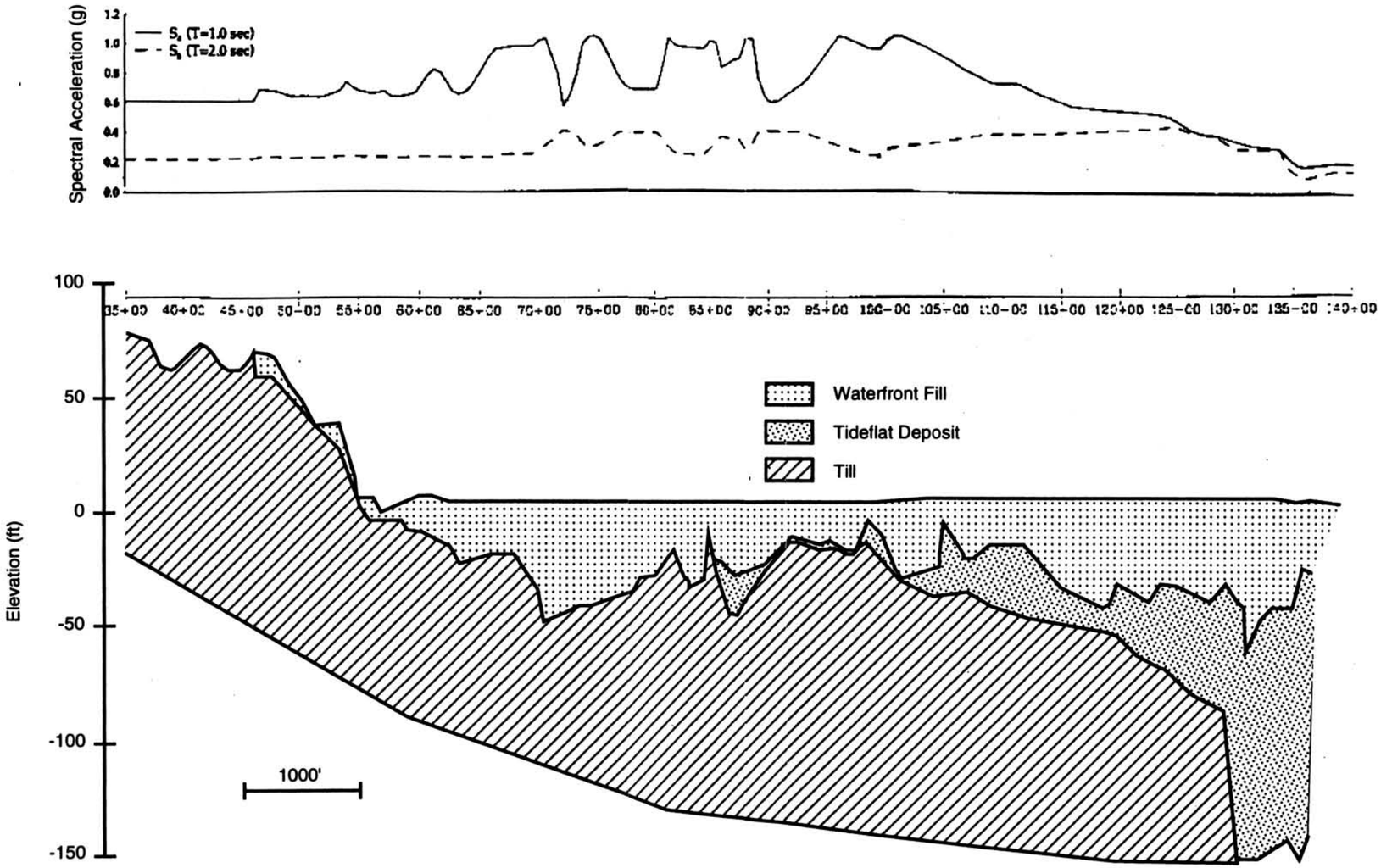

Figure 4.18. Variation of Computed Spectral Acceleration for T = 1.0 Sec and T = 2.0 Sec along the Length of the Alaskan Way Viaduct

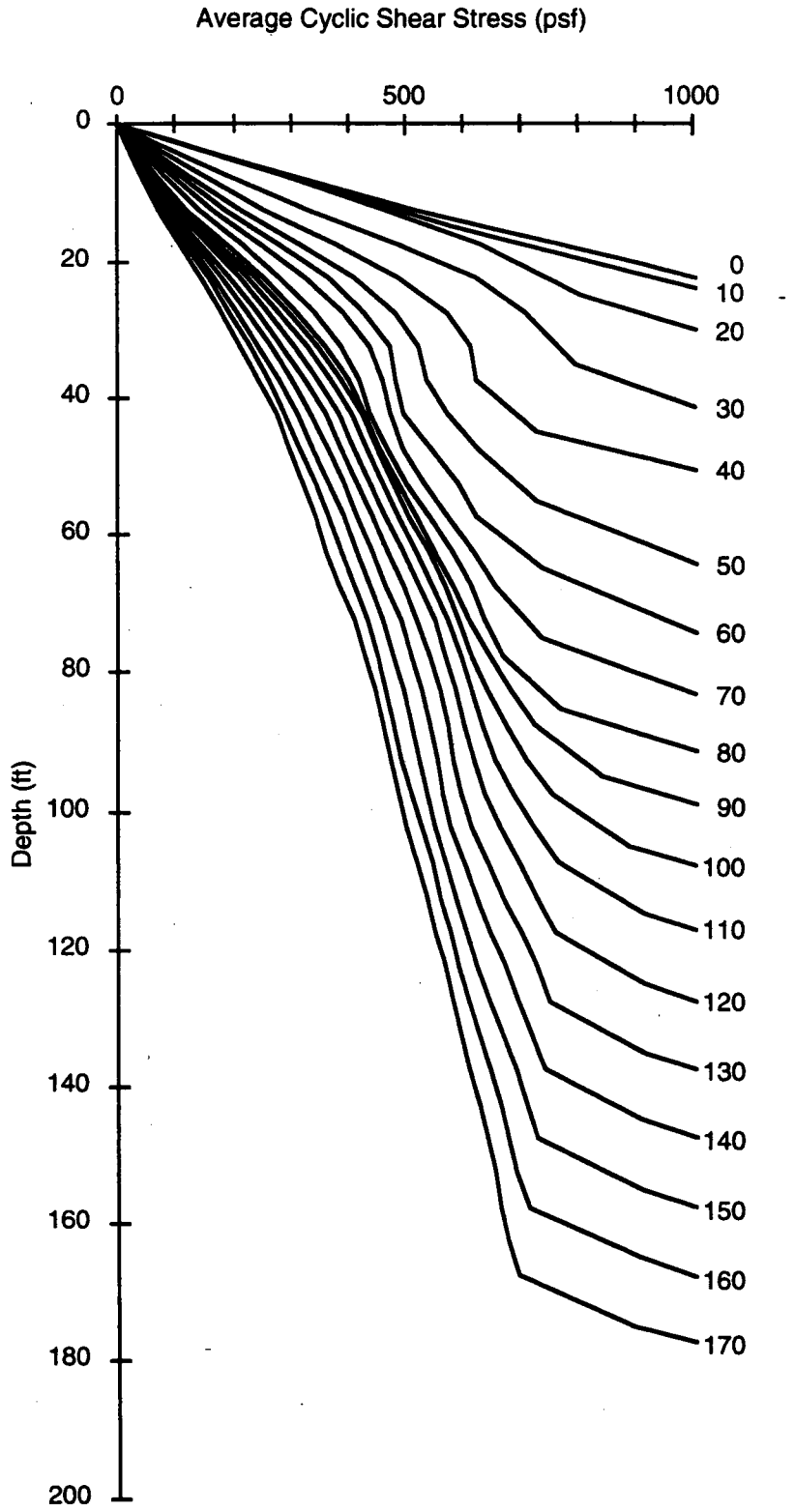

Figure 4.19. Variation of Computed Average Cyclic Shear Stress with Depth for Various Soft Soil Thicknesses

CHAPTER 5
FOUNDATION RESPONSE CHARACTERISTICS

5.1 MODES OF DEFORMATION

The dynamic response of a structure is strongly influenced by the interaction of the structure and the soil on which it is supported. That interaction takes place through the foundations of the structure, and evaluation of that interaction requires knowledge of the stiffness and damping characteristics of the foundation. Dynamic pile group stiffness and damping coefficients were required for dynamic analyses of the Alaskan Way Viaduct superstructure. Researchers evaluating the structural response of the bridge performed detailed analyses of a typical WSDOT section (which extended from Bents 151-154) and a Seattle section (from Bents 106-109). The stiffness and damping coefficients were computed for the foundations at these typical sections.

The finite element model used for the typical section superstructure contained nodes at the centers of the footings; consequently, the stiffness and damping coefficients were computed with respect to those points. The mass of each footing was included in the finite element model of the superstructure, so the foundation stiffness and damping coefficients were calculated with the assumption of a weightless footing. Six degrees of freedom exist for a rigid footing: translational movements in the vertical and two orthogonal horizontal directions, and rotation about the vertical and two orthogonal horizontal axes. Horizontal translation is often referred to as "swaying." Rotation about a horizontal axis is called "rocking," and rotation about the vertical axis is referred to as "torsion." The stiffness and damping matrices are diagonal except for terms caused by coupling between swaying in the x-direction and rocking about the y-axis, and between swaying in the y-direction and rocking about the x-axis. The result is eight independent terms in the stiffness and damping matrices.

5.2 METHOD OF ANALYSIS

Determination of stiffness and damping matrices was accomplished with the computer program DYNA4, developed at the University of Western Ontario, Canada (Novak et al. 1993). DYNA4 is intended for the dynamic response analysis of various types of foundations under a variety of loading conditions, including earthquake loading. DYNA4 is frequently used for evaluation of foundation stiffness and damping characteristics; its use in this regard was recommended by a WSDOT-sponsored study of seismic design of bridge foundations (ref). The theory upon which DYNA4 is based (Novak and Aboul-Ella, 1978a, 1978b) assumes linear elastic material, with the soil characterized by shear wave velocity, unit weight, Poisson's ratio, and material damping. Material damping is assumed to be hysteretic and frequency independent. The pile and the soil profile considered for the east foundation of Bent 152 are shown in Figure 5.1.

Sources of Stiffness and Damping

The interaction of a pile group with an embedded footing and the surrounding soil is a complicated problem. Both stiffness and damping may be provided by different physical mechanisms. The total stiffness of the pile group includes the stiffness provided by the piles and that provided by the embedded footing. The total damping includes hysteretic and radiation damping from the soil, and material damping from the piles themselves.

Dynamic pile load tests were planned at the beginning of this investigation. However, DYNA4 analyses showed that a considerable portion of the swaying stiffness of the Alaskan Way Viaduct foundations was provided by the footings rather than the piles themselves. Because of this observation, and because the dynamic load tests would have yielded more information about the surficial soils than the deeper soils that are actually providing lateral resistance to the Alaskan Way Viaduct piles, dynamic load tests were not considered cost effective and were not performed.

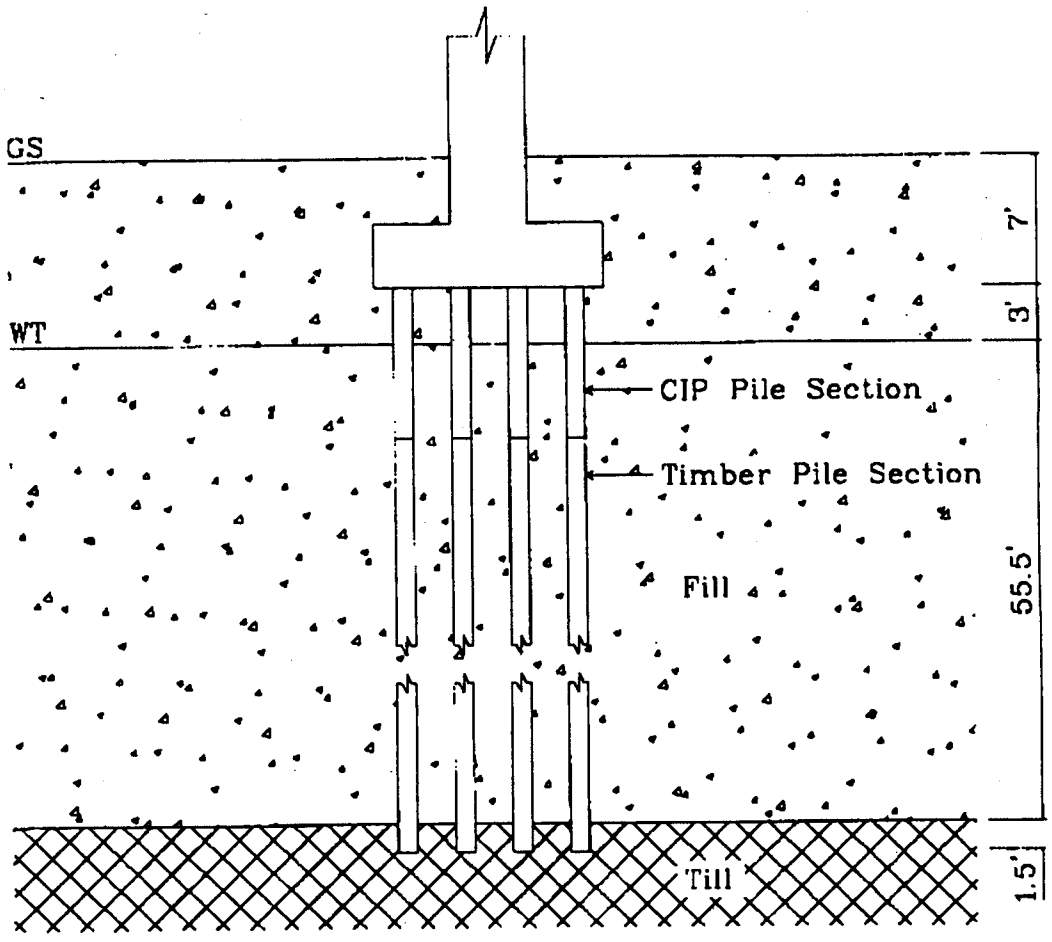

Figure 5.1. Foundation and Soil Profile Used for Foundation Stiffness and Damping Analyses

Effects of Ground Motion Frequency

Pile group stiffness and damping characteristics generally vary with the frequency of the input motion. However, the finite element model used for the analysis of Alaskan Way Viaduct superstructure required stiffness and damping coefficients that were independent of frequency. Therefore, these coefficients had to be determined at a frequency representative of that at which the primary response of the structure was expected. To estimate this frequency, a typical Viaduct section was analyzed under the assumptions of fixed and then pinned conditions at the foundation level; the fundamental periods were found to be 0.9 sec for the fixed case and 2.0 sec for the pinned case (Eberhard et al., 1995a). Because the actual foundations were assumed to be much closer to fixed than to pinned, the stiffness and damping coefficients were computed at a frequency of 1 Hz. Subsequent structural analyses verified the accuracy of this assumption.

Pile Group Interaction

Pile-soil-pile interaction can also influence the behavior of pile groups. Pile-soil-pile interaction includes the effects of the displacement of each pile within a group on the displacements of all of the other piles in the group. Its analysis generally reduces the pile group stiffness to a value below that obtained by the summation of individual pile stiffnesses. This effect is more significant in groups with closely spaced piles, and DYNA4 provides an option to consider the group interaction. A study conducted by Dames & Moore for the WSDOT (Dames & Moore, 1993) suggested that a previous version of the DYNA4 program (DYNA3, 1991) produced stiffnesses that were much lower than the observed experimental values when the interaction option was used. However, the soil properties used in the present analyses were obtained from samples located far enough from the foundations that they were not influenced by pile driving. Consequently, the reduction in stiffness due to pile-soil-pile interaction was expected to be compensated for by the effects of pile driving-induced densification. Given these observations, the analyses were based on soil properties from measurements taken away from the zone influenced by pile driving densification and without use of the interaction option.

Effects of Soil Nonlinearity

Soils are well known as nonlinear materials, and the nonlinear load-deformation behavior of foundations that rely on the mobilization of soil strength is well established. The nonlinear behavior of laterally loaded piles has been an important issue in the design of offshore structures as well as bridges. DYNA4, however, like other dynamic foundation analyses, treats the soil as a linear elastic material. To approximate the effects of nonlinear soil behavior, the following approach was taken:

1. A set of static, nonlinear pile analyses was performed using the computer program COM625 (Kramer and Won, 1987). COM625 is a modified version of the commonly used program COM624 , but the modifications had no influence on the problem analyzed here. The piles were assumed to be fixed against rotation at the pile/pile cap connection, and p-y curves were obtained using the hyperbolic tangent method (O'Neill and Murchison). The analyses were performed for a series of lateral loads applied at the level of the base of the pile cap.

2. The pile deflections and deflection-compatible soil moduli obtained from the iterative COM625 solution were recorded for each lateral load level.

3. Modulus reduction factors, defined as the ratio of the soil modulus at a particular pile head deflection and the initial soil modulus, were computed for various depths and pile head deflections.

4. The computed modulus reduction factors were applied to the maximum shear moduli obtained from the subsurface investigation to obtain moduli for the DYNA4 analyses.

These reduction factors were also used, along with the Seed and Idriss (1970) modulus reduction and damping curves for sand, to estimate the damping ratios at various depths for the DYNA4 analyses. Consequently, the DYNA4 results were expressed in terms of total translational displacement of the pile cap.

5.3 RESULTS OF ANALYSES

The eight independent stiffness and damping coefficients for the foundations at the WSDOT and Seattle sections are tabulated in Table 5.1 through Table 5.9. Stiffness and damping coefficients were calculated for a range of 0 to 7 inches of total translational displacement of the footing. As expected, the stiffness coefficients decreased as the footing deflection increased because of the reduction in the shear moduli values. Damping coefficients,

however, increased initially and then showed a slight decrease. Damping coefficients are functions of both shear moduli and hysteretic material damping, and initially the increase in hysteretic material damping over-compensated for the reduction because of the decrease in the shear moduli. However, this process reversed as the footing deflection increased.

The stiffness and damping coefficients at the interior column foundations were about 30 percent higher than those at the exterior column foundations. Further, for the typical sections considered, the Seattle section stiffness coefficients were about 30 percent higher and damping coefficients were about 80 percent higher than those at the WSDOT section. The stiffness and damping coefficients were similar in the longitudinal and transverse direction of the Viaduct for the translational degrees of freedom, but they differed for the rotational degrees of freedom. In general, the footings were longer and had more piles per row in the transverse direction than in the longitudinal direction, and this resulted in larger rotational stiffness and damping coefficients about the longitudinal direction, of the viaduct than those about the transverse direction.

Structural analyses using the stiffnesses and damping coefficients developed in this analyses indicated that the response of the superstructure was close to that observed assuming fixed conditions at the foundations.

The eight independent stiffness and damping coefficients for the foundations at the WSDOT and Seattle sections are tabulated in Table 5.1-5.9.

5.4 SUMMARY

Foundation dynamics analyses were performed to estimate foundation stiffness and damping characteristics for the pile group foundations that support the Alaskan Way Viaduct. The analyses were based on the site-specific soil conditions described in Chapter 2 and on the actual foundation conditions described in Chapter 3. The effects of loading frequency and soil nonlinearity were approximated in a rational manner. Structural analyses of the typical sections were conducted with three different foundation conditions: pinned at the foundation level, fixed at the foundation level, and using the stiffness and damping coefficients developed in this analysis. The structural response of the Alaskan Way Viaduct using the stiffness and damping

coefficients developed in this analysis were found to be similar to those observed under the assumption of a fixed condition at the foundation level.

Table 5.1 Stiffness and Damping Coefficient for the East Column at Bent 106

Horizontal Disp. at Pile Cap (in)	0.0	0.1	0.2	0.5	1.0	1.5	2.0	2.5	3.0	3.5	4.0	4.5	5.0	6.0	7.0
Stiffness Coefficients															
Horizontal Translation (X) (lb/ft)	1.31E+08	1.30E+08	1.27E+08	1.11E+08	8.67E+07	6.92E+07	5.69E+07	4.89E+07	4.28E+07	3.85E+07	3.52E+07	3.23E+07	2.99E+07	2.63E+07	2.35E+07
Horizontal Translation (Y) (lb/ft)	1.31E+08	1.30E+08	1.27E+08	1.11E+08	8.67E+07	6.92E+07	5.69E+07	4.89E+07	4.28E+07	3.85E+07	3.52E+07	3.23E+07	2.99E+07	2.63E+07	2.35E+07
Vertical Translation (Z) (lb/ft)	4.26E+08	4.25E+08	4.23E+08	4.12E+08	3.92E+08	3.76E+08	3.62E+08	3.52E+08	3.44E+08	3.37E+08	3.32E+08	3.26E+08	3.22E+08	3.14E+08	3.08E+08
Rotation About (X) (lb.ft/rad)	1.21E+10	1.21E+10	1.20E+10	1.16E+10	1.10E+10	1.04E+10	1.00E+10	9.72E+09	9.46E+09	9.26E+09	9.10E+09	8.94E+09	8.80E+09	8.59E+09	8.40E+09
Rotation About (Y) (lb.ft/rad)	4.48E+09	4.47E+09	4.44E+09	4.29E+09	4.02E+09	3.80E+09	3.64E+09	3.52E+09	3.41E+09	3.34E+09	3.27E+09	3.21E+09	3.16E+09	3.08E+09	3.00E+09
Torsion About (Z) (lb.ft/rad)	6.28E+09	6.22E+09	6.08E+09	5.33E+09	4.11E+09	3.23E+09	2.63E+09	2.24E+09	1.94E+09	1.74E+09	1.58E+09	1.45E+09	1.33E+09	1.17E+09	1.04E+09
Cross-Stiffness (YZ Plane) (lb/rad)	1.50E+08	1.50E+08	1.48E+08	1.40E+08	1.24E+08	1.11E+08	1.01E+08	9.25E+07	8.56E+07	8.07E+07	7.66E+07	7.28E+07	6.95E+07	6.43E+07	6.00E+07
Cross-Stiffness (XZ Plane) (lb/rad)	-1.50E+08	-1.50E+08	-1.48E+08	-1.40E+08	-1.24E+08	-1.11E+08	-1.01E+08	-9.25E+07	-8.56E+07	-8.07E+07	-7.66E+07	-7.28E+07	-6.95E+07	-6.43E+07	-6.00E+07
Damping Coefficients															
Horizontal Translation (X) (lb/ft/s)	1.17E+06	1.26E+06	1.45E+06	2.14E+06	2.62E+06	2.66E+06	2.52E+06	2.37E+06	2.22E+06	2.08E+06	1.96E+06	1.86E+06	1.77E+06	1.61E+06	1.48E+06
Horizontal Translation (Y) (lb/ft/s)	1.17E+06	1.26E+06	1.45E+06	2.14E+06	2.62E+06	2.66E+06	2.52E+06	2.37E+06	2.22E+06	2.08E+06	1.96E+06	1.86E+06	1.77E+06	1.61E+06	1.48E+06
Vertical Translation (Z) (lb/ft/s)	3.90E+06	3.97E+06	4.12E+06	4.71E+06	5.24E+06	5.41E+06	5.40E+06	5.34E+06	5.24E+06	5.14E+06	5.05E+06	4.97E+06	4.88E+06	4.72E+06	4.56E+06
Rotation About (X) (lb.ft/rad/s)	9.95E+07	1.02E+08	1.07E+08	1.28E+08	1.47E+08	1.53E+08	1.53E+08	1.51E+08	1.48E+08	1.45E+08	1.42E+08	1.40E+08	1.37E+08	1.32E+08	1.28E+08
Rotation About (Y) (lb.ft/rad/s)	3.63E+07	3.73E+07	3.95E+07	4.82E+07	5.58E+07	5.82E+07	5.81E+07	5.72E+07	5.59E+07	5.46E+07	5.35E+07	5.26E+07	5.16E+07	4.97E+07	4.80E+07
Torsion About (Z) (lb.ft/rad/s)	3.56E+07	4.06E+07	5.14E+07	9.07E+07	1.19E+08	1.23E+08	1.16E+08	1.08E+08	1.00E+08	9.32E+07	8.71E+07	8.19E+07	7.72E+07	6.96E+07	6.33E+07
Cross-Damping (YZ Plane) (lb/rad/s)	6.12E+05	6.64E+05	7.73E+05	1.23E+06	1.74E+06	2.01E+06	2.16E+06	2.22E+06	2.23E+06	2.20E+06	2.17E+06	2.15E+06	2.12E+06	2.06E+06	2.00E+06
Cross-Damping (XZ Plane) (lb/rad/s)	-6.12E+05	-6.64E+05	-7.73E+05	-1.23E+06	-1.74E+06	-2.01E+06	-2.16E+06	-2.22E+06	-2.23E+06	-2.20E+06	-2.17E+06	-2.15E+06	-2.12E+06	-2.06E+06	-2.00E+06

Table 5.2 Stiffness and Damping Coefficients for the West Column of Bent 106

Horizontal Disp. at Pile Cap (in)	0.0	0.1	0.2	0.5	1.0	1.5	2.0	2.5	3.0	3.5	4.0	4.5	5.0	6.0	7.0
Stiffness Coefficients															
Horizontal Translation (X) (lb/ft)	1.08E+08	1.07E+08	1.04E+08	9.17E+07	7.12E+07	5.69E+07	4.67E+07	3.99E+07	3.51E+07	3.17E+07	2.89E+07	2.64E+07	2.46E+07	2.17E+07	1.95E+07
Horizontal Translation (Y) (lb/ft)	1.32E+08	1.31E+08	1.28E+08	1.14E+08	9.12E+07	7.48E+07	6.27E+07	5.43E+07	4.83E+07	4.40E+07	4.05E+07	3.72E+07	3.49E+07	3.10E+07	2.80E+07
Vertical Translation (Z) (lb/ft)	3.87E+08	3.86E+08	3.84E+08	3.73E+08	3.55E+08	3.39E+08	3.27E+08	3.17E+08	3.09E+08	3.03E+08	2.98E+08	2.93E+08	2.89E+08	2.82E+08	2.76E+08
Rotation About (X) (lb.ft/rad)	1.12E+10	1.12E+10	1.11E+10	1.08E+10	1.02E+10	9.67E+09	9.26E+09	8.96E+09	8.72E+09	8.54E+09	8.38E+09	8.23E+09	8.11E+09	7.91E+09	7.73E+09
Rotation About (Y) (lb.ft/rad)	3.98E+09	3.96E+09	3.94E+09	3.80E+09	3.54E+09	3.35E+09	3.19E+09	3.08E+09	2.99E+09	2.92E+09	2.86E+09	2.81E+09	2.77E+09	2.69E+09	2.63E+09
Torsion About (Z) (lb.ft/rad)	5.69E+09	5.64E+09	5.50E+09	4.84E+09	3.74E+09	2.96E+09	2.41E+09	2.05E+09	1.79E+09	1.61E+09	1.46E+09	1.33E+09	1.24E+09	1.09E+09	9.73E+08
Cross-Stiffness (YZ Plane) (lb/rad)	1.71E+08	1.70E+08	1.69E+08	1.62E+08	1.49E+08	1.37E+08	1.26E+08	1.17E+08	1.10E+08	1.05E+08	1.01E+08	9.61E+07	9.27E+07	8.68E+07	8.16E+07
Cross-Stiffness (XZ Plane) (lb/rad)	-1.01E+08	-1.01E+08	-9.99E+07	-9.48E+07	-8.53E+07	-7.74E+07	-7.04E+07	-6.49E+07	-6.05E+07	-5.72E+07	-5.44E+07	-5.17E+07	-4.96E+07	-4.62E+07	-4.33E+07
Damping Coefficients															
Horizontal Translation (X) (lb/ft/s)	9.60E+05	1.05E+06	1.22E+06	1.78E+06	2.18E+06	2.22E+06	2.09E+06	1.96E+06	1.84E+06	1.73E+06	1.64E+06	1.54E+06	1.46E+06	1.34E+06	1.23E+06
Horizontal Translation (Y) (lb/ft/s)	1.05E+06	1.14E+06	1.33E+06	1.96E+06	2.46E+06	2.54E+06	2.45E+06	2.33E+06	2.21E+06	2.09E+06	1.99E+06	1.88E+06	1.80E+06	1.66E+06	1.55E+06
Vertical Translation (Z) (lb/ft/s)	3.57E+06	3.64E+06	3.79E+06	4.33E+06	4.84E+06	4.98E+06	4.98E+06	4.91E+06	4.82E+06	4.73E+06	4.65E+06	4.55E+06	4.48E+06	4.35E+06	4.22E+06
Rotation About (X) (lb.ft/rad/s)	9.13E+07	9.39E+07	9.92E+07	1.19E+08	1.37E+08	1.43E+08	1.43E+08	1.41E+08	1.38E+08	1.36E+08	1.33E+08	1.30E+08	1.28E+08	1.24E+08	1.20E+08
Rotation About (Y) (lb.ft/rad/s)	3.21E+07	3.31E+07	3.53E+07	4.33E+07	5.04E+07	5.24E+07	5.22E+07	5.12E+07	5.00E+07	4.88E+07	4.78E+07	4.66E+07	4.58E+07	4.42E+07	4.27E+07
Torsion About (Z) (lb.ft/rad/s)	2.92E+07	3.43E+07	4.47E+07	7.95E+07	1.06E+08	1.10E+08	1.04E+08	9.67E+07	8.99E+07	8.39E+07	7.86E+07	7.32E+07	6.94E+07	6.26E+07	5.70E+07
Cross-Damping (YZ Plane) (lb/rad/s)	5.09E+05	5.56E+05	6.57E+05	1.07E+06	1.61E+06	1.93E+06	2.15E+06	2.28E+06	2.33E+06	2.34E+06	2.34E+06	2.33E+06	2.32E+06	2.29E+06	2.27E+06
Cross-Damping (XZ Plane) (lb/rad/s)	-2.00E+05	-2.35E+05	-3.10E+05	-6.05E+05	-9.71E+05	-1.18E+06	-1.31E+06	-1.38E+06	-1.42E+06	-1.42E+06	-1.41E+06	-1.39E+06	-1.38E+06	-1.35E+06	-1.32E+06

Table 5.3 Stiffness and Damping Coefficients for the East Column of Bent 107

Horizontal Disp. at Pile Cap (in)	0.0	0.1	0.2	0.5	1.0	1.5	2.0	2.5	3.0	3.5	4.0	4.5	5.0	6.0	7.0
Stiffness Coefficients															
Horizontal Translation (X) (lb/ft)	1.83E+08	1.82E+08	1.77E+08	1.56E+08	1.22E+08	9.75E+07	8.04E+07	6.91E+07	6.05E+07	5.45E+07	4.98E+07	4.58E+07	4.24E+07	3.73E+07	3.34E+07
Horizontal Translation (Y) (lb/ft)	1.83E+08	1.82E+08	1.77E+08	1.56E+08	1.22E+08	9.75E+07	8.04E+07	6.91E+07	6.05E+07	5.45E+07	4.98E+07	4.58E+07	4.24E+07	3.73E+07	3.34E+07
Vertical Translation (Z) (lb/ft)	6.02E+08	6.01E+08	5.98E+08	5.82E+08	5.54E+08	5.31E+08	5.12E+08	4.98E+08	4.85E+08	4.76E+08	4.68E+08	4.60E+08	4.54E+08	4.43E+08	4.34E+08
Rotation About (X) (lb.ft/rad)	9.63E+09	9.61E+09	9.55E+09	9.25E+09	8.71E+09	8.28E+09	7.93E+09	7.68E+09	7.46E+09	7.30E+09	7.17E+09	7.04E+09	6.93E+09	6.75E+09	6.60E+09
Rotation About (Y) (lb.ft/rad)	3.24E+10	3.23E+10	3.22E+10	3.12E+10	2.96E+10	2.82E+10	2.71E+10	2.63E+10	2.56E+10	2.51E+10	2.47E+10	2.42E+10	2.39E+10	2.33E+10	2.28E+10
Torsion About (Z) (lb.ft/rad)	1.49E+10	1.48E+10	1.45E+10	1.27E+10	9.83E+09	7.77E+09	6.34E+09	5.41E+09	4.71E+09	4.22E+09	3.84E+09	3.52E+09	3.25E+09	2.85E+09	2.54E+09
Cross-Stiffness (YZ Plane) (lb/rad)	2.19E+08	2.18E+08	2.16E+08	2.03E+08	1.80E+08	1.61E+08	1.45E+08	1.33E+08	1.23E+08	1.16E+08	1.10E+08	1.05E+08	9.98E+07	9.23E+07	8.60E+07
Cross-Stiffness (XZ Plane) (lb/rad)	-2.19E+08	-2.18E+08	-2.16E+08	-2.03E+08	-1.80E+08	-1.61E+08	-1.45E+08	-1.33E+08	-1.23E+08	-1.16E+08	-1.10E+08	-1.05E+08	-9.98E+07	-9.23E+07	-8.60E+07
Damping Coefficients															
Horizontal Translation (X) (lb/ft/s)	1.61E+06	1.74E+06	2.00E+06	2.97E+06	3.63E+06	3.70E+06	3.52E+06	3.32E+06	3.10E+06	2.92E+06	2.75E+06	2.61E+06	2.48E+06	2.26E+06	2.08E+06
Horizontal Translation (Y) (lb/ft/s)	1.61E+06	1.74E+06	2.00E+06	2.97E+06	3.63E+06	3.70E+06	3.52E+06	3.32E+06	3.10E+06	2.92E+06	2.75E+06	2.61E+06	2.48E+06	2.26E+06	2.08E+06
Vertical Translation (Z) (lb/ft/s)	5.54E+06	5.64E+06	5.84E+06	6.66E+06	7.41E+06	7.66E+06	7.66E+06	7.59E+06	7.45E+06	7.32E+06	7.19E+06	7.10E+06	6.97E+06	6.74E+06	6.53E+06
Rotation About (X) (lb.ft/rad/s)	7.98E+07	8.18E+07	8.61E+07	1.03E+08	1.19E+08	1.24E+08	1.24E+08	1.23E+08	1.20E+08	1.18E+08	1.15E+08	1.14E+08	1.12E+08	1.08E+08	1.04E+08
Rotation About (Y) (lb.ft/rad/s)	2.72E+08	2.79E+08	2.92E+08	3.44E+08	3.92E+08	4.09E+08	4.10E+08	4.07E+08	3.99E+08	3.91E+08	3.84E+08	3.79E+08	3.72E+08	3.60E+08	3.48E+08
Torsion About (Z) (lb.ft/rad/s)	8.96E+07	1.01E+08	1.26E+08	2.16E+08	2.81E+08	2.91E+08	2.76E+08	2.58E+08	2.39E+08	2.24E+08	2.10E+08	1.98E+08	1.87E+08	1.69E+08	1.54E+08
Cross-Damping (YZ Plane) (lb/rad/s)	9.46E+05	1.02E+06	1.19E+06	1.88E+06	2.62E+06	2.99E+06	3.19E+06	3.27E+06	3.26E+06	3.22E+06	3.17E+06	3.13E+06	3.08E+06	2.99E+06	2.90E+06
Cross-Damping (XZ Plane) (lb/rad/s)	-9.46E+05	-1.02E+06	-1.19E+06	-1.88E+06	-2.62E+06	-2.99E+06	-3.19E+06	-3.27E+06	-3.26E+06	-3.22E+06	-3.17E+06	-3.13E+06	-3.08E+06	-2.99E+06	-2.90E+06

Table 5.4 Stiffness and Damping Coefficients for the West Column of Bents 107 and 108

Horizontal Disp. at Pile Cap (in)	0.0	0.1	0.2	0.5	1.0	1.5	2.0	2.5	3.0	3.5	4.0	4.5	5.0	6.0	7.0
Stiffness Coefficients															
Horizontal Translation (X) (lb/ft)	1.83E+08	1.82E+08	1.77E+08	1.56E+08	1.22E+08	9.75E+07	8.04E+07	6.91E+07	6.05E+07	5.45E+07	4.98E+07	4.58E+07	4.24E+07	3.73E+07	3.34E+07
Horizontal Translation (Y) (lb/ft)	1.83E+08	1.82E+08	1.77E+08	1.56E+08	1.22E+08	9.75E+07	8.04E+07	6.91E+07	6.05E+07	5.45E+07	4.98E+07	4.58E+07	4.24E+07	3.73E+07	3.34E+07
Vertical Translation (Z) (lb/ft)	6.07E+08	6.05E+08	6.03E+08	5.87E+08	5.59E+08	5.36E+08	5.17E+08	5.03E+08	4.90E+08	4.81E+08	4.73E+08	4.66E+08	4.59E+08	4.49E+08	4.40E+08
Rotation About (X) (lb.ft/rad)	1.69E+10	1.69E+10	1.68E+10	1.63E+10	1.54E+10	1.47E+10	1.41E+10	1.37E+10	1.33E+10	1.31E+10	1.28E+10	1.26E+10	1.24E+10	1.21E+10	1.19E+10
Rotation About (Y) (lb.ft/rad)	1.04E+10	1.04E+10	1.03E+10	9.98E+09	9.41E+09	8.95E+09	8.59E+09	8.32E+09	8.09E+09	7.92E+09	7.78E+09	7.64E+09	7.53E+09	7.34E+09	7.18E+09
Torsion About (Z) (lb.ft/rad)	9.79E+09	9.70E+09	9.48E+09	8.31E+09	6.44E+09	5.08E+09	4.15E+09	3.54E+09	3.08E+09	2.76E+09	2.51E+09	2.30E+09	2.13E+09	1.86E+09	1.66E+09
Cross-Stiffness (YZ Plane) (lb/rad)	2.19E+08	2.18E+08	2.16E+08	2.03E+08	1.80E+08	1.61E+08	1.45E+08	1.33E+08	1.23E+08	1.16E+08	1.10E+08	1.05E+08	9.98E+07	9.23E+07	8.60E+07
Cross-Stiffness (XZ Plane) (lb/rad)	-2.19E+08	-2.18E+08	-2.16E+08	-2.03E+08	-1.80E+08	-1.61E+08	-1.45E+08	-1.33E+08	-1.23E+08	-1.16E+08	-1.10E+08	-1.05E+08	-9.98E+07	-9.23E+07	-8.60E+07
Damping Coefficients															
Horizontal Translation (X) (lb/ft/s)	1.56E+06	1.69E+06	1.95E+06	2.92E+06	3.59E+06	3.66E+06	3.49E+06	3.29E+06	3.08E+06	2.89E+06	2.73E+06	2.59E+06	2.46E+06	2.24E+06	2.07E+06
Horizontal Translation (Y) (lb/ft/s)	1.56E+06	1.69E+06	1.95E+06	2.92E+06	3.59E+06	3.66E+06	3.49E+06	3.29E+06	3.08E+06	2.89E+06	2.73E+06	2.59E+06	2.46E+06	2.24E+06	2.07E+06
Vertical Translation (Z) (lb/ft/s)	5.47E+06	5.57E+06	5.78E+06	6.61E+06	7.36E+06	7.61E+06	7.62E+06	7.55E+06	7.40E+06	7.27E+06	7.15E+06	7.05E+06	6.92E+06	6.69E+06	6.47E+06
Rotation About (X) (lb.ft/rad/s)	1.40E+08	1.43E+08	1.50E+08	1.78E+08	2.04E+08	2.13E+08	2.13E+08	2.11E+08	2.07E+08	2.03E+08	1.99E+08	1.96E+08	1.92E+08	1.86E+08	1.80E+08
Rotation About (Y) (lb.ft/rad/s)	8.52E+07	8.74E+07	9.19E+07	1.10E+08	1.26E+08	1.32E+08	1.32E+08	1.31E+08	1.28E+08	1.25E+08	1.23E+08	1.21E+08	1.19E+08	1.15E+08	1.11E+08
Torsion About (Z) (lb.ft/rad/s)	5.73E+07	6.49E+07	8.12E+07	1.41E+08	1.84E+08	1.90E+08	1.80E+08	1.68E+08	1.56E+08	1.46E+08	1.37E+08	1.29E+08	1.21E+08	1.10E+08	1.00E+08
Cross-Damping (YZ Plane) (lb/rad/s)	1.01E+06	1.09E+06	1.25E+06	1.93E+06	2.67E+06	3.04E+06	3.23E+06	3.30E+06	3.29E+06	3.25E+06	3.20E+06	3.16E+06	3.11E+06	3.01E+06	2.92E+06
Cross-Damping (XZ Plane) (lb/rad/s)	-1.01E+06	-1.09E+06	-1.25E+06	-1.93E+06	-2.67E+06	-3.04E+06	-3.23E+06	-3.30E+06	-3.29E+06	-3.25E+06	-3.20E+06	-3.16E+06	-3.11E+06	-3.01E+06	-2.92E+06

Table 5.5 Stiffness and Damping Coefficients for the East Column of Bent 109

Horizontal Disp. at Pile Cap (in)	0.0	0.1	0.2	0.5	1.0	1.5	2.0	2.5	3.0	3.5	4.0	4.5	5.0	6.0	7.0
Stiffness Coefficients															
Horizontal Translation (X) (lb/ft)	1.31E+08	1.30E+08	1.27E+08	1.11E+08	8.67E+07	6.92E+07	5.69E+07	4.89E+07	4.28E+07	3.85E+07	3.52E+07	3.23E+07	2.99E+07	2.63E+07	2.36E+07
Horizontal Translation (Y) (lb/ft)	1.31E+08	1.30E+08	1.27E+08	1.11E+08	8.67E+07	6.92E+07	5.69E+07	4.89E+07	4.28E+07	3.85E+07	3.52E+07	3.23E+07	2.99E+07	2.63E+07	2.36E+07
Vertical Translation (Z) (lb/ft)	4.32E+08	4.31E+08	4.29E+08	4.18E+08	3.98E+08	3.82E+08	3.69E+08	3.58E+08	3.50E+08	3.43E+08	3.38E+08	3.33E+08	3.28E+08	3.21E+08	3.15E+08
Rotation About (X) (lb.ft/rad)	7.07E+09	7.06E+09	7.02E+09	6.79E+09	6.39E+09	6.07E+09	5.82E+09	5.64E+09	5.48E+09	5.37E+09	5.27E+09	5.18E+09	5.10E+09	4.98E+09	4.87E+09
Rotation About (Y) (lb.ft/rad)	1.23E+10	1.23E+10	1.22E+10	1.18E+10	1.12E+10	1.06E+10	1.02E+10	9.89E+09	9.63E+09	9.43E+09	9.27E+09	9.12E+09	8.98E+09	8.77E+09	8.58E+09
Torsion About (Z) (lb.ft/rad)	7.26E+09	7.20E+09	7.03E+09	6.16E+09	4.75E+09	3.73E+09	3.03E+09	2.58E+09	2.24E+09	2.00E+09	1.82E+09	1.67E+09	1.54E+09	1.34E+09	1.20E+09
Cross-Stiffness (YZ Plane) (lb/rad)	1.50E+08	1.50E+08	1.48E+08	1.40E+08	1.24E+08	1.11E+08	1.01E+08	9.25E+07	8.56E+07	8.07E+07	7.66E+07	7.28E+07	6.95E+07	6.43E+07	6.00E+07
Cross-Stiffness (XZ Plane) (lb/rad)	-1.50E+08	-1.50E+08	-1.48E+08	-1.40E+08	-1.24E+08	-1.11E+08	-1.01E+08	-9.25E+07	-8.56E+07	-8.07E+07	-7.66E+07	-7.28E+07	-6.95E+07	-6.43E+07	-6.00E+07
Damping Coefficients															
Horizontal Translation (X) (lb/ft/s)	1.20E+06	1.29E+06	1.48E+06	2.17E+06	2.64E+06	2.68E+06	2.54E+06	2.39E+06	2.24E+06	2.10E+06	1.98E+06	1.88E+06	1.78E+06	1.63E+06	1.50E+06
Horizontal Translation (Y) (lb/ft/s)	1.20E+06	1.29E+06	1.48E+06	2.17E+06	2.64E+06	2.68E+06	2.54E+06	2.39E+06	2.24E+06	2.10E+06	1.98E+06	1.88E+06	1.78E+06	1.63E+06	1.50E+06
Vertical Translation (Z) (lb/ft/s)	3.92E+06	3.99E+06	4.14E+06	4.72E+06	5.24E+06	5.39E+06	5.38E+06	5.32E+06	5.21E+06	5.11E+06	5.01E+06	4.94E+06	4.85E+06	4.68E+06	4.51E+06
Rotation About (X) (lb.ft/rad/s)	5.69E+07	5.84E+07	6.17E+07	7.45E+07	8.58E+07	8.94E+07	8.92E+07	8.79E+07	8.59E+07	8.40E+07	8.23E+07	8.09E+07	7.93E+07	7.63E+07	7.36E+07
Rotation About (Y) (lb.ft/rad/s)	9.95E+07	1.02E+08	1.07E+08	1.28E+08	1.47E+08	1.54E+08	1.53E+08	1.51E+08	1.48E+08	1.45E+08	1.42E+08	1.40E+08	1.37E+08	1.32E+08	1.27E+08
Torsion About (Z) (lb.ft/rad/s)	4.15E+07	4.73E+07	5.97E+07	1.05E+08	1.38E+08	1.43E+08	1.35E+08	1.25E+08	1.16E+08	1.08E+08	1.01E+08	9.49E+07	8.94E+07	8.07E+07	7.33E+07
Cross-Damping (YZ Plane) (lb/rad/s)	5.69E+05	6.22E+05	7.31E+05	1.19E+06	1.71E+06	1.98E+06	2.13E+06	2.20E+06	2.20E+06	2.18E+06	2.15E+06	2.13E+06	2.10E+06	2.04E+06	1.98E+06
Cross-Damping (XZ Plane) (lb/rad/s)	-5.69E+05	-6.22E+05	-7.31E+05	-1.19E+06	-1.71E+06	-1.98E+06	-2.13E+06	-2.20E+06	-2.20E+06	-2.18E+06	-2.15E+06	-2.13E+06	-2.10E+06	-2.04E+06	-1.98E+06

Table 5.6 Stiffness and Damping Coefficients for the West Column of Bent 109

Horizontal Disp. at Pile Cap (in)	0.0	0.1	0.2	0.5	1.0	1.5	2.0	2.5	3.0	3.5	4.0	4.5	5.0	6.0	7.0
Stiffness Coefficients															
Horizontal Translation (X) (lb/ft)	1.31E+08	1.30E+08	1.27E+08	1.11E+08	8.67E+07	6.92E+07	5.69E+07	4.89E+07	4.28E+07	3.85E+07	3.52E+07	3.23E+07	2.99E+07	2.63E+07	2.36E+07
Horizontal Translation (Y) (lb/ft)	1.31E+08	1.30E+08	1.27E+08	1.11E+08	8.67E+07	6.92E+07	5.69E+07	4.89E+07	4.28E+07	3.85E+07	3.52E+07	3.23E+07	2.99E+07	2.63E+07	2.36E+07
Vertical Translation (Z) (lb/ft)	4.32E+08	4.31E+08	4.29E+08	4.18E+08	3.98E+08	3.82E+08	3.69E+08	3.58E+08	3.50E+08	3.43E+08	3.38E+08	3.33E+08	3.28E+08	3.21E+08	3.15E+08
Rotation About (X) (lb.ft/rad)	1.22E+10	1.22E+10	1.21E+10	1.18E+10	1.11E+10	1.06E+10	1.02E+10	9.88E+09	9.62E+09	9.42E+09	9.26E+09	9.11E+09	8.97E+09	8.76E+09	8.58E+09
Rotation About (Y) (lb.ft/rad)	4.53E+09	4.52E+09	4.49E+09	4.34E+09	4.07E+09	3.86E+09	3.69E+09	3.57E+09	3.47E+09	3.39E+09	3.33E+09	3.27E+09	3.22E+09	3.13E+09	3.06E+09
Torsion About (Z) (lb.ft/rad)	6.28E+09	6.22E+09	6.08E+09	5.33E+09	4.11E+09	3.23E+09	2.63E+09	2.24E+09	1.94E+09	1.74E+09	1.58E+09	1.45E+09	1.33E+09	1.17E+09	1.04E+09
Cross-Stiffness (YZ Plane) (lb/rad)	1.50E+08	1.50E+08	1.48E+08	1.40E+08	1.24E+08	1.11E+08	1.01E+08	9.25E+07	8.56E+07	8.07E+07	7.66E+07	7.28E+07	6.95E+07	6.43E+07	6.00E+07
Cross-Stiffness (XZ Plane) (lb/rad)	-1.50E+08	-1.50E+08	-1.48E+08	-1.40E+08	-1.24E+08	-1.11E+08	-1.01E+08	-9.25E+07	-8.56E+07	-8.07E+07	-7.66E+07	-7.28E+07	-6.95E+07	-6.43E+07	-6.00E+07
Damping Coefficients															
Horizontal Translation (X) (lb/ft/s)	1.17E+06	1.26E+06	1.45E+06	2.14E+06	2.62E+06	2.66E+06	2.52E+06	2.37E+06	2.22E+06	2.08E+06	1.96E+06	1.86E+06	1.77E+06	1.61E+06	1.48E+06
Horizontal Translation (Y) (lb/ft/s)	1.17E+06	1.26E+06	1.45E+06	2.14E+06	2.62E+06	2.66E+06	2.52E+06	2.37E+06	2.22E+06	2.08E+06	1.96E+06	1.86E+06	1.77E+06	1.61E+06	1.48E+06
Vertical Translation (Z) (lb/ft/s)	3.89E+06	3.96E+06	4.10E+06	4.69E+06	5.22E+06	5.38E+06	5.37E+06	5.31E+06	5.20E+06	5.10E+06	5.01E+06	4.93E+06	4.84E+06	4.67E+06	4.51E+06
Rotation About (X) (lb.ft/rad/s)	9.91E+07	1.02E+08	1.07E+08	1.27E+08	1.46E+08	1.52E+08	1.52E+08	1.50E+08	1.47E+08	1.44E+08	1.41E+08	1.39E+08	1.36E+08	1.31E+08	1.27E+08
Rotation About (Y) (lb.ft/rad/s)	3.62E+07	3.72E+07	3.94E+07	4.80E+07	5.56E+07	5.80E+07	5.78E+07	5.69E+07	5.56E+07	5.43E+07	5.31E+07	5.22E+07	5.12E+07	4.93E+07	4.75E+07
Torsion About (Z) (lb.ft/rad/s)	3.56E+07	4.06E+07	5.14E+07	9.07E+07	1.19E+08	1.23E+08	1.16E+08	1.08E+08	1.00E+08	9.31E+07	8.71E+07	8.19E+07	7.72E+07	6.96E+07	6.33E+07
Cross-Damping (YZ Plane) (lb/rad/s)	6.12E+05	6.64E+05	7.73E+05	1.23E+06	1.74E+06	2.01E+06	2.16E+06	2.22E+06	2.23E+06	2.20E+06	2.17E+06	2.15E+06	2.11E+06	2.06E+06	2.00E+06
Cross-Damping (XZ Plane) (lb/rad/s)	-6.12E+05	-6.64E+05	-7.73E+05	-1.23E+06	-1.74E+06	-2.01E+06	-2.16E+06	-2.22E+06	-2.23E+06	-2.20E+06	-2.17E+06	-2.15E+06	-2.11E+06	-2.06E+06	-2.00E+06

Table 5.7 Stiffness and Damping Coefficients for the East and West Columns of Bent 151

Horizontal Disp. at Pile Cap (in)	0.0	0.1	0.2	0.5	1.0	1.5	2.0	2.5	3.0	3.5	4.0	4.5	5.0	6.0	7.0
Stiffness Coefficients															
Horizontal Translation (X) (lb/ft)	9.94E+07	9.86E+07	9.70E+07	8.76E+07	7.11E+07	5.71E+07	4.70E+07	4.04E+07	3.57E+07	3.19E+07	2.91E+07	2.67E+07	2.47E+07	2.17E+07	1.94E+07
Horizontal Translation (Y) (lb/ft)	9.94E+07	9.86E+07	9.70E+07	8.76E+07	7.11E+07	5.71E+07	4.70E+07	4.04E+07	3.57E+07	3.19E+07	2.91E+07	2.67E+07	2.47E+07	2.17E+07	1.94E+07
Vertical Translation (Z) (lb/ft)	2.60E+08	2.59E+08	2.58E+08	2.51E+08	2.35E+08	2.21E+08	2.09E+08	1.99E+08	1.92E+08	1.86E+08	1.81E+08	1.76E+08	1.72E+08	1.66E+08	1.61E+08
Rotation About (X) (lb.ft/rad)	3.29E+09	3.28E+09	3.26E+09	3.14E+09	2.91E+09	2.70E+09	2.53E+09	2.40E+09	2.30E+09	2.22E+09	2.15E+09	2.09E+09	2.05E+09	1.96E+09	1.90E+09
Rotation About (Y) (lb.ft/rad)	2.36E+09	2.35E+09	2.34E+09	2.26E+09	2.09E+09	1.94E+09	1.82E+09	1.72E+09	1.65E+09	1.59E+09	1.55E+09	1.50E+09	1.47E+09	1.41E+09	1.36E+09
Torsion About (Z) (lb.ft/rad)	2.72E+09	2.70E+09	2.66E+09	2.41E+09	1.94E+09	1.54E+09	1.25E+09	1.07E+09	9.37E+08	8.32E+08	7.53E+08	6.86E+08	6.33E+08	5.52E+08	4.92E+08
Cross-Stiffness (YZ Plane) (lb/rad)	1.24E+08	1.23E+08	1.22E+08	1.17E+08	1.06E+08	9.61E+07	8.75E+07	8.07E+07	7.55E+07	7.10E+07	6.74E+07	6.42E+07	6.15E+07	5.70E+07	5.35E+07
Cross-Stiffness (XZ Plane) (lb/rad)	-1.24E+08	-1.23E+08	-1.22E+08	-1.17E+08	-1.06E+08	-9.61E+07	-8.75E+07	-8.07E+07	-7.55E+07	-7.10E+07	-6.74E+07	-6.42E+07	-6.15E+07	-5.70E+07	-5.35E+07
Damping Coefficients															
Horizontal Translation (X) (lb/ft/s)	4.27E+05	4.91E+05	5.92E+05	1.08E+06	1.53E+06	1.71E+06	1.68E+06	1.60E+06	1.52E+06	1.44E+06	1.36E+06	1.29E+06	1.22E+06	1.11E+06	1.02E+06
Horizontal Translation (Y) (lb/ft/s)	4.27E+05	4.91E+05	5.92E+05	1.08E+06	1.53E+06	1.71E+06	1.68E+06	1.60E+06	1.52E+06	1.44E+06	1.36E+06	1.29E+06	1.22E+06	1.11E+06	1.02E+06
Vertical Translation (Z) (lb/ft/s)	1.28E+06	1.34E+06	1.42E+06	1.91E+06	2.49E+06	2.83E+06	2.95E+06	2.99E+06	2.98E+06	2.94E+06	2.89E+06	2.83E+06	2.77E+06	2.66E+06	2.59E+06
Rotation About (X) (lb.ft/rad/s)	1.69E+07	1.78E+07	1.91E+07	2.67E+07	3.51E+07	3.98E+07	4.11E+07	4.11E+07	4.06E+07	3.98E+07	3.90E+07	3.79E+07	3.70E+07	3.54E+07	3.42E+07
Rotation About (Y) (lb.ft/rad/s)	1.22E+07	1.29E+07	1.39E+07	1.93E+07	2.53E+07	2.86E+07	2.95E+07	2.96E+07	2.93E+07	2.87E+07	2.81E+07	2.74E+07	2.68E+07	2.57E+07	2.49E+07
Torsion About (Z) (lb.ft/rad/s)	1.13E+07	1.33E+07	1.65E+07	3.20E+07	4.63E+07	5.22E+07	5.11E+07	4.82E+07	4.51E+07	4.21E+07	3.95E+07	3.69E+07	3.48E+07	3.12E+07	2.84E+07
Cross-Damping (YZ Plane) (lb/rad/s)	7.39E+05	7.75E+05	8.31E+05	1.13E+06	1.49E+06	1.74E+06	1.85E+06	1.92E+06	1.95E+06	1.96E+06	1.94E+06	1.91E+06	1.88E+06	1.82E+06	1.77E+06
Cross-Damping (XZ Plane) (lb/rad/s)	-7.39E+05	-7.75E+05	-8.31E+05	-1.13E+06	-1.49E+06	-1.74E+06	-1.85E+06	-1.92E+06	-1.95E+06	-1.96E+06	-1.94E+06	-1.91E+06	-1.88E+06	-1.82E+06	-1.77E+06

Table 5.8 Stiffness and Damping Coefficients for the East and West Columns of Bents 152 and 153

Horizontal Disp. at Pile Cap (in)	0.0	0.1	0.2	0.5	1.0	1.5	2.0	2.5	3.0	3.5	4.0	4.5	5.0	6.0	7.0
Stiffness Coefficients															
Horizontal Translation (X) (lb/ft)	1.42E+08	1.41E+08	1.39E+08	1.25E+08	1.02E+08	8.19E+07	6.75E+07	5.81E+07	5.14E+07	4.60E+07	4.19E+07	3.84E+07	3.56E+07	3.13E+07	2.81E+07
Horizontal Translation (Y) (lb/ft)	1.42E+08	1.41E+08	1.39E+08	1.25E+08	1.02E+08	8.19E+07	6.75E+07	5.81E+07	5.14E+07	4.60E+07	4.19E+07	3.84E+07	3.56E+07	3.13E+07	2.81E+07
Vertical Translation (Z) (lb/ft)	3.77E+08	3.76E+08	3.74E+08	3.63E+08	3.41E+08	3.20E+08	3.03E+08	2.89E+08	2.78E+08	2.69E+08	2.62E+08	2.56E+08	2.50E+08	2.41E+08	2.34E+08
Rotation About (X) (lb.ft/rad)	5.29E+09	5.28E+09	5.25E+09	5.07E+09	4.71E+09	4.37E+09	4.10E+09	3.89E+09	3.73E+09	3.60E+09	3.50E+09	3.40E+09	3.33E+09	3.20E+09	3.09E+09
Rotation About (Y) (lb.ft/rad)	5.29E+09	5.28E+09	5.25E+09	5.07E+09	4.71E+09	4.37E+09	4.10E+09	3.89E+09	3.73E+09	3.60E+09	3.50E+09	3.40E+09	3.33E+09	3.20E+09	3.09E+09
Torsion About (Z) (lb.ft/rad)	4.92E+09	4.88E+09	4.81E+09	4.35E+09	3.52E+09	2.80E+09	2.28E+09	1.94E+09	1.71E+09	1.52E+09	1.37E+09	1.25E+09	1.16E+09	1.01E+09	8.99E+08
Cross-Stiffness (YZ Plane) (lb/rad)	1.81E+08	1.81E+08	1.79E+08	1.71E+08	1.55E+08	1.40E+08	1.28E+08	1.18E+08	1.10E+08	1.04E+08	9.82E+07	9.35E+07	8.96E+07	8.31E+07	7.79E+07
Cross-Stiffness (XZ Plane) (lb/rad)	-1.81E+08	-1.81E+08	-1.79E+08	-1.71E+08	-1.55E+08	-1.40E+08	-1.28E+08	-1.18E+08	-1.10E+08	-1.04E+08	-9.82E+07	-9.35E+07	-8.96E+07	-8.31E+07	-7.79E+07
Damping Coefficients															
Horizontal Translation (X) (lb/ft/s)	6.13E+05	7.03E+05	8.47E+05	1.54E+06	2.18E+06	2.43E+06	2.40E+06	2.29E+06	2.18E+06	2.06E+06	1.95E+06	1.84E+06	1.75E+06	1.60E+06	1.47E+06
Horizontal Translation (Y) (lb/ft/s)	6.13E+05	7.03E+05	8.47E+05	1.54E+06	2.18E+06	2.43E+06	2.40E+06	2.29E+06	2.18E+06	2.06E+06	1.95E+06	1.84E+06	1.75E+06	1.60E+06	1.47E+06
Vertical Translation (Z) (lb/ft/s)	1.85E+06	1.93E+06	2.05E+06	2.75E+06	3.59E+06	4.09E+06	4.27E+06	4.32E+06	4.31E+06	4.26E+06	4.19E+06	4.10E+06	4.01E+06	3.86E+06	3.76E+06
Rotation About (X) (lb.ft/rad/s)	2.71E+07	2.85E+07	3.06E+07	4.25E+07	5.58E+07	6.33E+07	6.54E+07	6.55E+07	6.48E+07	6.36E+07	6.23E+07	6.07E+07	5.93E+07	5.68E+07	5.50E+07
Rotation About (Y) (lb.ft/rad/s)	2.71E+07	2.85E+07	3.06E+07	4.25E+07	5.58E+07	6.33E+07	6.54E+07	6.55E+07	6.48E+07	6.36E+07	6.23E+07	6.07E+07	5.93E+07	5.68E+07	5.50E+07
Torsion About (Z) (lb.ft/rad/s)	2.09E+07	2.45E+07	3.01E+07	5.77E+07	8.30E+07	9.35E+07	9.18E+07	8.67E+07	8.13E+07	7.61E+07	7.14E+07	6.68E+07	6.31E+07	5.68E+07	5.17E+07
Cross-Damping (YZ Plane) (lb/rad/s)	1.08E+06	1.13E+06	1.22E+06	1.66E+06	2.19E+06	2.55E+06	2.71E+06	2.82E+06	2.86E+06	2.86E+06	2.84E+06	2.80E+06	2.75E+06	2.66E+06	2.58E+06
Cross-Damping (XZ Plane) (lb/rad/s)	-1.08E+06	-1.13E+06	-1.22E+06	-1.66E+06	-2.19E+06	-2.55E+06	-2.71E+06	-2.82E+06	-2.86E+06	-2.86E+06	-2.84E+06	-2.80E+06	-2.75E+06	-2.66E+06	-2.58E+06

Table 5.9 Stiffness and Damping Coefficients for the East and West Columns of Bent 154

Horizontal Disp. at Pile Cap (in)	0.0	0.1	0.2	0.5	1.0	1.5	2.0	2.5	3.0	3.5	4.0	4.5	5.0	6.0	7.0
Stiffness Coefficients															
Horizontal Translation (X) (lb/ft)	1.08E+08	1.07E+08	1.05E+08	9.49E+07	7.71E+07	6.19E+07	5.10E+07	4.38E+07	3.88E+07	3.47E+07	3.16E+07	2.90E+07	2.69E+07	2.36E+07	2.11E+07
Horizontal Translation (Y) (lb/ft)	1.08E+08	1.07E+08	1.05E+08	9.49E+07	7.71E+07	6.19E+07	5.10E+07	4.38E+07	3.88E+07	3.47E+07	3.16E+07	2.90E+07	2.69E+07	2.36E+07	2.11E+07
Vertical Translation (Z) (lb/ft)	2.83E+08	2.83E+08	2.81E+08	2.73E+08	2.56E+08	2.40E+08	2.27E+08	2.17E+08	2.09E+08	2.02E+08	1.97E+08	1.92E+08	1.88E+08	1.81E+08	1.76E+08
Rotation About (X) (lb.ft/rad)	3.96E+09	3.95E+09	3.93E+09	3.80E+09	3.53E+09	3.28E+09	3.07E+09	2.92E+09	2.80E+09	2.70E+09	2.62E+09	2.55E+09	2.49E+09	2.40E+09	2.32E+09
Rotation About (Y) (lb.ft/rad)	2.21E+09	2.20E+09	2.19E+09	2.11E+09	1.95E+09	1.81E+09	1.69E+09	1.60E+09	1.53E+09	1.48E+09	1.43E+09	1.39E+09	1.36E+09	1.30E+09	1.26E+09
Torsion About (Z) (lb.ft/rad)	2.93E+09	2.91E+09	2.87E+09	2.60E+09	2.10E+09	1.67E+09	1.36E+09	1.16E+09	1.01E+09	9.01E+08	8.15E+08	7.44E+08	6.87E+08	5.99E+08	5.34E+08
Cross-Stiffness (YZ Plane) (lb/rad)	1.36E+08	1.36E+08	1.35E+08	1.29E+08	1.17E+08	1.05E+08	9.59E+07	8.84E+07	8.26E+07	7.77E+07	7.37E+07	7.02E+07	6.72E+07	6.23E+07	5.84E+07
Cross-Stiffness (XZ Plane) (lb/rad)	-1.36E+08	-1.36E+08	-1.35E+08	-1.29E+08	-1.17E+08	-1.05E+08	-9.59E+07	-8.84E+07	-8.26E+07	-7.77E+07	-7.37E+07	-7.02E+07	-6.72E+07	-6.23E+07	-5.84E+07
Damping Coefficients															
Horizontal Translation (X) (lb/ft/s)	4.63E+05	5.32E+05	6.41E+05	1.17E+06	1.65E+06	1.85E+06	1.82E+06	1.74E+06	1.65E+06	1.56E+06	1.48E+06	1.39E+06	1.33E+06	1.21E+06	1.11E+06
Horizontal Translation (Y) (lb/ft/s)	4.63E+05	5.32E+05	6.41E+05	1.17E+06	1.65E+06	1.85E+06	1.82E+06	1.74E+06	1.65E+06	1.56E+06	1.48E+06	1.39E+06	1.33E+06	1.21E+06	1.11E+06
Vertical Translation (Z) (lb/ft/s)	1.39E+06	1.45E+06	1.54E+06	2.07E+06	2.71E+06	3.08E+06	3.21E+06	3.25E+06	3.24E+06	3.20E+06	3.15E+06	3.08E+06	3.02E+06	2.90E+06	2.82E+06
Rotation About (X) (lb.ft/rad/s)	2.03E+07	2.13E+07	2.29E+07	3.17E+07	4.17E+07	4.72E+07	4.88E+07	4.90E+07	4.85E+07	4.76E+07	4.66E+07	4.54E+07	4.44E+07	4.25E+07	4.11E+07
Rotation About (Y) (lb.ft/rad/s)	1.16E+07	1.22E+07	1.32E+07	1.84E+07	2.41E+07	2.73E+07	2.81E+07	2.81E+07	2.78E+07	2.73E+07	2.67E+07	2.60E+07	2.54E+07	2.43E+07	2.35E+07
Torsion About (Z) (lb.ft/rad/s)	1.23E+07	1.44E+07	1.78E+07	3.45E+07	4.98E+07	5.61E+07	5.51E+07	5.19E+07	4.86E+07	4.54E+07	4.26E+07	3.98E+07	3.75E+07	3.37E+07	3.07E+07
Cross-Damping (YZ Plane) (lb/rad/s)	8.10E+05	8.51E+05	9.13E+05	1.25E+06	1.65E+06	1.92E+06	2.04E+06	2.12E+06	2.15E+06	2.15E+06	2.13E+06	2.10E+06	2.07E+06	2.00E+06	1.93E+06
Cross-Damping (XZ Plane) (lb/rad/s)	-8.10E+05	-8.51E+05	-9.13E+05	-1.25E+06	-1.65E+06	-1.92E+06	-2.04E+06	-2.12E+06	-2.15E+06	-2.15E+06	-2.13E+06	-2.10E+06	-2.07E+06	-2.00E+06	-1.93E+06

CHAPTER 6
LIQUEFACTION HAZARDS

Reclamation of tidal areas by the placement of earth fills has been a key part of the economic development of many major port cities around the world. On the seismically active west coast of the United States, much of this earthwork activity took place in the mid to late 1800s and early 1900s, before the discipline of geotechnical engineering had been developed. As a result, many of these waterfront fills were placed by techniques that would not be considered acceptable by modern standards and that produced waterfront fills that are susceptible to liquefaction. In cities such as San Francisco and Seattle, where waterfront areas built on liquefiable soils are relied upon by both the shipping and tourist industries, earthquake-induced failures would have tremendous economic impacts.

Damage caused by liquefaction of waterfront fills has been observed in many earthquakes in different parts of the world. In San Francisco, liquefaction of waterfront fills was observed following the 1868 Hayward, 1906 San Francisco, and 1989 Loma Prieta earthquakes (Clough and Chameau, 1983; Chameau et al., 1991). Liquefaction of loosely placed backfills caused the failure of a number of quay walls in the 1964 Niigata earthquake in Japan (Seed and Idriss, 1966). Liquefaction-induced failures of quay walls that were retaining waterfront fills were observed at the ports of Valparaiso and San Antonio in the 1985 Chilean earthquake (JICA, 1986; Ortigosa et al., 1993).

Liquefaction is most commonly observed in saturated, loose, cohesionless soils. As indicated in Chapter 2, both the natural and fill soils that have been deposited on top of the dense till beneath the Alaskan Way Viaduct are largely loose and cohesionless. Because these soils are saturated at depths of greater than about 10 feet (3.5 m), they must be considered potentially liquefiable. This chapter presents the results of a detailed evaluation of the liquefaction potential of these soils and discusses the anticipated effects of liquefaction on the seismic vulnerability of the Alaskan Way Viaduct.

6.1 HISTORICAL EVIDENCE OF LIQUEFACTION

Post-earthquake investigations have shown that liquefaction often recurs at the same location when soil and groundwater conditions have remained unchanged (Youd, 1984). Thus, historical evidence of liquefaction can serve as a useful indicator of liquefaction susceptibility. The waterfront fill and tideflat deposits that underly the Alaskan Way Viaduct have not been subjected to severe ground shaking, but they were subjected to moderate shaking during the 1949 and 1965 earthquakes.

Minor effects of liquefaction were observed near the Alaskan Way Viaduct following both the 1949 and 1965 earthquakes (Grant et al., 1992). At Pier 66, the 1949 earthquake "resulted in displacement of the transit shed in a seaward direction. The column displacement amounted to a maximum of about 9 inches in a lesser displacement at the north end of the north portion" (Olsen, 1978). Reports noted that further south, near Pier 36, a

> "concrete wall around a tank farm adjacent to the Duwamish waterway indicated considerable earth movement. One east-west wall about 100 feet long and 12 feet high reveals three vertical construction joints opened 1-5/8, 2, 1-3/4 inches, or a total of 6 inches during or since the quake. The joint filler in a north-south wall was squeezed out a maximum of 3 inches at the bottom of one joint. The wall nearest to the Duwamish waterway and parallel to it has settled 2 inches below adjacent walls and is out of plumb. Lateral and vertical movement of ground is evident" (U.S. Army Corps of Engineers, 1949).

Reports also noted that somewhat to the east of the Viaduct, at 177 SW Massachusetts,

> "Examination of the ground around the Albers Brothers Elevators shows no evidence of settlement except that a number of sand boils developed from 5 to 15 feet [1.5 to 4.6 m] away from the elevators on the northeast side. The ground around a large fuel tank has settled differentially from zero to 1/2 inch (1.3 cm) as evidenced by the soil contact mark" (U.S. Army Corps of Engineers, 1949).

Following the 1965 earthquake, breaks in underground water supply mains were observed near Piers 64 through 66. Such damage is commonly produced by liquefaction in waterfront fill areas. Along Elliot Avenue just north of the Viaduct, the Perfection Smokery building appeared "to have suffered additional damage due to the earthquake in that the front wall... bulged at the northwest corner" (MacPherson, 1965).

Clearly, the effects of liquefaction near the Alaskan Way Viaduct following the 1949 and 1965 earthquakes were modest. However, the levels of shaking in both earthquakes were

relatively low. If either earthquake had produced stronger shaking, or if the duration of shaking of either had been greater, much more liquefaction-induced damage would likely have occurred. It is important to note that the levels of shaking around the Alaskan Way Viaduct in both the 1949 and 1965 earthquakes were well below that anticipated in the present design-level earthquake.

6.2 PREVIOUS INVESTIGATIONS OF LIQUEFACTION POTENTIAL

Liquefaction hazards have been evaluated in conjunction with the design of a number of constructed facilities in the Puget Sound area. In recent years, the U.S. Geological Survey has supported research into the liquefaction characteristics of soils in the Puget Sound and, more specifically, the Seattle area. Though these research investigations were conducted on regional scales, the Alaskan Way Viaduct site is within the regions of interest, and the results of the investigations apply to the site.

Mabey and Youd (1991) used Newmark sliding block analyses to develop an empirical relationship between slope displacement and various ground motion, slope geometry, and soil strength parameters. By combining the results of sliding block analyses for slopes of different geometry and material properties with data from previous subsurface investigations and a digital elevation model of the Seattle South Quadrangle, they were able to identify areas where liquefaction hazards were high. The results of the analyses were used to prepare a map indicating lateral spreading displacements that could be expected in two earthquake scenarios: a magnitude 7.5 event producing a peak acceleration of 0.30 g and a magnitude 7.5 event producing a peak acceleration of 0.15 g. The resulting hazard map is shown in Figure 6.1. The Alaskan Way Viaduct is largely within the most hazardous area, where large lateral spreading displacements are anticipated. While the regional analysis conducted by Mabey and Youd (1991) was not intended to portray liquefaction hazards at specific sites with great accuracy, it indicated that liquefaction hazards near the Alaskan Way Viaduct are considerable.

Grant et al. (1992) also evaluated liquefaction hazards in Seattle. Subsurface data, principally in the form of Standard Penetration Resistances, from over 350 borings in Seattle

were compiled and stored in a digital database. Ground motions corresponding to two deterministic earthquake scenarios, a magnitude 7.5 event producing a peak acceleration of 0.30 g and a magnitude 7.5 event producing a peak acceleration of 0.15 g, were selected. For each of these scenarios, the minimum corrected Standard Penetration Resistance required to resist liquefaction was computed and compared with the SPT data available from the subsurface conditions database. The liquefaction hazard potential was then evaluated using both threshold criteria and thickness criteria. The threshold criteria used the fraction of SPT resistances that were below the threshold values required to produce liquefaction: >50 percent was assigned a high hazard rating; 25 percent to 50 percent was considered to represent moderate hazard; 10 percent to 25 percent was called low hazard; and less than 10 percent was considered very low hazard. The thickness criteria considered computed liquefaction to exist if the cumulative thickness of liquefied soil exceeded 10 feet (3.5 m) for the 0.30 g motion or 3.6 inches (9.1 cm) for the 0.15 g motion. High hazard ratings were assigned when more than 50 percent of the borings showed computed liquefaction. Areas in which 25 percent to 50 percent of the borings showed computed liquefaction were considered to have moderate hazard. Lower percentages were assigned low hazard ratings. Both the threshold and thickness criteria were applied to soil conditions classified as fills, Holocene deposits, and Pleistocene deposits. The fill sites were concentrated around the Duwamish tideflat area, and tests of both the threshold and thickness criteria revealed that they had a high liquefaction hazard. Areas within about 200 feet (61 m) of open bodies of water were singled out as posing even greater hazards on the basis of historical performance and the potential for lateral spreading. Though this study did not explicitly address the fills that exist beneath the Alaskan Way Viaduct, the similarity between those fills and the fills it considered is sufficient that the general conclusions are likely to apply to both.

6.3 SITE-SPECIFIC EVALUATION OF LIQUEFACTION POTENTIAL

To evaluate the potential for liquefaction-induced damage to the Alaskan Way Viaduct, a site-specific liquefaction evaluation was performed. Its purpose was to evaluate the potential for the occurrence of liquefaction and to estimate the effects of liquefaction along the alignment of

the Viaduct. The liquefaction evaluation used the results of the subsurface investigations described in Chapter 2 and the ground response analyses described in Chapter 4.

A complete evaluation of liquefaction hazards addresses three primary issues: the susceptibility of the soil to liquefaction, the potential for initiation of liquefaction, and the effects of liquefaction. The procedures and results of the investigation of each of these issues are described in the following sections.

Liquefaction Susceptibility

The susceptibility of a soil to liquefaction can be evaluated in a number of ways. Geologic origin, composition, stress-density conditions, and historical performance can all be used to evaluate the susceptibility of a soil deposit to liquefaction.

Soil deposits that are susceptible to liquefaction are formed within a relatively narrow range of geological environments (Youd and Hoose, 1977; Youd, 1991). Loose fills, particularly those placed without compaction by settling through water, are very likely to be susceptible to liquefaction. Liquefaction only occurs in saturated soils, so the depth to groundwater also influences liquefaction susceptibility; the effects of liquefaction are most commonly observed at sites where groundwater is within a few meters of the ground surface. As described in Chapter 2, the waterfront fills beneath the Alaskan Way Viaduct were deposited without compaction by dumping soil into the waters of Elliot Bay or by hydraulic filling. The current groundwater level beneath the Viaduct is about 8 to 10 feet (2.4 to 3.5 m). The history and characteristics of the fills along the waterfront of Seattle are similar in many respects to the waterfront fills that liquefied and produced extensive damage in San Francisco in the 1989 Loma Prieta earthquake (Clough and Chameau, 1983; Chameau et al., 1991). Given the available geologic criteria, the waterfront fills beneath the Alaskan Way Viaduct must be considered susceptible to liquefaction.

Because liquefaction requires the development of excess pore pressure, liquefaction susceptibility is influenced by the compositional characteristics that influence volume change behavior. Compositional characteristics associated with high volume change potential tend to be associated with high liquefaction susceptibility. These characteristics include particle size,

shape, and gradation. For many years, liquefaction-related phenomena were thought to be limited to sands. More recently, the bounds on gradation criteria for liquefaction susceptibility have broadened. Liquefaction of non-plastic silts has been observed (Ishihara, 1984; 1985) in the laboratory and in the field, indicating that plasticity characteristics, rather than grain size alone, influence the liquefaction susceptibility of fine-grained soils. Coarse silts with bulky particle shape, which are nonplastic and cohesionless, have been found to be susceptible to liquefaction. Liquefaction susceptibility is also influenced by gradation. Field evidence indicates that most liquefaction failures have involved uniformly-graded soils. As discussed in Chapter 2, the waterfront fills near the Alaskan Way Viaduct consist primarily of clean and silty fine sands of relatively uniform gradation. The silty soil that is present in the fill is nonplastic. Thus, soil composition criteria indicate that the waterfront fill beneath the Alaskan Way Viaduct is susceptible to liquefaction.

Liquefaction susceptibility also depends on the initial state of the soil, i.e., the stress and density characteristics at the time of the earthquake. Because the tendency to generate excess pore pressure of a particular soil is strongly influenced by both density and initial stress conditions, liquefaction susceptibility depends strongly on the initial state of the soil. Though earthquake shaking can induce pore pressures in both loose and dense sands, higher pore pressures are induced and liquefaction is more commonly observed in loose sands. The method of deposition, and the results of the insitu and laboratory tests performed as part of the subsurface investigations, indicate that the waterfront fill beneath the Alaskan Way Viaduct is loose and, consequently, susceptible to liquefaction.

Historical susceptibility criteria (Youd, 1984; 1991) suggest that soils that have previously liquefied are susceptible to liquefaction in the future, particularly in earthquakes that produce stronger shaking than the soil has been subjected to in the past. As discussed in Section 6.1, liquefaction was clearly observed in the waterfront fills near the Alaskan Way Viaduct (and in similarly deposited soils nearby) in both the 1949 and 1965 earthquakes. Thus, historical

criteria indicate that the waterfront fill beneath the Alaskan Way Viaduct is susceptible to liquefaction.

In summary, all of the criteria commonly used to evaluate liquefaction susceptibility indicate that the waterfront fill beneath and near the Alaskan Way Viaduct is susceptible to liquefaction.

Initiation of Liquefaction

Since the liquefaction susceptibility of the waterfront fill soils to liquefaction is well-established, the potential for initiation of liquefaction must be evaluated. Liquefaction is initiated when the amplitude and duration of ground motion are sufficient to cause porewater pressures to rise to a critical level. The amplitude and duration of motion required to initiate liquefaction depend on the characteristics of the soil. Liquefaction may be initiated in very loose soils by low amplitude and/or short duration ground motions; dense soils may require large amplitudes and/or very long durations to develop sufficient pore pressure to initiate liquefaction. Therefore, evaluation of the potential for liquefaction requires comparison of the level of loading produced by the earthquake of interest with the level of loading required to initiate liquefaction in the soil of interest. To make this comparison, the earthquake loading and soil liquefaction resistance must be characterized in a consistent manner.

Characterization of Earthquake Loading

The generation of excess pore pressure that is required to initiate liquefaction is related to the amplitude and duration of earthquake-induced cyclic loading. The cyclic stress approach is based on the assumption that the generation of excess pore pressure is fundamentally related to the cyclic shear stresses; hence seismic loading is expressed in terms of cyclic shear stresses. In this evaluation, cyclic shear stresses were computed as part of the ground response analyses described in Chapter 4.

Earthquakes produce transient and highly irregular shear stresses in soil deposits. To compare this transient loading with the uniform loading commonly used in laboratory

liquefaction tests, the concept of a cyclic stress ratio was developed. The cyclic stress ratio is defined as

$$CSR = \frac{0.65\,\tau_{max}}{\sigma_v'} \qquad \text{Equation 6.1}$$

where τ_{max} is the maximum shear stress induced in the soil and σ_v' is the vertical effective stress prior to the earthquake. The 0.65 term suggests that, for equivalent durations, an irregular time history of shear stress with a peak value, τ_{max}, is equivalent to a uniform (sinusoidal) time history of shear stress with amplitude $0.65\tau_{max}$.

The ground response analyses used to predict the site-specific ground motions described in Chapter 4 were also used to compute the variation of maximum cyclic shear stress with depth for different soil profiles. The shear modulus of the waterfront fill and tideflat deposits, as indicated by shear wave velocity measurements, were indistinguishable. Consequently, peak shear stress profiles were computed for various soft soil thicknesses without regard for the relative thicknesses of fill and tideflat soils. The variation of peak shear stress with depth for various soft soil thicknesses were shown in Figure 4.18

Characterization of Liquefaction Resistance

The liquefaction resistance of soils can be characterized in a number of different ways. Laboratory tests on undisturbed and reconstituted soil samples have been commonly used to measure liquefaction resistance for many years, but they have fallen into disfavor as their inherent limitations have become increasingly recognized. In recent years, the use of insitu tests has become generally accepted as the preferred method to characterize the liquefaction resistance of soils. The detailed subsurface investigation performed as part of this study included three types of insitu tests: standard penetration tests, cone penetration tests, and downhole (seismic cone) shear wave velocity tests. These tests were performed to allow liquefaction resistance to be characterized in terms of three independent insitu test parameters.

Standard Penetration Resistance. Standard Penetration Tests were routinely performed in the subsurface investigation conducted for design of the Viaduct in 1948 and in later

subsurface investigations. Additional Standard Penetration Tests were performed in the supplemental subsurface investigations conducted as part of this project. The total of both subsurface investigations is 284 Standard Penetration Tests performed along the length of the Alaskan Way Viaduct.

To compare the results of the 1948 and 1993 Standard Penetration Tests, several of the 1993 borings were located near the 1948 borings. Comparison of the SPT resistances of these two borings and the SPT resistances of 1948 and 1993 revealed no systematic differences. As a result, the SPT resistances from the 1948 and 1993 subsurface investigations were treated equally in all geotechnical analyses. After anomalously high SPT resistances (for which evidence of obstructions such as gravel, wood chunks, debris, or other material was explicitly noted in the boring logs) were removed, the SPT resistances were corrected for hammer energy and overburden pressure (Chapter 2). The resulting variation of SPT resistance within the waterfront fill and tideflat deposits is shown in Figure 6.2.

Cone Penetration Resistance. Cone Penetration Tests were performed in cone soundings at 16 locations along the length of the Alaskan Way Viaduct. A total of 617 feet (188 m) of cone soundings were obtained during the supplemental subsurface investigations conducted as part of this project. For analysis of liquefaction hazards, the measured CPT resistances were corrected to a standard effective overburden pressure of 1 tsf (100 kPa), as described in Chapter 2. The resulting variation of corrected CPT resistance within the waterfront fill and tideflat deposit is shown in Figure 6.3.

Shear Wave Velocity. Using WSDOT's seismic cone equipment, shear wave velocity measurements were made at the same locations as the CPT measurements. A total of 120 shear wave velocity measurements were made during the supplemental subsurface investigation. The measured shear wave velocities were normalized to a standard effective overburden pressure of 1 tsf (96 kPa), as described in Chapter 2. The resulting variation of corrected shear wave velocity within the waterfront fill and tideflat deposit is shown in Figure 6.4.

Liquefaction Potential.

Liquefaction potential is commonly evaluated by expressing earthquake loading and liquefaction resistance in common terms and then by comparing the values of each. Earthquake loading is most commonly expressed in terms of the cyclic shear stresses (or cyclic shear stress ratios) produced by the earthquake. However, by using empirical relationships between various insitu test parameters and the cyclic stress ratio required to produce liquefaction, earthquake loading can also be expressed in terms of the minimum insitu test parameter value required to resist liquefaction for a particular cyclic stress ratio. The second approach, which allows liquefaction potential to be easily visualized in deposits with variable insitu parameters, was used in the present study. The results of the liquefaction potential analyses are expressed below for each type of insitu test.

Standard Penetration Resistance. The empirical liquefaction resistance relationships of Seed et al. (1985) were used to determine the minimum SPT resistances required to resist liquefaction in the fill and tideflat deposits when they were subjected to the design-level ground motions. Figures 6.5 through 6.10 show the actual measured SPT resistances and the minimum SPT resistances required to resist liquefaction for soft soil thicknesses of 20 to 70 feet (6.1 to 21.3 m). Obviously, the great majority of the corrected SPT resistances were well below the minimum values required to resist liquefaction.

By defining the factor of safety against liquefaction in the conventional manner, i.e., as

$$FS_L = \frac{\text{Cyclic shear stress required to cause liquefaction}}{\text{Equivalent cyclic shear stress induced byearthquake}} \qquad \text{Equation 6.2}$$

a factor of safety can be defined for each SPT data point. By this definition, a factor of safety of less than 1 indicates that liquefaction is expected to occur. In using a moving average with a 10-foot-long triangular weighting function, the average factor of safety against liquefaction varies with depth, as shown in Figure 6.11. Note that the average factor of safety is generally less than 1 to considerable depths; at locations where the soft soil thickness is relatively low, the average

factor of safety is well below 1. The fraction of corrected SPT resistances that fell below the minimum values required to resist liquefaction are shown in Table 6.1. Using SPT resistance as a measure of liquefaction resistance, extensive liquefaction of the waterfront fill and tideflat deposits appears very likely.

Table 6.1. Percentage of SPT resistance values lower than the minimum values required to resist liquefaction

Soft Soil Thickness	Percentage
20 ft (6.1 m)	99%
30 ft (9.1 m)	91% - 97%
40 ft (12.2 m)	78% - 92%
50 ft (15.2 m)	74% - 89%
60 ft (18.3 m)	70% - 80%
70 ft (21.3 m)	64% - 74%

Cone Penetration Resistance. The empirical liquefaction resistance relationships of Mitchell and Tseng (1990) were used to determine the minimum CPT resistances required to resist liquefaction in the fill and tideflat deposits when they were subjected to the design input motions. Figures 6.12 through 6.17 show the actual corrected CPT resistances and the minimum CPT resistances required to resist liquefaction for soft soil thicknesses of 20 to 70 feet (6.1 to 21.3 m). Obviously, the great majority of the measured CPT resistances were well below the minimum values required to resist liquefaction. The fraction of corrected CPT resistances that fell below the minimum values required to resist liquefaction are shown in Table 6.2. Given these CPT resistances, extensive liquefaction of the waterfront fill and tideflat deposits appears very likely.

Table 6.2. Percentage of CPT resistance values lower than the minimum values required to resist liquefaction

Soft Soil Thickness	Percentage
20 ft (6.1 m)	82% - 84%
30 ft (9.1 m)	76% - 78%
40 ft (12.2 m)	71% - 78%
50 ft (15.2 m)	69% - 77%
60 ft (18.3 m)	66% - 75%
70 ft (21.3 m)	63% - 72%

Shear Wave Velocity. The empirical liquefaction resistance relationship of Tokimatsu et al. (1991) was used to determine the minimum shear wave velocities that would be required to resist liquefaction in the waterfront fill and tideflat deposits when they were subjected to the design input motions. Figures 6.18 through 6.23 show the actual corrected shear wave velocities and the minimum shear wave velocities required to resist liquefaction for soft soil thicknesses of 20 to 70 feet (6.1 to 21.3 m) Obviously, the great majority of the corrected shear wave velocities were well below the minimum values required to resist liquefaction. The fraction of corrected shear wave velocities that fell below the minimum shear wave velocities required to resist liquefaction are shown in Table 6.3. Though the fraction of shear wave velocities that were less than that required to resist liquefaction was lower than the corresponding fractions for SPT and CPT resistance, extensive liquefaction of the waterfront fill and tideflat deposits still appears very likely.

Table 6.3. Percentage of shear wave velocity values lower than the minimum values required to resist liquefaction

Soft Soil Thickness	Percentage
20 ft (6.1 m)	48% - 55%
30 ft (9.1 m)	53% - 59%
40 ft (12.2 m)	25% - 60%
50 ft (15.2 m)	13% - 45%
60 ft (18.3 m)	9% - 27%
70 ft (21.3 m)	8% - 21%

Discussion

The potential for initiation of liquefaction was investigated through three independent approaches to the characterization of liquefaction resistance. Each of these independent approaches indicated that extensive liquefaction of the fills and tideflat deposits is likely to occur in response to the design ground motions. It is important to note that the waterfront fill and tideflat deposits are so loose that less severe ground motions could also cause extensive liquefaction. An approximate analysis suggests that widespread liquefaction could be produced by a ground motion with a 50 percent probability of exceedance in a 50-year period, i.e., a ground motion five times more likely than the design ground motion.

As a check on the procedures used in these liquefaction potential analyses, identical analyses were performed using measured ground motions from the 1965 earthquake. For these analyses, the input motion was taken as the ground motion measured at the Federal Building in Seattle multiplied by a factor of 1.5 to approximately account for the effects of soil-structure interaction inherent in the recorded motion. The peak ground surface acceleration of the resulting motion was approximately 0.12 g. The results of the liquefaction analyses, expressed in terms of the SPT resistances required to resist liquefaction, are presented in Figures 6.24 through 6.29. Obviously, some of the measured SPT resistances were below the minimum values required to resist liquefaction, but most were above (except for 20 feet (6.1 m) of waterfront fill). The fraction of measured SPT resistances that fell below the estimated minimum values required to resist liquefaction in the 1965 earthquake are shown in Table 6.4.

Table 6.4. Percentage of SPT resistance values lower than the minimum values required to resist liquefaction for the 1965 Seattle-Tacoma earthquake motion.

Soft Soil Thickness	Percentage
20 ft (6.1 m)	56% - 68%
30 ft (9.1 m)	37% - 48%
40 ft (12.2 m)	50% - 52%
50 ft (15.2 m)	48% - 50%
60 ft (18.3 m)	44%
70 ft (21.3 m)	36%

A weighted average of the factor of safety with depth is shown in Figure 6.30. These analyses indicated that limited occurrence of liquefaction should have occurred in the 1965 earthquake, and only occasional evidence should have been observed at the ground surface. The fact that the observed effects following the 1965 earthquake were consistent with this modeled behavior supports the validity of the procedures used to evaluate liquefaction potential.

Effects of Liquefaction

The results described in the previous sections revealed that the waterfront fills beneath the Alaskan Way Viaduct are susceptible to liquefaction and that the design-level ground motions are likely to trigger widespread liquefaction. Therefore, the researchers needed to evaluate the potential effects of liquefaction on the Alaskan Way Viaduct and the area that surrounds it.

Liquefaction has caused extensive damage to waterfront structures and nearby facilities in earthquakes around the world. This damage has resulted primarily from movements of liquefied soil and from reductions in soil strength near foundations and retaining structures. All of these potential causes of damage are relevant to the Alaskan Way Viaduct site and are discussed in the following sections.

Development of Sand Boils

The cyclic shear stresses and strains induced by earthquake shaking generate positive excess porewater pressures in saturated, liquefiable soils. Beneath a level ground surface, such as the surface below the Alaskan Way Viaduct, these excess pore pressures are dissipated predominantly by the upward flow of porewater. If the hydraulic gradient driving the flow reaches a critical value, the vertical effective stress can drop to zero and the soil can reach a quick condition. In such cases, the water velocities may be sufficient to carry soil particles to the surface. In the field, soil conditions are rarely uniform, so the escaping porewater tends to flow at high velocity through localized cracks or channels. Sand particles can be carried through these channels and ejected at the ground surface to form sand boils.

The potential for development of sand boils depends on the level of excess porewater pressure generated in the soil, the thickness of the soil in which high porewater pressures are generated, and the thickness of the overlying soil. Ishihara (1985) developed an empirical relationship between excess porewater pressure and the factor of safety against liquefaction. Applying this relationship to the individual factors of safety corresponding to each of the SPT tests and applying a 10-ft-long (3.5-m-long) triangular moving average to the results produces the anticipated pore pressure ratio ($r_u = \Delta u/\sigma'_{vo}$) profiles shown in Figures 6.31 through 6.36. Ishihara (1985) examined the soil conditions associated with various liquefaction-related damage reports from two large Japanese earthquakes and estimated the thickness of the overlying layer required to prevent level-ground liquefaction-related damage. Considering the depth of the water table beneath the Alaska Way Viaduct, sand boils are expected along most of its length.

Post-Earthquake Settlement

Earthquake-induced stresses and strains cause densification of dry, cohesionless soils (seismic compaction) and the buildup of porewater pressures in liquefiable soils. As porewater pressures dissipate after an earthquake, the soil reconsolidates. The volumetric strain that results from densification of dry soil and reconsolidation of saturated soil is manifested at the ground surface as settlement. The magnitude of the settlement depends on the level of porewater pressure generated during the earthquake.

Seismic Compaction of Fill Above the Water Table

The densification of dry sands subjected to earthquake loading depends on (1) the density of the sand (2) the amplitude of the cyclic shear strain induced in the sand and (3) the number of cycles of shear strain applied during the earthquake (Silver and Seed, 1971). For the fill material above the water table at the Alaskan Way Viaduct site (in approximately the upper 10 feet (3.5 m)) settlements were estimated from the corrected SPT resistances (based on field measurements) and computed cyclic shear strains (based on site-specific ground response analyses) (Tokimatsu and Seed, 1987). The computed settlements are indicated in Table 6.5.

Table 6.5. Computed settlements due to seismic compaction of fill above water table.

Soft Soil Thickness (ft)	Computed Settlement (in)
10 ft (3.1 m)	0.87 in (2.2 cm)
20 ft (6.1 m)	0.64 in (1.6 cm)
30 ft (9.1 m)	0.26 in (0.7 cm)
40 ft (12.2 m)	0.11 in (2.8 mm)
50 ft (15.2 m)	0.10 in (2.5 mm)
60 ft (18.3 m)	0.08 in (2.0 mm)
70 ft (21.3 m)	0.07 in (1.8 mm)

Settlement of Soil Below the Water Table

The post-earthquake densification of saturated sands is influenced by (1) the density of the sand (2) the maximum shear strain induced in the sand and (3) the amount of excess pore pressure generated by an earthquake. Using the corrected SPT resistance to characterize the density of the waterfront fills and tideflat deposits, post-earthquake settlements of these saturated soils were calculated with two independent procedures.

Tokimatsu and Seed (1987) used a correlation between corrected SPT resistance and relative density, and an estimate of the shear strain potential of liquefied soil (Seed et al., 1984) to estimate the volumetric strain after liquefaction directly from the cyclic stress ratio and corrected SPT resistance. Ishihara and Yoshimine (1992) used results from cyclic simple shear and cyclic triaxial tests that measured the volumetric strain after liquefaction as a function of relative density, along with correlations between SPT and CPT resistance and relative density, to predict post-liquefaction volumetric strain. This procedure also indicates that negligible settlement of the till will occur. Anticipated settlements of the saturated soils above the till are given in Table 6.6. Post-earthquake settlement of the till is expected to be negligible.

The computed settlements shown in Tables 6.5 and 6.6 should be added together to obtain the anticipated post-earthquake ground surface settlements at different locations along the length of the Viaduct. These anticipated settlements are considerable and could impose substantial downdrag loads on the existing pile foundations as the liquefied soil reconsolidated. Substantial vertical loads from the soil above the pile caps could also be transmitted to the piles.

Table 6.6. Computed settlements of saturated waterfront fill and tideflat deposits following design-level earthquake.

Soft Soil Thickness	Computed Post-Earthquake Ground Surface Settlement		
	Tokimatsu and Seed (1987)	Ishihara and Yoshimine (1992)	Average
20 ft (6.1 m)	3.7 in (9 cm)	4.5 in (11 cm)	4.1 in (10 cm)
30 ft (9.1 m)	7.4 in (19 cm)	8.4 in (21 cm)	7.9 in (20 cm)
40 ft (12.2 m)	12.1 in (31 cm)	13.0 in (33 cm)	12.5 in (32 cm)
50 ft (15.2 m)	17.3 in (44 cm)	17.7 in (45 cm)	17.5 in (44 cm)
60 ft (18.3 m)	21.3 in (54 cm)	20.9 in (53 cm)	21.1 in (54 cm)
70 ft (21.3 m)	24.9 in (63 cm)	24.5 in (62 cm)	24.7 in (63 cm)

Vertical Foundation Movements

Subsurface investigations have shown that the relatively soft waterfront fill and tideflat soils are underlain by very dense, glacially overconsolidated, cohesionless soils. Pile driving records suggest that the piles that support the Alaskan Way Viaduct do not penetrate far—typically 2 feet to 3 feet (61 cm to 90.5 cm)—into the underlying dense soils. As a result, the vertical capacity of the piles depends on mobilization of the shear strength of the soil in the upper portion of the dense, cohesionless soil.

The excess porewater pressure in the dense soil underlying the soft waterfront and tideflat deposits would be much lower than that in the overlying soils at the end of an earthquake. As a result, the hydraulic gradient in the lower portion of the softer soils would initially cause water to flow down into the dense soil. The excess porewater pressure in the underlying dense soil would therefore continue to increase after earthquake shaking had ended before the pressure would eventually dissipate. Since these soils are cohesionless, their shear strength would be reduced by the increased porewater pressure. If the strength was reduced sufficiently, the bearing capacities of the piles could be reduced below the values required to support the Viaduct, resulting in significant vertical settlements of the pile foundations. Because the permeabilities of the waterfront fill and tideflat soils immediately above the dense soils appear to vary substantially over relatively short distances, these movements could be highly irregular. Note that these movements would be expected to occur at some time after earthquake shaking had ended.

As illustrated in Figures 6.31 through 6.36, earthquake-induced porewater pressures are expected to reach high values in the waterfront fill and tideflat deposits. An independent estimate of earthquake-induced porewater pressures was obtained with the nonlinear, effective stress-based, ground response analysis program TESS3 (Pyke, 1985; 1993). TESS3 predicts the generation of excess porewater pressure during earthquake shaking and also the pressure's redistribution and dissipation during and after shaking. As illustrated in Figure 6.37 through 6.42, the generated porewater pressures were consistent with those obtained from the empirical procedure used to develop Figures 6.31 through 6.36. Figures 6.37 through 6.42 show the variation of excess porewater pressure with depth both during and after earthquake shaking. The major soil units were assumed to have uniform permeability characteristics in theses analyses.

Figures 6.37 through 6.42 also show the variation of excess porewater pressure with time at a depth of 2.5 feet (76 cm) below the top of the glacial till. These figures show clearly that high porewater pressures could develop at and below the tips of the Alaskan Way Viaduct piles after earthquake shaking had ended. The bearing capacities of these piles would likely be substantially reduced. Given the loss of skin resistance caused by liquefaction, the subsequent downdrag caused by reconsolidation of the overlying liquefied soil, and the additional vertical load due to the weight of the soil above the pile caps, bearing capacity failure of the pile foundations could occur at a number of locations. Pile capacity analyses indicate that bearing capacity failures could develop if pore pressure ratios in the soil beneath the tips of the piles exceed values of 0.55 to 0.60. The spatial distribution of these bearing capacity failures is impossible to predict; however, the observed randomness of the waterfront fill characteristics suggests that foundation failures could occur at footings adjacent to footings that did not fail, thereby imposing substantial differential settlements on the Viaduct.

Transverse Stability and Lateral Foundation Movements

The dynamic lateral displacements of the Alaska Way Viaduct during earthquake shaking will depend on the foundation stiffness and damping characteristics described in Chapter 5. These dynamic displacements are measured relative to the average free-field soil displacements.

For perfectly level sites underlain by liquefiable soil, very little permanent lateral soil displacement would be expected. However, for sloping sites or sites near a vertical face, static driving stresses could lead to the development of substantial permanent lateral free-field displacements caused by flow liquefaction or lateral spreading. Such lateral displacements could be particularly damaging to pile-supported structures. Because a large portion of the Alaska Way Viaduct is near the eastern edge of Elliot Bay, significant permanent lateral soil displacements are possible.

Influence of the Sea Wall. Evaluation of earthquake-induced permanent lateral displacements in liquefiable soils is extremely difficult. At this point, the geotechnical engineering profession is only able to provide rough estimates of permanent lateral displacements under the simplest and most uniform conditions. When complicating factors are present, estimation of permanent lateral displacements becomes even more difficult. Evaluation of permanent lateral displacements near the Alaskan Way Viaduct is complicated by the presence of the seawall described in Chapter 2. Because the waterfront fill and tideflat deposits are so loose and susceptible to liquefaction, they will be prone to significant permanent lateral displacements. Similar liquefiable soils have been involved in flow slides in past earthquakes with tens of feet of permanent lateral displacement. However, the extent of the displacements of the waterfront fill at the site of the Alaskan Way Viaduct will be limited by the presence of the seawall. The permanent lateral displacement of the soils immediately beneath the Viaduct will be limited by the permanent lateral displacement of the seawall.

The seawall, as illustrated in Figure 2.3, is a complicated structure that includes a timber pile-supported relieving platform. As-built drawings could not be located, but design drawings and written descriptions of construction (Engineering News-Record, 1934) indicated that the relieving platform is supported by both vertical and battered timber piles. 12-inch by 12-inch horizontal cap beams between the relieving platform and the tops of the piles connect the vertical piles in rows parallel to the wall. Battered piles appear to fit into shallow notches on the bottom of the 12-inch by 16-inch beams that extend back from the face of the seawall. The piles appear

to be connected to the relieving platform by 24-inch long drift bolts that extend through the relieving platform and into the centers of the piles. The current conditions of the piles, relieving platform, and their connections after some 50 years of service are not known.

Detailed analysis of the seismic vulnerability of the seawall was beyond the scope of the current investigation. However, on the basis of a review of the design drawings, the following general observations can be made.

1. Driving the timber piles that support the relieving platform is likely to have densified the waterfront fill that existed beneath the relieving platform through the combined effects of displacement and vibration.

2. The sheetpiling that retains the waterfront fill beneath the precast concrete wall section does not appear to penetrate far into the underlying dense glacial till. Historically, lack of adequate sheetpile penetration has been a significant factor in the failure of waterfront retaining structures during earthquakes.

3. The connections between the piles and the relieving platform appear to be tenuous, and they might not remain intact during an episode of strong earthquake shaking.

4. It seems unlikely that the vertical and battered timber piles that support the relieving platform and provide resistance to lateral earth pressures would have been driven more than a few feet into the dense soil underlying the waterfront fill. Consequently, the bearing capacities of these piles could be significantly reduced because of redistribution of porewater pressure during and following strong earthquake shaking.

5. The seawall appears to have been designed to resist lateral earth pressures on the basis of static loading conditions. Liquefaction of the waterfront fill and tideflat deposits would be expected to impose considerably greater lateral pressures on the seawall. Lateral pressures exerted by liquefied soil could be up to 3 times greater than the static lateral earth pressures.

Despite the beneficial effects of densification noted in Item 1 above, it appears likely that the seawall would be damaged by strong earthquake shaking such as that associated with the design-level earthquake. The precise nature of the damage is difficult to predict, but it appears likely that significant permanent lateral displacements would be involved. There is ample historical precedent for the occurrence of such damage under similar circumstances; several examples are briefly described below.

1. The 1964 Niigata earthquake (M=7.5) caused catastrophic damage to many sheet pile quay walls at Fishery Pier in the Niigata Port area (Hamada, 1992). The quay walls were constructed by driving steel sheet piles in front of existing, concrete

piers. From the epicenter located approximately 31.1 miles (50 km) from the port, the earthquake delivered peak ground accelerations for the entire city ranging from 0.08g to 0.25g. The backfill at the pier typically consisted of medium fine sand with SPT resistances of less than or equal to 10 to about 33 feet (10 m) below the ground surface. As a result of liquefaction, a great portion of this wall slid some 6 to 12 feet (2 to 4 m) towards the water and sank. The ground surface also subsided by about 3 to 9 feet (1 to 3 m).

2. In 1983, the Nihonkai Chubu earthquake (M=7.7) caused damage to quay walls at Akita Port, located some 63 miles (100 km) from the epicenter (Iai and Kameoka, 1993). The quay walls were anchored bulkheads consisting of steel sheet piles attached by a 65.6-foot (20-m) long, high-strength steel tie rod to a continuous anchor supported by pairs of steel pipe piles. The backfill, within approximately 33 feet (10 m) of the ground surface, consisted of clean, uniform sand placed by pluviation through water. This backfill had SPT resistances of less than or equal to 10. The earthquake, which produced peak accelerations of 0.24 g at a nearby site, caused gradual lateral and vertical deformations of the wall and anchor. Lateral displacements of both the wall and anchor were generally between about 5 feet (1.5 m) and 6.5 feet (2.0 m). The ground surface immediately behind the sheet pile wall settled up to 5 feet (1.5 m).

3. The 1983 Nihonkai Chubu earthquake also caused the displacement and inclination of concrete caisson quay walls at Gaiko Wharf in Akita Harbor (Hamada, 1992). The quay wall of Pier C was made of caissons 52.5 feet (16 m) long, 42.6 feet (13 m) wide, and 47.6 feet (14.5 m) high. The subsurface of a borehole taken near this location consisted of medium sand with typical SPT-values of N less than or equal to 10 to a depth of approximately 46 feet (14 m) below the ground surface. The earthquake caused up to 5 feet (1.5 m) of seaward displacement and up to 3 degrees of inclination to the caissons.

4. The Chilean earthquake of 1985 consisted of two main shocks that were delivered within 11 seconds of each other and damaged many waterfront retaining structures at the Ports of Valparaiso and San Antonio (Ortigosa et al, 1993). An example was a newly constructed anchored bulkhead consisting of sheet pile walls connected to concrete anchor blocks by 82-foot (25-m) long, 2.56-inch diameter (65-mm) tie rods at Berth 3 in the Port of San Antonio. The backfill for this structure, which extended to depths of approximately 33 feet (10 m) below the ground surface, ranged from nonplastic fine sands to rockfills poured over the seabed without special compaction techniques. SPT resistances for this material were less than or equal to 20. The earthquake delivered a maximum peak ground acceleration of 0.67g for the N10E component at a recording site about 2.8 miles (4.5 km) away from San Antonio, and caused seaward deformations at the copeline ranging from 21.7 to 47.2 inches (55 to 120 cm). Post-earthquake investigations revealed a lack of tension in the tie-rods, which implied a seaward displacement of the segmented deadman beam. The tie rods, however, exhibited vertical and horizontal maximum displacements of up to 20 inches (50 cm), and some segments of the deadman beam tilted vertically and horizontally up to 4.5 degrees.

5. In 1986, the Kalamata earthquake (M = 6.2) caused damage to quay walls at the Port of Kalamata, located approximately 7.5 miles (12 km) south of the epicenter (Pitilakis and Moutsakis, 1989). The damaged quay walls were gravity retaining walls about 38 feet (11.6 m) long founded through 8.2 to 9.8 feet (2.5 to 3.0 m) of silty sand and sandy gravel overlain by loose, sandy backfill. The total weight of

the quay wall was 48 ton/ft (1400 kN/m), but buoyancy effects made the effective unit weight 29 to 31 tons/ft (850 to 900 kN/m). The main shock of the earthquake delivered peak accelerations of approximately 0.27 g and caused horizontal displacements in the quay wall of about 5.9 +/- 2.0 inches (15 +/- 5 cm) after surface measurements. The quay wall also rotated 4 to 5 degrees toward the sea. Within 30 to 40 feet (9 to 12 m) of the wall face, the backfill subsided up to 7.9 inches (20 cm), with the surface settlements decreasing with increasing distance from the face of the wall. The quay wall was not put out of service by these deformations.

Previous Lateral Displacement Estimate. As part of a research project supported by the U.S. Geological Survey, Mabey and Youd (1991) mapped maximum expected permanent lateral spreading displacements throughout the Seattle south quadrangle for two different earthquake scenarios. For a magnitude 7.5 earthquake producing a peak horizontal acceleration of 0.30 g, permanent lateral displacements exceeding 100 inches (2.54 m) were predicted for all but the southernmost end of the Alaskan Way Viaduct. Maximum permanent lateral displacements of 14 to 100 inches (36 cm to 2.54 m) were predicted for a magnitude 7.5 earthquake with 0.15 g peak horizontal acceleration.

Lateral Stability Evaluations. In an attempt to bound the level of permanent lateral displacements that could occur at the location of the Alaskan Way Viaduct, a series of lateral displacement calculations were performed. The calculations used a variety of existing methods for estimating permanent lateral displacements of liquefied soils. However, none of the methods was directly applicable to the conditions that exist at the Alaska Way Viaduct site. Their resulting lack of accuracy must be considered when their results are interpreted.

Estimation of permanent lateral displacements is complicated by the presence of the seawall. Because the structural integrity of the seawall is unknown and cannot be assured, it was treated in an approximate, but conservative, manner in these calculations. Any available structural resistance to lateral deformation was neglected; instead, the waterfront fill below the relieving platform was treated as a densified fill. Given the volume of the timber piles that were driven through the fill and the volume of the zone below the relieving platform, the densified fill was assumed to be 7.4 percent greater than the original waterfront fill. Assuming that the difference between the maximum and minimum void ratios of the waterfront fill was typical of

that for similar materials (Holtz and Kovacs, 1981) and using the relative density-SPT resistance correlation of Marcuson and Bieganousky (1977), the corrected SPT resistance of the densified fill was estimated to be approximately 21.

Several available methods for estimating permanent lateral displacements are based on the residual (or steady state) shear strength of the liquefied soils. Evaluation of the residual strength of liquefied soils is one of the most challenging tasks in contemporary geotechnical earthquake engineering; it is not presently possible to estimate residual strengths with great accuracy. Residual strengths are most commonly determined by correlation to insitu test parameters. Correlations between residual strength and SPT resistance based on back-calculation of actual liquefaction failures are most commonly used. For the purposes of stability analysis and lateral displacement estimation, low-, mid-, and high-range estimates of residual strength were obtained from the correlation of Seed and Harder (1990). The low-, mid-, and high-range strengths for the loose waterfront fill were 100 psf (48 kPa), 305 psf (146 kPa), and 570 psf (273 kPa), respectively. The corresponding values for the densified waterfront fill were 1070 psf (512 kPa), 1345 psf (644 kPa), and 1620 psf 776 kPa), respectively.

If the residual strength of a liquefied soil is smaller than the shear stresses required to maintain static equilibrium, flow sliding may occur. Flow slides are characterized by large and rapid permanent lateral displacements and can cause tremendous damage to constructed facilities. To evaluate the potential for flow slide development, a series of limit equilibrium stability analyses was performed. The stability analyses were performed for an idealized profile that corresponded to the transverse soil profile near Columbia Street shown in Figure 2.7.

A series of noncircular potential failure surfaces were analyzed using low-, mid-, and high-range residual strengths for the loose waterfront fill and densified waterfront fill. The waterfront fill above the water table was assumed, on the basis of the triaxial tests described in Chapter 2, to have a constant friction angle of 30°. The stability of seven potential failure surfaces, each of which extended to different distances behind the face of the wall, was analyzed using Spencer's method (Spencer, 1967). The results of the stability analyses are shown in

Figure 6.43. The stability analyses indicated that, even for the low-range residual strengths, large-scale flow sliding is unlikely. However, this result does not preclude the possibility of large lateral deformations developing as a result of lateral spreading.

Permanent Lateral Displacement Estimation. Though currently available procedures for estimating permanent lateral displacements of liquefied soils are very approximate, they can provide at least a general indication of the levels of permanent lateral displacement that can be expected at a particular site. In an attempt to obtain a rough estimate of the range of permanent lateral displacement of the Columbia Street section, several approaches were used.

- Hamada et al. Approach

  Hamada et al. (1986) investigated permanent lateral displacements due to lateral spreading in a number of earthquakes in Japan. Empirical analyses suggested a very simple procedure for estimating displacements on the basis of slope height and slope angle. The Hamada et al. approach suggested that permanent lateral displacements of the Columbia Street section on the order of 12 feet (3.7 m) may be possible.

- Lucia et al. Approach

  To estimate the runout distances of liquefied soils, with emphasis on the types of materials stored in mine tailings ponds, Lucia et al. (1981) developed a strength- and volume-compatible limit equilibrium analysis that was calibrated against numerous tailings pond failures. Use of the Lucia et al. procedure with a volume-weighted average residual strength produced the following estimated wall face displacements:

Residual Strength	Displacement
Low-range	117 ft (35.7 m)
Mid-range	0 ft (0 m)
High-range	0 ft (0 m)

The procedure is very approximate, but it does suggest that significant permanent lateral displacements could develop if the actual residual strengths were much lower than the mid-range estimated strengths.

- Bartlett and Youd Approach

Bartlett and Youd developed empirical correlations for estimating permanent lateral displacements due to lateral spreading from lateral spreading case histories. Some of the conditions that exist at the Alaska Way Viaduct lie outside the recommended range of conditions for application of the Bartlett and Youd correlation, so its results must be interpreted with caution. The correlation depends on earthquake magnitude and distance, as well as on a variety of material and geometric parameters. For a failure surface that extends back as far as the Viaduct, the Bartlett and Youd approach estimated the following permanent lateral displacements for a magnitude 7.5 earthquake at different distances from the site:

Distance (km)	Displacement
6.2 miles (10 km)	56 ft (17 m)
12.4 miles (20 km)	20 ft (6 m)
31.0 miles (50 km)	3 ft (1 m)
62.0 miles (100 km)	4 in (0.1 m)

- Byrne Approach

Another approach to estimating permanent lateral displacements was proposed by Byrne et al. (1992). By estimating the effective stiffnesses of a potentially liquefiable soil before and after liquefaction, stress-deformation analyses can be used to estimate the permanent deformations associated with a reduction of soil stiffness due to liquefaction. The Byrne et al. approach was applied to a discretized idealization of the Columbia Street profile with the finite element analysis program ANSYS. By assuming a zero displacement boundary condition (pinned nodal points) along the bottom of the waterfront fill and neglecting any resistance that might be provided by the structural

elements of the seawall, the analysis produced the estimated deformed shapes of the Columbia Street profile before and after liquefaction shown in Figure 6.44. This analysis shows approximately 3.6 ft (1.1 m) of permanent lateral displacement at the top of the seawall and approximately 2.6 ft (79 cm) of permanent lateral ground surface displacement near the Alaska Way Viaduct.

The Byrne et al. (1992) analysis, though very approximate, is the only method that relates the lateral displacement at the location of the Alaska Way Viaduct to the lateral displacement at the face of the wall. For the boundary conditions described above, the permanent lateral displacement at the Viaduct is about 70 percent to 75 percent of the displacement at the face of the seawall.

Summary of Permanent Lateral Displacement Predictions. All available methods for estimating permanent lateral displacements of liquefied soils are very approximate. Furthermore, the conditions along the Seattle waterfront near and seaward of the Alaskan Way Viaduct make application of these methods difficult. For that reason, none of the individual analyses can be assumed to be very accurate. However, considered as a group, the analyses suggest that large, permanent lateral displacements of the liquefied soil are not only possible, but probably very likely. When combined with observations of the effects of previous earthquakes, both in Seattle and in other parts of the world, the analyses indicate that significant permanent lateral displacements of the soil near and beneath the Alaska Way Viaduct should be expected during and following an earthquake that produces the design-level ground motion.

Effects of Lateral Soil Displacements on Pile Foundations

The lateral displacement of soils during lateral spreading imposes lateral loads on pile foundations. The magnitude and distribution of these loads depend on the relative stiffnesses of the soil and the pile, and on the displacement pattern of the soil. Piles that are flexible (relative to the soil) will tend to assume the same deformed shape as the soil profile. Because the relative displacement between the pile and soil is small, the soil-induced lateral loads on the pile are

illustrates, the pile generally followed the free-field soil displacements. The flexural stiffness of the pile allowed it to maintain a straighter shape than the free-field displacement profile, but it also caused the pile to displace slightly more than the free-field at the ground surface. Computed bending moment, shear, and soil resistance profiles for the same case are presented in Figures 6.46-6.48. Maximum curvatures for piles of various flexural stiffnesses (for pinned and fixed head conditions) are shown in Figures 6.49 and 6.50. These curves assume linear elastic pile behavior; they can be used to determine whether piles of given flexural stiffnesses will be loaded beyond their elastic limits. Analysis of typical piles indicates that lateral spreading displacements of 10 to 12 inches (25 to 30 cm) would cause flexural failure of many piles; lateral spreading displacements of 24 inches (60 cm) would produce ultimate bending moments in most piles.

6.4 SUMMARY

Liquefaction is one of the most common causes of damage to structures and facilities in seismically active areas. A detailed evaluation of the liquefaction potential of the soils beneath and near the Alaskan Way Viaduct indicated that they are highly susceptible to liquefaction. Analyses of the anticipated response of these soils to the design-level ground motion indicated that widespread liquefaction will occur in the waterfront fill and tideflat deposits. The effects of this liquefaction are expected to include post-earthquake settlement of the ground surface, variable settlement of the pile foundations with possible loss of bearing capacity, and permanent lateral displacement of the liquefied soil. Though the level of permanent lateral soil displacement cannot be predicted accurately, available evidence suggests that the displacements will be large enough to cause substantial damage to the existing pile foundations that support the Viaduct.

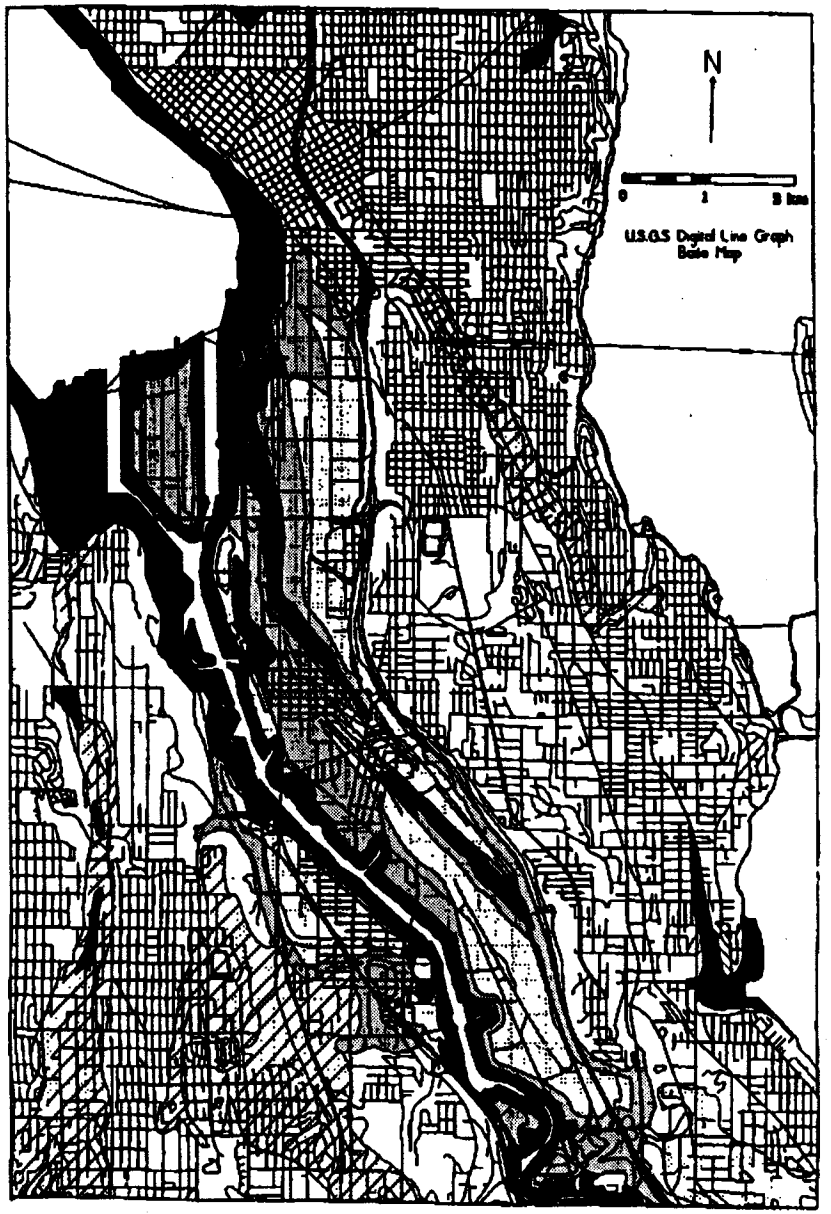

	Scenario Earthquake #1	Scenario Earthquake #2
M	7.5	7.5
a_{max}	0.30 g	0.15 g
	Displacement (in.)	
	>100	14 - 100
	84 - 100	6 - 48
	45 - 84	2 - 12
	10 - 45	0 - 4
	Little liquefaction susceptibility but in areas with steep slopes. Liquefaction is unlikely, but if it were to occur, large displacements are possible.	
	No displacement likely due to liquefaction.	

Figure 6.1. Map of Lateral Spreading Displacement Hazard for the Seattle South Quadrangle (Displacements indicated by legend represent maximum expected lateral spreading displacements (After Mabey and Youd, 1991)

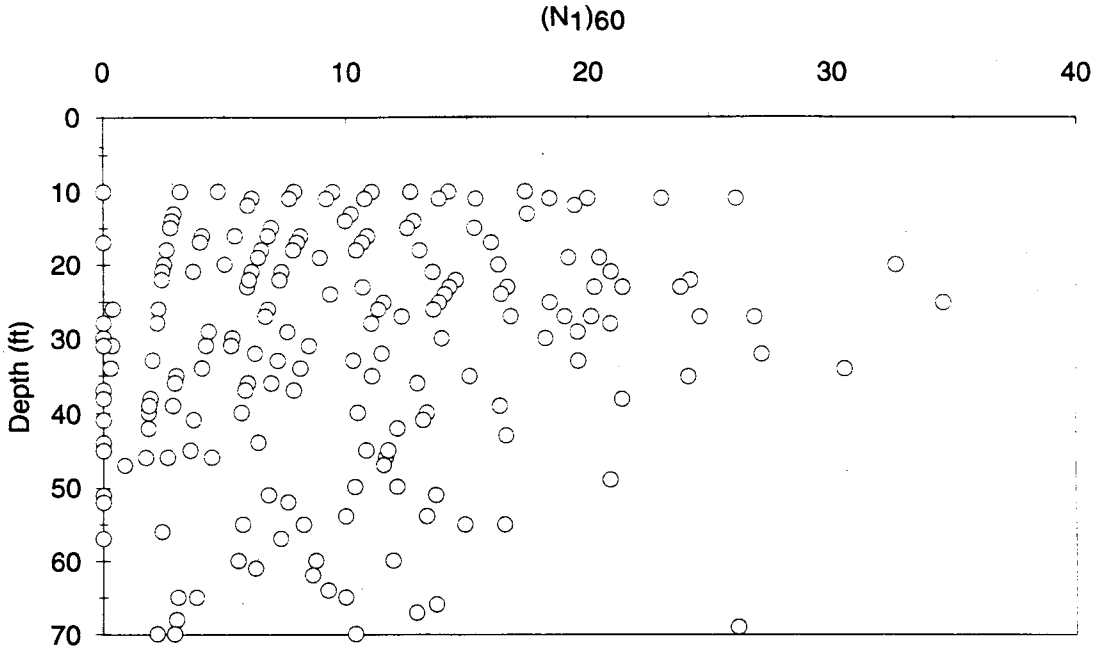

Figure 6.2. Corrected SPT Resistances Used for Liquefaction Analyses of Saturated Soils

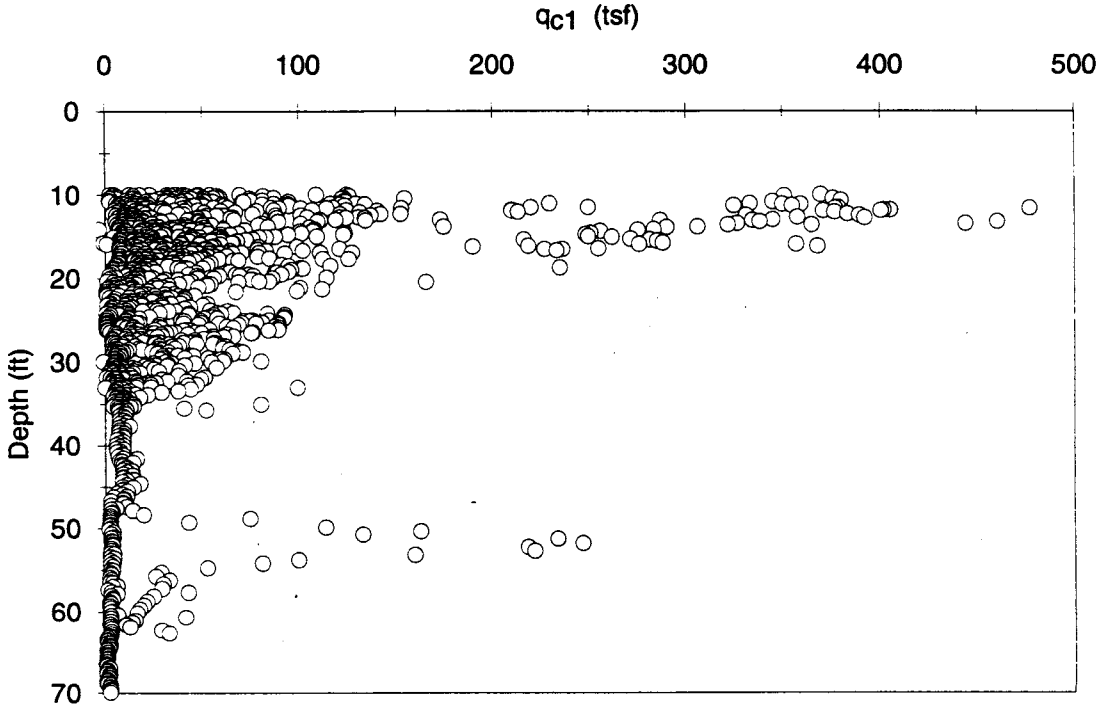

Figure 6.3. Corrected CPT Tip Resistances Used for Liquefaction Analyses of Saturated Soils

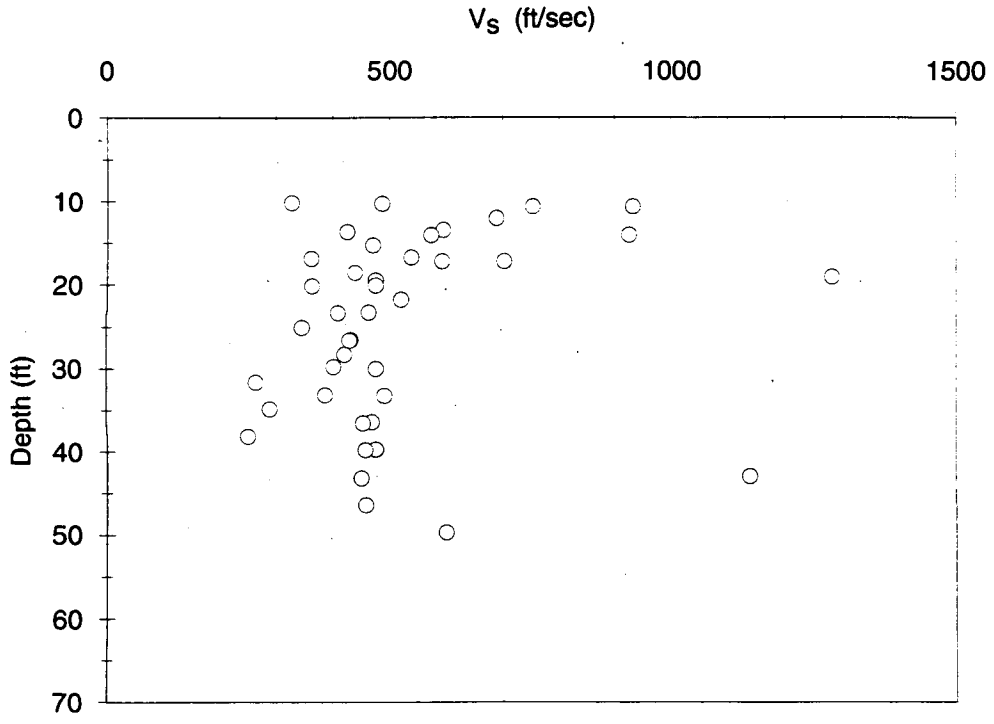

Figure 6.4. Corrected Shear Wave Velocities Used for Liquefaction Analyses of Saturated Soils

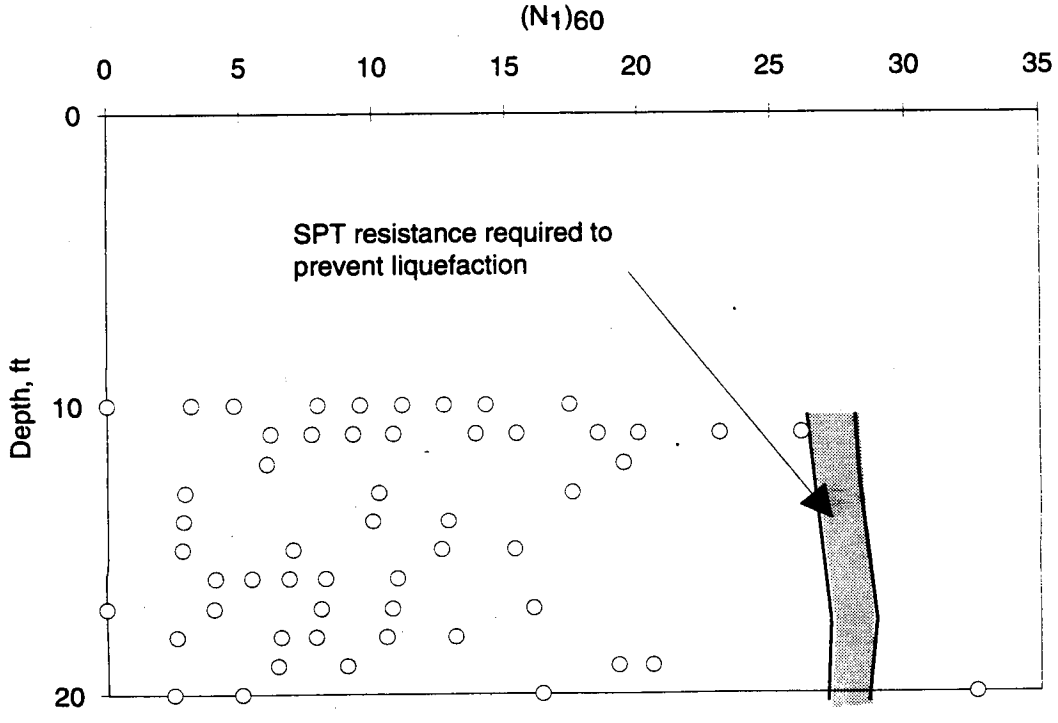

Figure 6.5. Comparison of Measured SPT Resistances with SPT Resistance Required to Resist Liquefaction for 20 Ft Soft Soil

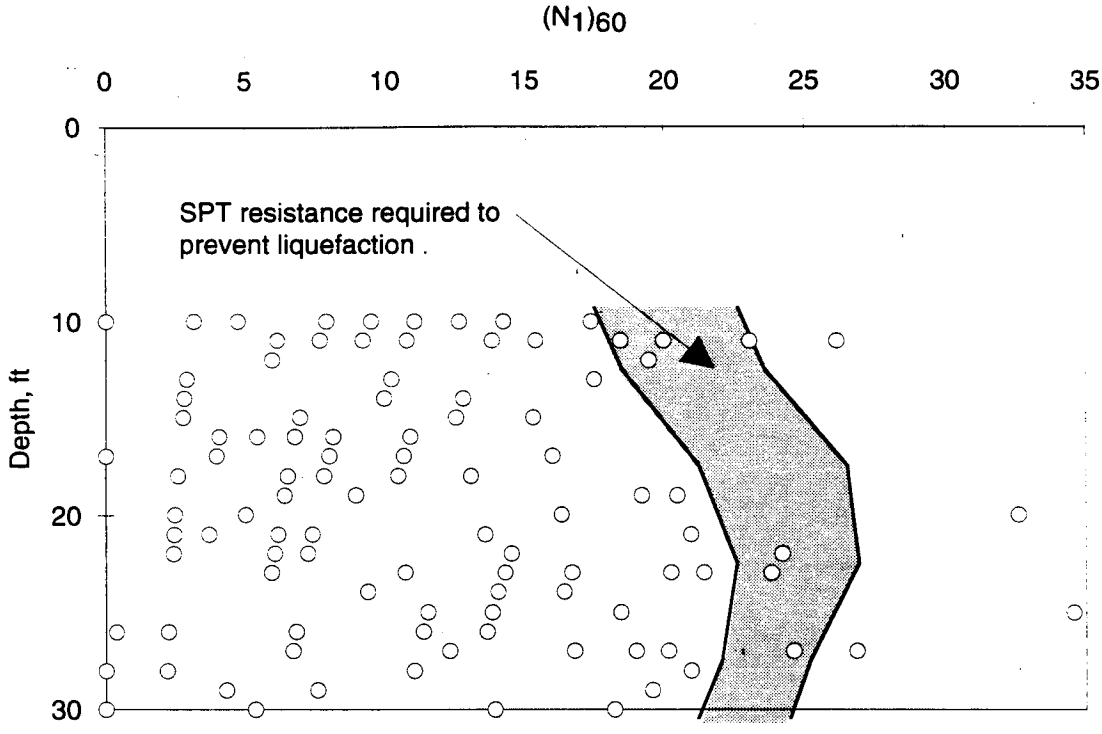

Figure 6.6. Comparison of Measured SPT Resistances with SPT Resistance Required to Resist Liquefaction for 30 Ft Soft Soil

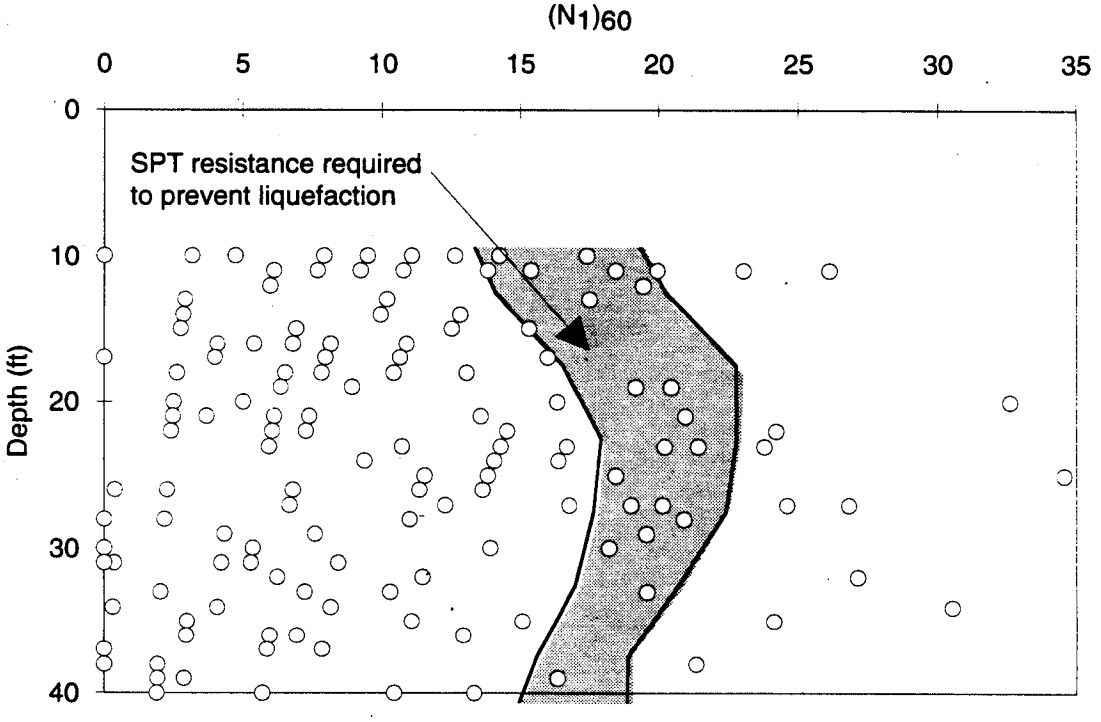

Figure 6.7. Comparison of Measured SPT Resistances with SPT Resistance Required to Resist Liquefaction for 40 Ft Soft Soil

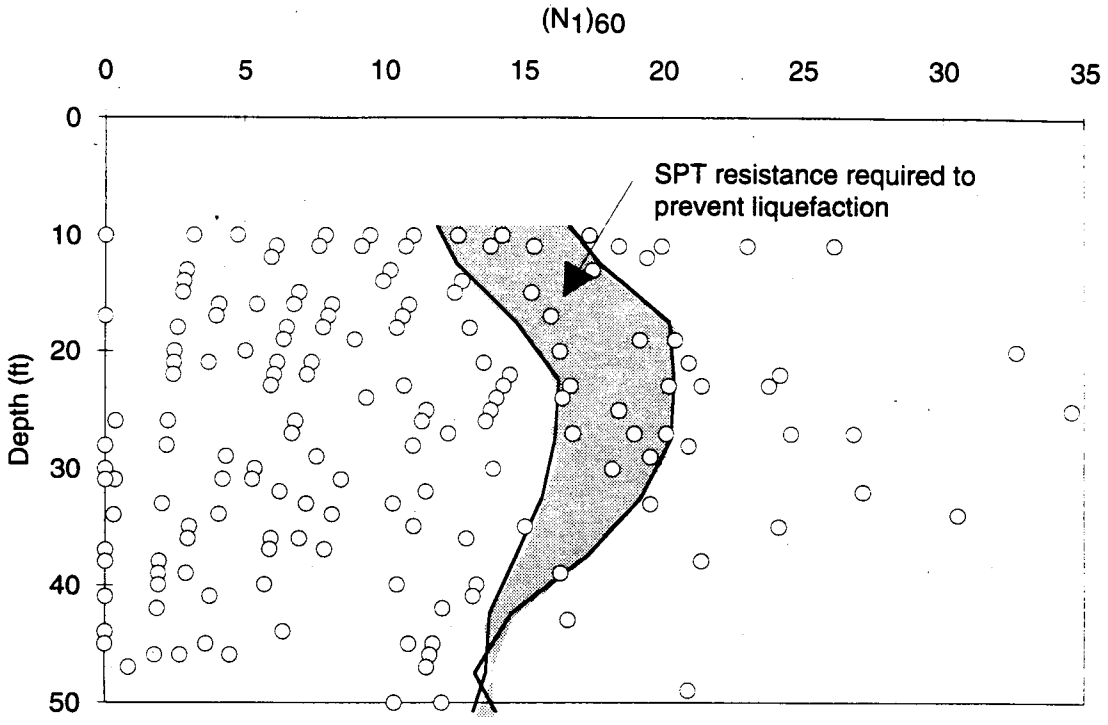

Figure 6.8. Comparison of Measured SPT Resistances with SPT Resistance Required to Resist Liquefaction for 50 Ft Soft Soil

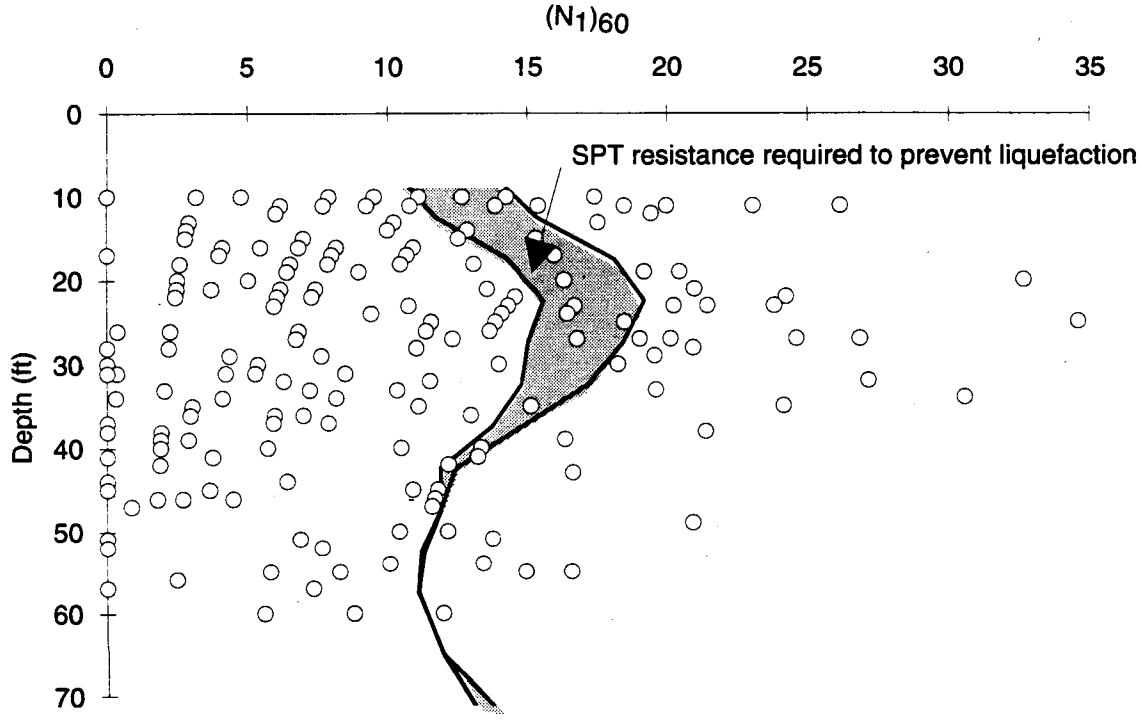

Figure 6.9. Comparison of Measured SPT Resistances with SPT Resistance Required to Resist Liquefaction for 60 Ft Soft Soil

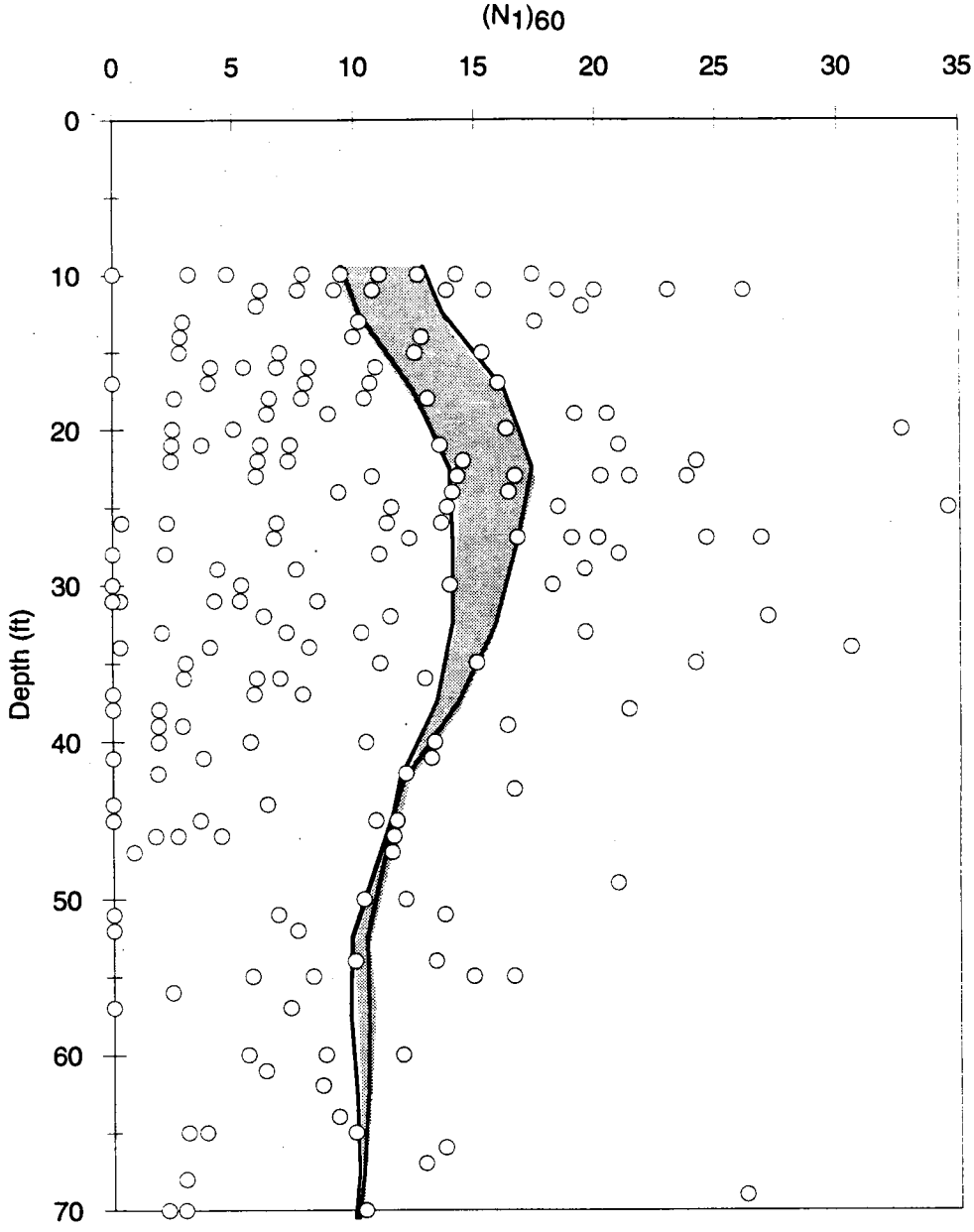

Figure 6.10. Comparison of Measured SPT Resistances with SPT Resistance Required to Resist Liquefaction for 70 Ft Soft Soil

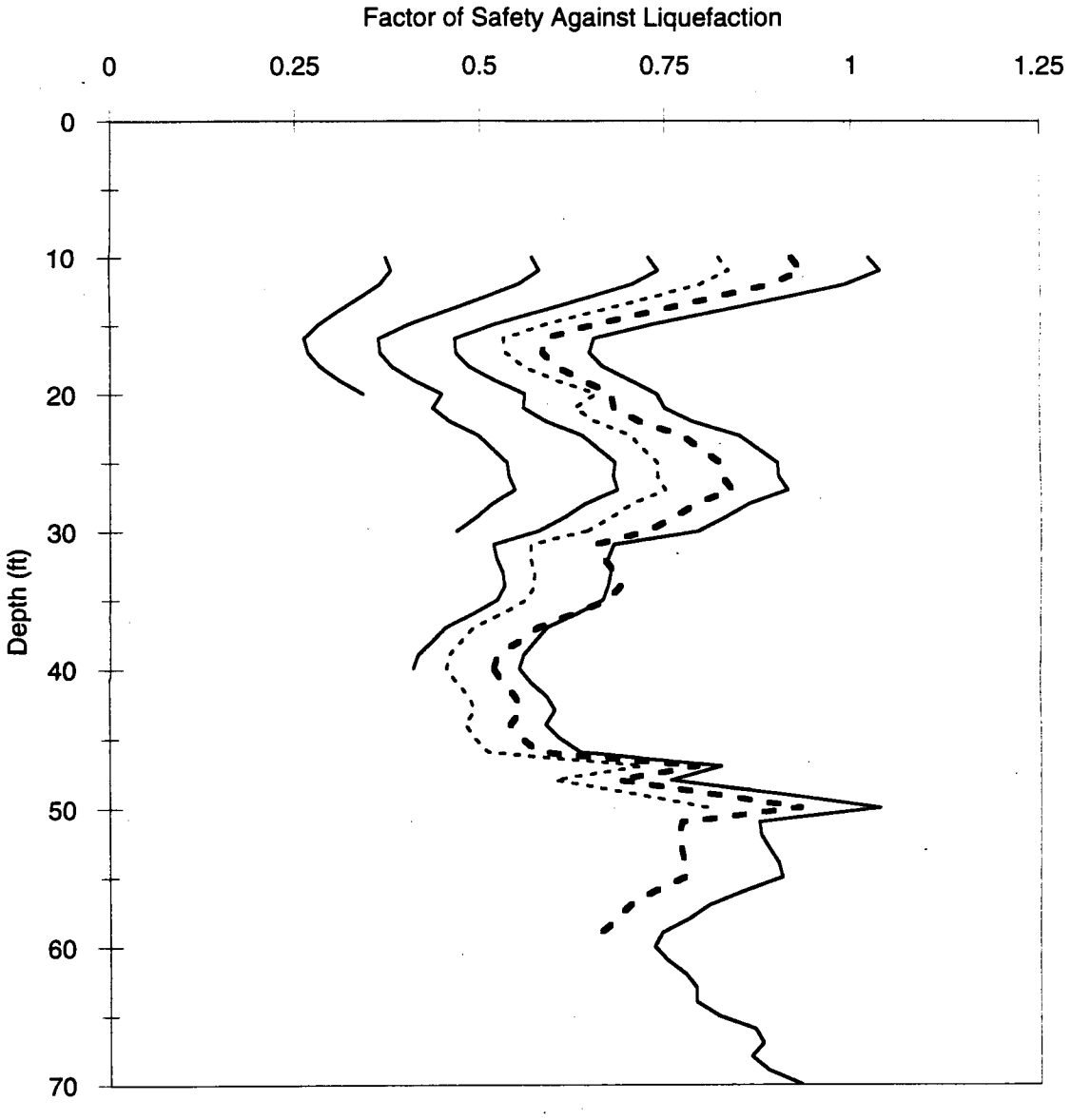

Figure 6.11. Variation of Average Factor of Safety Against Liquefaction with Depth for Design-Level Ground Motions

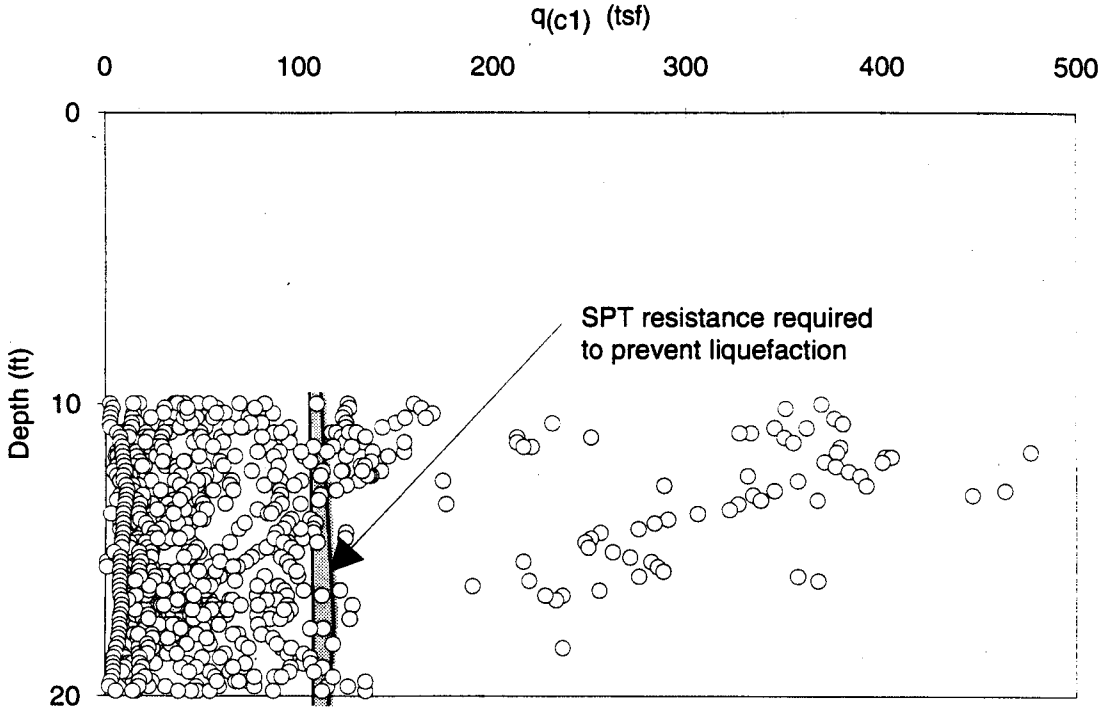

Figure 6.12. Comparison of Measured CPT Resistances with CPT Resistance Required to Resist Liquefaction for 20 Ft Soft Soil

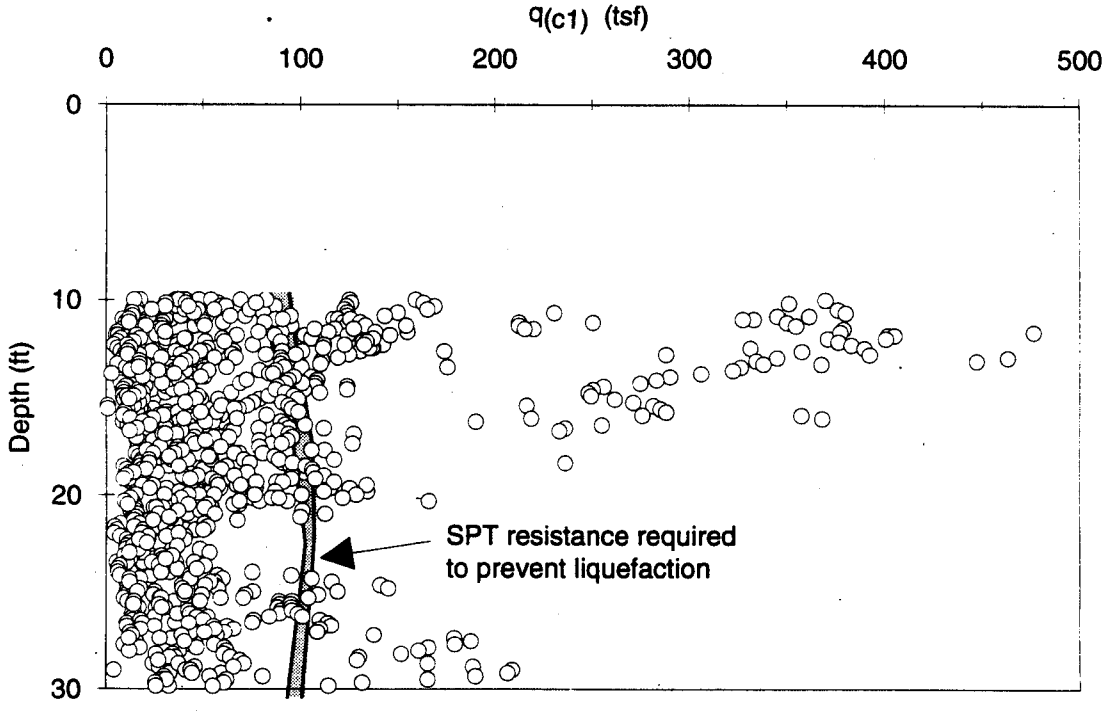

Figure 6.13. Comparison of Measured CPT Resistances With CPT Resistance Required to Resist Liquefaction for 30 Ft Soft Soil

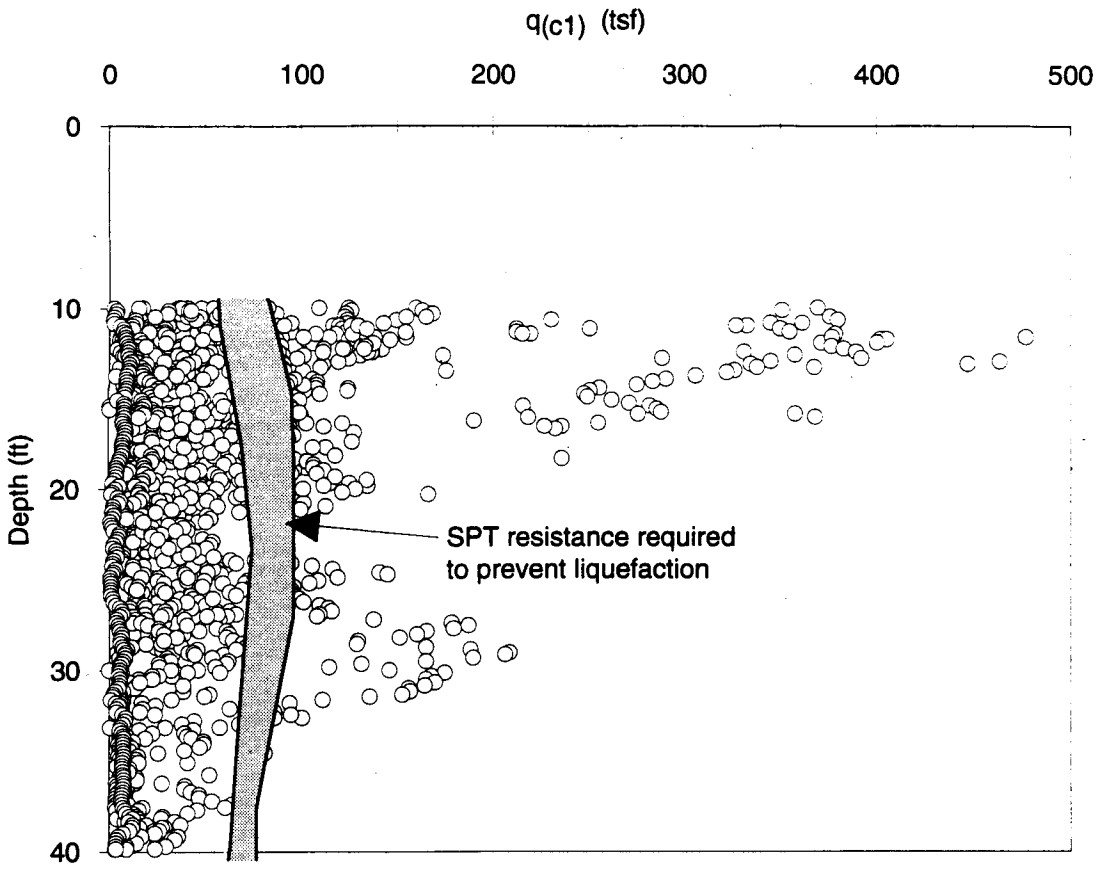

Figure 6.14. Comparison of Measured CPT Resistances with CPT Resistance Required to Resist Liquefaction for 40 Ft Soft Soil

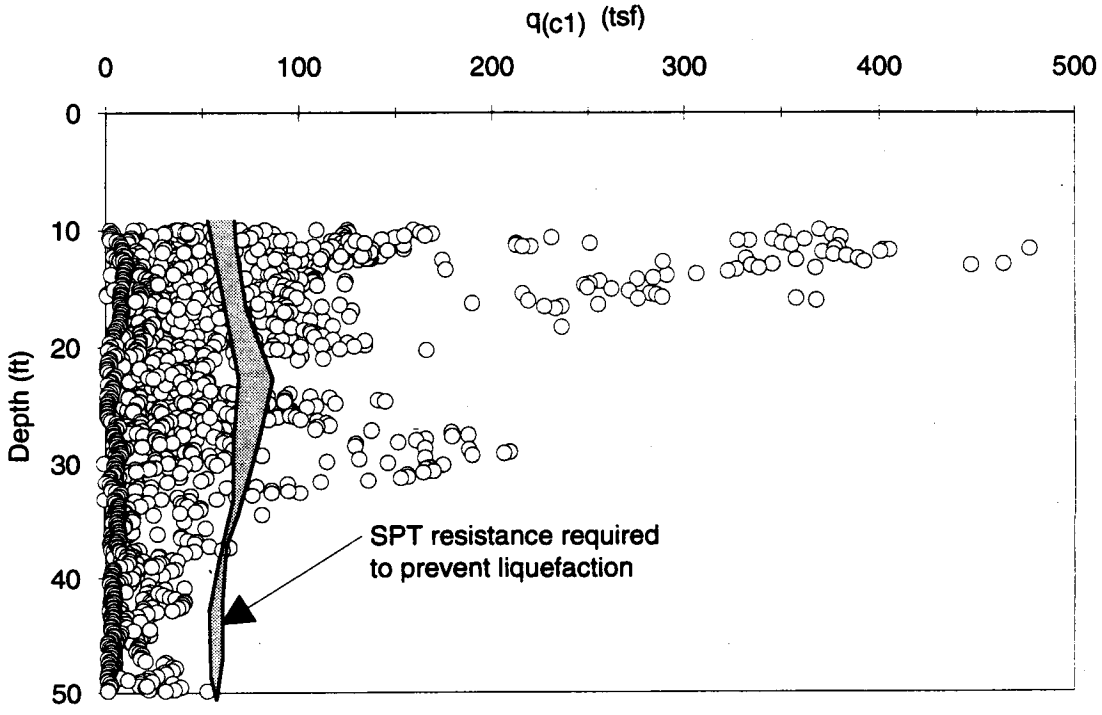

Figure 6.15. Comparison of Measured CPT Resistances with CPT Resistance Required to Resist Liquefaction for 50 Ft Soft Soil

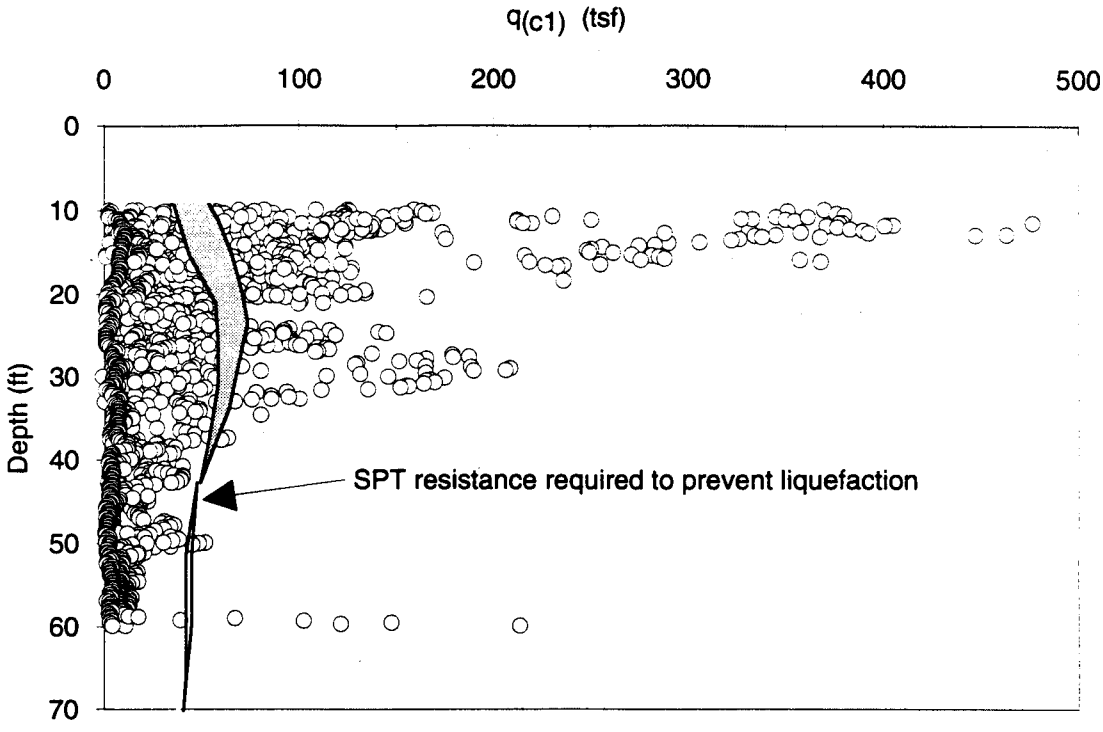

Figure 6.16. Comparison of Measured CPT Resistances with CPT Resistance Required to Resist Liquefaction for 26 Ft Soft Soil

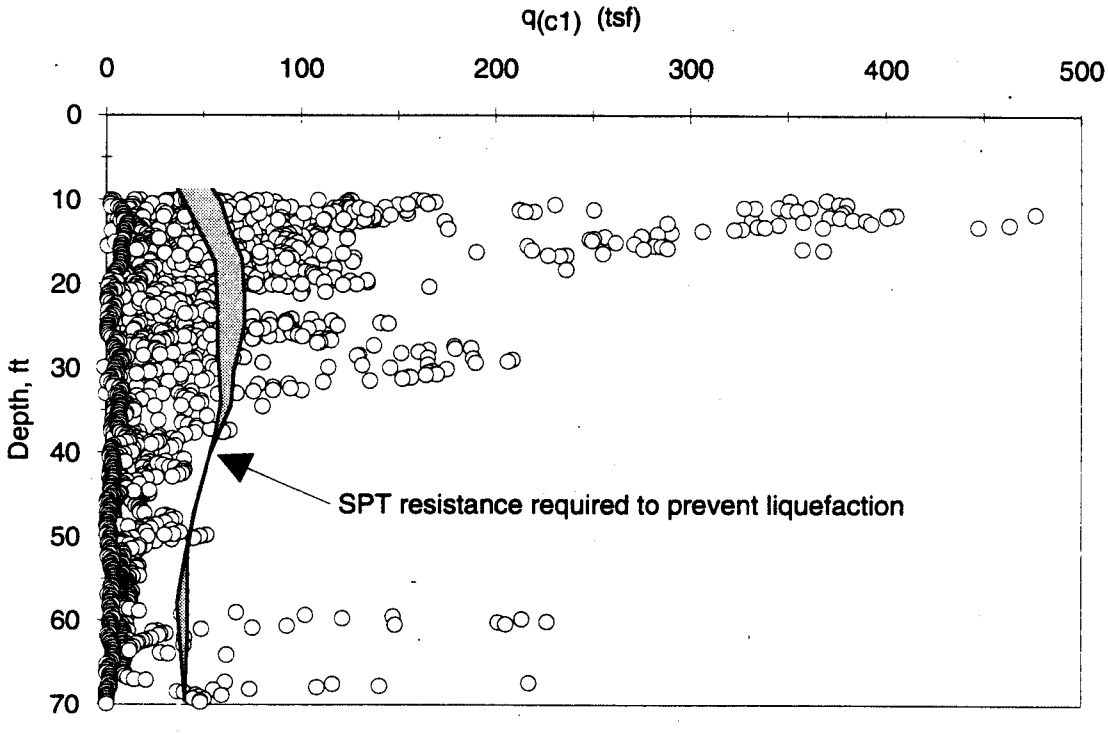

Figure 6.17. Comparison of Measured CPT Resistances with CPT Resistance Required to Resist Liquefaction for 70 Ft Soft Soil

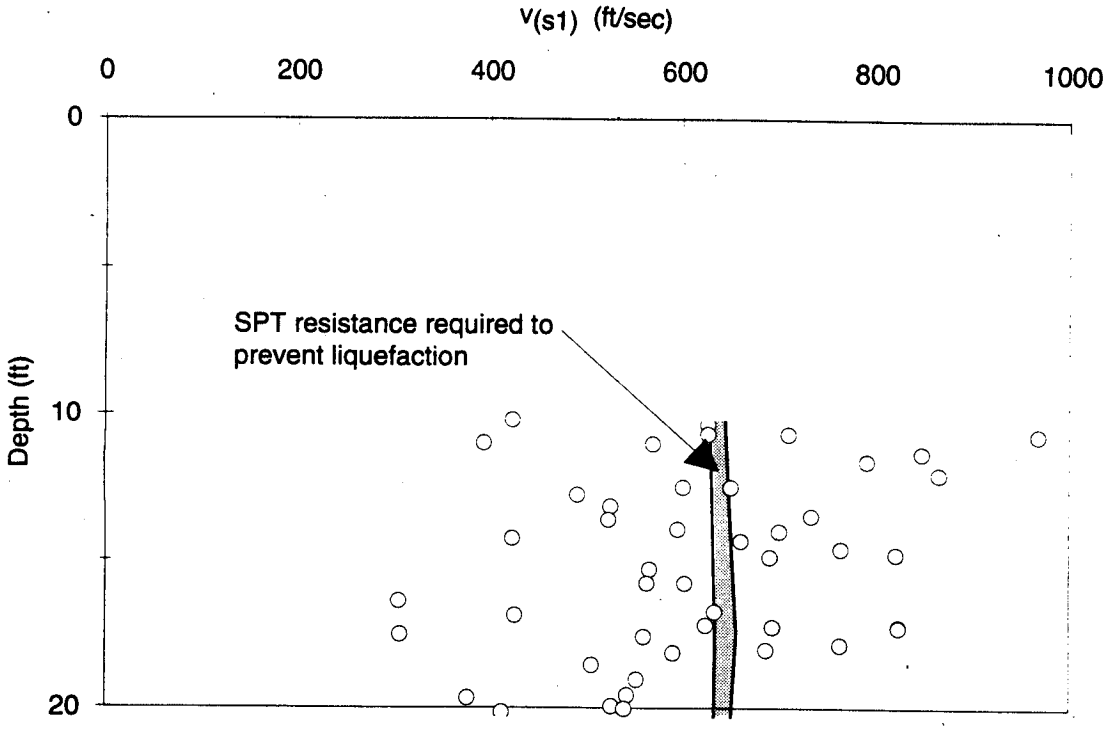

Figure 6.18. Comparison of Measured Shear Wave Velocities With Shear Wave Velocities Required to Resist Liquefaction for 20 Ft Soft Soil

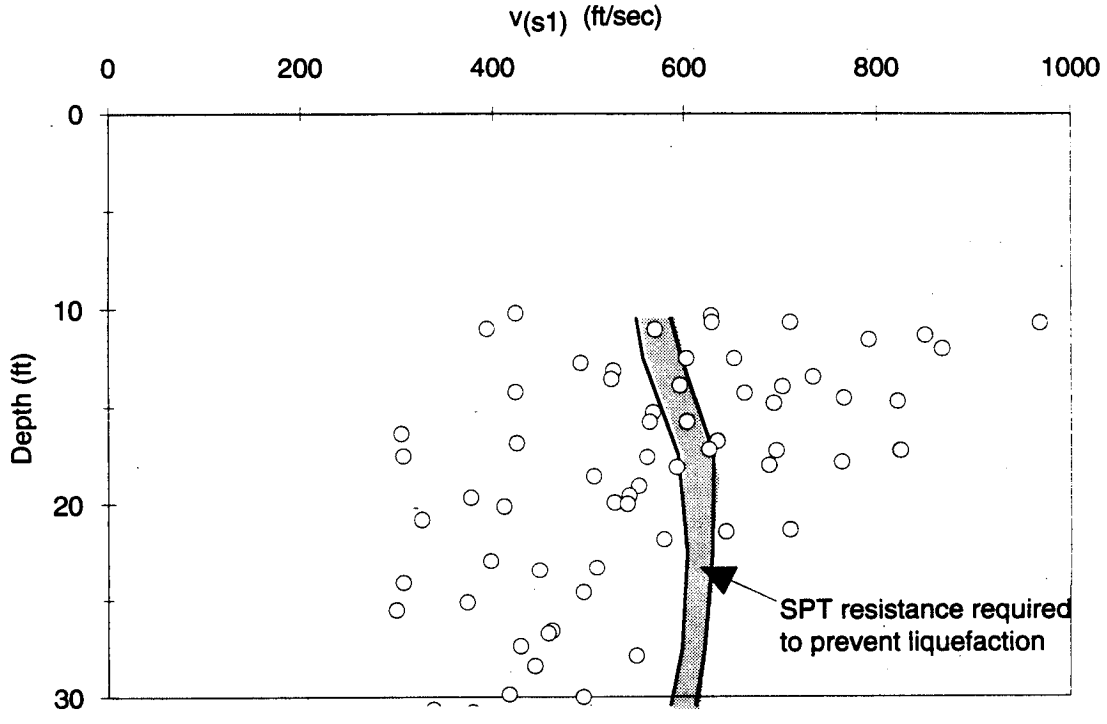

Figure 6.19. Comparison of Measured Shear Wave Velocities with Shear Wave Velocities Required to Resist Liquefaction for 30 Ft Soft Soil

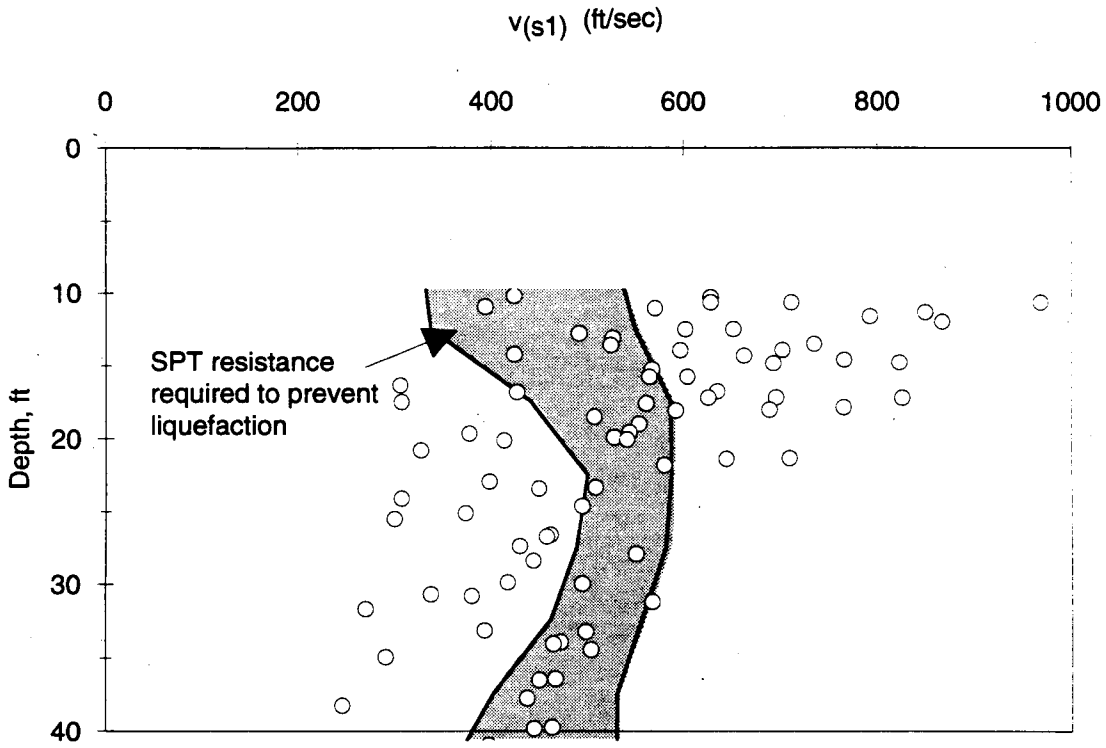

Figure 6.20. Comparison of Measured Shear Wave Velocities with Shear Wave Velocities Required to Resist Liquefaction for 40 Ft Soft Soil

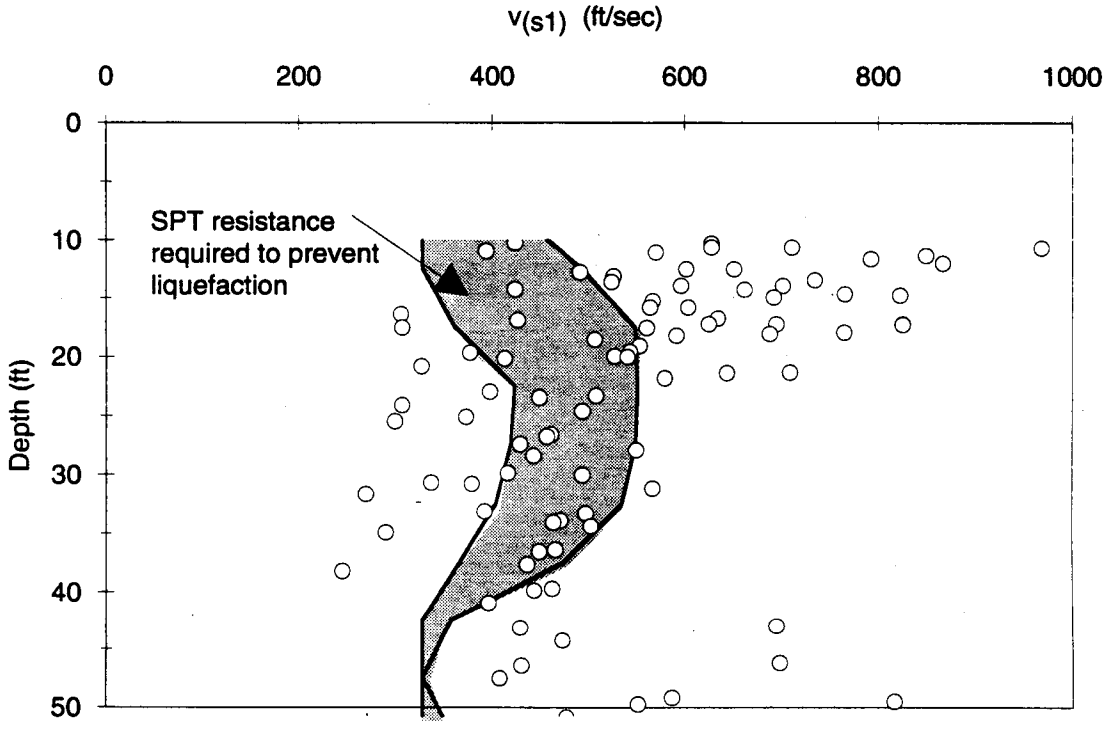

Figure 6.21. Comparison of Measured Shear Wave Velocities with Shear Wave Velocities Required to Resist Liquefaction for 50 Ft Soft Soil

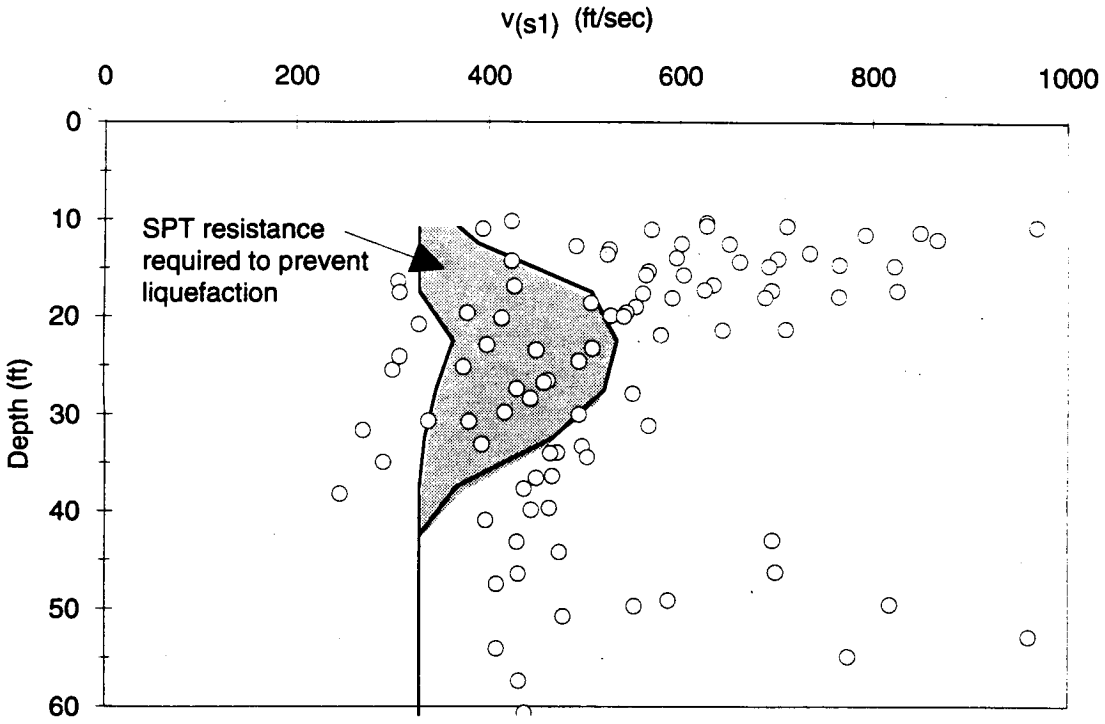

Figure 6.22. Comparison of Measured Shear Wave Velocities with Shear Wave Velocities Required to Resist Liquefaction for 60 Ft Soft Soil

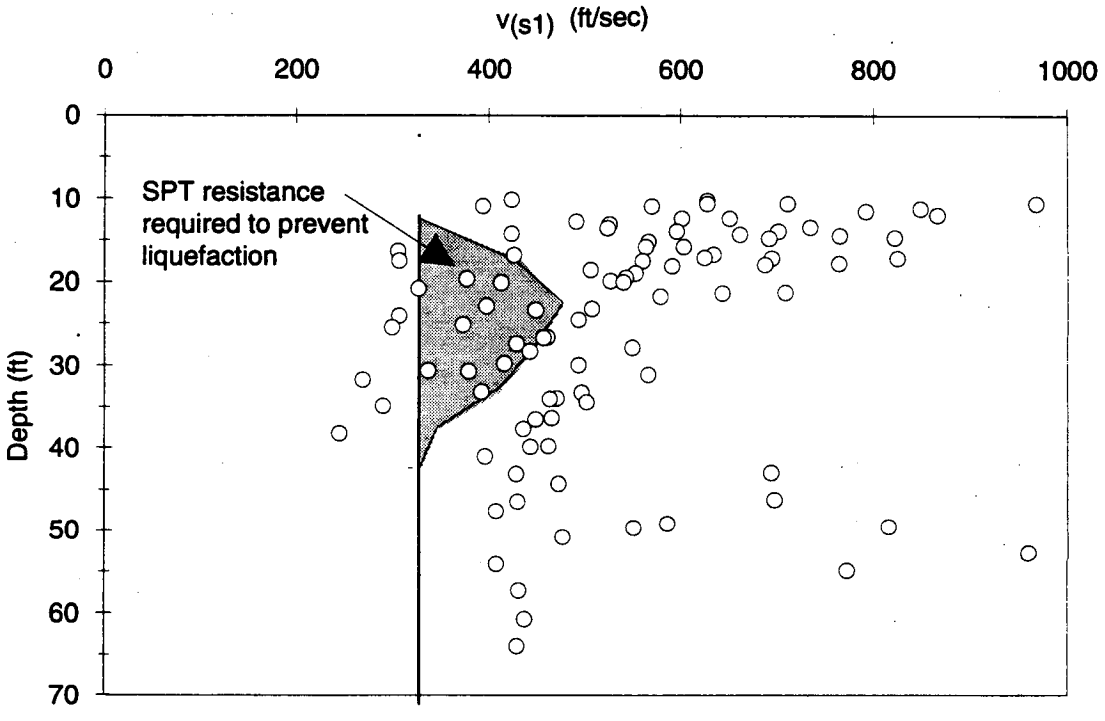

Figure 6.23. Comparison of Measured Shear Wave Velocities with Shear Wave Velocities Required to Resist Liquefaction for 70 Ft Soft Soil

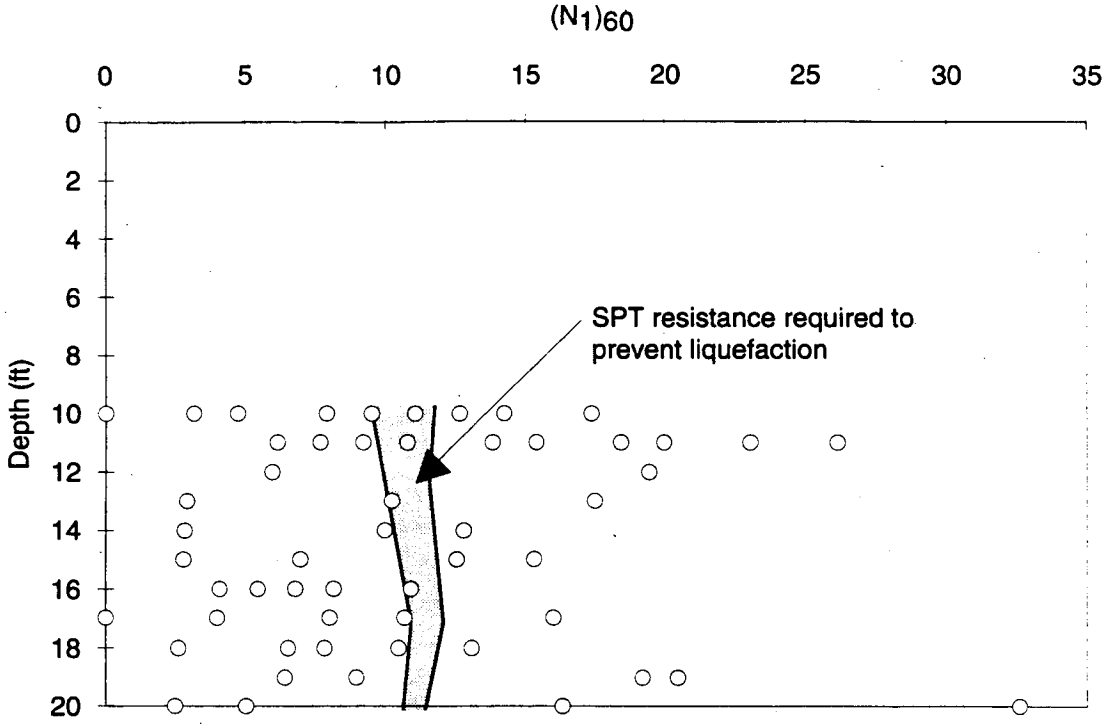

Figure 6.24. Comparison of Measured SPT Resistances with SPT Resistance Required to Resist Liquefaction for 20 Ft Soft Soil for the 1965 Seattle Earthquake Motion

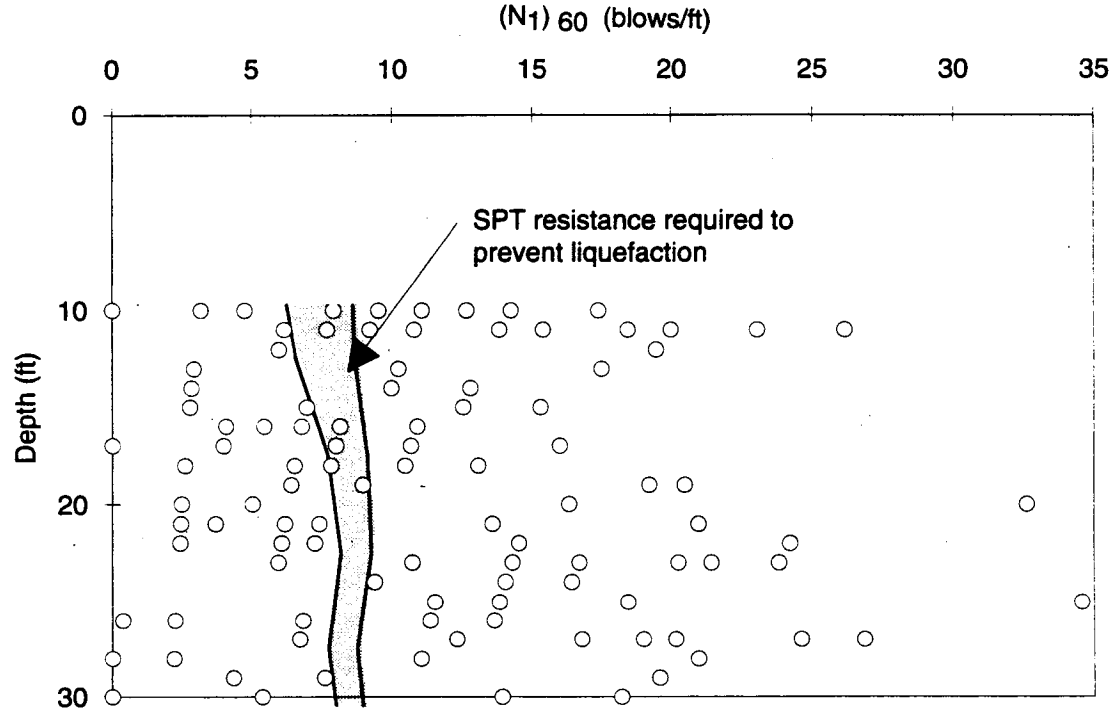

Figure 6.25. Comparison of Measured SPT Resistances with SPT Resistance Required to Resist Liquefaction for 30 Ft Soft Soil for the 1965 Seattle Earthquake Motion

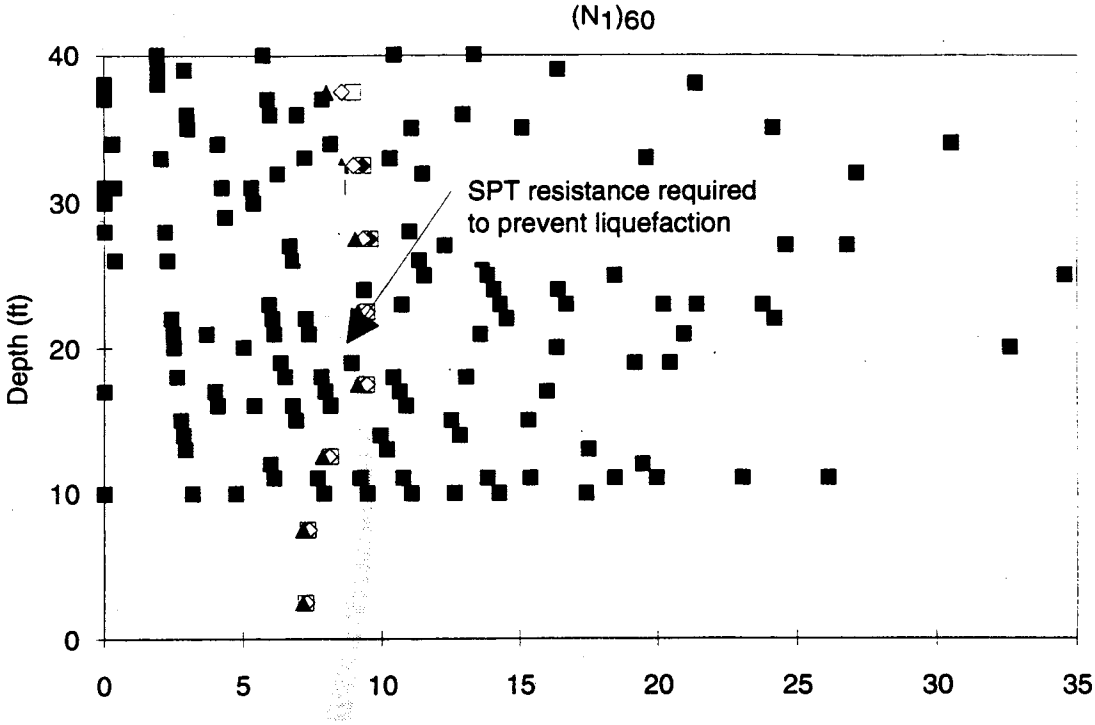

Figure 6.26. Comparison of Measured SPT Resistances with SPT Resistance Required to Resist Liquefaction for 40 Ft Soft Soil for the 1965 Seattle Earthquake Motion

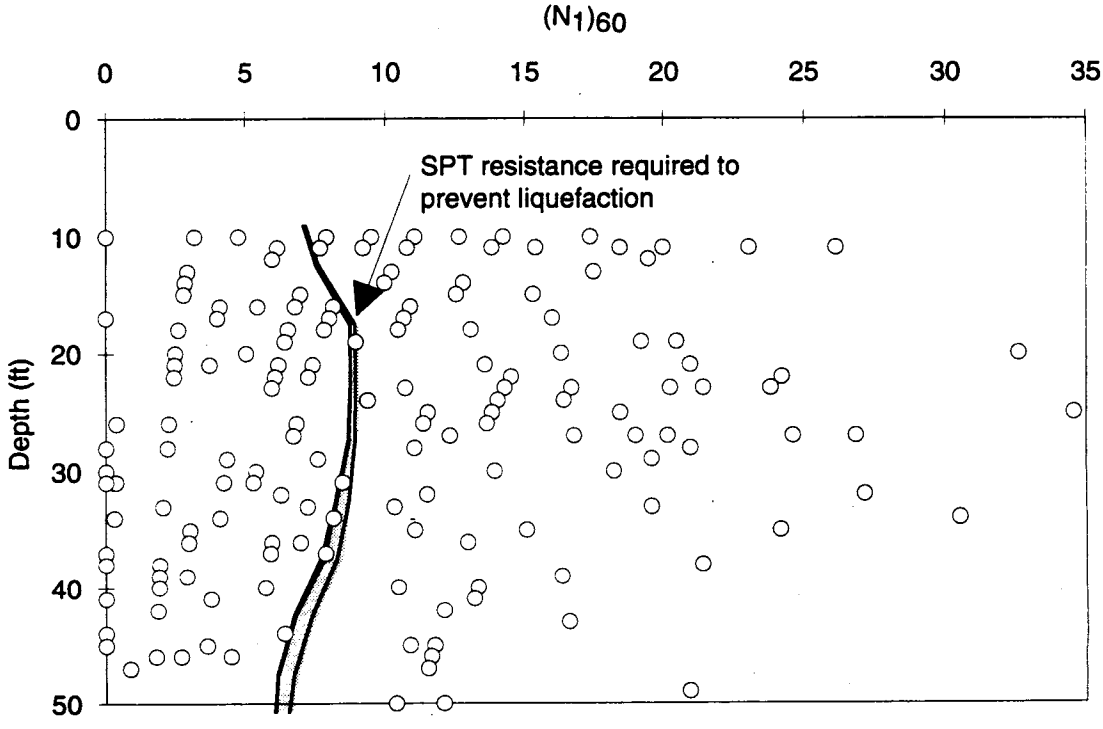

Figure 6.27. Comparison of Measured SPT Resistances with SPT Resistance Required to Resist Liquefaction for 50 Ft Soft Soil for the 1965 Seattle Earthquake Motion

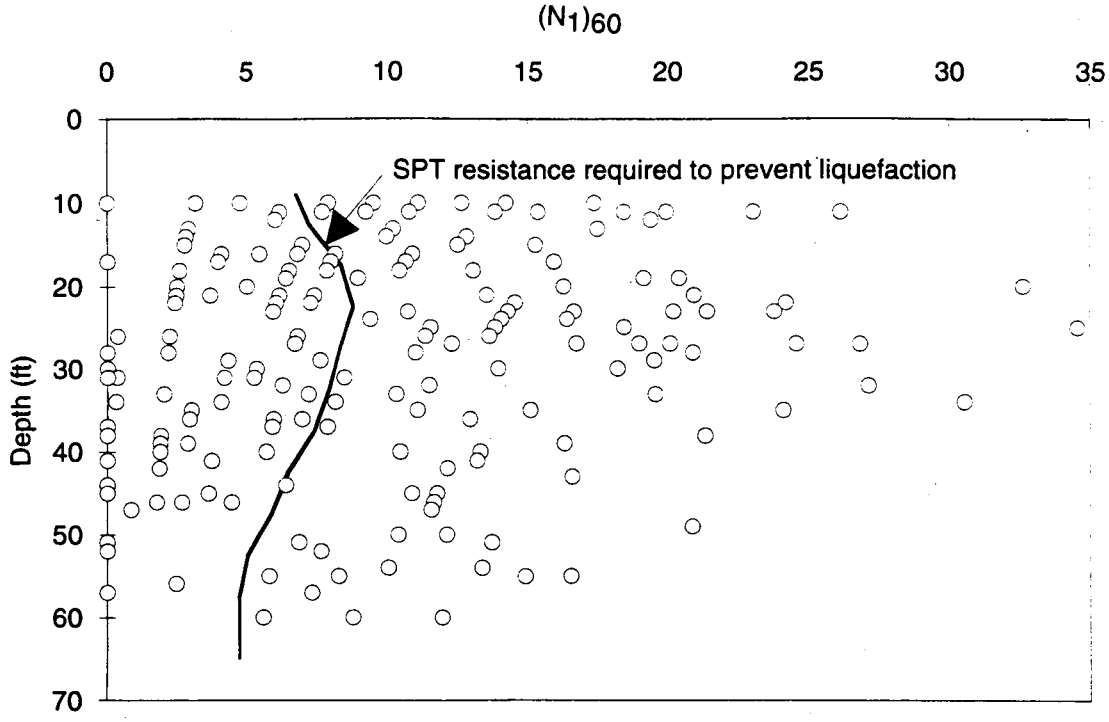

Figure 6.28. Comparison of Measured SPT Resistances With SPT Resistance Required to Resist Liquefaction for 60 Ft Soft Soil for the 1965 Seattle Earthquake Motion

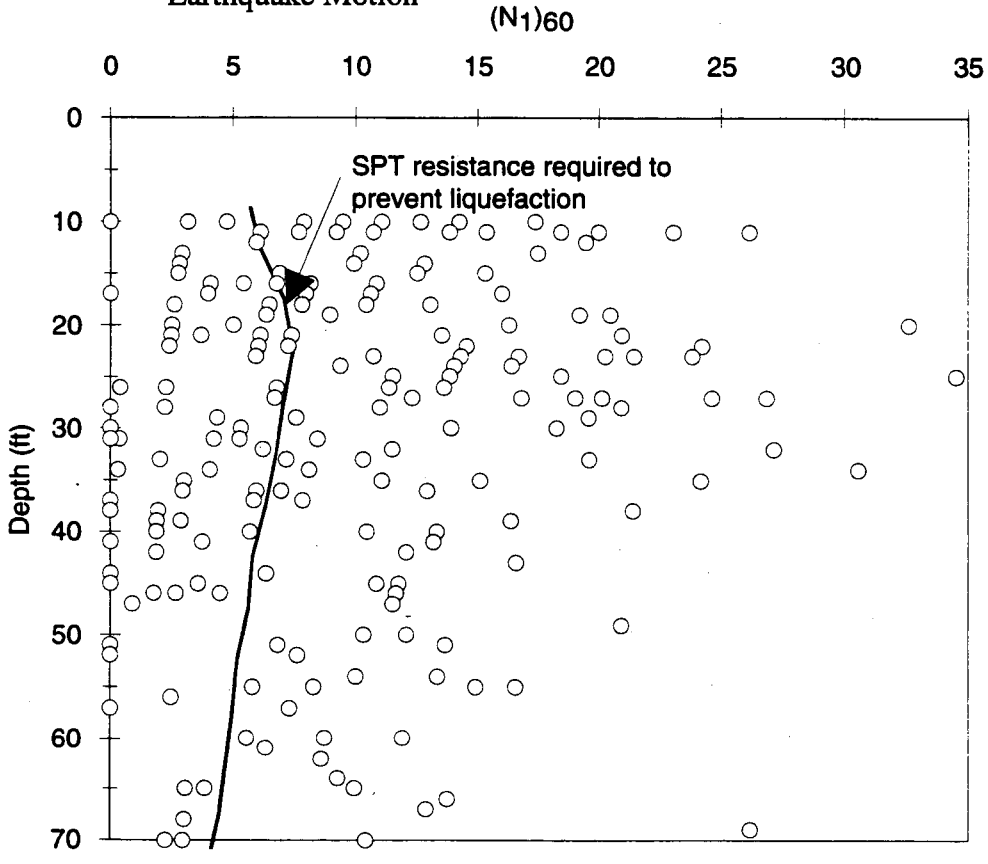

Figure 6.29. Comparison of Measured SPT Resistances with SPT Resistance Required to Resist Liquefaction for 70 Ft Soft Soil for the 1965 Seattle Earthquake Motion

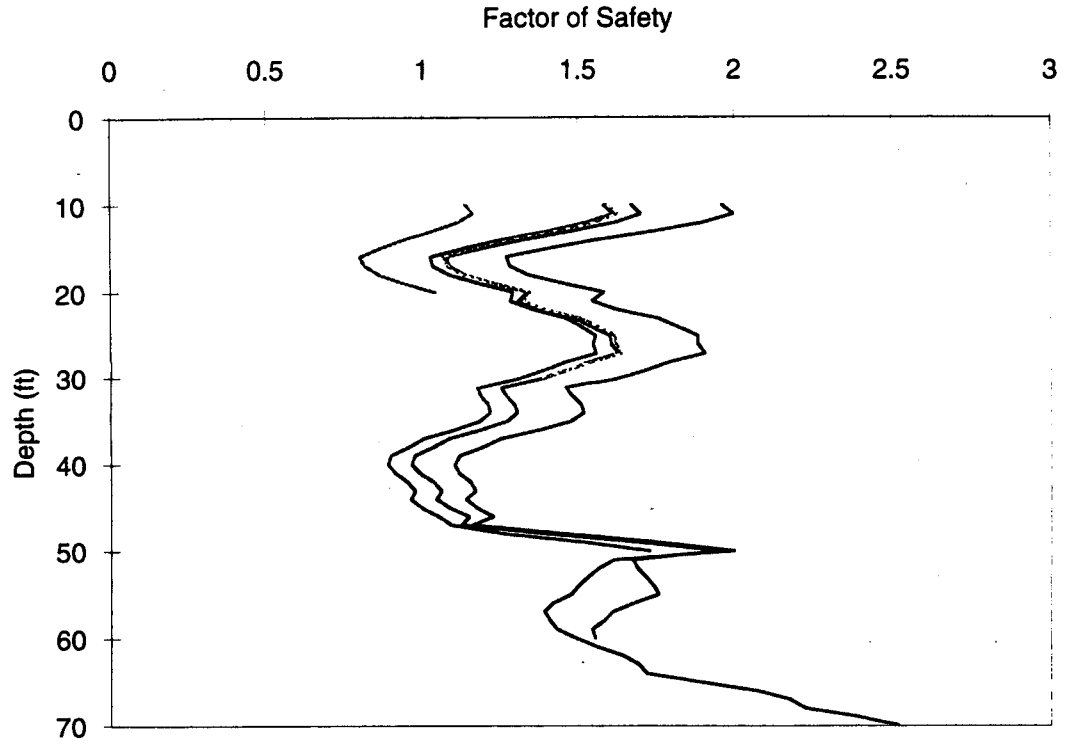

Figure 6.30. Variation of Average Factor of Safety Against Liquefaction with Depth for the 1965 Seattle Earthquake Motion

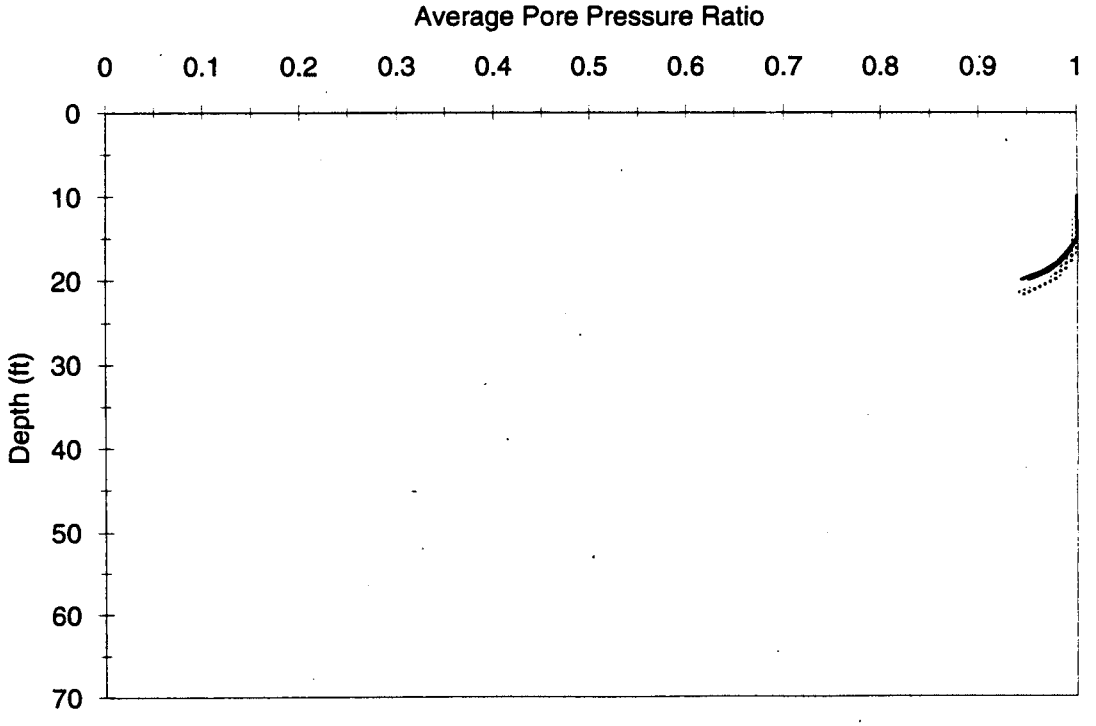

Figure 6.31. Variation of Average Peak Pore Pressure Ratio with Depth for 20 Ft Soft Soil

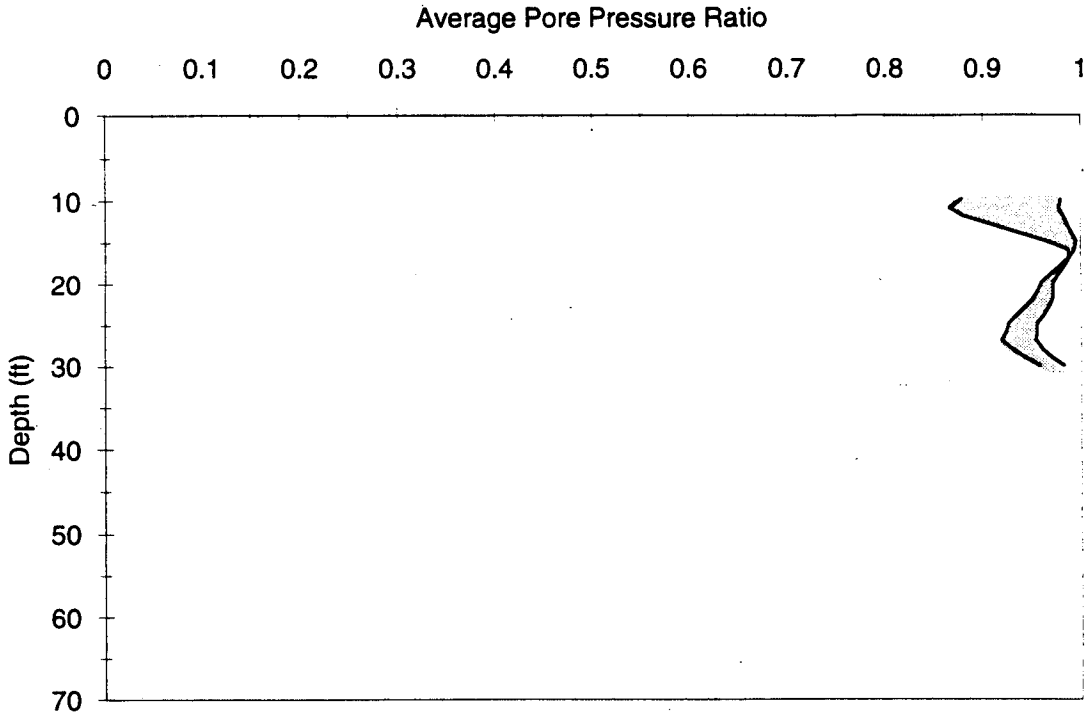

Figure 6.32. Variation of Average Peak Pore Pressure Ratio with Depth for 30 Ft Soft Soil

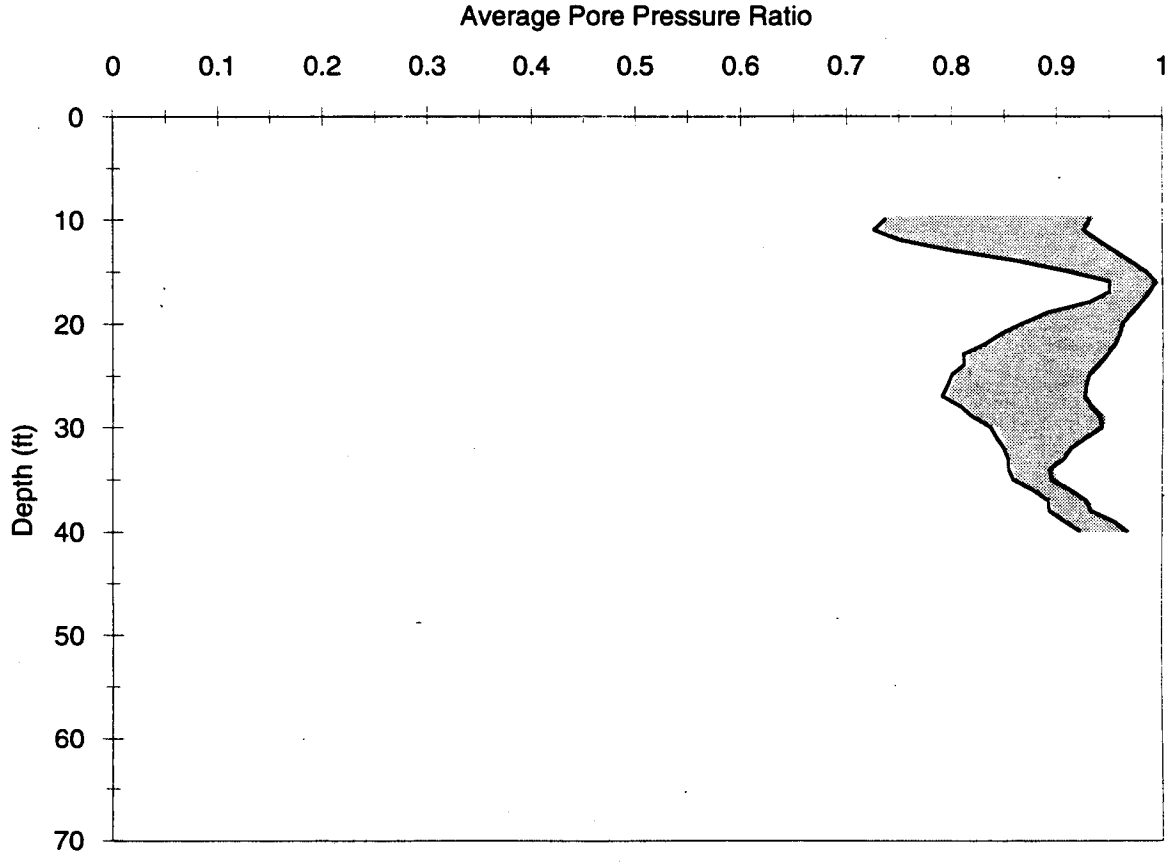

Figure 6.33. Variation of Average Peak Pore Pressure Ratio with Depth for 40 Ft Soft Soil

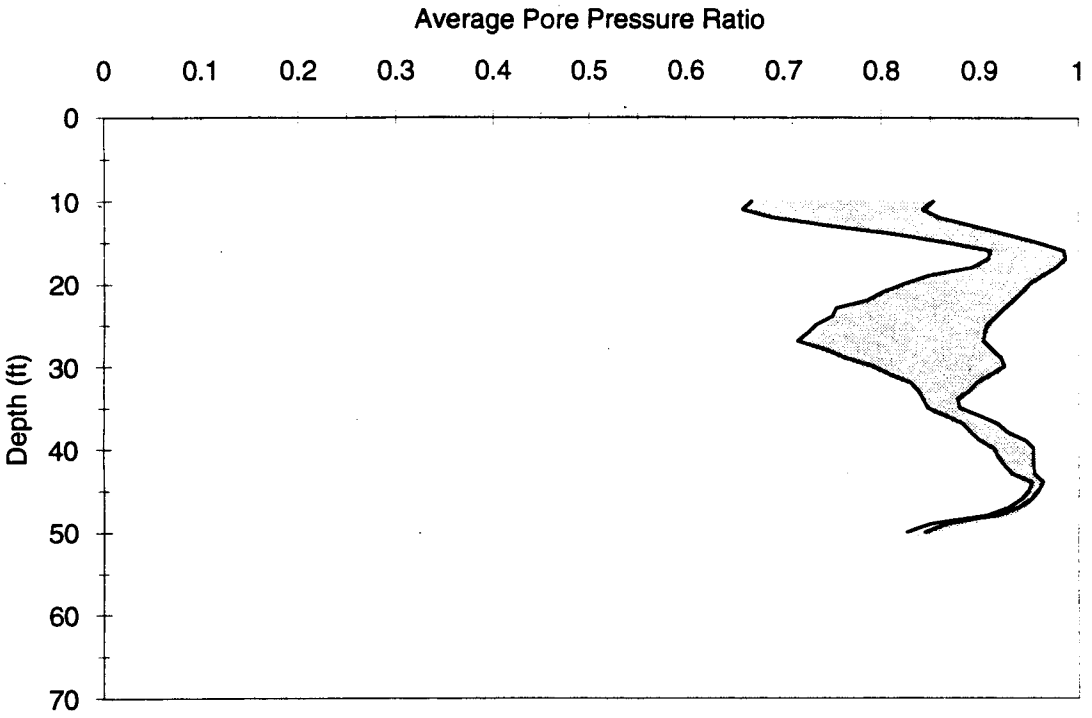

Figure 6.34. Variation of Average Peak Pore Pressure Ratio with Depth for 50 Ft Soft Soil

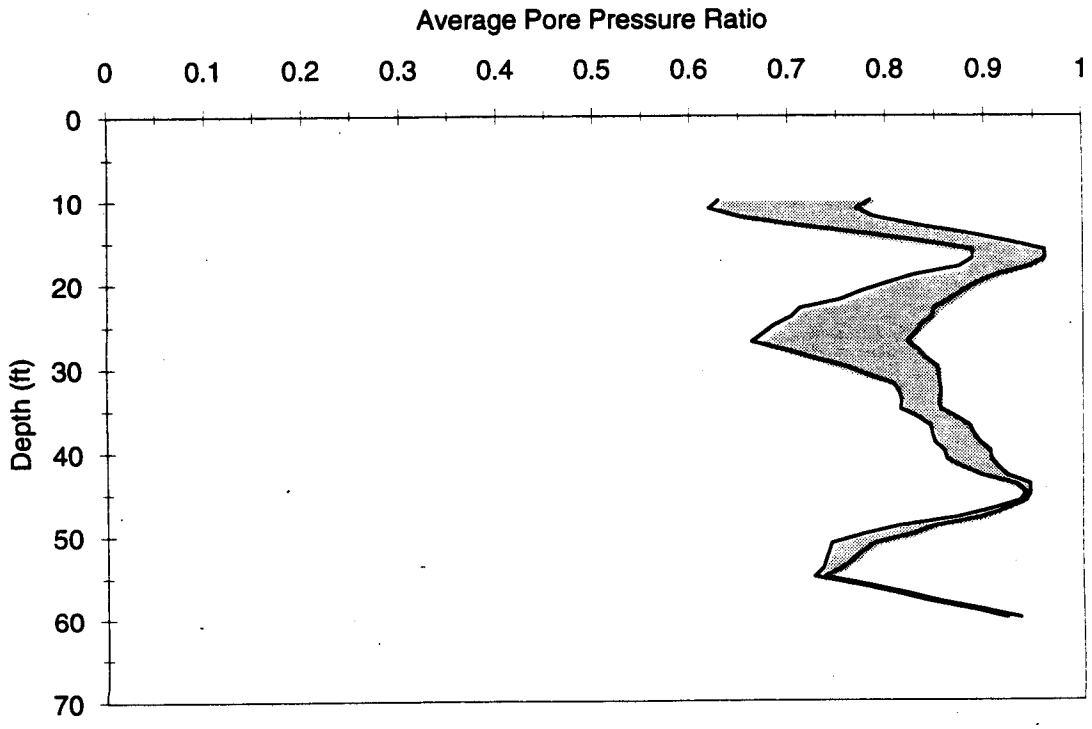

Figure 6.35. Variation of Average Peak Pore Pressure Ratio with Depth for 60 Ft Soft Soil

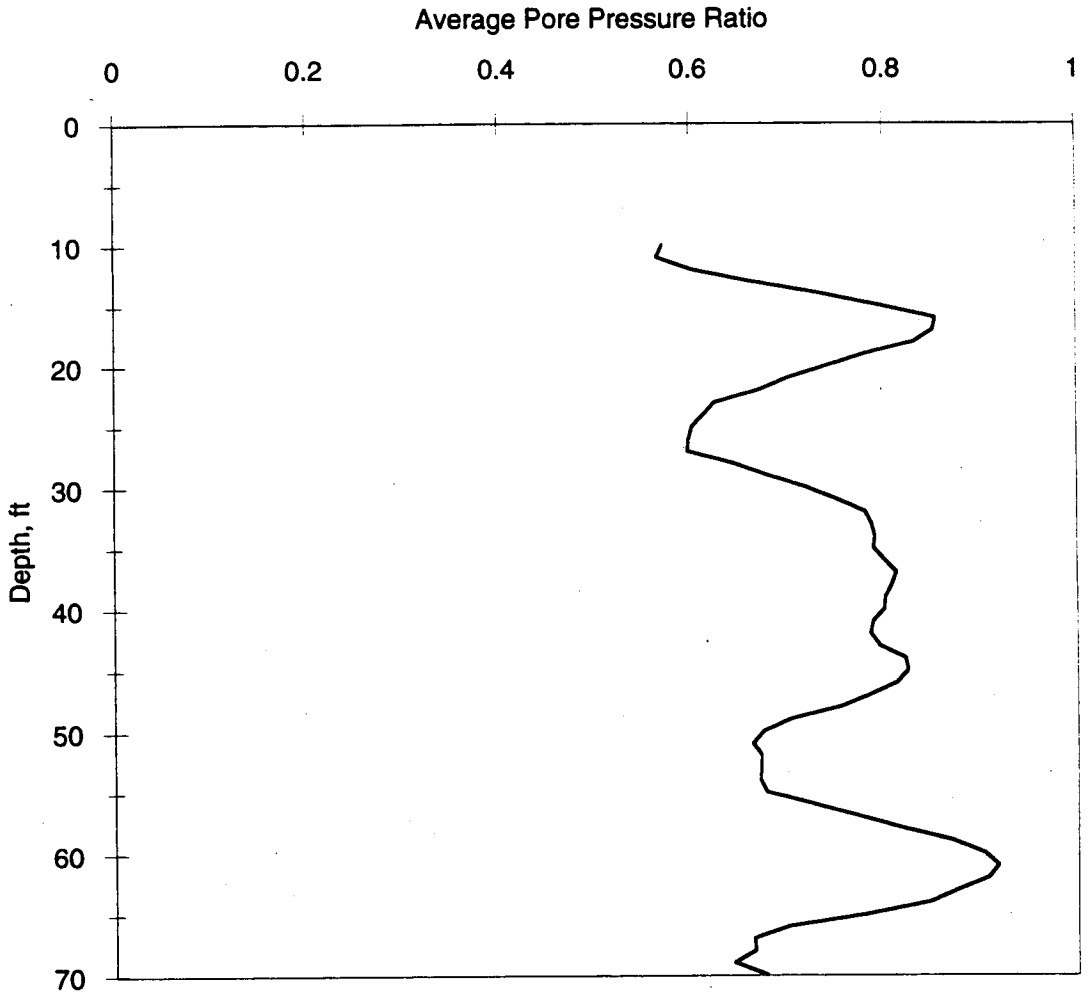

Figure 6.36. Variation of Average Peak Pore Pressure Ratio with Depth for 70 Ft Soft Soil

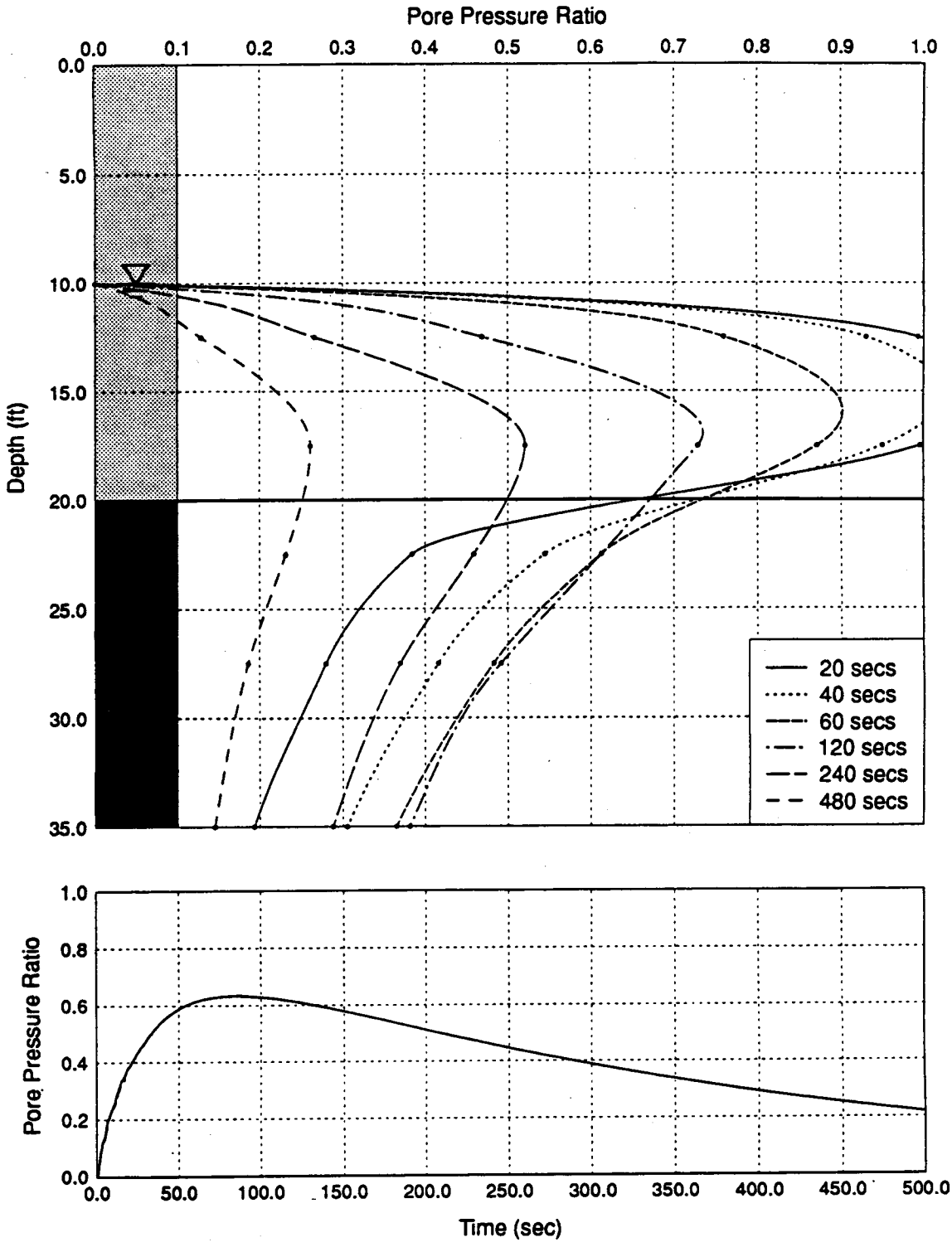

Figure 6.37 (a) Variation of Pore Pressure Ratio with Depth at Different Times after the Beginning of Earthquake Shaking for 20 Ft Soft Soil, and (B) Variation of Pore Pressure Ratio with Time in the Vicinity of the Tips of the Existing Pile Foundations (2.5 Ft Below Top of Till)

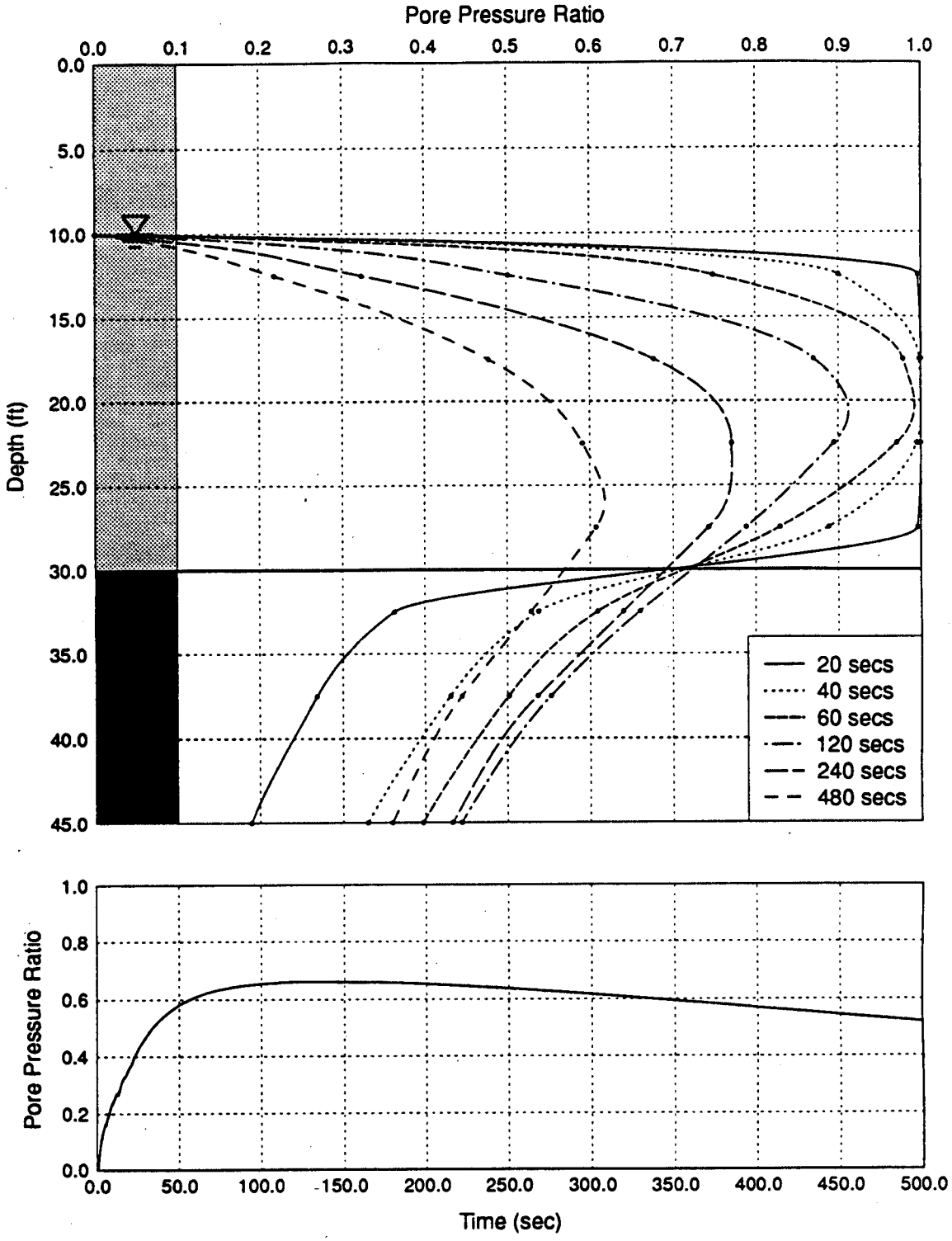

Figure 6.38 (a) Variation of Pore Pressure Ratio with Depth at Different Times after the Beginning of Earthquake Shaking for 30 Ft Soft Soil, and (B) Variation of Pore Pressure Ratio with Time in the Vicinity of the Tips of the Existing Pile Foundations (2.5 Ft Below Top of Till)

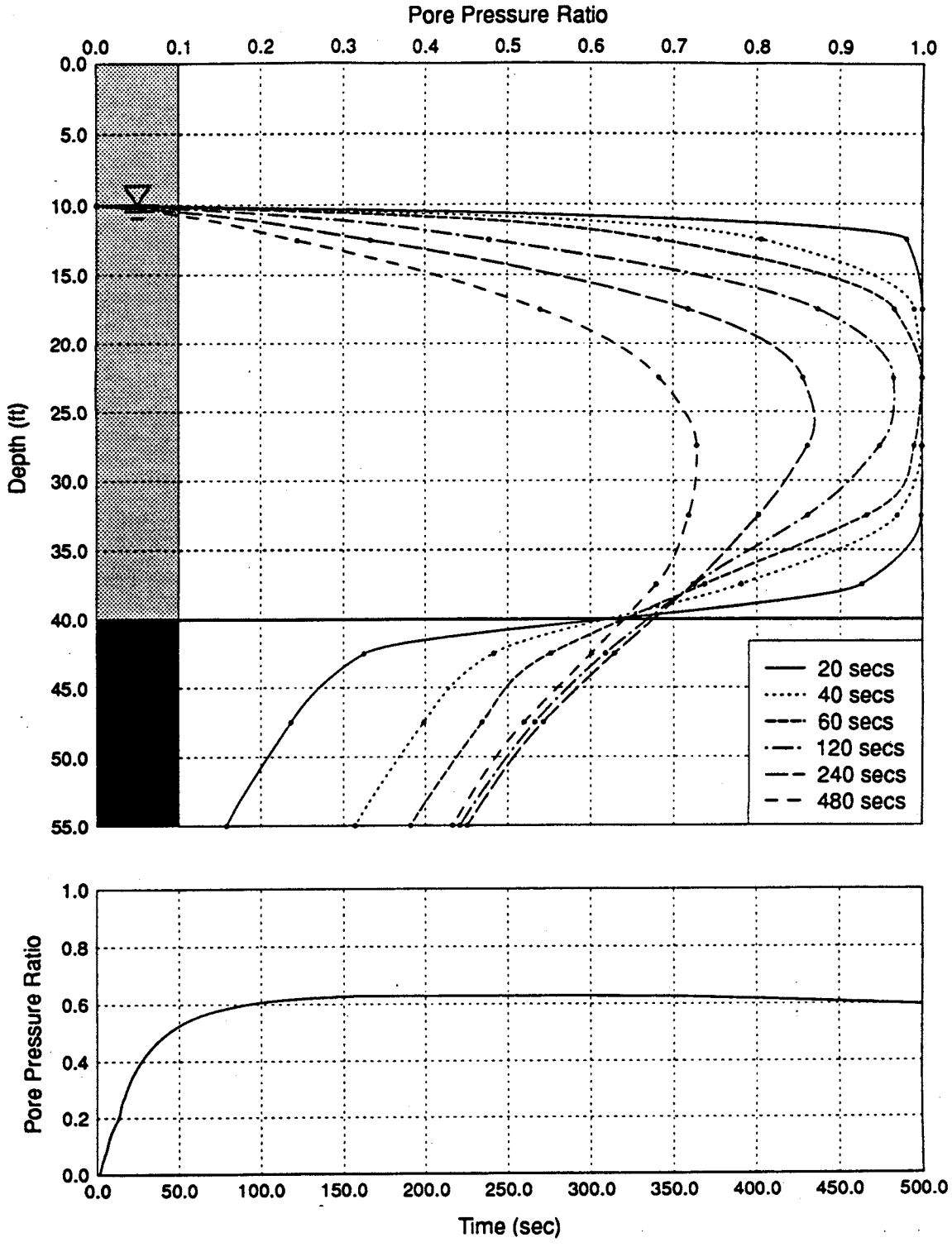

Figure 6.39 (a) Variation of Pore Pressure Ratio with Depth at Different Times after the Beginning of Earthquake Shaking for 40 Ft Soft Soil, and (B) Variation of Pore Pressure Ratio with Time in the Vicinity of the Tips of the Existing Pile Foundations (2.5 Ft Below Top of Till)

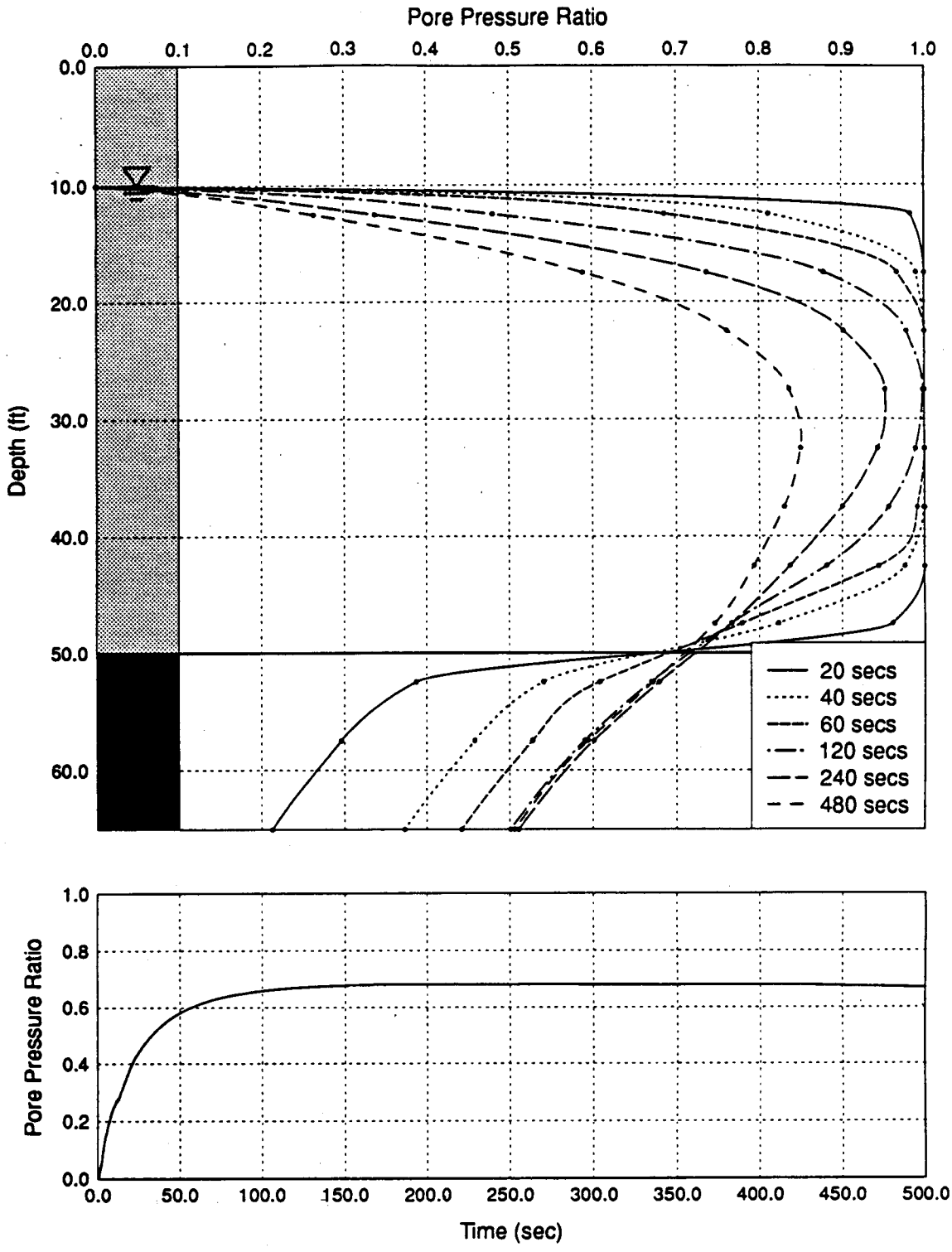

Figure 6.40 (a) Variation of Pore Pressure Ratio with Depth at Different Times after the Beginning of Earthquake Shaking for 50 Ft Soft Soil, and (B) Variation of Pore Pressure Ratio with Time in the Vicinity of the Tips of the Existing Pile Foundations (2.5 Ft Below Top of Till)

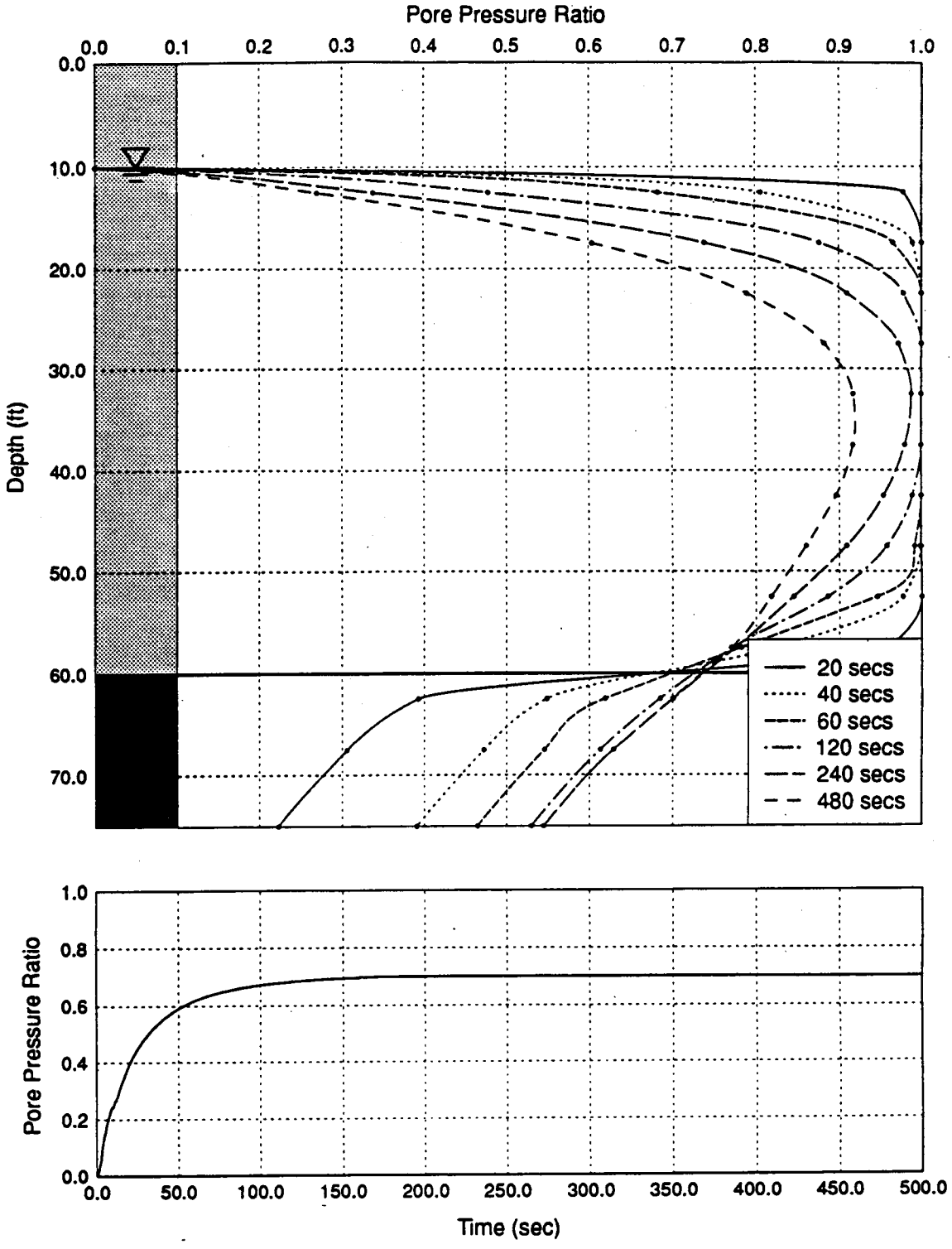

Figure 6.41 (a) Variation of Pore Pressure Ratio with Depth at Different Times after the Beginning of Earthquake Shaking for 60 Ft Soft Soil, and (B) Variation of Pore Pressure Ratio with Time in the Vicinity of the Tips of the Existing Pile Foundations (2.5 Ft Below Top of Till)

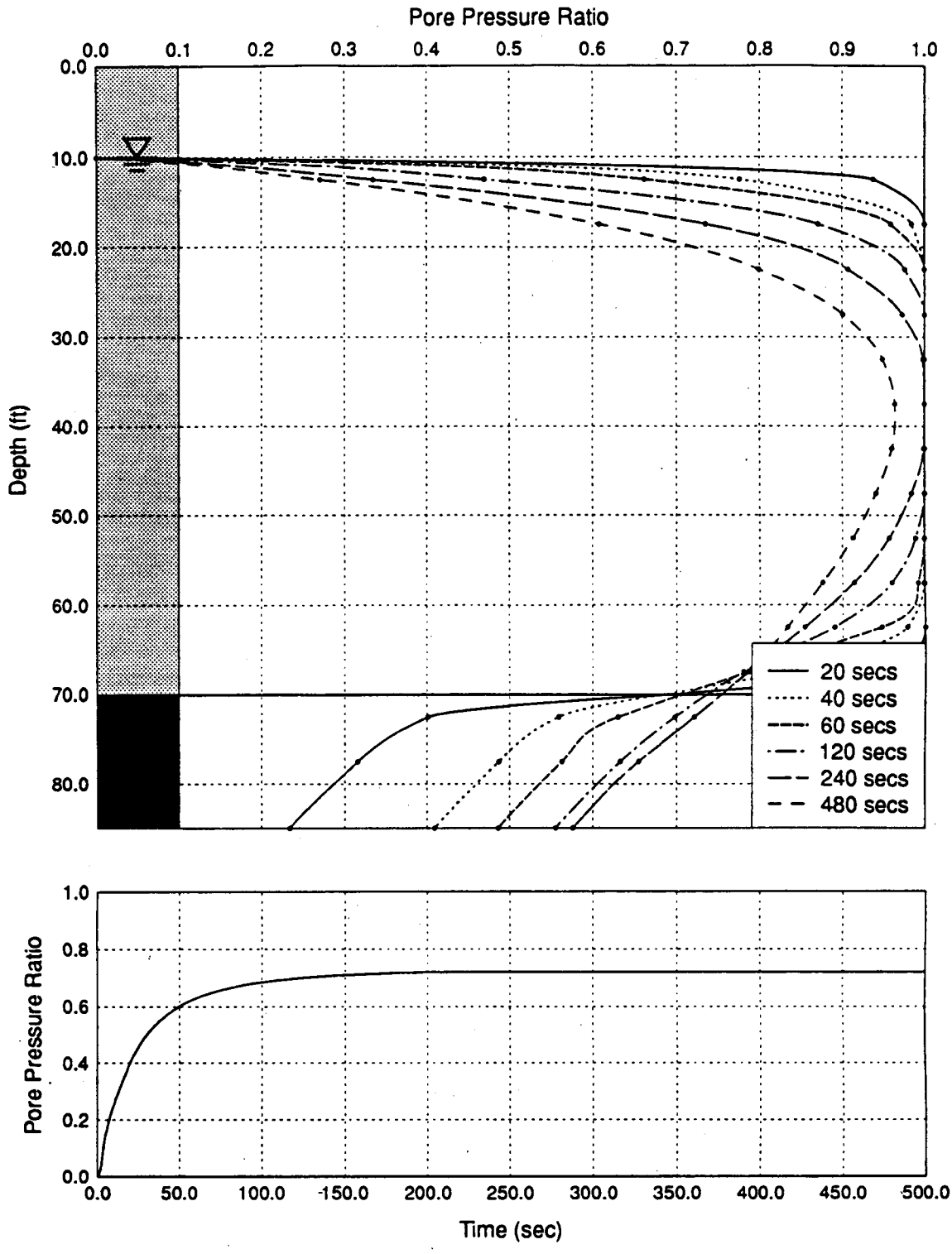

Figure 6.42 (a) Variation of Pore Pressure Ratio with Depth at Different Times after the Beginning of Earthquake Shaking for 70 Ft Soft Soil, and (B) Variation of Pore Pressure Ratio with Time in the Vicinity of the Tips of the Existing Pile Foundations (2.5 Ft Below Top of Till)

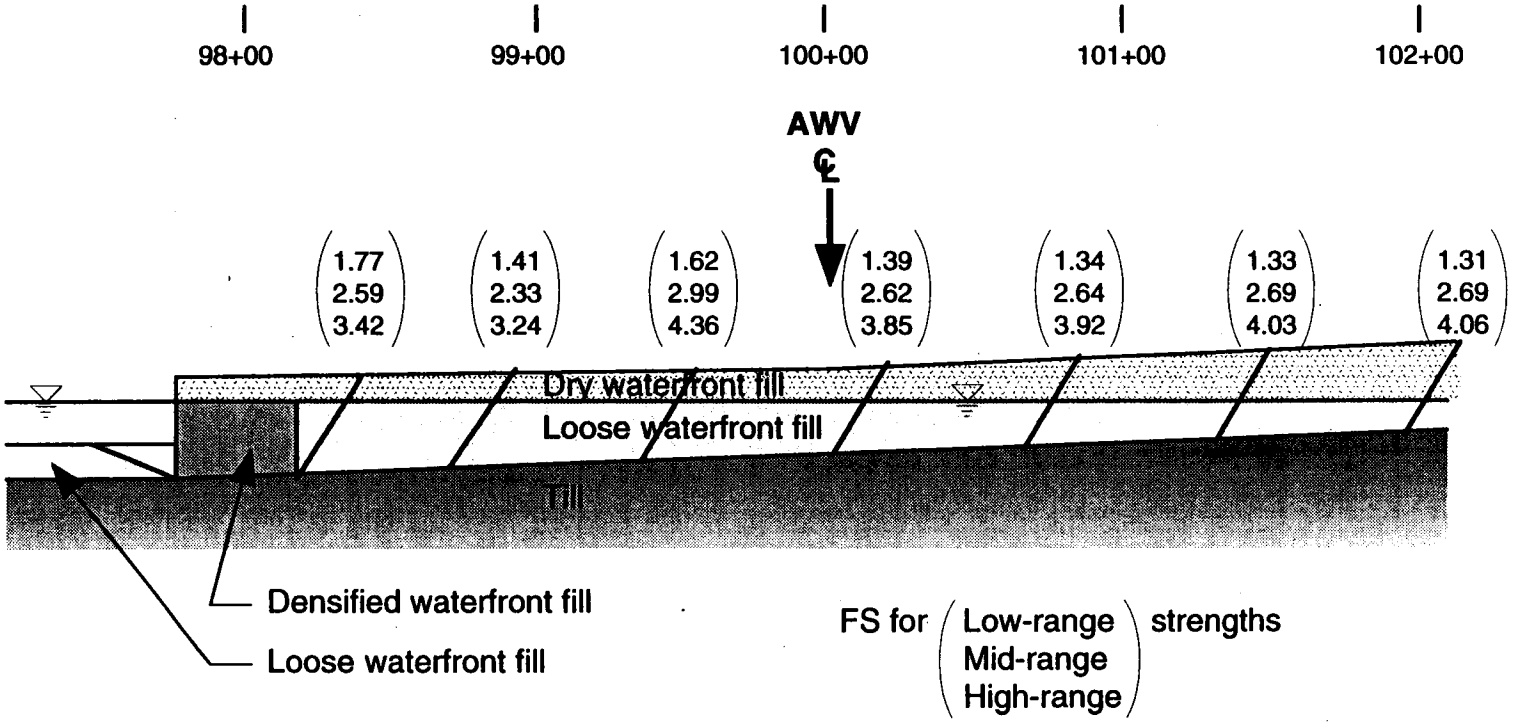

Figure 6.43. Idealized Soil Profile at Columbia Street Cross-Section with Computed Factors of Safety for Various Potential Failure Surfaces

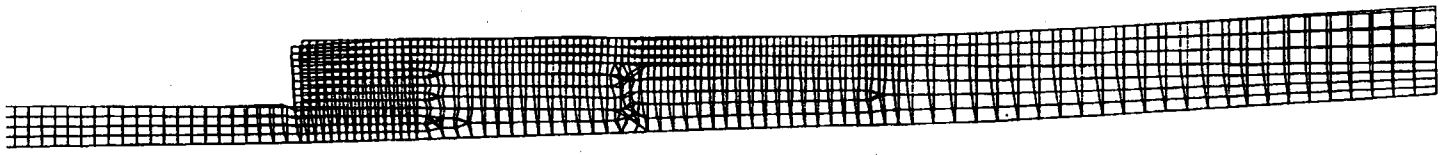

Figure 6.44. Original and Final Configurations of the Columbia Street Cross-Section as Estimated by Byrne et al. (1991) Approach

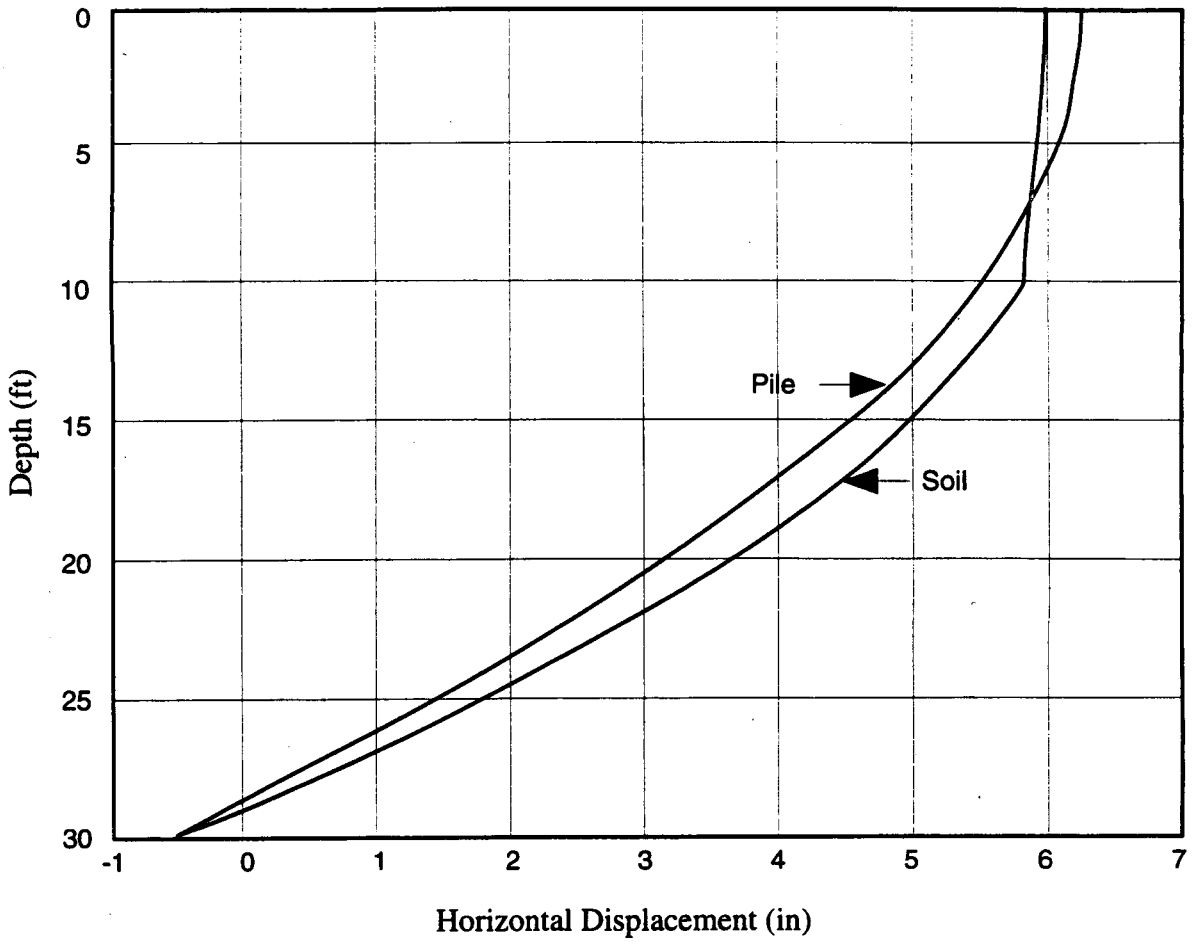

Figure 6.45. Displaced Shape of Fixed Head Pile with EI = 5 x 10^{10} lb-in^2 due to 6-inch Lateral Spreading Displacement

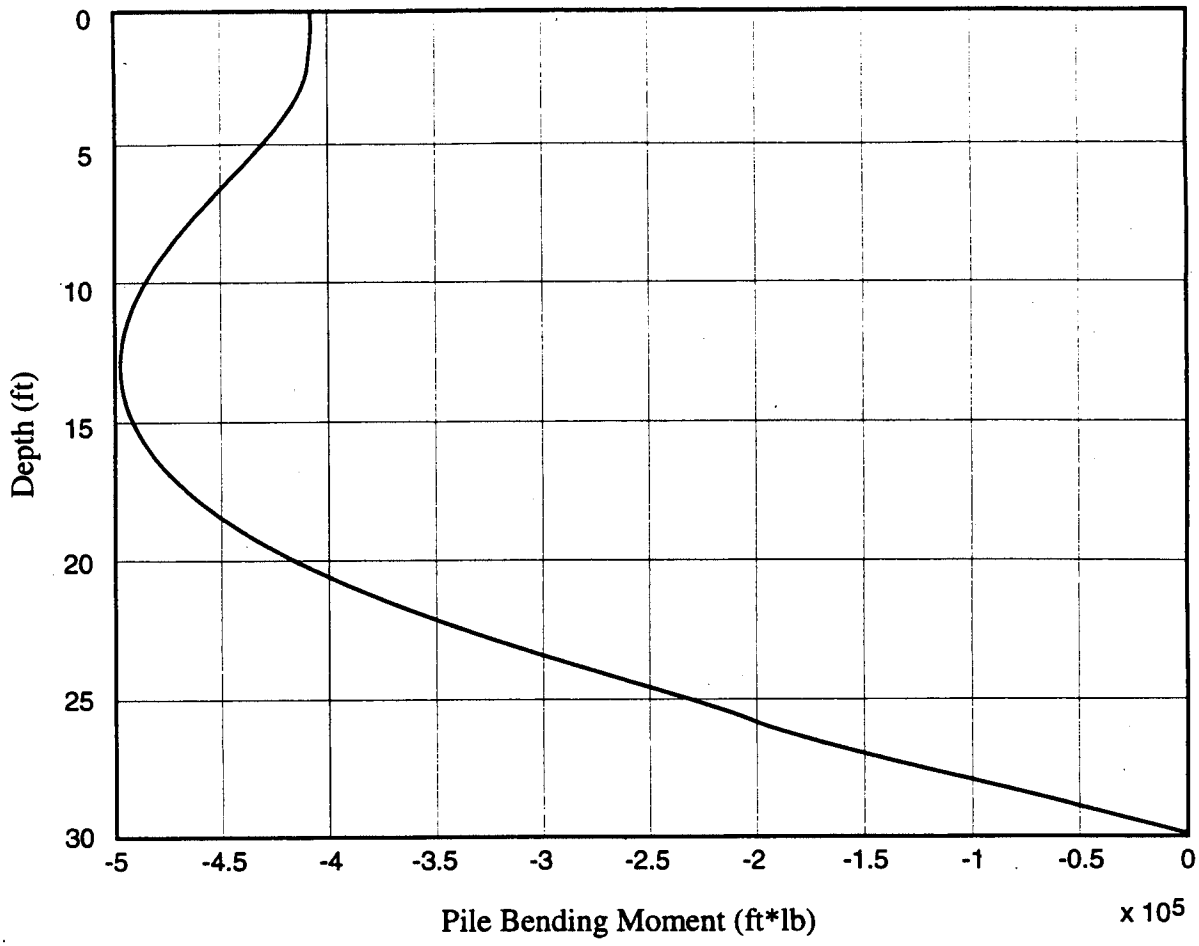

Figure 6.46. Computed Bending Moments in Fixed Head Pile with $EI = 5 \times 10^{10}$ lb-in^2 Due to 6-inch Lateral Spreading Displacement

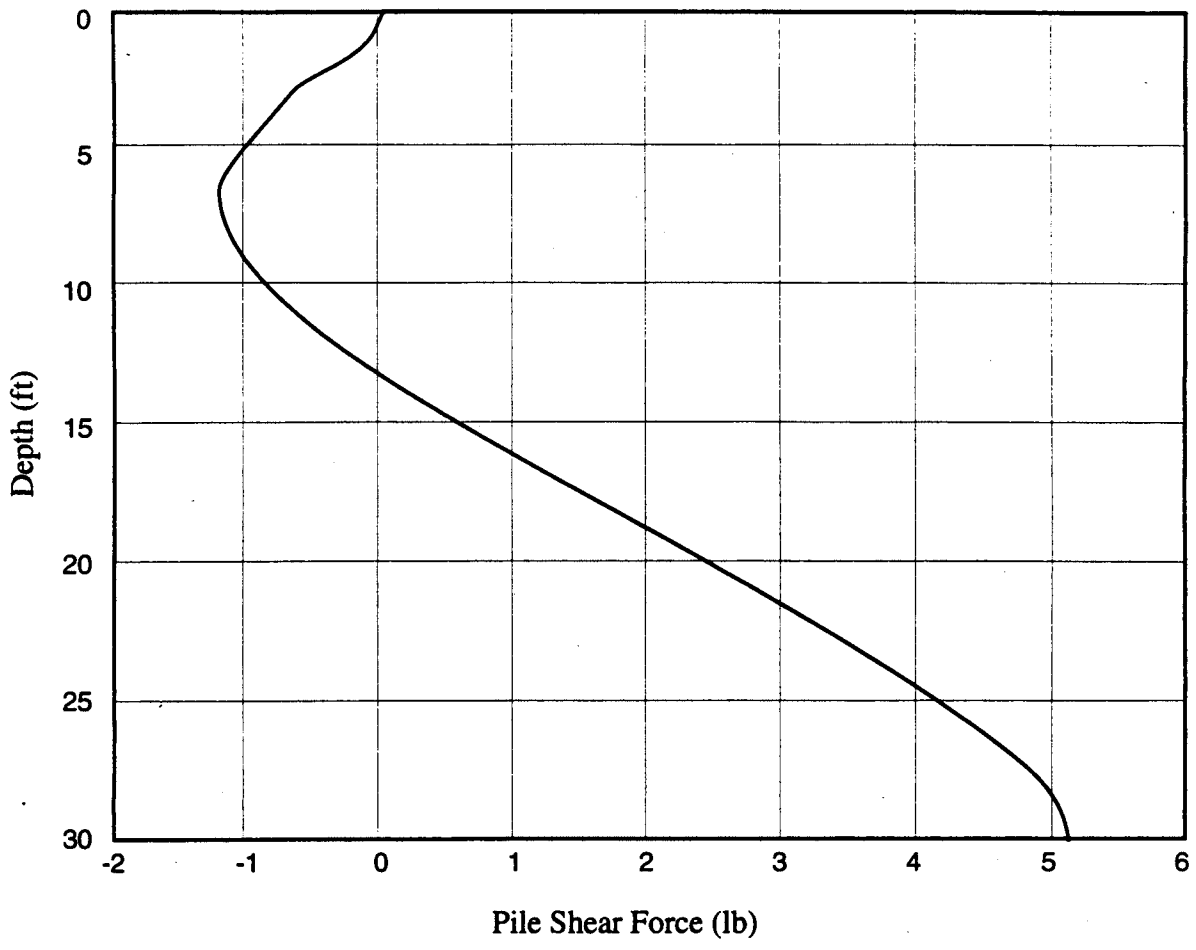

Figure 6.47. Computed Shear in Fixed Head Pile with EI = 5 x 10^{10} lb-in^2 due to 6-inch Lateral Spreading Displacement

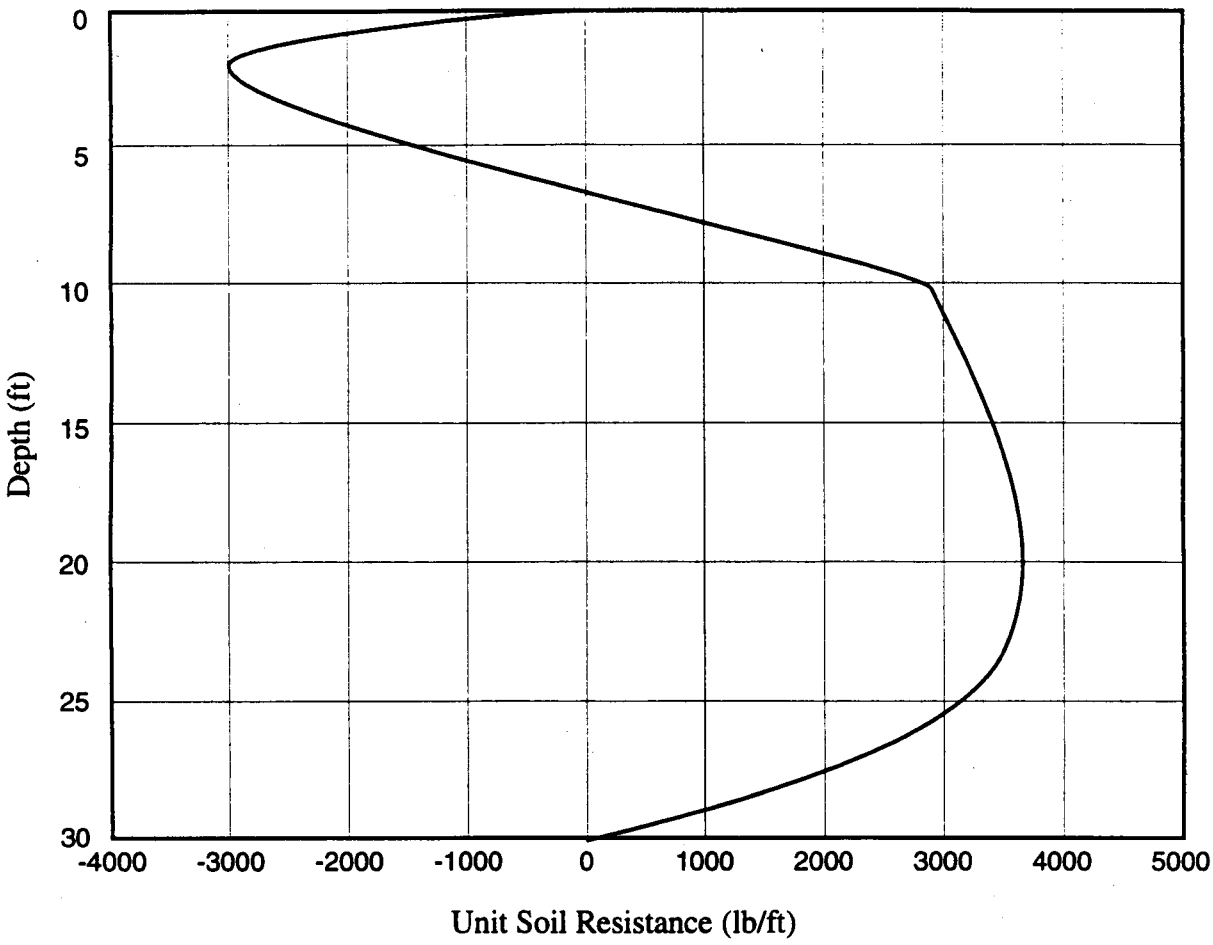

Figure 6.48. Computed Unit Soil Resistance for Fixed Head Pile with EI = 5 x 10^{10} lb-in^2 due to 6-inch Lateral Spreading Displacement

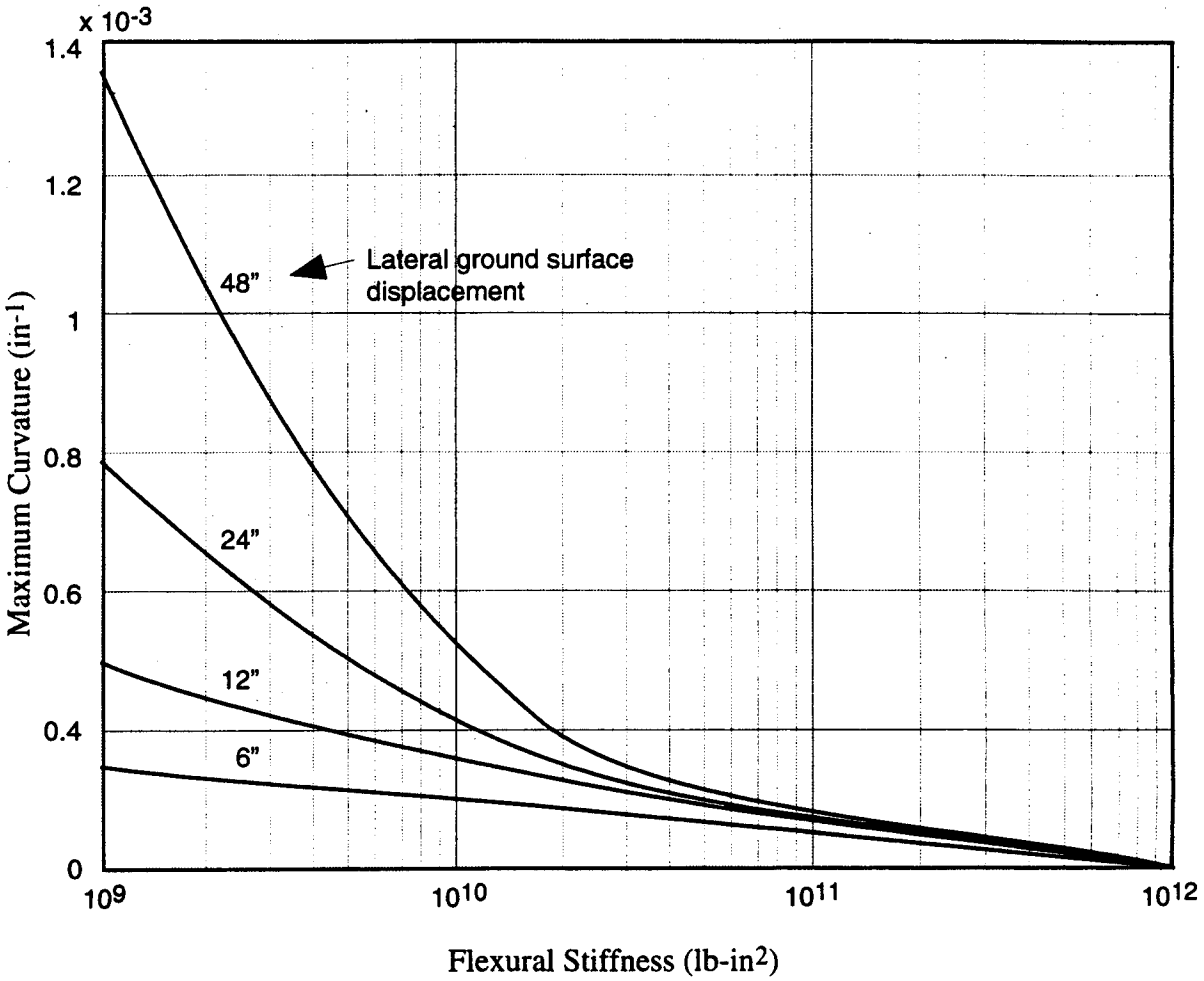

Figure 6.49. Computed Maximum Bending Moments for Piles of Various Flexural Stiffnesses—Pinned Head Conditions

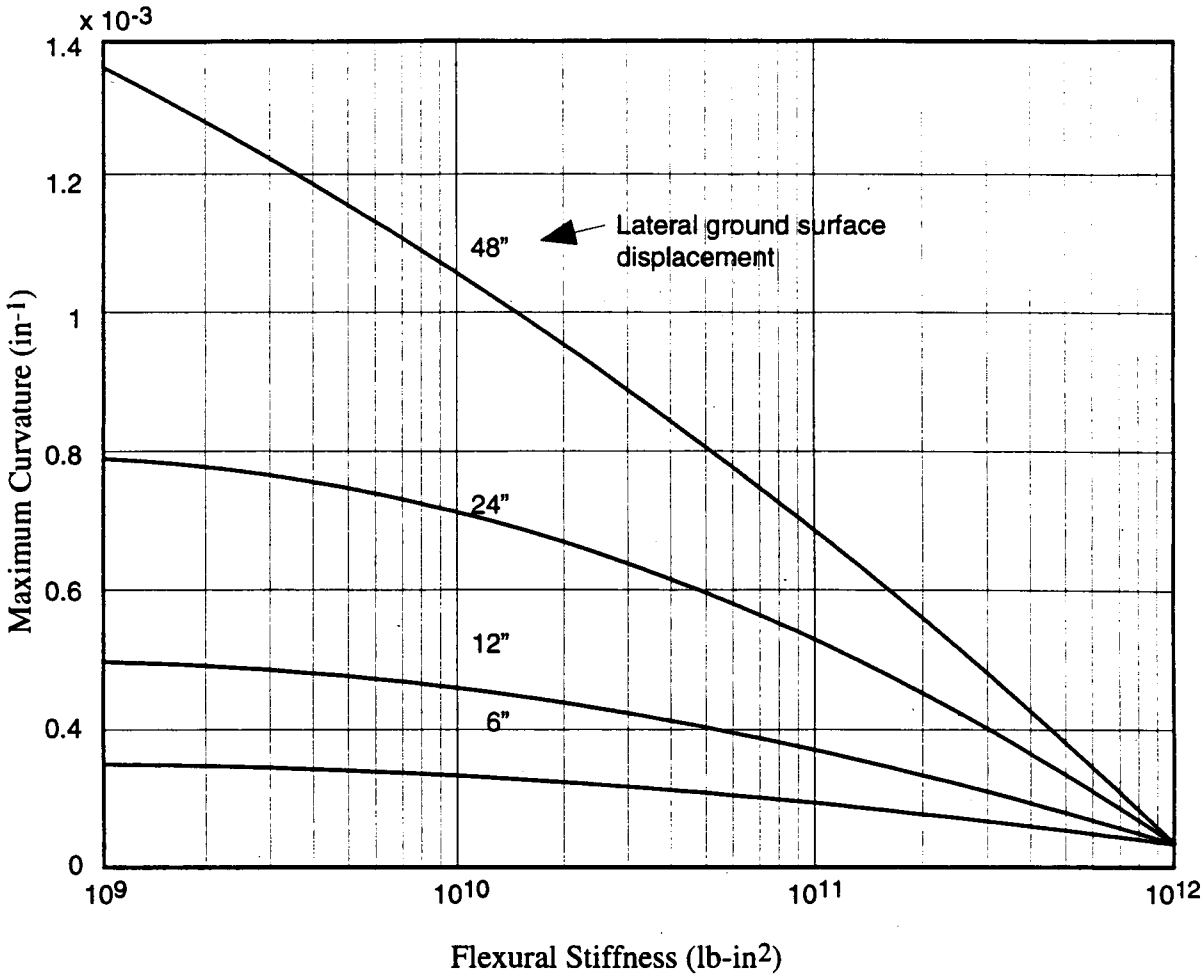

Figure 6.50. Computed Maximum Bending Moments for Piles of Various Flexural Stiffnesses—Fixed Head Conditions

CHAPTER 7
SUMMARY AND CONCLUSIONS

The Alaskan Way Viaduct, which carries some 86,000 vehicles per day as one of only two north-south highways through Seattle, is one of a number of major highway bridges identified by the Washington State Department of Transportation as potentially vulnerable to seismic loading. The Viaduct was constructed in two main sections. Construction on the northern portion of the current Viaduct, designed by the City of Seattle, began in 1949. The southern portion was designed by the Washington State Department of Highways and completed in 1953.

The collapse of the Cypress Viaduct in Oakland, California, during the 1989 Loma Prieta earthquake motivated WSDOT to undertake a series of analyses of the seismic vulnerability of the Alaskan Way Viaduct. This report, and companion reports by Eberhard et al. (1995a; 1995b), describe the results of detailed evaluations of these analyses. The companion reports describe structural earthquake engineering aspects of the seismic vulnerability of the Viaduct. This report describes the geotechnical earthquake engineering investigation of the vulnerability of the Viaduct. The geotechnical investigation included characterization of subsurface soil conditions, evaluation of site-specific ground motions, identification of existing foundation conditions, evaluation of dynamic foundation response characteristics, and evaluation of liquefaction hazards.

SUMMARY

The researchers investigated subsurface conditions by reviewing historical accounts of the development of the Seattle waterfront, reviewing available records in the archives of WSDOT and the City of Seattle Engineering Department, performing supplemental subsurface investigations with insitu testing, and performing laboratory tests on specimens obtained from the supplemental subsurface investigation. The results of these efforts clearly established that the subsurface soil along most of the length of the Alaskan Way Viaduct is dominated by a loose,

saturated, hydraulically-placed fill of variable thickness. This fill is retained along most of the length of the Viaduct by a 60-year-old seawall at the current edge of Elliot Bay. Along the northern portion of the Viaduct, the waterfront fill is underlain by a dense, gravelly glacial till. Along the southern portion, a loose, saturated tideflat deposit of variable thickness lies between the waterfront fill and the dense till. The waterfront fill and tideflat deposits are of similar origin and were deposited in a similar manner; consequently, many of their engineering properties are similar.

The Alaskan Way Viaduct is supported on pile foundations that extend through the waterfront fill and tideflat deposits near the ground surface to the underlying dense till. Each column of the Viaduct is supported by a group of piles which support a buried footing. The number and arrangement of piles in each group varies along the length of the Viaduct and between interior and exterior columns, and the sizes of the pile caps vary to accommodate the sizes of the pile groups. The northern section of the Viaduct (the Seattle section) is typically supported by groups of 14 to 20 concrete-filled steel pipe piles, precast concrete piles, and H-piles. The southern section (the WSDOT section) is typically supported by groups of 11 to 16 composite piles and H-piles. The composite piles consist of timber piles (driven until their butts were below the water table) spliced to overlying concrete-filled pipe pile sections. Available pile driving records indicate that the piles in both the Seattle and WSDOT sections derive their vertical capacities from end bearing within a few feet of the top of the dense till.

Design-level ground motions were determined with the aid of a probabilistic seismic hazard analysis (PSHA). Following discussions with the WSDOT Bridge and Structures office, the PSHA was performed to determine ground motion parameters with a 10 percent probability of exceedance in a 50-year period. This probability is consistent with current AASHTO seismic design criteria. Both shallow and deep seismic source zones, with appropriate attenuation relationships for each, were included in the PSHA. Hazards associated with earthquakes on the Cascadia subduction zone and postulated Seattle fault were estimated and found to have little influence on the design-level ground motion. Peak accelerations, spectral accelerations at a

variety of structural periods, and bracketed durations were all obtained from the PSHA. Synthetic ground motions with these characteristics were then developed and deconvolved through a variety of soil profiles to obtain equivalent bedrock motions. The equivalent bedrock motions were then propagated upward through models of the actual soil conditions at various points along the alignment of the Alaskan Way Viaduct. The resulting ground motions were used in the remainder of the geotechnical earthquake engineering analyses.

To provide input for dynamic analyses of the Alaskan Way Viaduct superstructure, the available soil and foundation conditions were used to estimate the stiffness and damping characteristics of the existing foundations systems. Stiffness and damping coefficients were determined for vertical and horizontal translational movement (in two orthogonal directions), and for rocking (about two orthogonal, horizontal axes) and torsional rotational movements. The contributions of both the piles and the pile cap were considered for each foundation. Cross-coupling effects between swaying and rocking modes of vibration, and the nonlinear response of the soil surrounding the piles were also considered.

Historical accounts of the placement of the waterfront fill and results of the subsurface investigations suggested that the liquefaction potential of the waterfront fills and tideflat deposits may be high. Consequently, a great deal of effort in the geotechnical investigation was devoted to evaluation of liquefaction hazards. The liquefaction hazards investigation was divided into three main portions: (1) evaluation of the susceptibility of the soils underlying the Alaskan Way Viaduct to liquefaction, (2) evaluation of the potential for the design-level ground motions to initiate liquefaction at various locations along the length of the Viaduct, and (3) evaluation of the effects of any liquefaction that was considered likely to occur. Evaluation of the effects of liquefaction required consideration of the potential response of the seawall that runs along the waterfront roughly parallel to the Viaduct.

CONCLUSIONS

A great deal of information on the subsurface and foundation conditions along the length of the Alaskan Way Viaduct was obtained during this investigation. This information, and a

variety of analyses based upon it, have illustrated the influence of geotechnical factors on the seismic vulnerability of the Viaduct. Some of the geotechnical factors will influence the dynamic response of the Viaduct during an earthquake. The effects of these factors will be manifested in the structural response of the Viaduct; their influence is inherent in the results of the seismic vulnerability evaluations described by Eberhard et al. (1995a; 1995b). Other geotechnical factors have a direct influence on the seismic vulnerability of the Viaduct. Specific conclusions regarding the effects of geotechnical factors on the seismic vulnerability of the Alaskan Way Viaduct are listed below.

1. Over all but its very northern portion, the Alaskan Way Viaduct is supported by pile foundations that extend through a waterfront fill deposit that is underlain by a natural tideflat deposit in some areas. The thicknesses of the waterfront fill and tideflat deposits vary considerably over the length of the Viaduct. The piles extend to the dense till that underlies the waterfront fill and tideflat deposits.

2. The waterfront fill consists of a clean to silty sand, most of which was placed without compaction by dumping through the waters of Elliot Bay, or by hydraulic filling operations. The waterfront fill contains occasional organic matter and debris.

3. The waterfront fill and tideflat deposits both exhibit very low standard penetration resistance, very low cone penetration tip resistance, and low shear wave velocities. Each of these characteristics indicates that the waterfront fill and tideflat deposits exist in a very loose state. From the standpoints of material composition, stiffness, and apparent density, the waterfront fill and tideflat deposits are so similar that they can be considered as a single "soft soil" deposit for the purpose of ground response analyses.

4. Under static conditions, the piles that support the Alaskan Way Viaduct derive the great majority of their vertical capacity from end bearing in the dense till beneath the waterfront fill and tideflat deposits. Available records indicate that the piles penetrate only a few feet into the dense till. Consequently, the capacity of the piles derives primarily from mobilization of the shear strength of the upper portion of the dense till.

5. Given a criterion of 10 percent probability of exceedance in a 50-year period, the design-level ground motion represents much stronger shaking at the Alaskan Way Viaduct site than was produced by the 1949 Olympia earthquake or the 1965 Seattle-Tacoma earthquake. Although the Viaduct survived the 1965 Seattle-Tacoma earthquake with little apparent damage, the level of shaking experienced in that event was much lower than the design-level ground motion.

6. Subsurface conditions will strongly influence the nature of any earthquake ground motions that are transmitted to the Alaskan Way Viaduct superstructure. At locations where the soft soils are thin or nonexistent, ground surface motions will be characterized by high accelerations that will occur at relatively high frequencies. At locations where the soft soils are thick, ground surface accelerations will be considerably lower but will also occur at lower frequencies.

7. Peak spectral accelerations for a period of 1.0 sec (the approximate fundamental period of vibration of the Alaskan Way Viaduct superstructure) reach their maximum values at locations where the Viaduct is underlain by about 40 feet (12.2 m) of soft soil. The level of shaking at these locations in a design-level earthquake is expected to be quite strong.

8. The pile group foundations that support the Viaduct would offer resistance to relative displacement between the bases of the columns of the superstructure and the surrounding soil. A considerable portion of that resistance would come from passive resistance of the soil adjacent to the vertical surfaces of the footings.

9. According to all applicable criteria, the waterfront fill and tideflat deposits are highly susceptible to liquefaction. The composition of each soil is consistent with that of soils that have liquefied in past earthquakes; each was deposited in a manner that has been shown to produce liquefiable soils in other areas; and each is currently in a loose condition, as evidenced by three types of insitu tests. Furthermore, evidence of some liquefaction was observed in both the 1949 and 1965 earthquakes.

10. The design-level ground motion is expected to cause widespread liquefaction of the waterfront fill and tideflat deposits that underlie most of the Viaduct. Liquefaction analyses based on three independent measures of liquefaction resistance consistently indicated that extensive liquefaction should be expected in the design-level earthquake. Identical analyses indicated that limited occurrences of liquefaction, with occasional expression at the ground surface, would be produced by a ground motion equivalent to that produced by the 1965 Seattle-Tacoma earthquake; this result is consistent with the observed effects of that earthquake.

11. Widespread liquefaction could be produced by ground motions that are less intense than the design ground motion. Analyses suggest that a ground motion with 50 percent probability of exceedance in a 50-year period could cause

widespread liquefaction. Such a motion is five times more likely to occur than the design ground motion.

12. Liquefaction would have a number of potential effects on the Viaduct. Though precise prediction of the effects of liquefaction remains beyond the current abilities of the geotechnical engineering profession, a number of effects appear likely:

a. Numerous sand boils beneath the Alaskan Way Viaduct are expected following a design-level ground motion. The effect of these sand boils on the seismic vulnerability of the Viaduct should be negligible.

b. Significant ground surface settlements would develop during and after design-level ground motion. These settlements would cause significant downdrag loading on the pile foundations as the liquefied soil reconsolidated, and would also cause additional vertical loading from the soils above the footings. Because of variations in the thickness of soft soils and anticipated ground motions along the length of the Viaduct, the magnitudes of these settlements would also vary along the length of the Viaduct.

c. The design-level ground motion would generate high pore pressures in the waterfront fill and tideflat deposits along the length of the Viaduct. These high pore pressures would virtually eliminate any positive pile skin friction that could contribute to the support of the Viaduct. More importantly, the high pore pressures in the soft soils would cause a hydraulic gradient that would force water to flow from the liquefied soils

into the underlying dense till both during and after the earthquake. The result would be an increase in pore pressure with an accompanying decrease in effective stress, hence strength, of the soils in the upper portion of the dense till. Since the upper portion of the dense till provides support for the weight of the Viaduct superstructure, reduction of its strength could lead to bearing failure of the piles. The effects of bearing failure would be downward movements of the piles themselves. Heterogeneity of the strength and permeability of the soils near the top of the dense till suggest that these pile movements would be non-uniform. Consequently, the Alaskan Way Viaduct superstructure could be subjected to substantial differential vertical foundation movements.

d. The seismic and post-earthquake stability of the soils beneath the Viaduct would be influenced by the presence and performance of the seawall that runs along the Seattle waterfront parallel to much of the Viaduct. Little information on the current condition of the seawall is available, and detailed evaluation of the seawall was beyond the scope of this investigation. All conclusions regarding stability and potential lateral soil movement were based on assumptions about the seawall and a typical soil profile at a particular location. Though these assumptions were consistent with the available information, further study of the seawall is needed.

e. Stability analyses of a typical section perpendicular to the Viaduct indicate that flow sliding would not be expected if the seawall remained predominantly intact, i.e. if the structural elements of the seawall remained connected. If the seawall were to fail catastrophically, progressive slope failure could begin near the seawall and eventually extend back to the

Viaduct. Such failures could produce large foundation displacements. Further study of the stability of additional sections perpendicular to the Viaduct is needed.

f. Significant lateral permanent displacement of the soil beneath the Viaduct is expected in a design-level ground motion. The lateral displacements would vary with the thickness of the soft soil along the length of the Viaduct; they would also be influenced by the performance of the seawall. Though the magnitude of these displacements cannot be predicted with great accuracy, several approaches to their estimation indicated that they would likely be measured in feet. On the basis of all of the available information, it appears likely that the design-level ground motion would produce permanent lateral displacements on the order of 3 to 4 feet if the seawall remained predominantly intact. If the seawall failed catastrophically, (i.e., if the connections between the piles, relieving platform, and wall were lost), lateral displacements could be much larger.

g. Soil-pile interaction analyses indicated that bending failure of many of the piles that support the Viaduct would begin at permanent lateral displacements of approximately 10 to 12 inches (25 to 30 cm). Failure of the splices that connect the timber and concrete sections of the composite piles in the WSDOT section could occur at even smaller levels of displacement.

In summary, it is clear that liquefaction represents a severe threat to the structural integrity of the Alaskan Way Viaduct and to many other structures and facilities along the Seattle waterfront. The vertical and horizontal soil movements expected from liquefaction in a design-

level ground motion would cause failure of the piles that support the Viaduct and induce very large loads in the superstructure of the Viaduct. While specific conclusions regarding the dynamic response of the superstructure are presented in the companion reports by Eberhard et al. (1995a; 1995b), it appears unlikely that the Viaduct has sufficient strength or ductility to resist loads caused by liquefaction-induced soil movements without severe damage or collapse.

ACKNOWLEDGMENTS

The research described in this report was part of a comprehensive seismic vulnerability investigation funded by the Washington State Department of Transportation. The research was conducted by the University of Washington Department of Civil Engineering. Associate Professor Steven L. Kramer and Assistant Professor Marc Eberhard were the principal investigators.

The geotechnical aspects of the seismic vulnerability investigation were performed by Prof. Kramer, Research Associate N. Sivaneswaran, and Research Assistant Kathryn Tucker. Jim Strout was supported as an hourly assistant in the early part of the research. Dr. Sivaneswaran was heavily involved in the ground response analyses and dynamic analyses of foundation impedances. Ms. Tucker was involved in the interpretation of subsurface conditions, material characterization, ground response analyses, and liquefaction analyses. Mr. Strout assisted with the seismic hazard analyses.

A great deal of assistance was provided to the researchers by various WSDOT personnel. Al Kilian of the Materials Laboratory, Myint Lwin and Ed Henley of the Bridge & Structures office, and Keith Anderson of the Research Office were instrumental in developing the research plan and monitoring of the project progress. Tony Allen and Todd Harrison of the Material Laboratory also assisted in progress monitoring. Technical staff from the Materials Laboratory performed a variety of laboratory tests on specimens obtained from the supplemental subsurface investigation. The authors are grateful for all of this assistance.

Deep downhole seismic testing was performed and interpreted by Mr. Steve Palmer of the Washington State Department of Natural Resources. Mr. Palmer's efforts are also gratefully acknowledged.

REFERENCES

Bucknam, R.C., Hemphill-Haley, E., and Leopold, E.B. (1992) "Abrupt uplift within the past 1700 years at Southern Puget Sound, Washington," *Science*, Vol. 258, pp. 1611-1613.

Byrne, P.M., Jitno, H., and Salgado, R. (1992). "Earthquake-induced displacements of soil-structures systems," *Proceedings*, 10th World Conference on Earthquake Engineering, Madrid, Spain, Vol. 3, pp. 1407-1412.

Hamada, M. (1992). "Large ground deformation and their effects on lifelines: 1964 Niigata earthquake," Case Studies of Liquefaction and Lifeline Performance During Past Earthquakes, National Center for Earthquake Engineering Research, State University of New York at Buffalo, pp. 3-1,3-123.

Hamada, M. (1992). "Large ground deformation and their effects on lifelines: 1983 Nihonkai Chubu earthquake," Case Studies of Liquefaction and Lifeline Performance During Past Earthquakes, National Center for Earthquake Engineering Research, State University of New York at Buffalo, pp. 3-1,3-123.

Iai, S. and Kameoka, T. (1993). "Finite element analysis of earthquake induced damage to anchored steel sheet pile quay walls," *Soils and Foundations*, Vol. 33, No. 1, pp. 71-91.

Ishihara, K. (1985). "Stability of natural deposits during earthquakes," *Proceedings*, Eleventh International Conference on Soil Mechanics and Foundation Engineering, Vol. 1, pp. 321-376.

Lee, M.K.W and Finn, W.D.L. (1978). "DESRA-2, Dynamic effective stress response analysis of soil deposits with energy transmitting boundary including assessment of liquefaction potential," *Soil Mechanics Series No. 38*, University of British Columbia, Vancouver, British Columbia.

Marcuson, W.F., III and Bieganousky, W.A. (1977). "SPT and relative density in coarse sands," *Journal of the Geotechnical Engineering Division*, ASCE, Vol. 103, No. GT11, pp. 1295-1309.

Mitchell, J.K. and Tseng, D.-J. (1990). "Assessment of liquefaction potential by cone penetration resistance," *Proceedings*, H. Bolton Seed Memorial Symposium, Berkeley, California, Vol. 2, J.M. Duncan ed., pp. 335-350.

O'Neill, M.W. and Murchison, J.M. (1983). "An evaluation of p-y relationships in sands," *Research Report PRAC 82-41-1*, American Petroleum Institute, University of Houston, Houston, Texas, 174 pp.

Ortigosa, P., Retamal, E., and Whitman, R.V. (1993). "Failures of quay walls during Chilean earthquake of March 1985," *Proceedings*, Third International Conference on Case Histories in Geotechnical Engineering, St. Louis, Missouri, Vol. 1, pp. 565-573.

Pitilakis, K. and Moutsakis, A. (1989). "Seismic analysis and behavior of gravity retaining walls - the case of Kalamata Harbor quay wall," *Soils and Foundations*, Vol. 29, No. 1, pp. 1-17.

Pyke, R.L. (1985). "TESS1 User's Guide," TAGA Engineering Software Services, Berkeley, California.

Pyke, R.L. (1993). Personal communication.

Silva, W.J. (1987). "WES RASCAL code for synthesizing earthquake ground motions," *Miscellaneous Paper S-73-1, Report 24*, U.S. Army Engineer Waterway Experiment Station, Vicksburg, Mississippi, 73 pp.

Appendix A

Supplementary Subsurface Investigation

Boring Logs

LOG OF TEST BORING

Washington State Department of Transportation

S.R. 99 SECTION Alaska Way Viaduct Job No. MS-1826

Hole No. H-1-93 Sub Section Seismic Study Cont. Sec. 1791

Station 135+15.2 Offset 30' Rt. Ground El. 9.2'

Type of Boring Wet Rotary Casing HW X 100', HQ X 182' W.T. El. See Log

Inspector Date June 16, 1993 Sheet 1 of 10

DEPTH	BLOWS PER FT.	PROFILE	SAMPLE TUBE NOS.			DESCRIPTION OF MATERIAL
						Ground surface - railroad fill, sand and gravel.
	4		STD PEN 35		3 2 2	Very loose, grayish brown, moist, gravelly SILT with fine sand and gravel layers. Retained 1.2 ft. See note at bottom of log for SPT-35.
5	5		STD PEN 1		2 3 2	**SP-SM, M.C. = 25.9%** Loose, dark brownish gray, wet, slightly silty, fine to medium **SAND** with shell fragments. Retained 1.5 ft.
			U-14		D E F	(400 p.s.i. to push sampler 2 ft.) Silty, fine to coarse SAND with a trace of shell and fine gravel. Retained 1.0 ft. See note at bottom of log for U-14.
10	6		STD PEN 2		2 3 3	Loose, dark brownish gray, wet, fine to medium **SAND** with shell fragments. Note: Tide flat material with high dilatancy. Retained 1.0 ft.
15			U-1		E F	(150 to 400 psi to push sampler 2 ft.) Dark gray, wet, fine to medium SAND with shell fragments. Note: high dilatancy. Retained 0.7 ft.
	8		STD PEN 3		3 4 4	Loose, dark gray, wet, fine to medium **SAND** with shell fragments. Note: high dilatancy.
20						

Continued Next Page

LOG OF TEST BORING

Washington State Department of Transportation

S.R. 99 SECTION Alaska Way Viaduct Job No. MS-1826

Hole No. H-1-93 Sub Section Seismic Study Cont. Sec. 1791

Station 135+15.2 Offset 30' Rt. Ground El. 9.2'

Type of Boring Wet Rotary Casing HW X 100', HQ X 182' W.T. El. See Log

Inspector Date June 16, 1993 Sheet 2 of 10

DEPTH	BLOWS PER FT.	PROFILE	SAMPLE TUBE NOS.		DESCRIPTION OF MATERIAL
			U-2	A THRU F	(Sampler sank with weight of drill.) **M.C. = 42.9%(A), 36.4%(B), 34.8%(C), 33.3%(D), 34.4%(E), 38.1%(F).** Top 4 inches: fine to medium SAND with silt lenses. Bottom 20 inches: fine sandy SILT with silt lenses and a trace of clay and shell. Recovered 2.0 ft.
	9		STD PEN 4	3 4 5	**ML, M.C. = 42.3% / SP-SM, M.C. = 26.4%** Top 8 inches: Loose, dark gray, wet, fine sandy **SILT**. Bottom 10 inches: Very dark gray, moist, fine to medium **SAND** with fibrous organic material and shell fragments (95% water recovery). Retained 1.5 ft.
25			U-3	E F	(450 psi to push sampler 2 ft.) Dark gray, wet, fine to medium SAND with shell fragments. Note: high dilatancy. Retained 0.7 ft.
	11		STD PEN 5	4 4 7	Medium dense, dark gray, wet, fine to medium **SAND** with shell fragments. Note: high dilatancy. (10% water loss down hole) Retained 1.5 ft.
30			U-4		(150 to 500 psi to push sampler 2 ft.) Dark gray, wet, fine to medium SAND with shell fragments. Note: high dilatancy. No recovery.
	26		STD PEN 6	8 11 15	Dense, dark gray, moist, fine to medium SAND with shell fragments (10% water loss). Retained 1.3 ft.
35			U-5	D E F	(500 psi to push sampler 2 ft.) Dark gray, moist, fine to medium SAND with shell fragments. Note: high dilatancy. Retained 1.0 ft.
	8		STD PEN 7	6 4 4	Loose, dark gray, wet, fine to medium **SAND** with shell fragments (5 to 10% water loss). Retained 1.5 ft.
40					

Continued Next Page

LOG OF TEST BORING

Washington State Department of Transportation

S.R. 99 SECTION Alaska Way Viaduct Job No. MS-1826

Hole No. H-1-93 Sub Section Seismic Study Cont. Sec. 1791

Station 135+15.2 Offset 30' Rt. Ground El. 9.2'

Type of Boring Wet Rotary Casing HW X 100', HQ X 182' W.T. El. See Log

Inspector _____ Date June 16, 1993 Sheet 3 of 10

DEPTH	BLOWS PER FT.	PROFILE	SAMPLE TUBE NOS.	DESCRIPTION OF MATERIAL
			U-6 E F	(400 psi to push sampler 2 ft.) **M.C. = 29.5%** Dark grey, wet, fine to medium SAND with shell fragments. Recovered 0.7 ft.
	13		STD PEN 8 5 7 6	Medium dense, dark gray, wet, fine to medium **SAND** with shells fragments. Note: high dilatancy. (10% water loss down hole) Retained 1.5 ft.
45			U-7 D E F	(500 psi to push sampler 2 ft.) **M.C. = 30.4%** Fine to medium **SAND** with shell fragments. Note: high dilatancy. Retained 1.0 ft.
	13		STD PEN 9 5 6 7	Medium dense, dark gray, wet, fine to medium **SAND** with shell fragments (5-10% water loss down hole). Retained 1.2 ft.
50			U-8	(200-500 psi to push sampler 2 ft.) Medium dense, dark gray, wet, fine to medium **SAND** with shell fragments. No recovery.
	9		STD PEN 10 3 4 5	**SP-SM, M.C. = 35.6%** Loose, very dark grey, wet, silty, fine SAND with laminated silt lenses, shell fragments and fibrous organic material. Retained 1.0 ft.
55			U-9 A THRU F	(400 psi to push sampler 2.0 ft.) Fine to medium SAND with traces of shell and wood fragments. Retained 2.0 ft.
	9		STD PEN 11 4 4 5	Loose, dark gray, wet, fine to medium **SAND** with layers of silt, a trace of decayed wood chunks and root hairs. (10% water loss) Retained 1.5 ft.
60				

Continued Next Page

LOG OF TEST BORING

Washington State Department of Transportation

S.R. 99 SECTION Alaska Way Viaduct Job No. MS-1826

Hole No. H-1-93 Sub Section Seismic Study Cont. Sec. 1791

Station 135+15.2 Offset 30' Rt. Ground El. 9.2'

Type of Boring Wet Rotary Casing HW X 100', HQ X 182' W.T. El. See Log

Inspector Date June 16, 1993 Sheet 4 of 10

DEPTH	BLOWS PER FT.	PROFILE	SAMPLE TUBE NOS.	DESCRIPTION OF MATERIAL
			U-10 A B C D E	(100-600 psi to push sampler 2.0 ft.) **M.C. = 35.1%** Silty, fine to medium SAND with shells, wood fragments and fine, rounded gravel. Retained 1.7 ft.
	11		STD PEN 12 3 4 7	Top 8 inches: Medium dense, dark grey, wet, fine sandy SILT with a trace of organics and shells. Bottom 10 inches: fine to medium SAND with silt lenses (5% water loss). Retained 1.5 ft.
65			U-11 A B C D E	(100-600 psi to push sample 2.0 ft.) **M.C. = 42.5%** Dark gray, wet, silty, fine SAND. Note: high dilatancy. Retained 1.7 ft.
	17		STD PEN 13 5 9 8	Medium dense, dark gray, wet, slightly silty, fine to medium **SAND** with a trace of shells (5% water loss). Retained 1.0 ft.
70			U-12 A B C D E	(600 psi to push sampler 2.0 ft.) Dark brown, wet, slightly silty, fine to medium SAND with trace of shells and decayed wood fragments. Retained 1.7 ft.
	17		STD PEN 14 5 8 9	**SP-SM, M.C. = 32.6%** Medium dense, very dark grey, wet, silty, fine to medium **SAND** with silt lenses and shell fragments (5% water loss). Retained 1.2 ft.
75			U-13 E F	(450 psi to push sampler 2 ft.) **M.C. = 39.3%** Very dark gray, wet, silty, fine to medium SAND with silt lenses and shell fragments (5% water loss). Retained 0.7 ft.
	3		STD PEN 15 1 2 1	**ML, M.C. = 32.2%** Very loose, dark gray, wet, fine sandy SILT with a trace of shell fragments. (5% water loss). Retained 1.3 ft.
80				

Continued Next Page

LOG OF TEST BORING

Washington State Department of Transportation

S.R. 99 SECTION Alaska Way Viaduct Job No. MS-1826

Hole No. H-1-93 Sub Section Seismic Study Cont. Sec. 1791

Station 135+15.2 Offset 30' Rt. Ground El. 9.2'

Type of Boring Wet Rotary Casing HW X 100', HQ X 182' W.T. El. See Log

Inspector _____ Date June 16, 1993 Sheet 5 of 10

DEPTH	BLOWS PER FT.	PROFILE	SAMPLE TUBE NOS.	DESCRIPTION OF MATERIAL
			S-1	(250 psi to push shelby tube 2.0 ft.) Dark gray, wet, silty, fine to medium SAND with a trace of shells. Retained 2.0 ft.
	14		STD 3 PEN 5 16 9	**SM, M.C. = 27.9%** Medium dense, very dark grey, moist, very silty, fine to medium SAND with shell fragments (5% water loss). Retained 1.5 ft.
85			S-2	(250 psi to push shelby tube 2.0 ft.) **M.C. = 40.2%** Very dark grey, wet, very silty, fine to medium SAND with shell fragments (5% water loss). Retained 2.0 ft.
	3		STD 1 PEN 1 17 2	Very loose, dark gray, moist, silty, fine SAND with a trace of shells (5% water loss). Retained 1.5 ft.
90			S-3	(500 psi to push shelby tube 2.0 ft.) **M.C. = 36.2%** Wet, silty, fine SAND with trace of shells and root hairs. Retained 2.0 ft.
	20		STD 5 PEN 9 18 11	Medium dense, gray, moist, fine SAND with silt lamination. Retained 1.5 ft.
95			S-4	Gray, moist, silty, fine SAND Retained 2.0 ft.
	19		STD 5 PEN 7 19 12	Medium dense, gray, moist, silty, fine SAND. Retained 1.5 ft.
100				

Continued Next Page

LOG OF TEST BORING

Washington State Department of Transportation

S.R. 99 SECTION Alaska Way Viaduct Job No. MS-1826

Hole No. H-1-93 Sub Section Seismic Study Cont. Sec. 1791

Station 135+15.2 Offset 30' Rt. Ground El. 9.2'

Type of Boring Wet Rotary Casing HW X 100', HQ X 182' W.T. El. See Log

Inspector _____ Date June 16, 1993 Sheet 6 of 10

DEPTH	BLOWS PER FT.	PROFILE	SAMPLE TUBE NOS.		DESCRIPTION OF MATERIAL
			S-5		Gray, moist, silty, fine SAND. Retained 2.0 ft.
	15		STD PEN 20	5 5 10	Medium dense, gray, moist, silty, fine SAND. Retained 1.5 ft.
105			S-6		Gray, moist, silty, fine SAND. Retained 2.0 ft.
	16		STD PEN 21	2 5 11	Medium dense, gray, moist, silty, fine SAND. Retained 1.5 ft.
110			S-7		**M.C. = 42.8%** Gray, moist, silty, fine SAND. Retained 2.0 ft.
	6		STD PEN 22	3 3 3	Loose, gray, wet, silty, fine SAND with wood fragments. Retained 0.7 ft.
115			S-8		Gray, wet, sandy SILT. Retained 2.0 ft.
	16		STD PEN 23	5 6 10	Medium dense, dark grey, wet, slightly silty, fine to coarse **SAND** with trace organics and wood fragments. Retained 1.5 ft.
120					

Continued Next Page

LOG OF TEST BORING

Washington State Department of Transportation

S.R. 99 SECTION Alaska Way Viaduct Job No. MS-1826

Hole No. H-1-93 Sub Section Seismic Study Cont. Sec. 1791

Station 135+15.2 Offset 30' Rt. Ground El. 9.2'

Type of Boring Wet Rotary Casing HW X 100', HQ X 182' W.T. El. See Log

Inspector Date June 16, 1993 Sheet 7 of 10

DEPTH	BLOWS PER FT.	PROFILE	SAMPLE TUBE NOS.		DESCRIPTION OF MATERIAL
	4		STD	2	Very loose, dark grey, moist, silty, fine SAND.
			PEN	2	Retained 1.5 ft.
			24	2	
125			S-9		No Recovery.
	8		STD	2	Loose, dark gray, moist, silty, fine SAND.
			PEN	2	Retained 1.5 ft.
			25	6	
130			S-10		**M.C. = 33.1%**
					Dark gray, moist, silty, fine SAND.
					Retained 2.0 ft.
	5		STD	1	Loose, dark gray, moist, fine sandy SILT.
			PEN	1	Retained 1.5 ft.
			26	4	
135	5		STD	1	Loose, dark gray, moist, fine sandy SILT.
			PEN	1	Retained 1.5 ft.
			27	4	
140					

Continued Next Page

LOG OF TEST BORING

Washington State Department of Transportation

S.R. 99 SECTION Alaska Way Viaduct Job No. MS-1826

Hole No. H-1-93 Sub Section Seismic Study Cont. Sec. 1791

Station 135+15.2 Offset 30' Rt. Ground El. 9.2'

Type of Boring Wet Rotary Casing HW X 100', HQ X 182' W.T. El. See Log

Inspector _____ Date June 16, 1993 Sheet 8 of 10

DEPTH	BLOWS PER FT.	PROFILE	SAMPLE TUBE NOS.		DESCRIPTION OF MATERIAL
			S-11		Dark gray, moist, fine sandy SILT. Retained 2.0 ft.
	5		STD	0	ML, M.C. = 31.4%
			PEN	2	Loose, gray, wet, fine sandy SILT.
			28	3	Retained 1.5 ft.
145					
	10		STD	0	Loose, dark gray, moist, silty, fine SAND with scattered,
			PEN	4	rounded fine GRAVEL (Coarse sand in tip of the sampler).
			29	6	Retained 1.5 ft.
150					
155					
	64		STD	15	SP, M.C. = 10.7%
			PEN	32	Very dense, gray, wet, slightly silty, gravelly, fine to
			30	32	coarse SAND (Till). Gravel is rounded to sub angular.
					(50% water loss) Retained 1.0 ft.
160					

Continued Next Page

LOG OF TEST BORING

Washington State Department of Transportation

S.R. 99 SECTION Alaska Way Viaduct Job No. MS-1826

Hole No. H-1-93 Sub Section Seismic Study Cont. Sec. 1791

Station 135+15.2 Offset 30' Rt. Ground El. 9.2'

Type of Boring Wet Rotary Casing HW X 100', HQ X 182' W.T. El. See Log

Inspector Date June 16, 1993 Sheet 9 of 10

DEPTH	BLOWS PER FT.	PROFILE	SAMPLE TUBE NOS.			DESCRIPTION OF MATERIAL
165	58/6"		STD PEN 31		15 58/6"	Very dense, gray, wet, silty, gravelly, fine to coarse SAND. Gravel is rounded to subangular, poorly graded, loosely bedded Glacial Till. Retained 0.6 ft.
170						(80-95% water recovery)
175	100/3"		STD PEN 32		49 100/3"	Very dense, Till material. No recovery.
	49		STD PEN 33		15 24 25	Dense, gray, moist SILT (massive, no structure) with a 3 inch layer of silty, coarse sand and gravel. Gravel is angular to subangular. (98% water recovery) Retained 1.5 ft.
180						

Continued Next Page

LOG OF TEST BORING

Washington State Department of Transportation

S.R. 99 SECTION Alaska Way Viaduct Job No. MS-1826

Hole No. H-1-93 Sub Section Seismic Study Cont. Sec. 1791

Station 135+15.2 Offset 30' Rt. Ground El. 9.2'

Type of Boring Wet Rotary Casing HW X 100', HQ X 182' W.T. El. See Log

Inspector _____ Date June 16, 1993 Sheet 10 of 10

DEPTH	BLOWS PER FT.	PROFILE	SAMPLE TUBE NOS.			DESCRIPTION OF MATERIAL
	70		STD		28	CL, M.C. = 27.4%
			PEN		33	Very hard, gray, moist, CLAY (massive, no structure)
			34		37	with a 1.25" X 0.5" piece of subangular gravel. (100% water recovery) Retained 1.5 ft.
						End of the Test Hole Boring at 183 ft. below ground elevation.
185						Water Table Elevation High tide 0.2 ft. below ground elevation - 6/08/93. Low tide 5.2 ft. below ground elevation - 6/16/93 @ 7:35 A.M.
						Note: SPT-35 and U-14 were sampled after moving test hole 5.0 ft.
190						This is a Summary Log of the Test Hole Boring. Soil/Rock descriptions are derived from visual field identifications and laboratory test data.
195						
200						

DOT FORM 351-003 REVISED 12/79

LOG OF TEST BORING

Washington State Department of Transportation

S.R. 99 SECTION Alaska Way Viaduct Job No. MS-1826

Hole No. H-2-93 Sub Section Seismic Study Cont. Sec. 1791

Station 109+44.5 Offset CL Ground El. 6.6'

Type of Boring Rotary Casing Augers (3" I.D.) W.T. El. -2.4'

Inspector _____ Date July 13, 1993 Sheet 1 of 5

DEPTH	BLOWS PER FT.	PROFILE	SAMPLE TUBE NOS.	DESCRIPTION OF MATERIAL
	19		STD 10 PEN 11 1 8	Medium dense, very dark grayish brown to very dark grey, dry, gravelly, fine to medium sandy SILT with vitreous material (coal?). Retained 0.3 ft.
5				
	6		STD 4 PEN 2 2 4	**SM, M.C. = 16.0%** Loose, greenish gray, moist, gravelly, very silty, fine to coarse **SAND** with root hairs. Retained 1.0 ft.
				▽ 07/13/93
10				
			U-3 D E F	**M.C. = 16.3% (D), 12.8% (E), 19.5% (F)** Greenish gray, wet, gravelly, silty, fine to coarse SAND. Retained 1.8 ft.
	7		STD 2 PEN 3 4 4	Loose, greenish gray, wet, gravelly, silty, fine to coarse **SAND**. Retained 1.0 ft.
15				
			U-5	**SM, PI = 3.74** Greenish gray to dark greenish grey, gravelly, very silty, fine to coarse SAND. Note: No full tubes - bag sample.
	7		STD 3 PEN 3	**SP-SM, M.C. = 24.4%** Loose, gray, wet, stratified, fine to medium SAND with
20				

Continued Next Page

LOG OF TEST BORING

Washington State Department of Transportation

S.R. 99 SECTION Alaska Way Viaduct Job No. MS-1826

Hole No. H-2-93 Sub Section Seismic Study Cont. Sec. 1791

Station 109+44.5 Offset CL Ground El. 6.6'

Type of Boring Rotary Casing Augers (3" I.D.) W.T. El. -2.4'

Inspector _____ Date July 13, 1993 Sheet 2 of 5

DEPTH	BLOWS PER FT.	PROFILE	SAMPLE TUBE NOS.		DESCRIPTION OF MATERIAL
			6	4	fibrous organic material and very dark gray, wet, anoxic mud with woodchips and sawdust. Retained 1.0 ft.
			U-7	E F	**M.C. = 56.1% (E)** Gray, fine SAND and woody, anoxic MUD.
	8		STD PEN 8	5 4 4	Loose, dark gray, wet, stratified, fine to medium SAND with shell fragments and dark brownish gray, wet, organic rich **MUD**. Retained 0.8 ft.
25					
	2		STD PEN 9	1 1 1	Very loose, very dark gray, moist, fine SAND. Retained 1.5 ft.
	7		STD PEN 10	5 4 3	**SP-SM, M.C. = 24.0%** Loose, very dark gray, moist, slightly silty, fine SAND with shell fragments. Retained 1.5 ft.
30					
			U-11	B E F	Dark gray, wet, SILT and fine SAND.
	4		STD PEN 12	2 2 2	Very loose, very dark gray to dark gray, wet, stratified, fine **SAND** (Sample A) and Dark gray, saturated, **SILT** with shell fragments (Sample B). Retained 1.5 ft.
35					
			U-13	B C D E	**M.C. = 42.7** Dark gray, wet, slightly sandy, SILT with shell fragments and organics. Retained 1.9 ft.
	3		STD PEN	F 1	**ML, M.C. = 35.9%** Very loose, dark gray, wet, fine sandy SILT with a trace of
40					

Continued Next Page

LOG OF TEST BORING

Washington State Department of Transportation

S.R. 99 SECTION Alaska Way Viaduct Job No. MS-1826

Hole No. H-2-93 Sub Section Seismic Study Cont. Sec. 1791

Station 109+44.5 Offset CL Ground El. 6.6'

Type of Boring Rotary Casing Augers (3" I.D.) W.T. El. -2.4'

Inspector Date July 13, 1993 Sheet 3 of 5

DEPTH	BLOWS PER FT.	PROFILE	SAMPLE TUBE NOS.			DESCRIPTION OF MATERIAL
			14		0 3	shell fragments.
			U-15		B C D E	Dark gray, saturated, **SILT** with a trace of shells and organics. Retained 1.7 ft.
	7		STD PEN 16		2 2 5	Loose, gray to dark gray, saturated, gravelly, fine to coarse sandy SILT with shell fragments. Retained 1.5 ft.
45						
	69		STD PEN 17		20 27 42	**SW, M.C. = 10.6%** Very dense, dark gray, stratified, slightly silty, gravelly, fine to coarse SAND with shell fragments and organics. And olive gray, wet, silty, fine to coarse sandy GRAVEL. Retained 1.5 ft.
50						
	50/3"		STD PEN 18		48 50/3"	Very dense, greenish gray, wet, slightly silty, gravelly, fine to coarse SAND. Retained 0.6 ft.
55						
	70		STD PEN 19		22 23 47	Sand in lead auger. Very dense, greenish gray to very dark gray, wet, slightly silty, gravelly, fine to coarse SAND. Retained 0.6 ft.
60						

Continued Next Page

LOG OF TEST BORING

Washington State Department of Transportation

S.R. 99 SECTION Alaska Way Viaduct Job No. MS-1826

Hole No. H-2-93 Sub Section Seismic Study Cont. Sec. 1791

Station 109+44.5 Offset CL Ground El. 6.6'

Type of Boring Rotary Casing Augers (3" I.D.) W.T. El. -2.4'

Inspector _____ Date July 13, 1993 Sheet 4 of 5

DEPTH	BLOWS PER FT.	PROFILE	SAMPLE TUBE NOS.	DESCRIPTION OF MATERIAL
	50/4"		STD PEN 20 — 50/4"	Sand in lead auger Very dense, dark greenish gray, to dark gray, wet, gravelly, fine to coarse SAND. Retained 0.3 ft.
65				
	50/4"		STD PEN 21 — 50/4"	Very dense, greenish gray to gray, wet, silty, gravelly, fine to coarse SAND. Retained 0.5 ft.
70				
	70		STD PEN 22 — 20 32 38	Very dense, greenish gray to gray, wet, slightly silty, gravelly, fine to coarse SAND with slightly fractured cobbles. Retained 1.5 ft.
75				
	60		STD PEN 23 — 15 30 30	Very dense, greenish gray to gray, stratified, wet, slightly silty, fine SAND and fine to coarse SAND. Retained 1.2 ft.
80				

Continued Next Page

LOG OF TEST BORING

Washington State Department of Transportation

S.R. 99 SECTION Alaska Way Viaduct Job No. MS-1826

Hole No. H-2-93 Sub Section Seismic Study Cont. Sec. 1791

Station 109+44.5 Offset CL Ground El. 6.6'

Type of Boring Rotary Casing Augers (3" I.D.) W.T. El. -2.4'

Inspector _____ Date July 13, 1993 Sheet 5 of 5

DEPTH	BLOWS PER FT.	PROFILE	SAMPLE TUBE NOS.	DESCRIPTION OF MATERIAL
				End of the Test Hole Boring at 78.5 ft. below ground elevation.
				NOTE: This Test Hole Boring was numbered H-14-93 on the field log.
85				This is a Summary Log of the Test Hole Boring. Soil/Rock descriptions are derived from visual field identifications and laboratory test data.
90				
95				
100				

DOT FORM 351-003 REVISED 12/79

LOG OF TEST BORING

Washington State Department of Transportation

S.R. 99 SECTION Alaska Way Viaduct Job No. MS-1826

Hole No. H-3-93 Sub Section Seismic Study Cont. Sec. 1791

Station 87+99.5 Offset 21' Lt. Ground El. 5.5'

Type of Boring Rotary Casing Augers (3" I.D.) W.T. El. See Log

Inspector Date July 14, 1993 Sheet 1 of 1

DEPTH	BLOWS PER FT.	PROFILE	SAMPLE TUBE NOS.	DESCRIPTION OF MATERIAL
	7		STD PEN 1 — 8 4 3	Loose, black to dark gray, dry, gravelly, silty, fine to coarse **SAND**. Note: Material looks similar to Asphalt. Retained 0.2 ft.
5				
	3		STD PEN 2 S-3 — 1 1 2	Very loose, black to very dark gray, gravelly, silty, fine to coarse **SAND**. Retained 0.1 ft. Material appears similar to Asphalt and Tar. Test Hole has contaminated material. Removed augers, plugged and capped hole with concrete.
10				
				End of the Test Hole Boring at 11.5 ft. below ground elevation.
				Water Table Elevation: Not determined.
15				
				NOTE: This Test Hole Boring was numbered H-5-93 on the field log.
				This is a Summary Log of the Test Hole Boring. Soil/Rock descriptions are derived from visual field identifications.
20				

DOT FORM 351-003 REVISED 12/79

LOG OF TEST BORING

Washington State Department of Transportation

S.R. 99 SECTION Alaska Way Viaduct Job No. MS-1826

Hole No. H-4-93 Sub Section Seismic Study Cont. Sec. 1791

Station 70+53.5 Offset 37.7' Left Ground El. 5.0'

Type of Boring Rotary Casing Augers (3" I.D.) W.T. El. See Log

Inspector Date July 15, 1993 Sheet 1 of 5

DEPTH	BLOWS PER FT.	PROFILE	SAMPLE TUBE NOS.			DESCRIPTION OF MATERIAL
	8		STD PEN 1		5 4 4	Loose, very dark grayish brown, dry, slightly clayey, gravelly, silty, fine to coarse SAND. Retained 0.4 ft.
5	6		STD PEN 2		2 3 3	Loose, very dark gray to dark olive gray, wet, slightly clayey, gravelly, silty, fine to coarse SAND. Retained 0.7 ft.
10	6		STD PEN 3		3 3 3	Loose, black, wet, stratified, medium to coarse SAND (has diesel odor) with shell fragments and gray, wet, clayey SILT. Retained 0.9 ft.
15	6		STD PEN 4		3 2 4	Loose, black, wet, slightly silty, fine to medium SAND with wood chips, shell fragments, and organic material (has anoxic odor). Retained 0.7 ft.
20						

Continued Next Page

LOG OF TEST BORING

Washington State Department of Transportation

S.R. 99 SECTION Alaska Way Viaduct Job No. MS-1826

Hole No. H-4-93 Sub Section Seismic Study Cont. Sec. 1791

Station 70+53.5 Offset 37.7' Left Ground El. 5.0'

Type of Boring Rotary Casing Augers (3" I.D.) W.T. El. See Log

Inspector Date July 15, 1993 Sheet 2 of 5

DEPTH	BLOWS PER FT.	PROFILE	SAMPLE TUBE NOS.	DESCRIPTION OF MATERIAL
	3		STD 1 PEN 2 5 1	**SP-SM, M.C. = 76.2%** Very loose, black, saturated, gravelly, silty, fine to coarse **SAND** with fibrous organic material, wood, and shell fragments (has anoxic odor). Retained 0.7 ft.
25				
	2		STD 1 PEN 1 6 1	One ft. of heave at 26.0 ft. b.g.e. Very loose, black, wet, gravelly, silty, fine to coarse SAND with shell fragments (has anoxic odor). Retained 0.7 ft.
30				
	5		STD 1 PEN 2 7 3	**SP-SM, M.C. = 28.9%** Loose, black to very dark gray, wet, slightly silty, gravelly, fine to coarse SAND (has anoxic odor). Retained 1.5 ft.
35				
	13		STD 4 PEN 7 8 6	Medium dense, dark greenish gray to dark gray, wet, slightly clayey, slightly silty, gravelly, fine to coarse **SAND**. Retained 1.5 ft.
40				

Continued Next Page

LOG OF TEST BORING

Washington State Department of Transportation

S.R. 99 SECTION Alaska Way Viaduct Job No. MS-1826

Hole No. H-4-93 Sub Section Seismic Study Cont. Sec. 1791

Station 70+53.5 Offset 37.7' Left Ground El. 5.0'

Type of Boring Rotary Casing Augers (3" I.D.) W.T. El. See Log

Inspector Date July 15, 1993 Sheet 3 of 5

DEPTH	BLOWS PER FT.	PROFILE	SAMPLE TUBE NOS.			DESCRIPTION OF MATERIAL
	2		STD PEN 9		1 1 1	Very loose, wet, dark greenish gray to very dark gray, stratified, slightly clayey, slightly silty, fine **SAND** and very dark gray to black, wet, organic rich, reduced **MUD** with wood and shell fragments. Retained 1.5 ft.
45			U-10		B C D E F	**M.C. = 44.6%** Gray to dark gray, wet, fine to coarse sandy, slightly clayey **SILT** with shell fragments. Retained 1.8 ft.
	1		STD PEN 11		1 0 1	**SM-SC, M.C. = 23.7%** Very loose, gray to dark gray, massive, wet, gravelly, very silty, clayey, fine to coarse **SAND** with shell fragments.
50						
			U-12		A B	Gray to dark gray, wet, fine to coarse sandy, clayey, SILT with shell fragments. Retained 1.0 ft.
	53/6"		STD PEN 13		35 53	Very dense, greenish gray, slightly silty, fine to coarse sandy **GRAVEL** with a trace of shell fragments. Retained 0.6 ft.
55						
	65/6"		STD PEN 14		65/6"	Very dense, dark gray to gray, moist, gravelly, fine to coarse sandy, clayey **SILT**. Retained 0.3 ft.
60						

Continued Next Page

LOG OF TEST BORING

Washington State Department of Transportation

S.R. 99 SECTION Alaska Way Viaduct Job No. MS-1826

Hole No. H-4-93 Sub Section Seismic Study Cont. Sec. 1791

Station 70+53.5 Offset 37.7' Left Ground El. 5.0'

Type of Boring Rotary Casing Augers (3" I.D.) W.T. El. See Log

Inspector _____ Date July 15, 1993 Sheet 4 of 5

DEPTH	BLOWS PER FT.	PROFILE	SAMPLE TUBE NOS.	DESCRIPTION OF MATERIAL
	47		STD PEN 15 — 8 20 27	**SC, M.C. = 16.8%** Very dense, gray, massive, moist, gravelly, clayey, fine to coarse **SAND.** Retained 1.5 ft.
65				
	50/2"		STD PEN 16 — 50/2"	Very dense, gray, wet, clayey, silty, fine to coarse SAND. Retained 0.2 ft.
70				
	25		STD PEN 17 — 7 6 19	Dense, dark gray, moist, gravelly, slightly clayey, slightly silty, fine to coarse **SAND.** Retained 1.5 ft.
75				
				End of test hole boring at 77.0 ft. below ground elevation.
				Water Table Elevation: Not determined.
80				

Continued Next Page

LOG OF TEST BORING

Washington State Department of Transportation

S.R. 99 SECTION Alaska Way Viaduct Job No. MS-1826

Hole No. H-4-93 Sub Section Seismic Study Cont. Sec. 1791

Station 70+53.5 Offset 37.7' Left Ground El. 5.0'

Type of Boring Rotary Casing Augers (3" I.D.) W.T. El. See Log

Inspector _____ Date July 15, 1993 Sheet 5 of 5

DEPTH	BLOWS PER FT.	PROFILE	SAMPLE TUBE NOS.	DESCRIPTION OF MATERIAL
				NOTE: This Test Hole Boring was numbered H-7-93 on the field log.
				This is a Summary Log of the Test Hole Boring. Soil/Rock descriptions are derived from visual field identifications and laboratory test data.
85				
90				
95				
100				

DOT FORM 351-003 REVISED 12/79

LOG OF TEST BORING

Washington State Department of Transportation

S.R. 99 SECTION Alaska Way Viaduct Job No. MS-1826

Hole No. H-8-93 Sub Section Seismic Study Cont. Sec. 1791

Station 102+86.8 Offset CL Ground El. 5.6'

Type of Boring Dry Rotary Casing 3"OD Hollow Core Augers W.T. El. -6.4'

Inspector _____ Date October 28, 1993 Sheet 1 of 2

DEPTH	BLOWS PER FT.	PROFILE	SAMPLE TUBE NOS.			DESCRIPTION OF MATERIAL
						Silty, coarse sandy **GRAVEL.**
	12		SPT 1		14 6 6 10	Medium dense, black, moist, slightly silty, coarse SAND and GRAVEL with a trace of organics. Retained 1.1 ft. Note: Gravel coated with black oil.
5						
	2		SPT 2		2 1 1 10	Very loose, dark brown, moist, three inch layer of coarse **SAND** and **GRAVEL** and a four inch layer of creosote wood fragments. Retained 0.6 ft.
10						
	4		SPT 3		1 3 1 6	▽ 10/28/93 Very loose, dark brown, wet to saturated, fine **SAND** with gravel and wood fiber. Retained 1.0 ft.
15						
	6		SPT 4		4 3 3 4	Loose, dark brown to brown, wet to moist, 5 inch layer of silty, fine **SAND** with wood fragments and a 11 inch layer of sawdust. Retained 1.3 ft.
20						Note: Highly combustible methane gas detected. Test Hole abandoned at 19.0 ft. below ground elevation.

Continued Next Page

LOG OF TEST BORING

Washington State Department of Transportation

S.R. 99 SECTION Alaska Way Viaduct Job No. MS-1826

Hole No. H-8-93 Sub Section Seismic Study Cont. Sec. 1791

Station 102+86.8 Offset CL Ground El. 5.6'

Type of Boring Dry Rotary Casing 3"OD Hollow Core Augers W.T. El. -6.4'

Inspector _____ Date October 28, 1993 Sheet 2 of 2

DEPTH	BLOWS PER FT.	PROFILE	SAMPLE TUBE NOS.	DESCRIPTION OF MATERIAL
				End of Test Hole Boring at 19.0 ft. below ground elevation.
				NOTE: This Test Hole Boring was numbered H-blank-93 on the field log.
				This is a Summary Log of the Test Hole Boring. Soil/Rock descriptions are derived from visual field identifications.
25				
30				
35				
40				

DOT FORM 351-003 REVISED 12/79

LOG OF TEST BORING

Washington State Department of Transportation

S.R. 99 SECTION Alaska Way Viaduct Job No. MS-1826

Hole No. H-9-93 Sub Section Seismic Study Cont. Sec. 1791

Station 61+62.3 Offset 26.7' Lt. Ground El. 6.5'

Type of Boring Wet Rotary Casing HW X 172'/HQ X 222' W.T. El. -1.1'

Inspector _____ Date November 23, 1993 Sheet 1 of 12

DEPTH	BLOWS PER FT.	PROFILE	SAMPLE TUBE NOS.	DESCRIPTION OF MATERIAL	WELL PP
				ASPHALT	
				BALLAST	
				Gravelly, silty, fine **SAND** (Fill material).	
	7		SPT 1 6 4 3	Loose, brown, moist, fine **SAND** with silt lenses. Retained 0.75 ft.	
5					
				▽ 11-22-93	
	9		SPT 2 7 6 3	Loose, brown, moist, fine to coarse **SAND**. Retained 0.75 ft.	
10					
	7		SPT 3 4 4 3	Loose, black to brown, moist, silty, fine to coarse SAND and GRAVEL. Brown silt with a 2" X 1" piece of gravel in end of the sampler. Retained 0.7 ft.	
15					
	25		SPT 4 30 18 7	Dense, gray, wet, gravelly, silty, fine to coarse SAND with wood fragments. Retained 0.75 ft.	
20					

Continued Next Page

LOG OF TEST BORING

Washington State Department of Transportation

S.R. 99 SECTION Alaska Way Viaduct Job No. MS-1826

Hole No. H-9-93 Sub Section Seismic Study Cont. Sec. 1791

Station 61+62.3 Offset 26.7' Lt. Ground El. 6.5'

Type of Boring Wet Rotary Casing HW X 172'/HQ X 222' W.T. El. -1.1'

Inspector _____ Date November 23, 1993 Sheet 2 of 12

DEPTH	BLOWS PER FT.	PROFILE	SAMPLE TUBE NOS.			DESCRIPTION OF MATERIAL	WELL PP
	18		SPT 5	6	9 9	Medium dense, brown, wet, fine to coarse **SAND** with shells. Retained 1.0 ft.	
25						▼ 1-6-94	
	55		SPT 6	14	20 35	Very dense, black to gray, wet, fine to coarse SAND and **GRAVEL** with mica schist and shells. Retained 1.25 ft.	
30							
	100/6"		SPT 7	100/6"		Very dense, gray, wet, fine to coarse SAND. 2" X 2" piece of gravel in end of the sampler. Retained 0.2 ft. (No water loss)	
35							
	50/6"		SPT 8	37	50/6"	Very hard, gray, moist SILT with a 1" X 1" piece of gravel. Retained 0.75 ft.	
40							

Continued Next Page

LOG OF TEST BORING

Washington State Department of Transportation

S.R. 99 SECTION Alaska Way Viaduct Job No. MS-1826

Hole No. H-9-93 Sub Section Seismic Study Cont. Sec. 1791

Station 61+62.3 Offset 26.7' Lt. Ground El. 6.5'

Type of Boring Wet Rotary Casing HW X 172'/HQ X 222' W.T. El. -1.1'

Inspector Date November 23, 1993 Sheet 3 of 12

DEPTH	BLOWS PER FT.	PROFILE	SAMPLE TUBE NOS.	DESCRIPTION OF MATERIAL	WELL PP
	17		SPT 9 — 5 7 10	Very stiff, gray, moist, massive, structureless, moderately blocked, layered SILT. Retained 1.5 ft.	
45					
	21		SPT 10 — 6 9 12	Very stiff, gray, moist, massive, structureless, moderately blocked, layered SILT. Retained 1.5 ft. (Small water loss)	
50					
55	100/5"		SPT 11 — 00/5"	Very dense, gray, wet, gravelly, fine to coarse SAND. Retained 0.4 ft. (No water loss)	
60			C 12	Gray, moist, gravelly, fine to coarse SAND with silt lenses and 6" cobble.	

Continued Next Page

LOG OF TEST BORING

Washington State Department of Transportation

S.R. 99 SECTION Alaska Way Viaduct Job No. MS-1826

Hole No. H-9-93 Sub Section Seismic Study Cont. Sec. 1791

Station 61+62.3 Offset 26.7' Lt. Ground El. 6.5'

Type of Boring Wet Rotary Casing HW X 172'/HQ X 222' W.T. El. -1.1'

Inspector _____ Date November 23, 1993 Sheet 4 of 12

DEPTH	BLOWS PER FT.	PROFILE	SAMPLE TUBE NOS.		DESCRIPTION OF MATERIAL	WELL PP
					Blocky, clayey SILT with a trace of gravel and shells. Recovered 5.0 ft. (No water loss)	
65			C 13		Gray, moist, moderately blocky, clayey SILT with a trace of fine to medium sand, mica, and gravel. Recovered 5.0 ft. (No water loss)	
70			C 14		Gray, moist, moderately blocky, clayey SILT with a trace of fine to coarse sand, mica, organics, and gravel. Recovered 5.0 ft. (100% water recovery)	
	53		SPT 15 C 16	12 24 29	Hard, gray, moist, clayey SILT with a trace of fine sand, mica, organics, gravel, and a 1" layer of fine sand. Retained 1.5 ft.	
75					Gray, moist, gravelly, coarse sandy, blocky, clayey SILT with fine sand lenses. Recovered 4.0 ft .	
80			C 17		Gray, moist, gravelly, coarse sandy, blocky, clayey SILT with fine sand lenses. Recovered 2.0 ft. (100% water recovery)	

Continued Next Page

LOG OF TEST BORING

Washington State Department of Transportation

S.R. 99 SECTION Alaska Way Viaduct Job No. MS-1826

Hole No. H-9-93 Sub Section Seismic Study Cont. Sec. 1791

Station 61+62.3 Offset 26.7' Lt. Ground El. 6.5'

Type of Boring Wet Rotary Casing HW X 172'/HQ X 222' W.T. El. -1.1'

Inspector _____ Date November 23, 1993 Sheet 5 of 12

DEPTH	BLOWS PER FT.	PROFILE	SAMPLE TUBE NOS.	DESCRIPTION OF MATERIAL	WELL PP
			C 18	Gray, moist, gravelly, fine to coarse sandy, clayey, moderately blocky **SILT.** Recovered 5.0 ft. (100% water recovery)	
85			C 19	Gray, moist, gravelly, fine to coarse sandy, clayey, moderately blocky **SILT.** Recovered 1.5 ft. (100% water recovery)	
90			C 20	Gray, moist, gravelly, fine to coarse sandy, clayey, moderately blocky **SILT.** (100% water recovery) Recovered 1.5 ft	
95	59/6"		SPT 21 59/6"	Very dense, gray, moist, silty, gravelly, fine to coarse **SAND.** Retained 0.5 ft.	
100					

Continued Next Page

LOG OF TEST BORING

Washington State Department of Transportation

S.R. 99 SECTION Alaska Way Viaduct Job No. MS-1826

Hole No. H-9-93 Sub Section Seismic Study Cont. Sec. 1791

Station 61+62.3 Offset 26.7' Lt. Ground El. 6.5'

Type of Boring Wet Rotary Casing HW X 172'/HQ X 222' W.T. El. -1.1'

Inspector _____ Date November 23, 1993 Sheet 6 of 12

DEPTH	BLOWS PER FT.	PROFILE	SAMPLE TUBE NOS.	DESCRIPTION OF MATERIAL	WELL PP
			C 22	Gray, moist, massive, structureless, silty, fine SAND. Recovered 2.5 ft. (100% water recovery)	
105	79/6"		SPT 79/6" 23 C 24	Very hard, dark gray, wet, structureless, silty, fine SAND with fine sand lenses. Note: dilatant material.	
				Dark gray, moist, to wet, massive, structureless, fine sandy SILT with horizontally laminated fine Sand and blocky Silt layers. Recovered 4.0 ft.	
110			C 25	Gray, wet, medium to coarse sandy GRAVEL with a trace of Cobbles. Recovered 1.0 ft. (98% water recovery)	
115			C 26	Gray, wet, silty, gravelly, fine to medium SAND. Recovered 0.5 ft. (100% water recovery)	
120					

Continued Next Page

LOG OF TEST BORING

Washington State Department of Transportation

S.R. 99 SECTION Alaska Way Viaduct Job No. MS-1826

Hole No. H-9-93 Sub Section Seismic Study Cont. Sec. 1791

Station 61+62.3 Offset 26.7' Lt. Ground El. 6.5'

Type of Boring Wet Rotary Casing HW X 172'/HQ X 222' W.T. El. -1.1'

Inspector _____ Date November 23, 1993 Sheet 7 of 12

DEPTH	BLOWS PER FT.	PROFILE	SAMPLE TUBE NOS.	DESCRIPTION OF MATERIAL	WELL PP
			C 27	Dark gray, wet, gravelly, fine to medium **SAND** Retained 1.9 ft. (100% water recovery)	
125	50/3"		SPT 28 47 50/3"	Very dense, dark gray, wet, gravelly, fine to coarse **SAND.** Retained 0.75 ft.	
130				Very dense, dark gray, wet, gravelly, fine to coarse **SAND.** Note: No samples taken until 150.0' below ground elevation.	
135				(100% water recovery)	
140					

Continued Next Page

LOG OF TEST BORING

Washington State Department of Transportation

S.R. 99 SECTION Alaska Way Viaduct Job No. MS-1826

Hole No. H-9-93 Sub Section Seismic Study Cont. Sec. 1791

Station 61+62.3 Offset 26.7' Lt. Ground El. 6.5'

Type of Boring Wet Rotary Casing HW X 172'/HQ X 222' W.T. El. -1.1'

Inspector Date November 23, 1993 Sheet 8 of 12

DEPTH	BLOWS PER FT.	PROFILE	SAMPLE TUBE NOS.	DESCRIPTION OF MATERIAL	WELL PP
145				Note: No change in drilling from 125.0' to 150.0' below ground elevation. (Very little water loss)	
150	92/6"		SPT 29 92/6"	Very dense, dark gray, wet, gravelly, fine to coarse **SAND.** Retained 0.5 ft. Note: No samples taken until 168.0 ft. below ground elevation.	
155				Note: No change in drilling from 150.0' to 168.0' below ground elevation. (No water loss)	
160					

Continued Next Page

LOG OF TEST BORING

Washington State Department of Transportation

S.R. 99 SECTION Alaska Way Viaduct Job No. MS-1826

Hole No. H-9-93 Sub Section Seismic Study Cont. Sec. 1791

Station 61+62.3 Offset 26.7' Lt. Ground El. 6.5'

Type of Boring Wet Rotary Casing HW X 172'/HQ X 222' W.T. El. -1.1'

Inspector Date November 23, 1993 Sheet 9 of 12

DEPTH	BLOWS PER FT.	PROFILE	SAMPLE TUBE NOS.	DESCRIPTION OF MATERIAL	WELL PP
165				Note: No water loss.	
	50/2"		SPT 50/2"	Very dense, dark gray, wet, fine to medium SAND with a 1" X 1/2" piece of fine grain, black rock. Retained 0.2 ft.	
170			C 30	**Gravelly SAND** Recovered 0.6 ft.	
			C 31	Gravelly, fine to medium **SAND**. Recovered 1.6 ft. (No water loss)	
			C 32		
175			C 33	Gravelly, fine to medium **SAND**. Recovered 0.9 ft. (Very little water loss)	
180					

Continued Next Page

LOG OF TEST BORING

Washington State Department of Transportation

S.R. 99 SECTION Alaska Way Viaduct Job No. MS-1826

Hole No. H-9-93 Sub Section Seismic Study Cont. Sec. 1791

Station 61 + 62.3 Offset 26.7' Lt. Ground El. 6.5'

Type of Boring Wet Rotary Casing HW X 172'/HQ X 222' W.T. El. -1.1'

Inspector _____ Date November 23, 1993 Sheet 10 of 12

DEPTH	BLOWS PER FT.	PROFILE	SAMPLE TUBE NOS.	DESCRIPTION OF MATERIAL	WELL PP
				Note: No sampling until 193 ft. below ground elevation.	
185				Note: No change from 175.0' to 193.0' below ground elevation.	
190					
	100/4"		SPT 34 00/4"	Very dense, dark grey, wet, fine to coarse SAND and **GRAVEL.** Retained 0.4 ft. (No water loss)	
195				Note: No change from 193.0' to 206.0' below ground elevation.	
200					

Continued Next Page

LOG OF TEST BORING

Washington State Department of Transportation

S.R. 99 SECTION Alaska Way Viaduct Job No. MS-1826

Hole No. H-9-93 Sub Section Seismic Study Cont. Sec. 1791

Station 61+62.3 Offset 26.7' Lt. Ground El. 6.5'

Type of Boring Wet Rotary Casing HW X 172'/HQ X 222' W.T. El. -1.1'

Inspector Date November 23, 1993 Sheet 11 of 12

DEPTH	BLOWS PER FT.	PROFILE	SAMPLE TUBE NOS.	DESCRIPTION OF MATERIAL	WELL PP
				Note: Very little water loss.	
205					
				SILT (No water loss)	
	50/6"		SPT 35 50/6"	Hard, gray, moist, massive SILT with black and brown oxidation stains. Retained 0.5 ft. (No water loss)	
210					
				No sampling until 220.0' below ground elevation.	
215					
				No change from 206.0' to 221.5' below ground elevation.	
220					

Continued Next Page

LOG OF TEST BORING

Washington State Department of Transportation

S.R. 99 SECTION Alaska Way Viaduct Job No. MS-1826

Hole No. H-9-93 Sub Section Seismic Study Cont. Sec. 1791

Station 61+62.3 Offset 26.7' Lt. Ground El. 6.5'

Type of Boring Wet Rotary Casing HW X 172'/HQ X 222' W.T. El. -1.1'

Inspector _____ Date November 23, 1993 Sheet 12 of 12

DEPTH	BLOWS PER FT.	PROFILE	SAMPLE TUBE NOS.	DESCRIPTION OF MATERIAL	WELL PP
	88		SPT 24 36 38 50	Very hard, dark brown, moist, massive SILT with black and brown oxidation stains. Retained 1.5 ft.	
				End of the Test Hole Boring at 221.5 ft. below ground elevation.	
225				Installed 2.5" O.D. threaded PVC pipe to a depth of 220.0' below ground elevation in conjunction with a flush monument.	
				This is a Summary Log of the Test Hole Boring. Soil/Rock descriptions are derived from visual field identifications and laboratory test data.	
230					
235					
240					

DOT FORM 351-003 REVISED 12/79

End of boring at 221.5 feet.

LOG OF TEST BORING

Washington State Department of Transportation

S.R. 99 SECTION Alaska Way Viaduct Job No. MS-1826

Hole No. H-10-93 Sub Section Seismic Study Cont. Sec. 1791

Station 117+41.11 Offset 25' Lt. Ground El. 6.6'

Type of Boring Wet Rotary Casing HW X 139'/HQ X 250' W.T. El. -2.4'

Inspector _____ Date December 22, 1993 Sheet 1 of 13

DEPTH	BLOWS PER FT.	PROFILE	SAMPLE TUBE NOS.	DESCRIPTION OF MATERIAL	WELL PP
				Silty, sandy GRAVEL (Fill material) from 0.0' to 9.0' below ground elevation.	
5					
				▽ 12-14-93	
10				SAND and GRAVEL at 9.0' to 20.0' below ground elevation. (20% to 30% water loss)	
15					
20					

Continued Next Page

LOG OF TEST BORING

Washington State Department of Transportation

S.R. 99 SECTION Alaska Way Viaduct Job No. MS-1826

Hole No. H-10-93 Sub Section Seismic Study Cont. Sec. 1791

Station 117+41.11 Offset 25' Lt. Ground El. 6.6'

Type of Boring Wet Rotary Casing HW X 139'/HQ X 250' W.T. El. -2.4'

Inspector _____ Date December 22, 1993 Sheet 2 of 13

DEPTH	BLOWS PER FT.	PROFILE	SAMPLE TUBE NOS.	DESCRIPTION OF MATERIAL	WELL PP
				SAWDUST from 20.0' to 23.0' below ground elevation.	
				Fine to medium **SAND** from 23.0' to 50.0' below ground elevation. (100% water recovery from 23' b.g.e.)	
25					
30					
35					
40					

Continued Next Page

LOG OF TEST BORING

Washington State Department of Transportation

S.R. 99 SECTION Alaska Way Viaduct Job No. MS-1826

Hole No. H-10-93 Sub Section Seismic Study Cont. Sec. 1791

Station 117+41.11 Offset 25' Lt. Ground El. 6.6'

Type of Boring Wet Rotary Casing HW X 139'/HQ X 250' W.T. El. -2.4'

Inspector Date December 22, 1993 Sheet 3 of 13

DEPTH	BLOWS PER FT.	PROFILE	SAMPLE TUBE NOS.	DESCRIPTION OF MATERIAL	WELL PP
45				Fine to medium SAND from 23.0' to 50.0' below ground elevation. (100% water recovery from 23' b.g.e.)	
50					
55				Silty, sandy GRAVEL with COBBLES. (Till like material 55.0' to 75.0' below ground elevation)	
60					

Continued Next Page

LOG OF TEST BORING

Washington State Department of Transportation

S.R. 99 SECTION Alaska Way Viaduct Job No. MS-182(

Hole No. H-10-93 Sub Section Seismic Study Cont. Sec. 1791

Station 117+41.11 Offset 25' Lt. Ground El. 6.6'

Type of Boring Wet Rotary Casing HW X 139'/HQ X 250' W.T. El. -2.4'

Inspector _____ Date December 22, 1993 Sheet 4 of 13

DEPTH	BLOWS PER FT.	PROFILE	SAMPLE TUBE NOS.	DESCRIPTION OF MATERIAL	WEL PP
				Silty, sandy GRAVEL with COBBLES. (Till like material 55.0' to 75.0' below ground elevation)	
65					
70					
75				Gravelly, silty, fine to coarse SAND	
80					

Continued Next Page

LOG OF TEST BORING

Washington State Department of Transportation

S.R. 99 SECTION Alaska Way Viaduct Job No. MS-1826

Hole No. H-10-93 Sub Section Seismic Study Cont. Sec. 1791

Station 117+41.11 Offset 25' Lt. Ground El. 6.6'

Type of Boring Wet Rotary Casing HW X 139'/HQ X 250' W.T. El. -2.4'

Inspector _____ Date December 22, 1993 Sheet 5 of 13

DEPTH	BLOWS PER FT.	PROFILE	SAMPLE TUBE NOS.	DESCRIPTION OF MATERIAL	WELL PP
85				Silty, fine to coarse SAND with a trace of gravel. (No water loss)	
90					
95					
100					

Continued Next Page

LOG OF TEST BORING

Washington State Department of Transportation

S.R. 99 SECTION Alaska Way Viaduct Job No. MS-1826

Hole No. H-10-93 Sub Section Seismic Study Cont. Sec. 1791

Station 117+41.11 Offset 25' Lt. Ground El. 6.6'

Type of Boring Wet Rotary Casing HW X 139'/HQ X 250' W.T. El. -2.4'

Inspector _____ Date December 22, 1993 Sheet 6 of 13

DEPTH	BLOWS PER FT.	PROFILE	SAMPLE TUBE NOS.	DESCRIPTION OF MATERIAL	WELL PP
105					
110					
115				Fine to coarse SAND with a trace of gravel.	
120					

Continued Next Page

LOG OF TEST BORING

Washington State Department of Transportation

S.R. 99 SECTION Alaska Way Viaduct Job No. MS-1826

Hole No. H-10-93 Sub Section Seismic Study Cont. Sec. 1791

Station 117+41.11 Offset 25' Lt. Ground El. 6.6'

Type of Boring Wet Rotary Casing HW X 139'/HQ X 250' W.T. El. -2.4'

Inspector _____ Date December 22, 1993 Sheet 7 of 13

DEPTH	BLOWS PER FT.	PROFILE	SAMPLE TUBE NOS.	DESCRIPTION OF MATERIAL	WELL PP
				Changed to HQ Advancer. (No water loss)	
125					
130					
135					
140					

Continued Next Page

LOG OF TEST BORING

Washington State Department of Transportation

S.R. 99 SECTION Alaska Way Viaduct Job No. MS-1826

Hole No. H-10-93 Sub Section Seismic Study Cont. Sec. 1791

Station 117+41.11 Offset 25' Lt. Ground El. 6.6'

Type of Boring Wet Rotary Casing HW X 139'/HQ X 250' W.T. El. -2.4'

Inspector _____ Date December 22, 1993 Sheet 8 of 13

DEPTH	BLOWS PER FT.	PROFILE	SAMPLE TUBE NOS.	DESCRIPTION OF MATERIAL	WELL PP
				Silty, fine SAND with a trace of gravel. (No water loss)	
145					
150					
155					
160					

Continued Next Page

LOG OF TEST BORING

Washington State Department of Transportation

S.R. 99 SECTION Alaska Way Viaduct Job No. MS-1826

Hole No. H-10-93 Sub Section Seismic Study Cont. Sec. 1791

Station 117+41.11 Offset 25' Lt. Ground El. 6.6'

Type of Boring Wet Rotary Casing HW X 139'/HQ X 250' W.T. El. -2.4'

Inspector Date December 22, 1993 Sheet 9 of 13

DEPTH	BLOWS PER FT.	PROFILE	SAMPLE TUBE NOS.	DESCRIPTION OF MATERIAL	WELL PP
				No change from 143.0' to 205.0' below ground level.	
165					
170					
175					
180					

Continued Next Page

LOG OF TEST BORING

Washington State Department of Transportation

S.R. 99 SECTION Alaska Way Viaduct Job No. MS-1826

Hole No. H-10-93 Sub Section Seismic Study Cont. Sec. 1791

Station 117+41.11 Offset 25' Lt. Ground El. 6.6'

Type of Boring Wet Rotary Casing HW X 139'/HQ X 250' W.T. El. -2.4'

Inspector _____ Date December 22, 1993 Sheet 10 of 13

DEPTH	BLOWS PER FT.	PROFILE	SAMPLE TUBE NOS.	DESCRIPTION OF MATERIAL	WELL PP
				No change from 143.0' to 205.0' below ground level.	
185					
190					
195					
200					

Continued Next Page

LOG OF TEST BORING

Washington State Department of Transportation

S.R. 99 SECTION Alaska Way Viaduct Job No. MS-1826

Hole No. H-10-93 Sub Section Seismic Study Cont. Sec. 1791

Station 117+41.11 Offset 25' Lt. Ground El. 6.6'

Type of Boring Wet Rotary Casing HW X 139'/HQ X 250' W.T. El. -2.4'

Inspector Date December 22, 1993 Sheet 11 of 13

DEPTH	BLOWS PER FT.	PROFILE	SAMPLE TUBE NOS.	DESCRIPTION OF MATERIAL	WELL PP
				No change from 143.0' to 205.0' below ground level.	
205				Gray SILT Note: Drilled through layers of silty, sandy **GRAVEL** every 5.0' from 205.0' to 250.0' below ground elevation.	
210					
215					
220					

Continued Next Page

LOG OF TEST BORING

Washington State Department of Transportation

S.R. 99 SECTION Alaska Way Viaduct Job No. MS-1826

Hole No. H-10-93 Sub Section Seismic Study Cont. Sec. 1791

Station 117+41.11 Offset 25' Lt. Ground El. 6.6'

Type of Boring Wet Rotary Casing HW X 139'/HQ X 250' W.T. El. -2.4'

Inspector _____ Date December 22, 1993 Sheet 12 of 13

DEPTH	BLOWS PER FT.	PROFILE	SAMPLE TUBE NOS.	DESCRIPTION OF MATERIAL
225				No change from 205.0' to 232.0' below ground elevation.
230				(10% water loss down hole)
				Silty, sandy GRAVEL.
235				
240				

Continued Next Page

LOG OF TEST BORING

Washington State Department of Transportation

S.R. 99 SECTION Alaska Way Viaduct Job No. MS-1826

Hole No. H-10-93 Sub Section Seismic Study Cont. Sec. 1791

Station 117+41.11 Offset 25' Lt. Ground El. 6.6'

Type of Boring Wet Rotary Casing HW X 139'/HQ X 250' W.T. El. -2.4'

Inspector _____ Date December 22, 1993 Sheet 13 of 13

DEPTH	BLOWS PER FT.	PROFILE	SAMPLE TUBE NOS.	DESCRIPTION OF MATERIAL
				Silty, sandy GRAVEL.
245				
250				End of the Test Hole Boring at 250.0 ft. below ground elevation.
				Installed 2.5" threaded PVC pipe to a depth of 250 ft. below ground elevation.
255				This is a Summary Log of the Test Hole Boring. Soil/Rock descriptions are derived from visual field identifications.
260				

DOT FORM 351-003 REVISED 12/79

LOG OF TEST BORING

Washington State Department of Transportation

S.R. 99 SECTION Alaska Way Viaduct Job No. MS-1826

Hole No. H-11-94 Sub Section Seismic Study Cont. Sec. 1791

Station 103+28.8 Offset CL Ground El. 6.8'

Type of Boring Wet Rotary Casing HW X 45.5' W.T. El. -3.2'

Inspector _____ Date January 6, 1994 Sheet 1 of 3

DEPTH	BLOWS PER FT.	PROFILE	SAMPLE TUBE NOS.	DESCRIPTION OF MATERIAL
				Silty, sandy GRAVEL (Fill)
5	22		SPT 1 — 21 13 9	Medium dense, gray, moist, gravelly, silty, fine SAND (Fill material). Retained 0.9 ft. (Very little water loss)
				Wood fragments, woodchips with sand and gravel.
10				▽
15	37		SPT 2 — 26 27 10	Dense, brown, wet, gravelly, fine to coarse SAND with wood debris. (Fill material). Retained 0.6 ft. (No water loss)
20				Fine SAND and GRAVEL.

Continued Next Page

DOT FORM 351-003 REVISED 12/79

LOG OF TEST BORING

Washington State Department of Transportation

S.R. 99 SECTION Alaska Way Viaduct Job No. MS-1826

Hole No. H-11-94 Sub Section Seismic Study Cont. Sec. 1791

Station 103+28.8 Offset CL Ground El. 6.8'

Type of Boring Wet Rotary Casing HW X 45.5' W.T. El. -3.2'

Inspector _____ Date January 6, 1994 Sheet 2 of 3

DEPTH	BLOWS PER FT.	PROFILE	SAMPLE TUBE NOS.	DESCRIPTION OF MATERIAL
25	14		SPT 3 — 10, 6, 8	Medium dense, dark brown, wet, fine SAND mixed with shells, decayed wood fragments, and gravel. Retained 0.8 ft. (Very little water loss down hole)
30				
35	1/18"		SPT 4 — 1/18"	Very soft, dark brown, moist, clayey SILT with a trace of shells. Retained 1.5 ft. (No water loss)
40				Clayey SILT

Continued Next Page

LOG OF TEST BORING

Washington State Department of Transportation

S.R. 99 SECTION Alaska Way Viaduct Job No. MS-1826

Hole No. H-11-94 Sub Section Seismic Study Cont. Sec. 1791

Station 103+28.8 Offset CL Ground El. 6.8'

Type of Boring Wet Rotary Casing HW X 45.5' W.T. El. -3.2'

Inspector _____ Date January 6, 1994 Sheet 3 of 3

DEPTH	BLOWS PER FT.	PROFILE	SAMPLE TUBE NOS.	DESCRIPTION OF MATERIAL
45	82	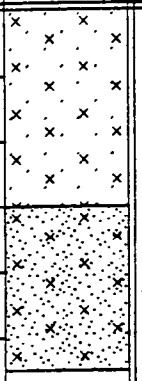	SPT 5 — 37 41 41	Very dense, dark brown, moist, gravelly, silty, fine to coarse **SAND.** (Till like material) Retained 1.5 ft. (No water loss)
				End of the Test Hole Boring at 45.5 ft. below ground elevation.
				This is a Summary Log of the Test Hole Boring. Soil/Rock descriptions are derived from visual field identifications.
50				
55				
60				

DOT FORM 351-003 REVISED 12/79

Appendix B

Supplementary Subsurface Investigation

Cone Penetration Test Soundings

Washington DOT

Elevation : 7.1 CPT Date : 06/14/93 14:00 Sounding : CPT-1 Pg 1 / 2

Location : 129+87 33.0' R Cone Used : 302 Job No. : MS 1826

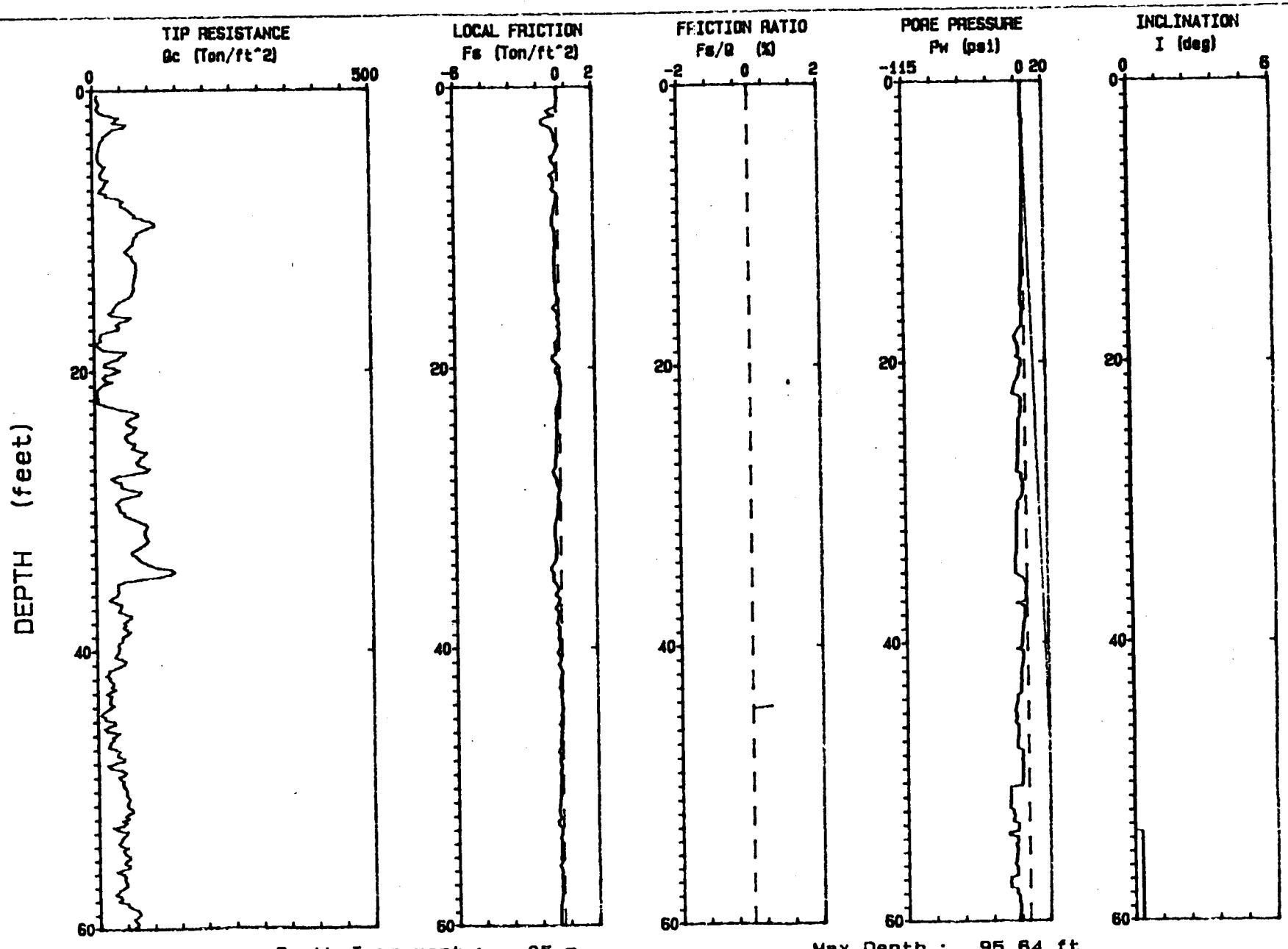

Depth Increment : .05 m

Max Depth : 95.64 ft

Washington DOT

Elevation : 7.1 CPT Date : 06/14/93 14:00 Sounding : CPT-1 Pg 2 / 2

Location : 129+87 33.0' R Cone Used : 302 Job No. : MS 1826

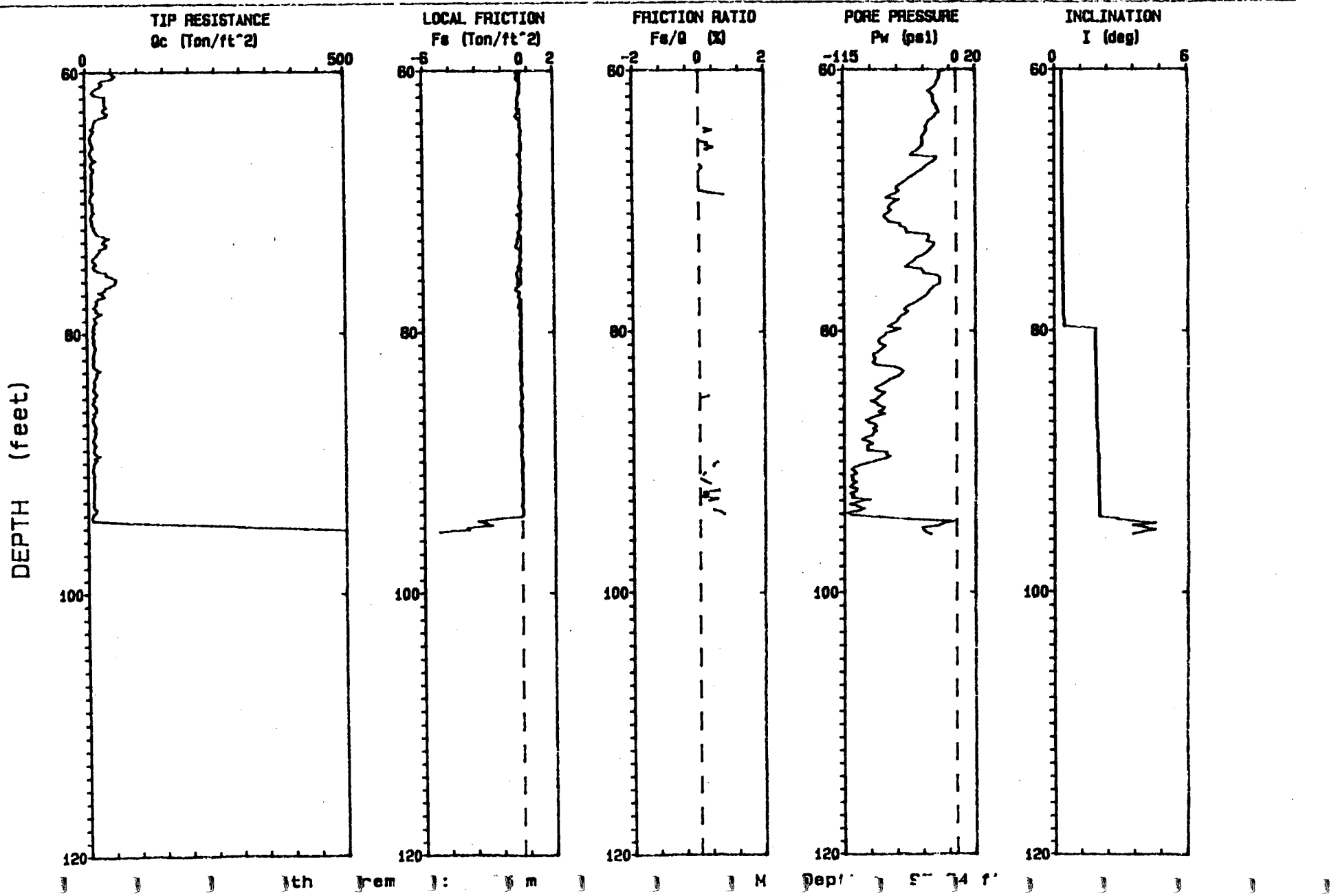

Washington DOT

Elevation : 7.1 CPT Date : 07/27/93 16:45 Sounding : CPT-1A Pg 1 / 2

Location : 129+87 33'R. Cone Used : 302 Job No. : MS1826

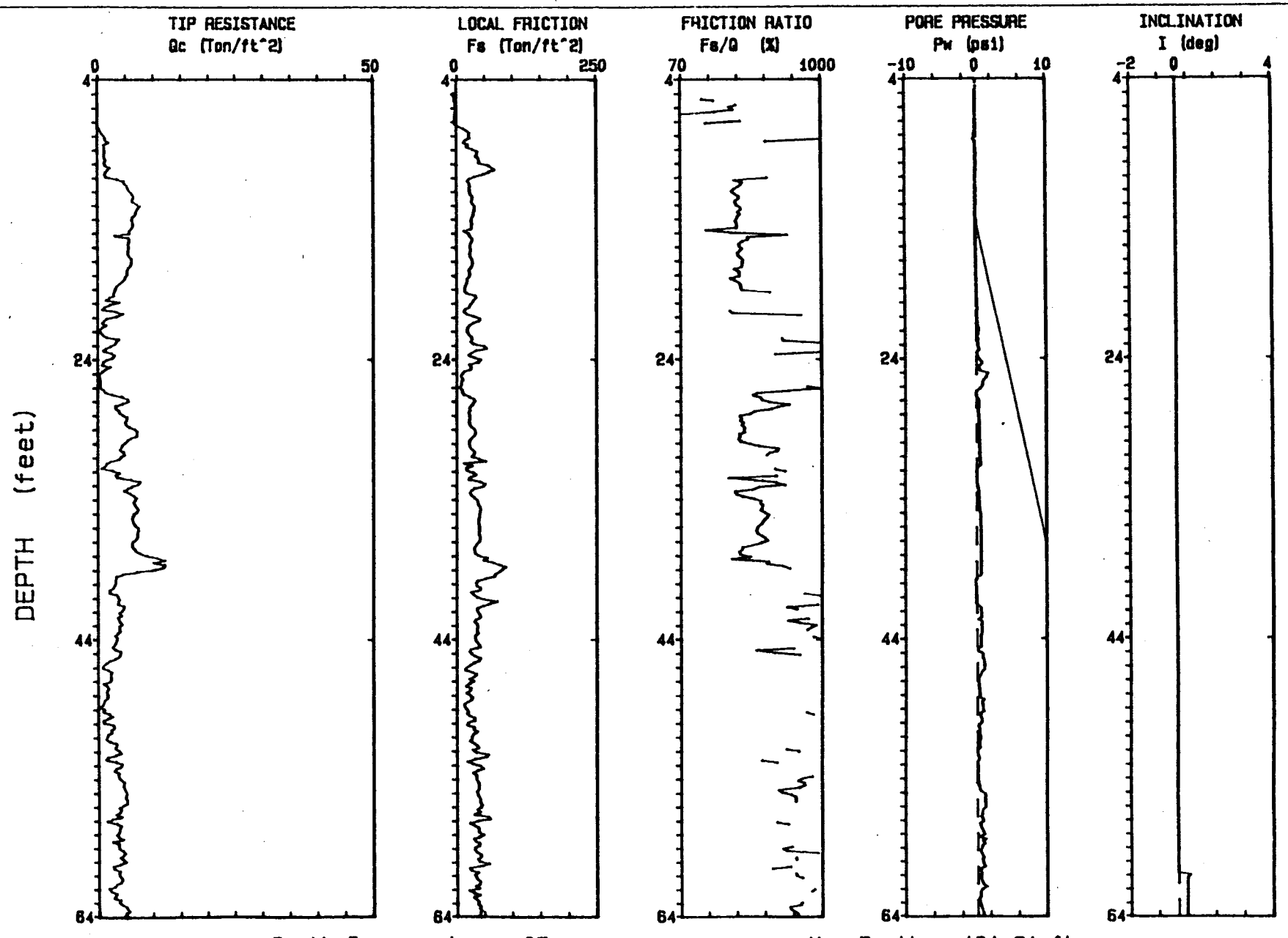

Depth Increment : .05 m

Max Depth : 101.21 ft

Washington DOT

Elevation : 7.1 CPT Date : 07/27/93 16:45 Sounding : CPT-1A Pg 2 / 2

Location : 129+87 33'R. Cone Used : 302 Job No. : MS1826

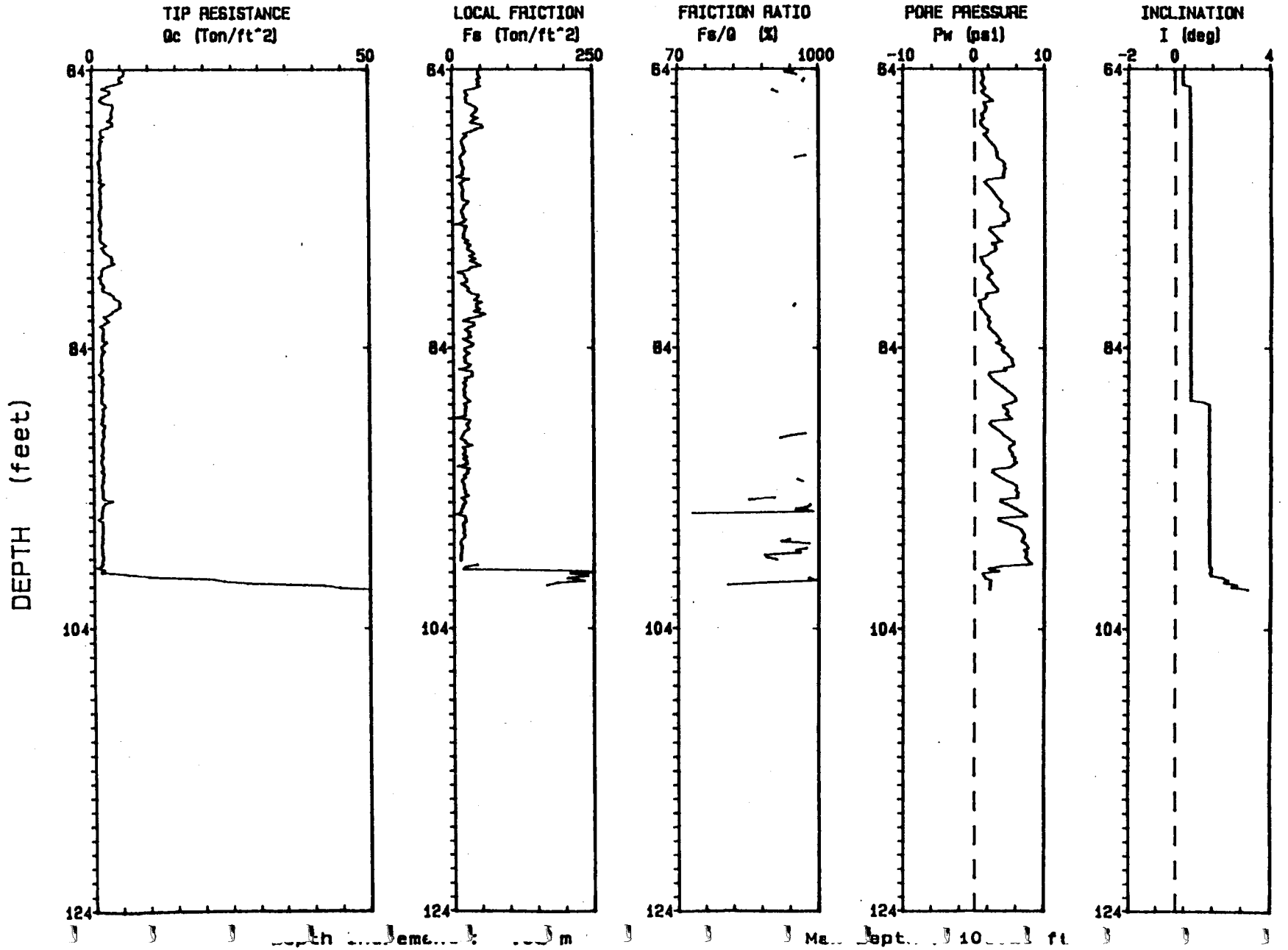

Washington DOT

Elevation : 6.5 CPT Date : 06/25/93 13:00 Sounding : CPT-3 Pg 1 / 1

Location : 89+31 18.4' L Cone Used : 302 Job No. : MS1826

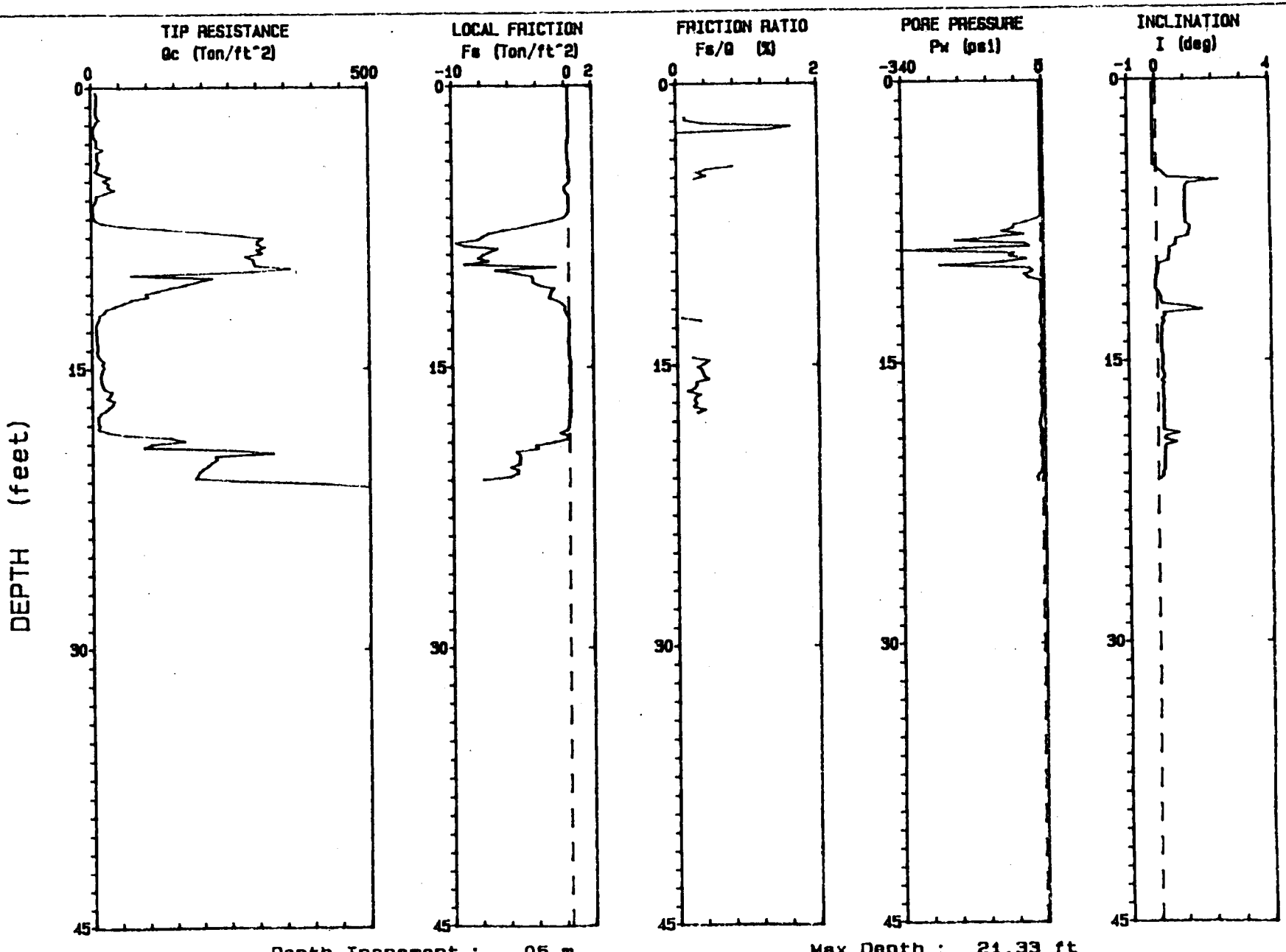

Depth Increment : .05 m

Max Depth : 21.33 ft

Washington DOT

Elevation : 6.5 | CPT Date : 06/30/93 8:30 | Sounding : CPT-4 | Pg 1 / 1

Location : 99+87 23.0 ℓ. | Cone Used : 302 MS1826 | Job No. :

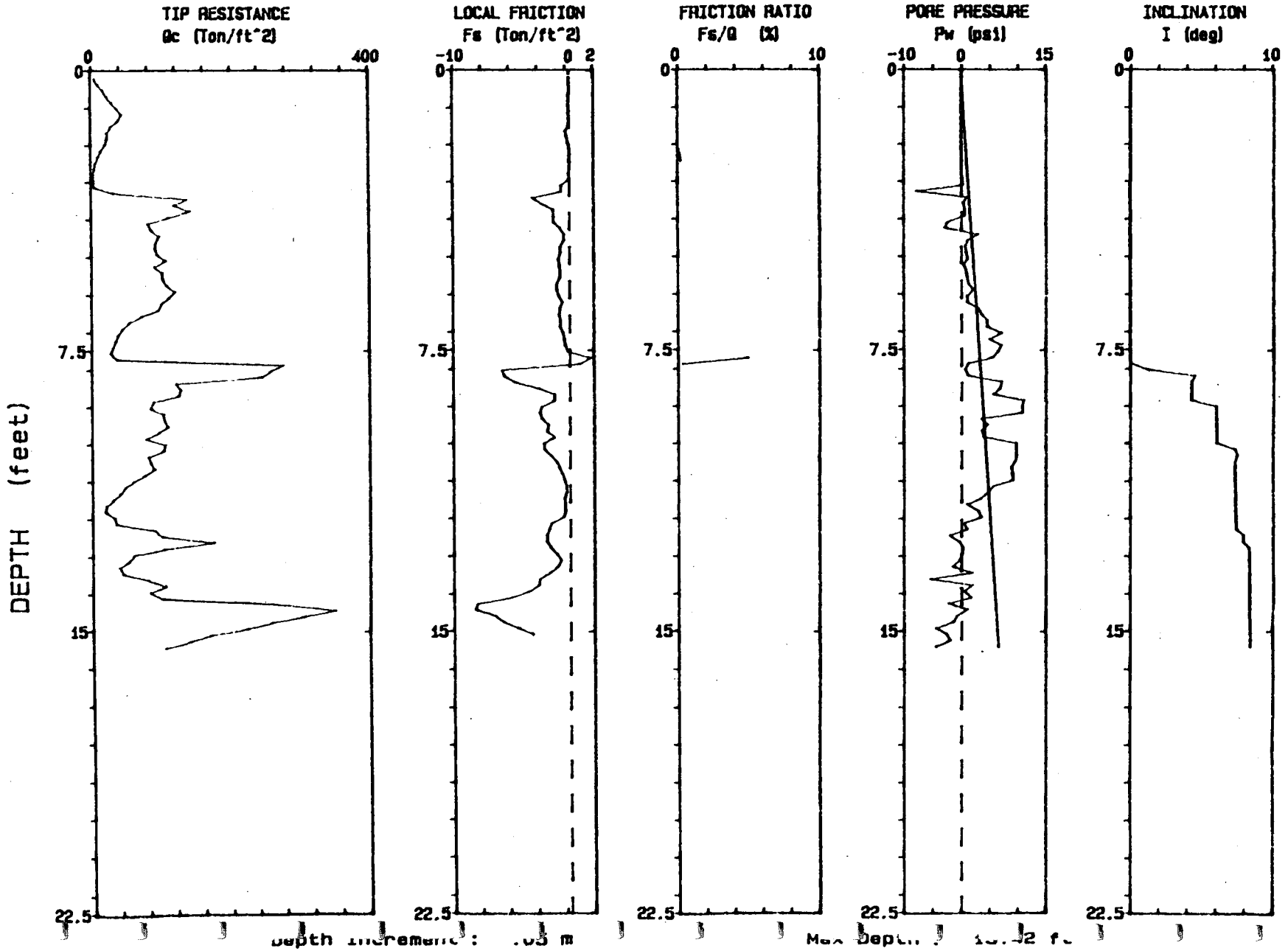

Depth Increment : .05 m Max Depth : 13.42 ft

Washington DOT

Elevation : 6.5' CPT Date : 07/21/93 14:25 Sounding : CPT-38 Pg 1 / 1

Location : 89+31 18.4' L Cone Used : . 247 Job No. : MS1826

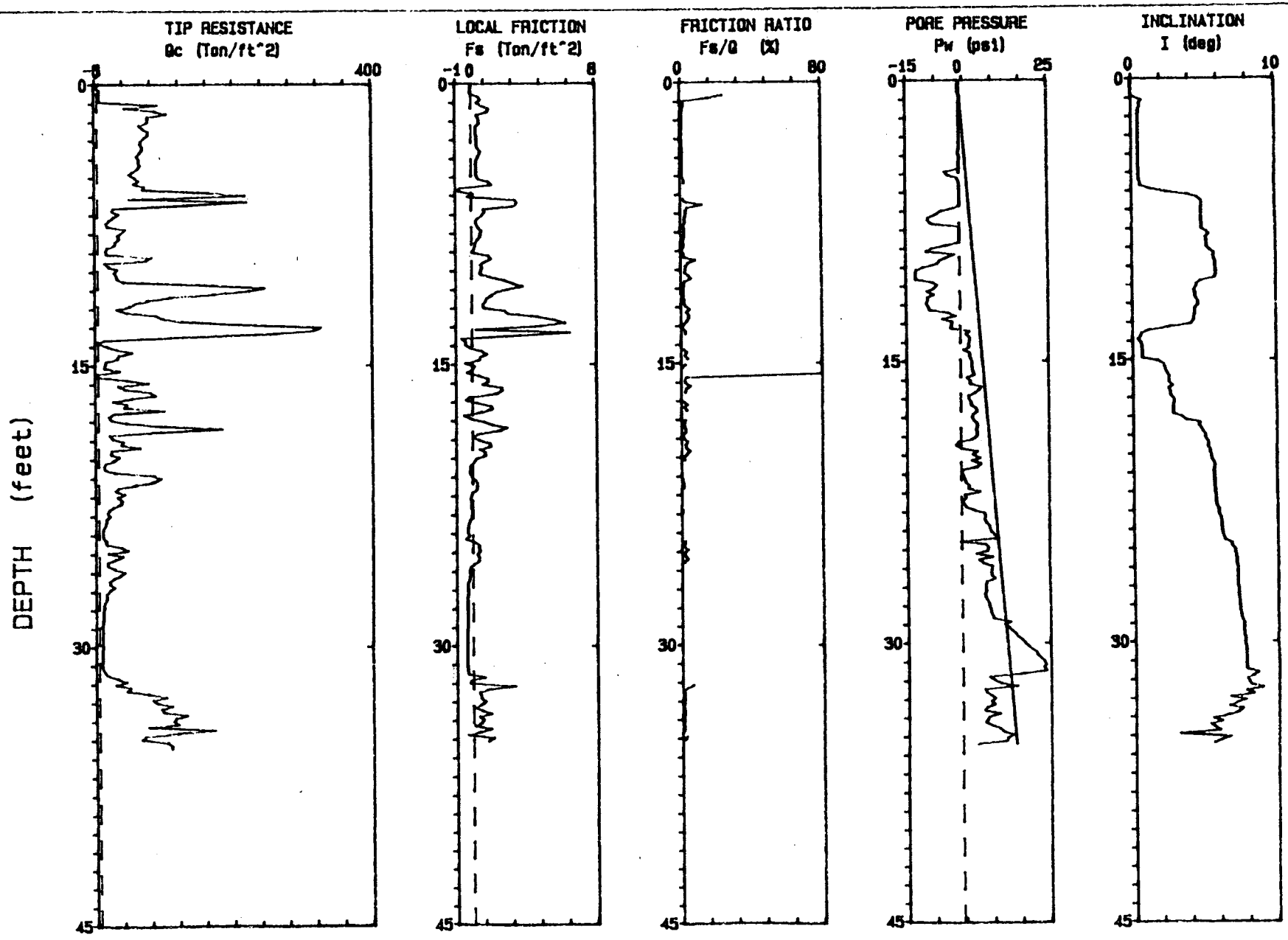

Depth Increment : .05 m

Max Depth : 35.43 ft

Washington DOT

Elevation : 6.5 CPT Date : 06/30/93 11:00 Sounding : CPT-4A Pg 1 / 1

Location : 99+87 23.0' Rt. Cone Used : 302 Job No. : MS1826

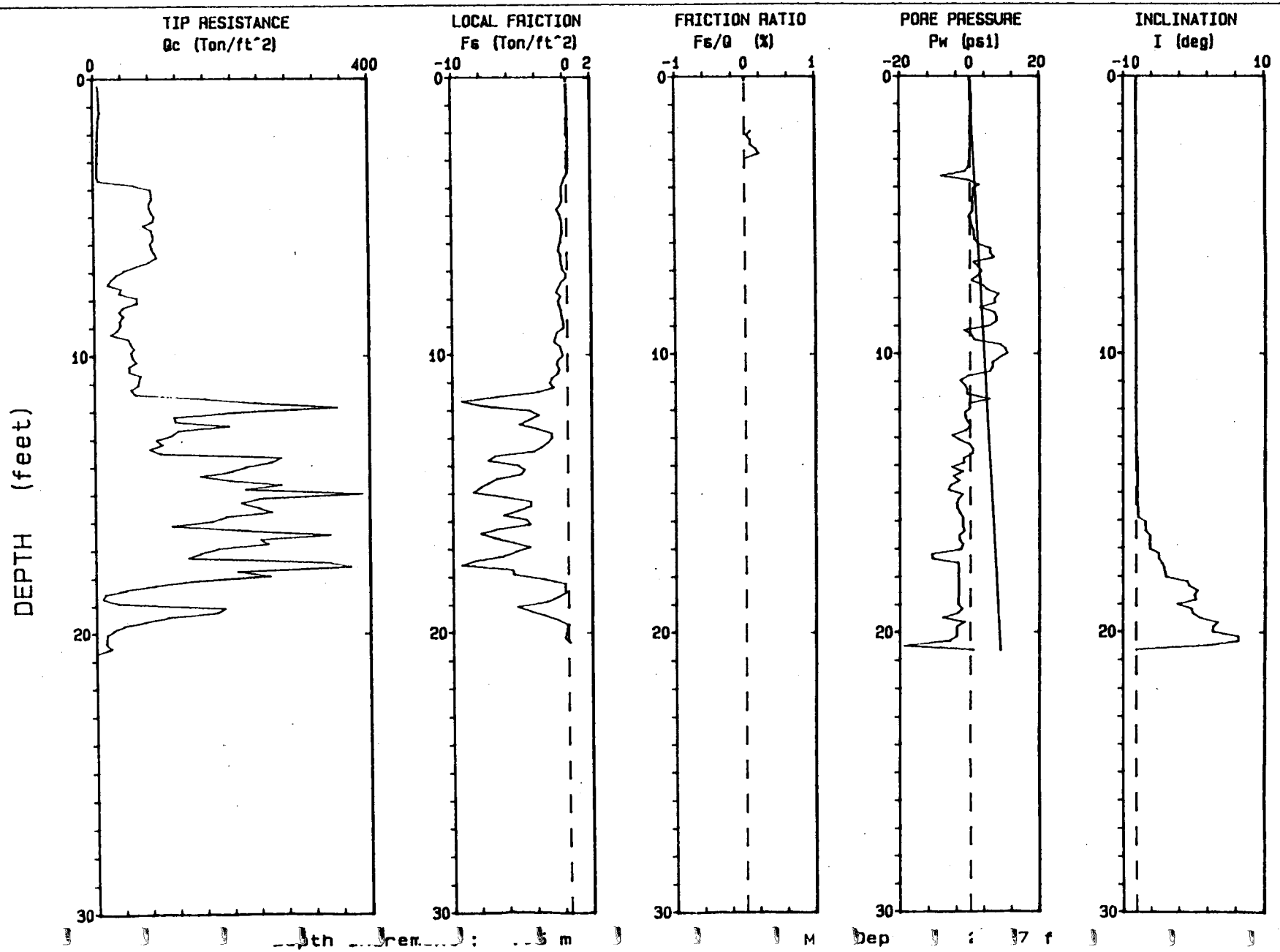

Washington DOT

Elevation : 6.5 CPT Date : 07/21/93 9:30 Sounding : CPT-4B Pg 1 / 1

Location : 99+87 23.0' R. Cone Used : 247 Job No. : MS1826

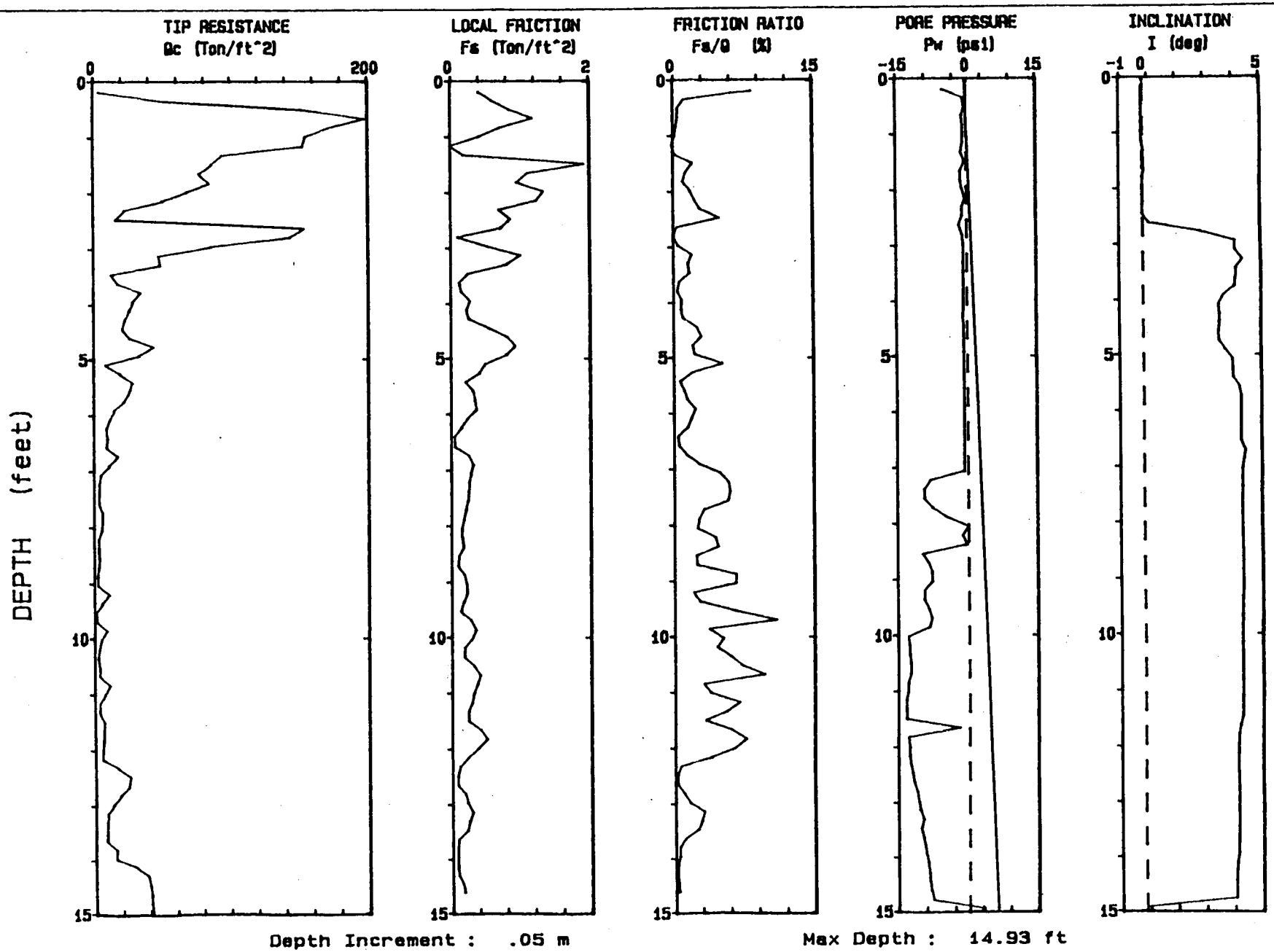

Depth Increment : .05 m

Max Depth : 14.93 ft

Washington DOT

Elevation : 6.5 | CPT Date : 07/21/93 10:45 | Sounding : CPT-4C Pg 1 / 1

Location : 99+87 23.0' R. | Cone Used : 247 | Job No. : MS1826

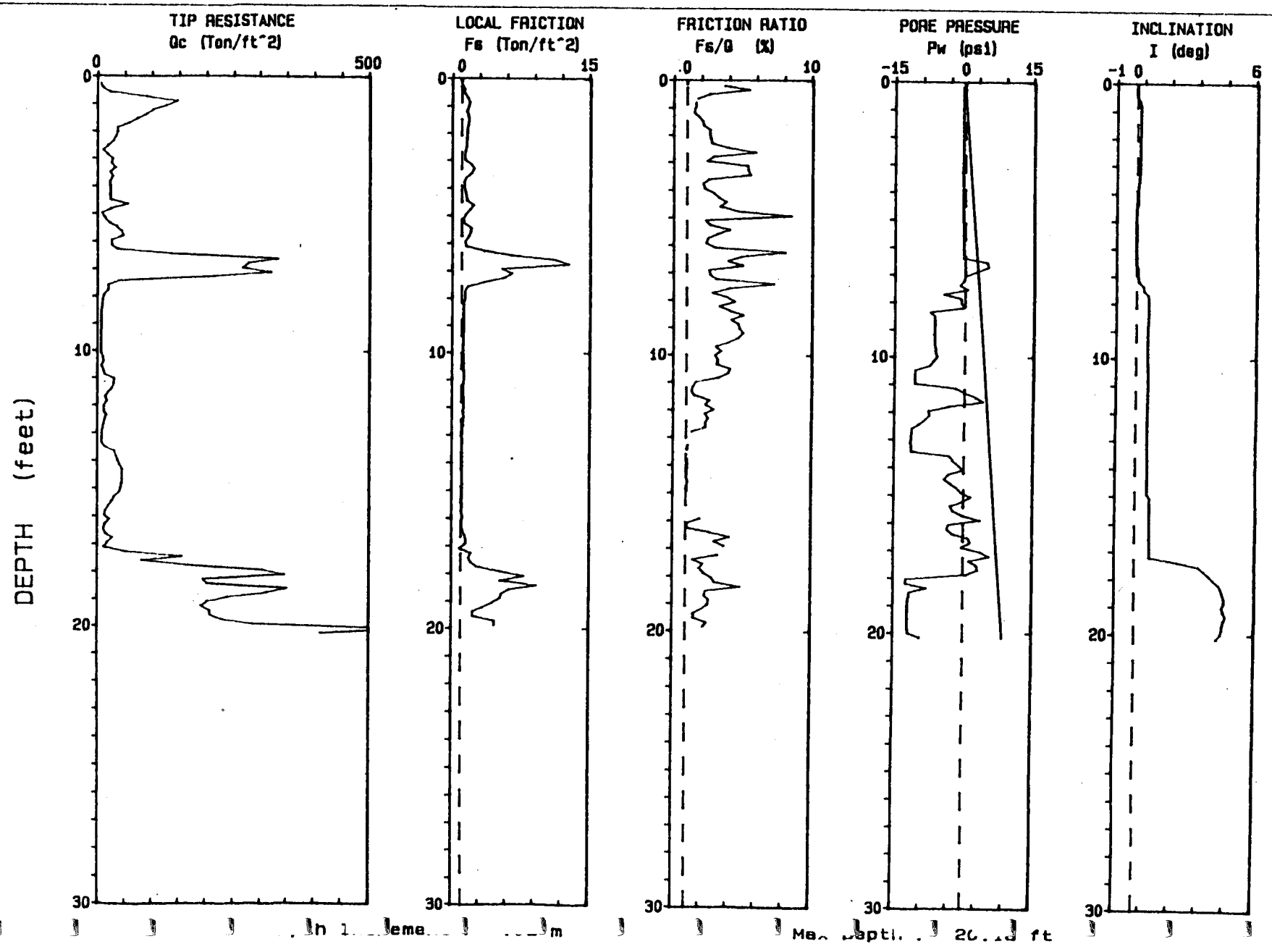

Washington DOT

Elevation : 6.6 CPT Date : 06/02/93 15:30 Sounding : CPT-5 Pg 1 / 1

Location : 77+07 23.0' L. Cone Used : 302 Job No. : MS1826

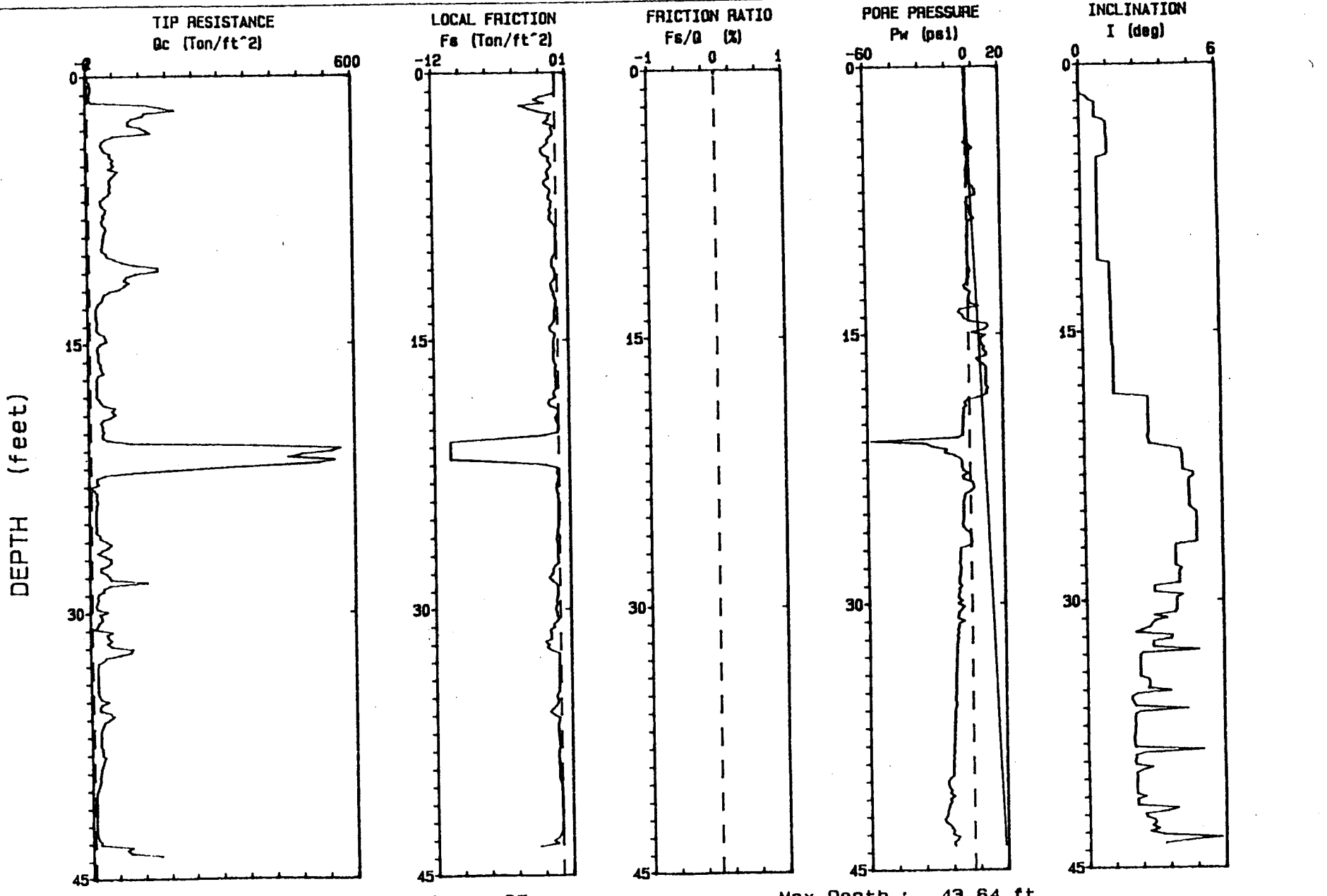

Depth Increment : .05 m

Max Depth : 43.64 ft

Washington DOT

Elevation : N/A
Location : 78+00 0.5' Lt.

CPT Date : 07/01/93 18:00
Cone Used : 247

Sounding : CPT-5A Pg 1 / 1
Job No. : MS-1826

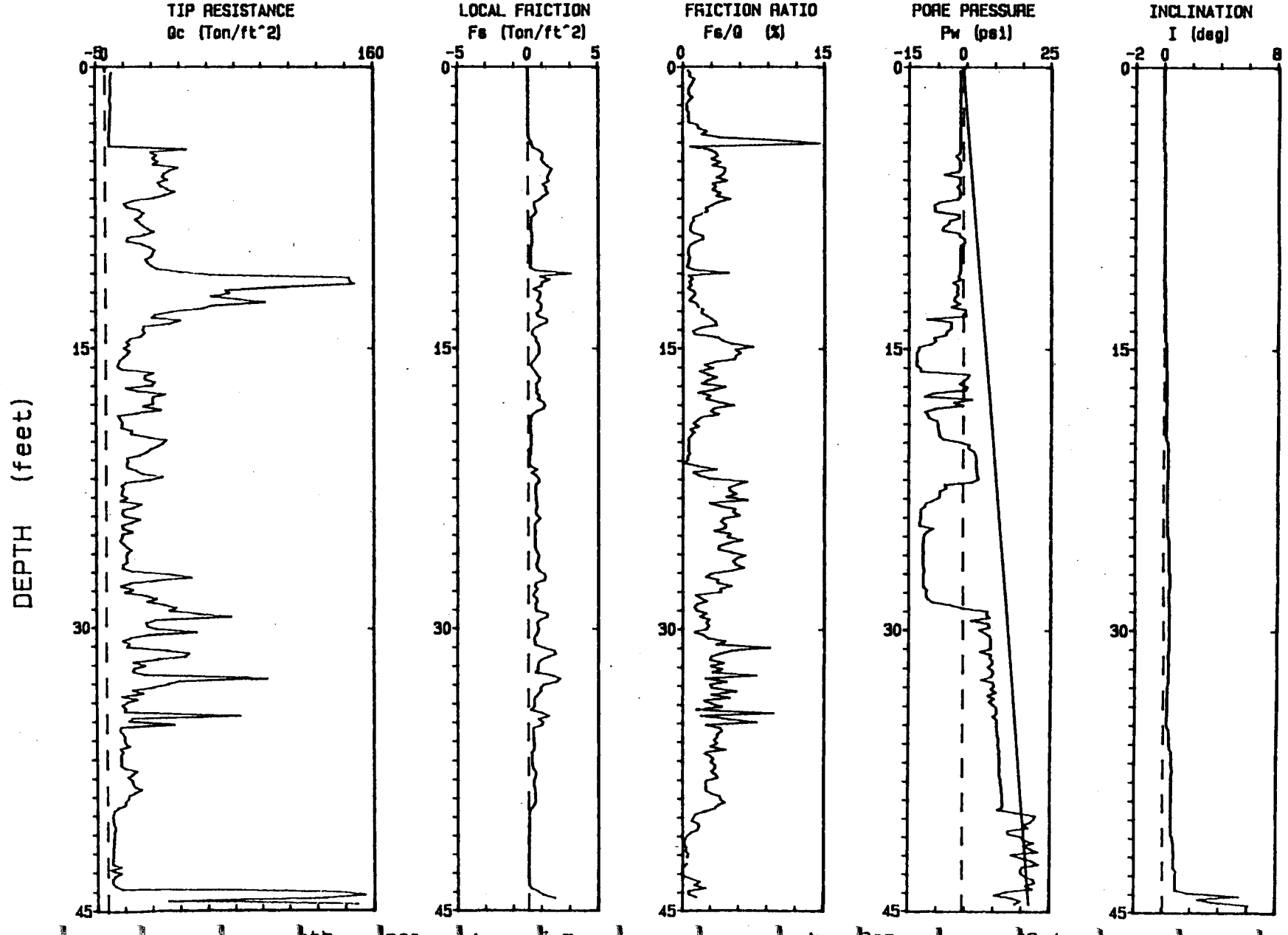

Washington DOT

Elevation : 6.0 CPT Date : 07/28/93 9:55 Sounding : CPT-6 Pg 1 / 1

Location : 63+14 24.0' L. Cone Used : 302 Job No. : MS1826

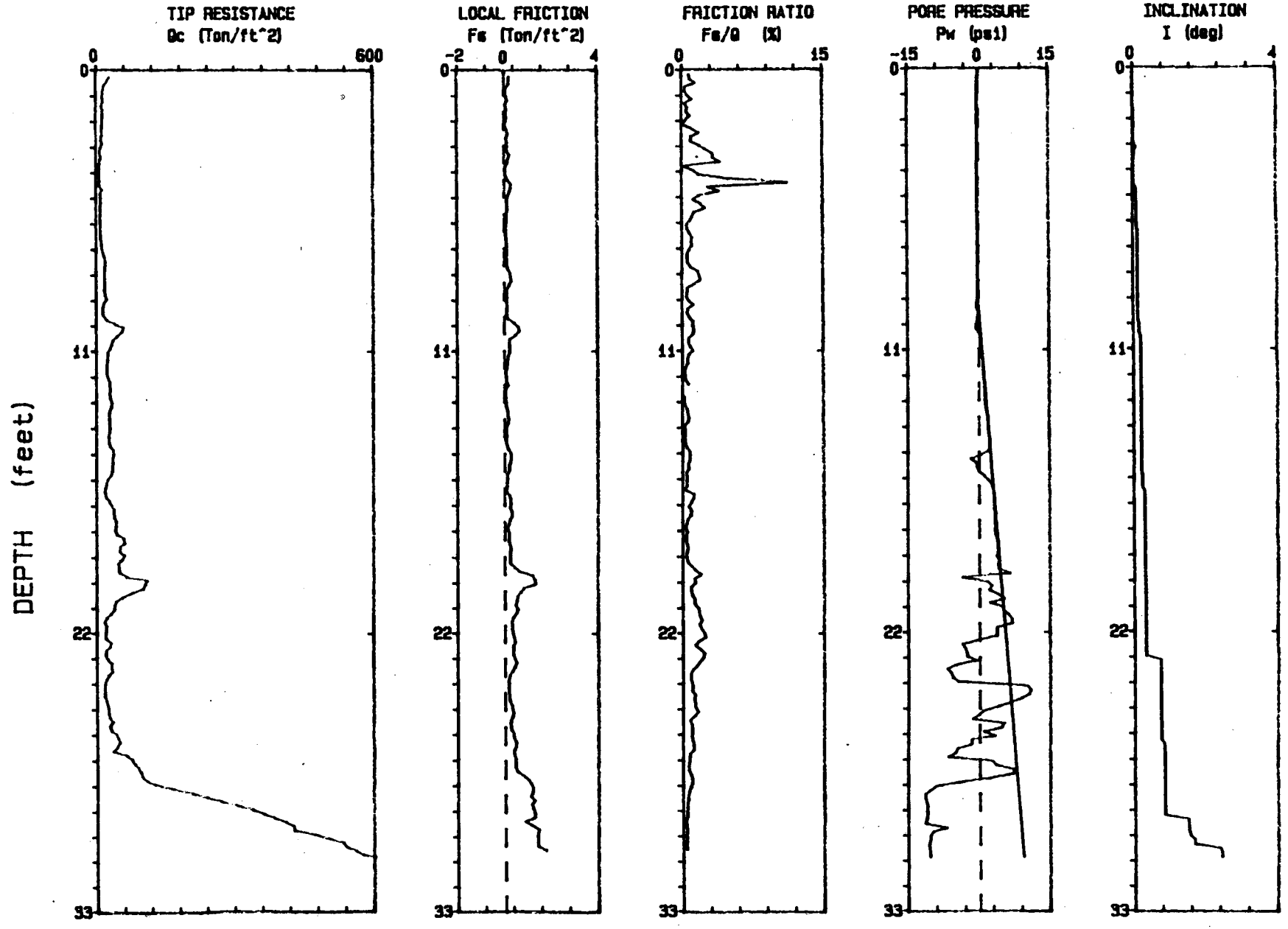

Depth Increment : .05 m

Max Depth : 30.84 ft

Washington DOT

Elevation : 7.1 | CPT Date : 10/06/93 12:45 | Sounding : CPT-21 Pg 1 / 1

Location : 126+60 33' R. | Cone Used : 302 | Job No. : MS 1826

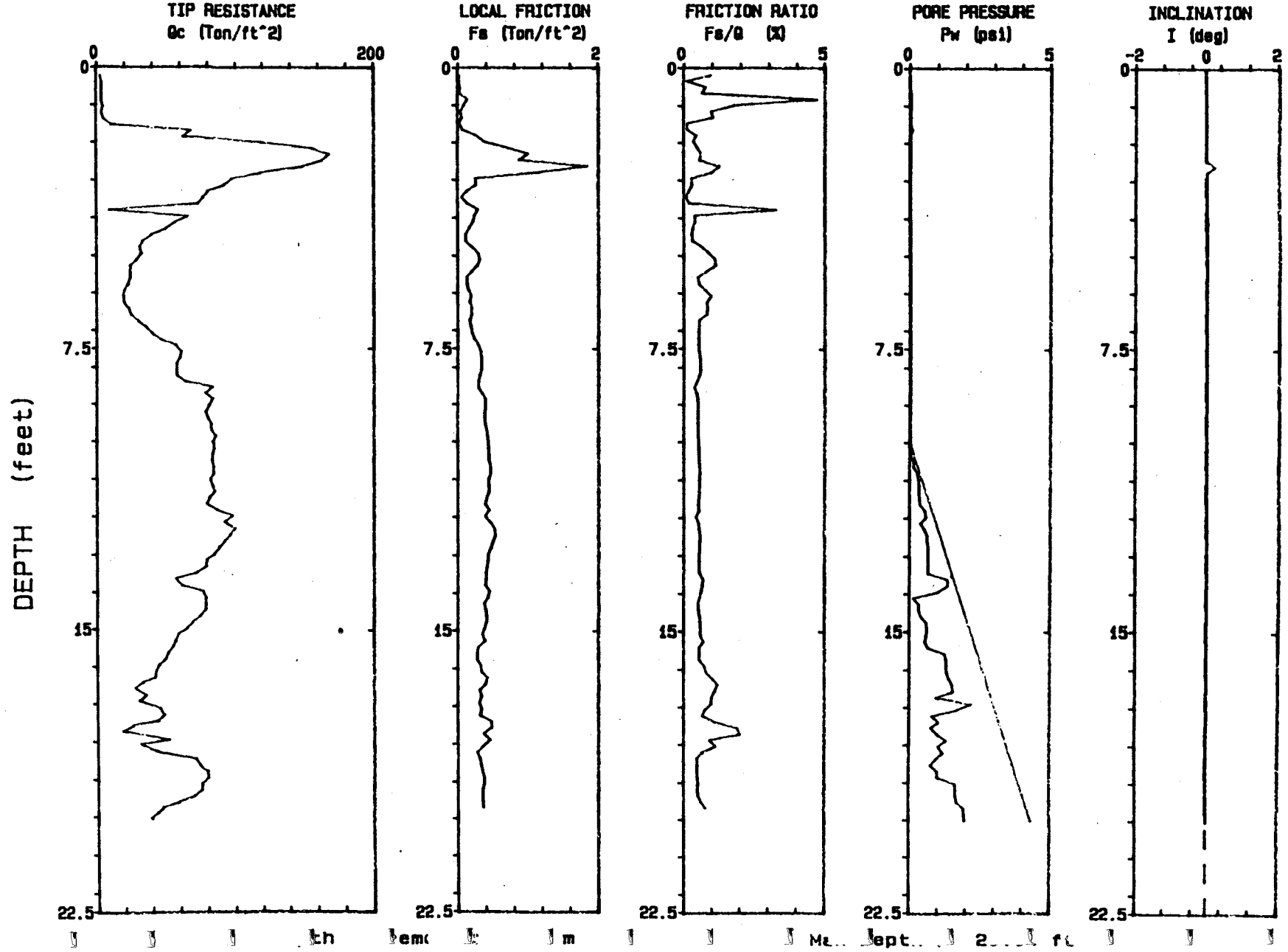

Washington DOT

Elevation : 6.6 | CPT Date : 10/07/93 9:40 | Sounding : CPT-22 Pg 1 / 1

Location : 117+47 25' L. | Cone Used : 302 | Job No. : MS1826 113+00

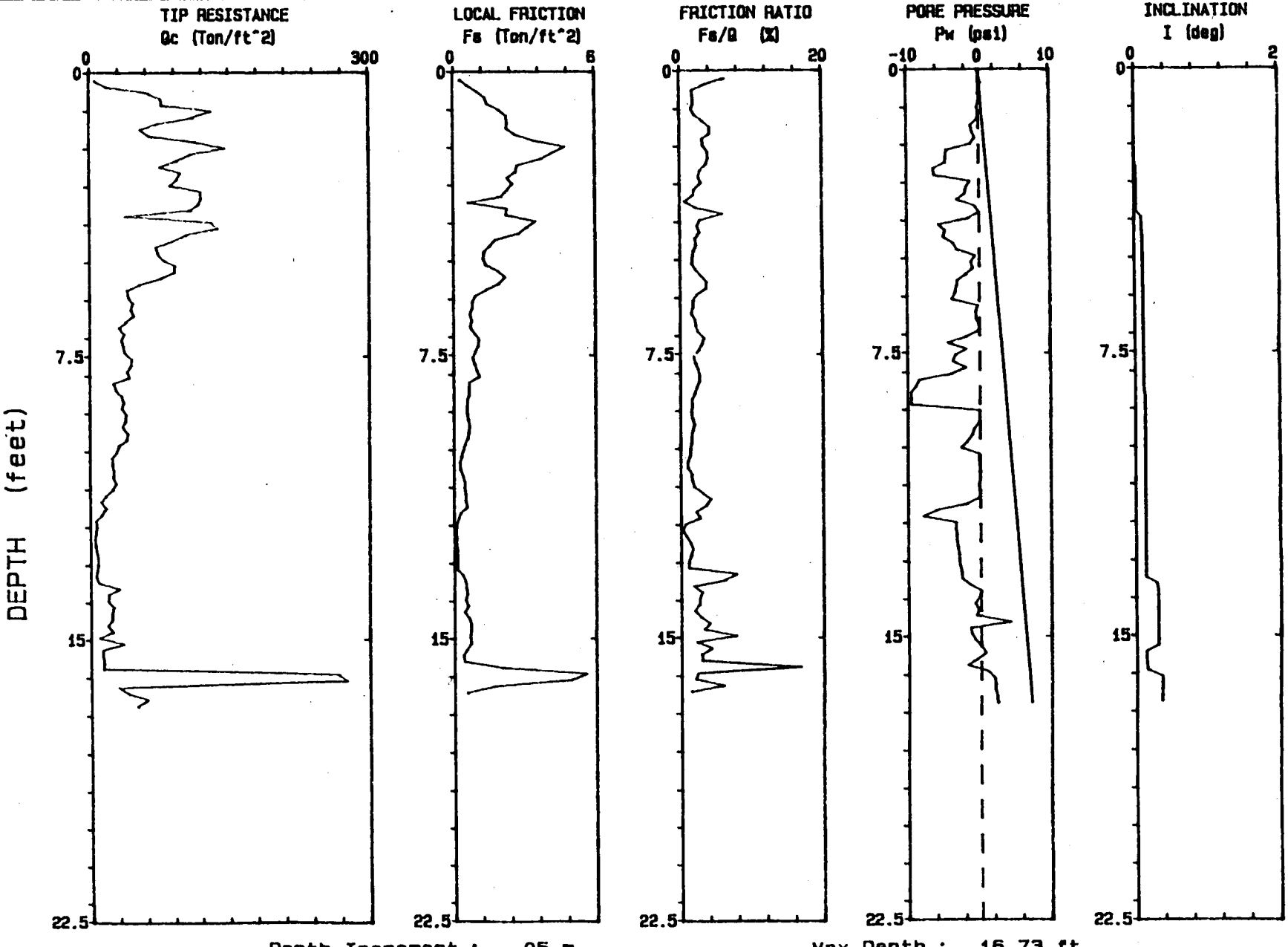

Depth Increment : .05 m

Max Depth : 16.73 ft

Washington DOT

Elevation : 6.6' CPT Date : 10/07/93 12:55 Sounding : CPT-23 Pg 1 / 1

Location : 117+52 25.0' L Cone Used : . 302 Job No. : MS1826

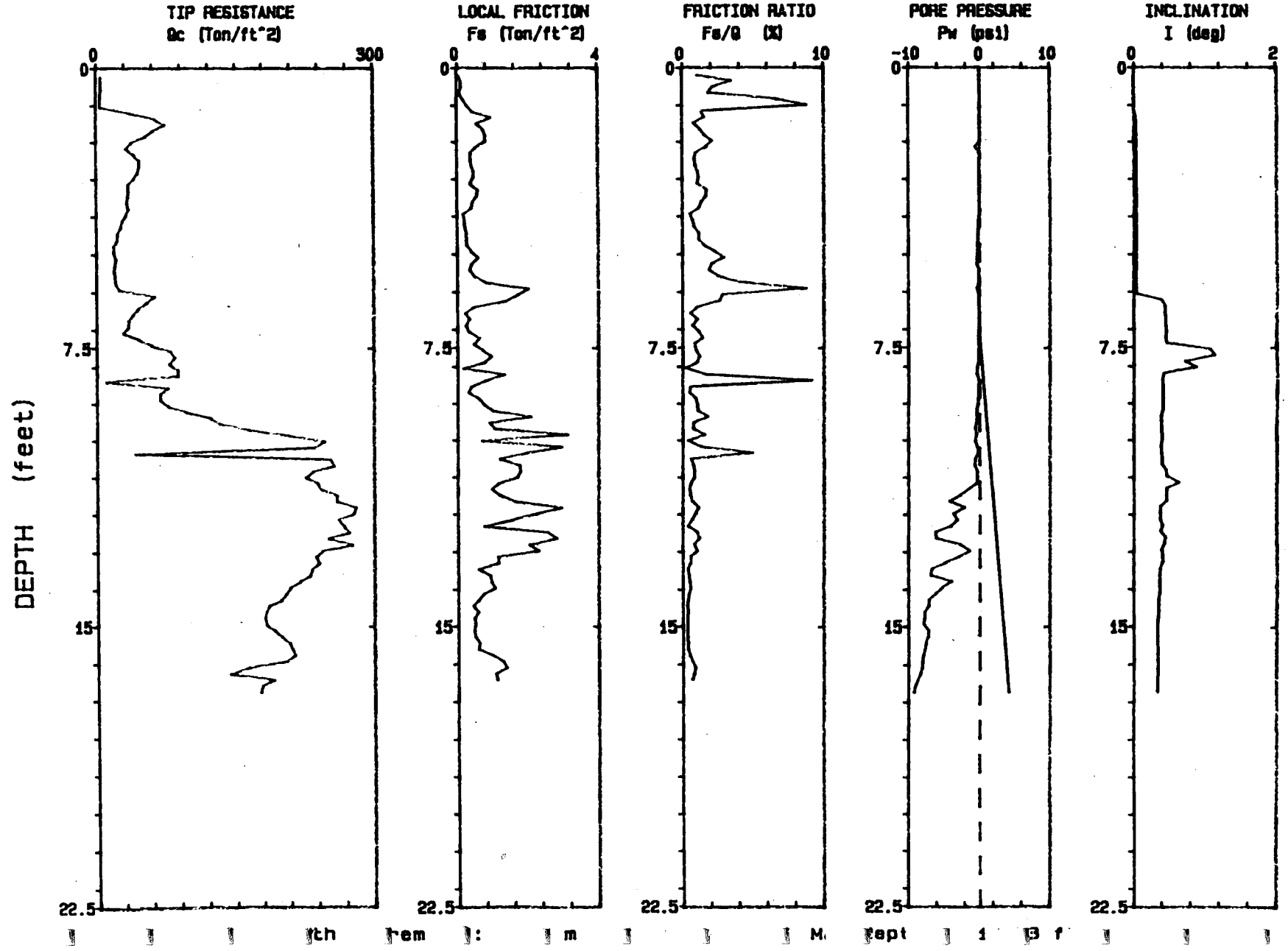

Washington DOT

Elevation : 5.6 | CPT Date : 10/12/93 7:30 | Sounding : CPT-24 Pg 1 / 1

Location : 102+34 C\L | Cone Used : 302 | Job No. : MS1826

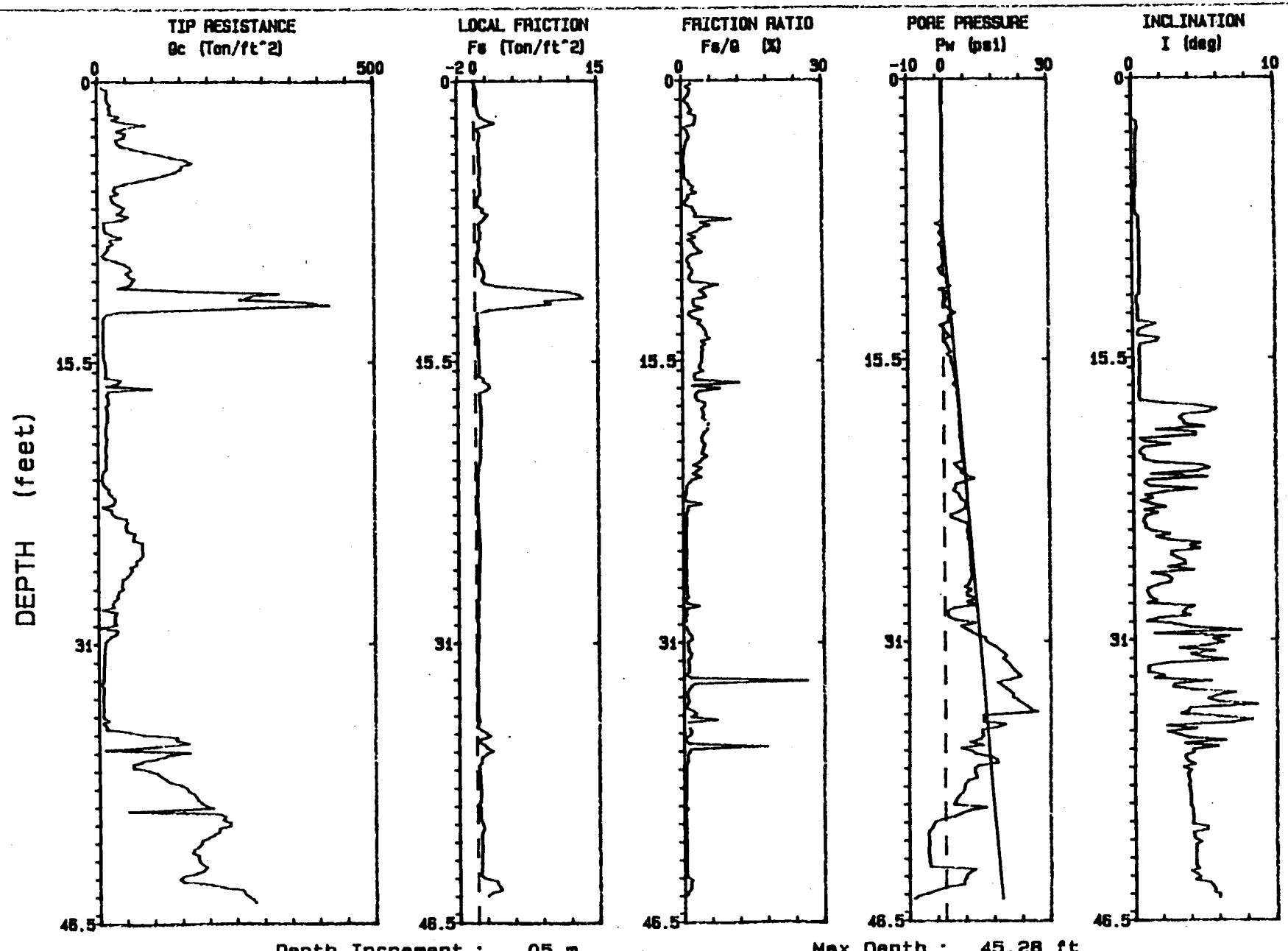

Depth Increment : .05 m

Max Depth : 45.28 ft

Washington DOT

Elevation : 6.3 CPT Date : 10/13/93 7:35 Sounding : CPT-25 Pg 1 / 2

Location : 121+52 22.0' R Cone Used : . 302 M Job No. : S1826

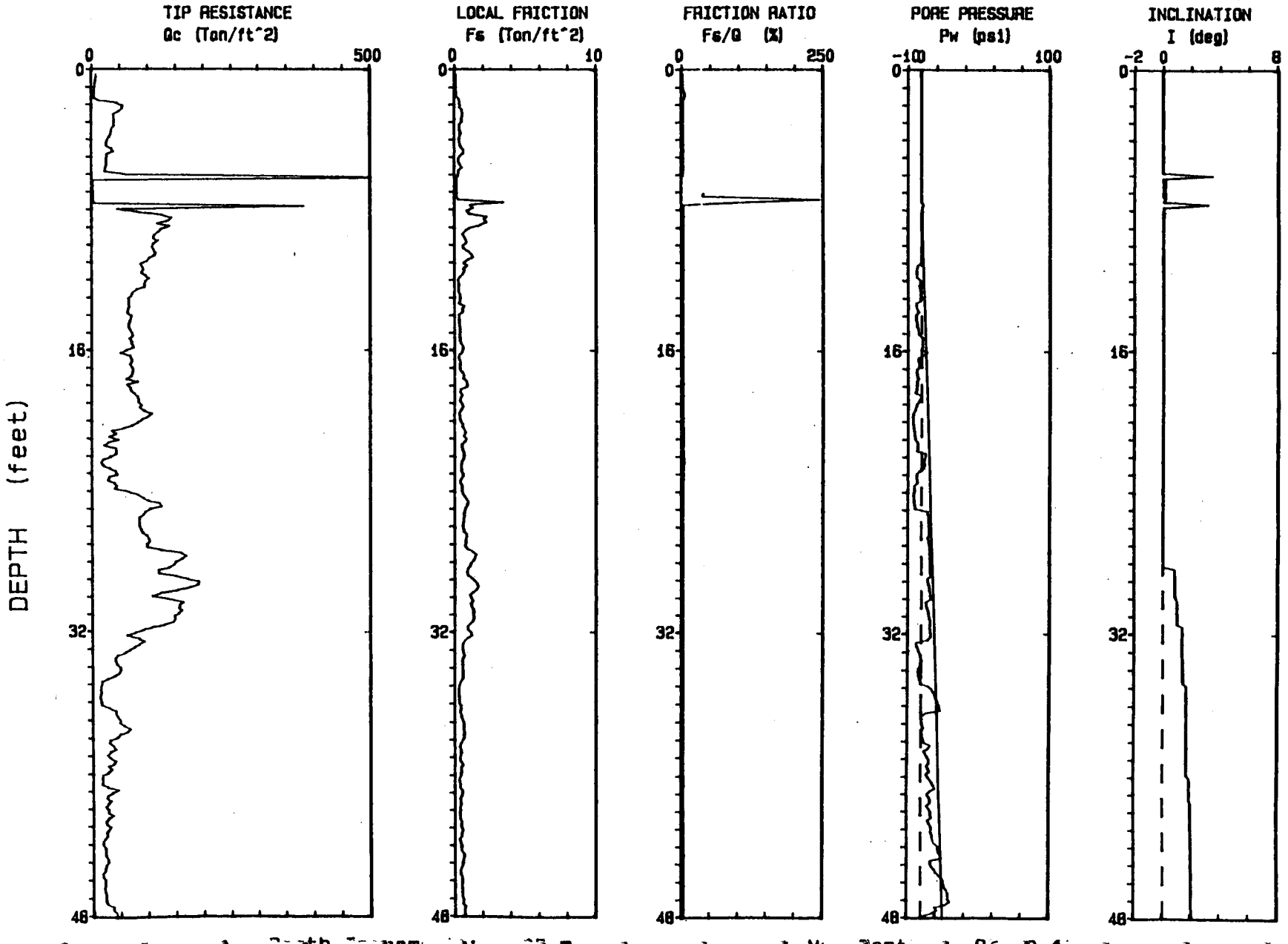

Washington DOT

Elevation : 6.3 CPT Date : 10/13/93 7:35 Sounding : CPT-25 Pg 2 / 2

Location : 121+52 22.0° R Cone Used : . 302 M Job No. : S1826

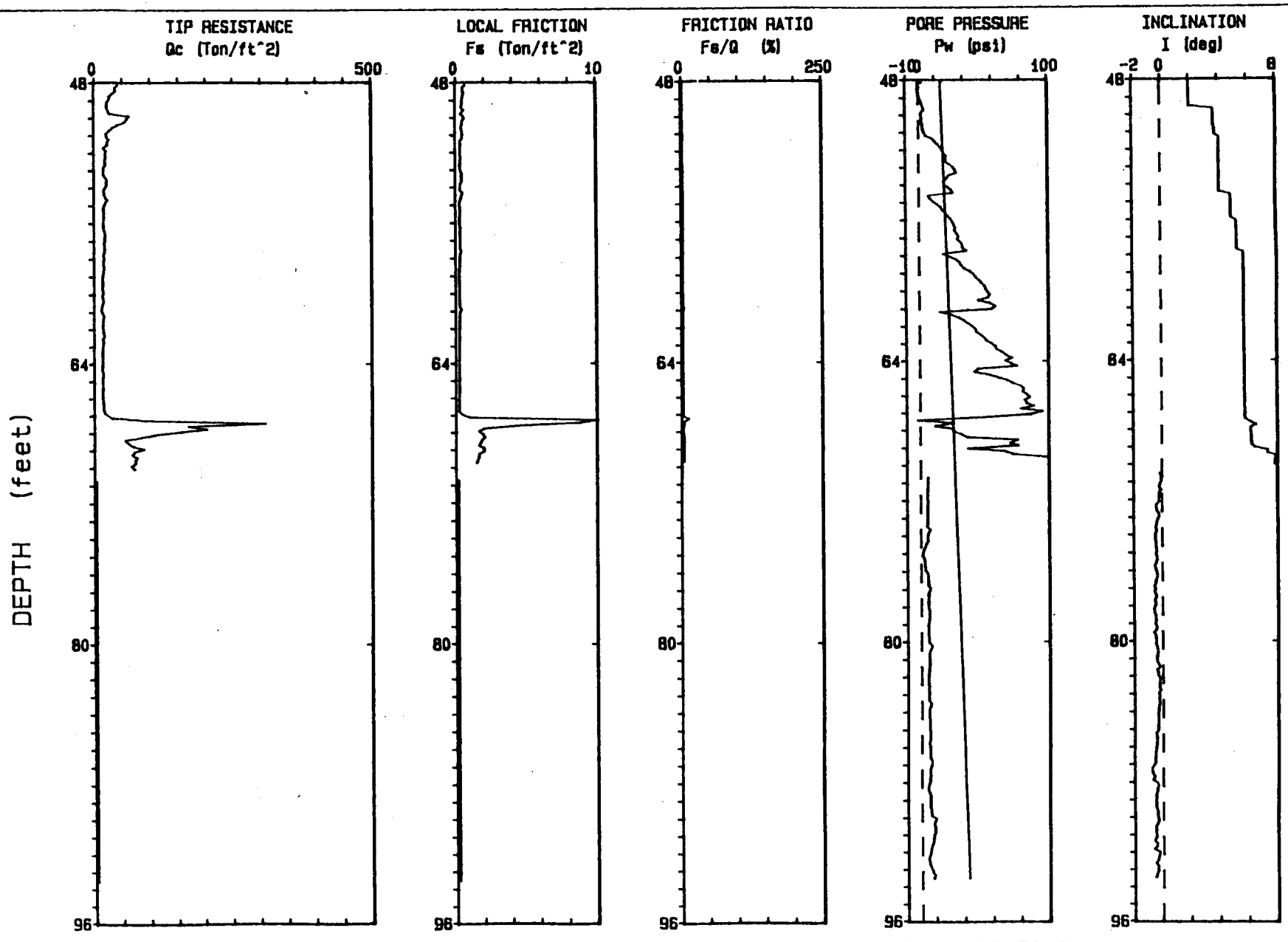

Depth Increment : .05 m

Max Depth : 93.50 ft

Washington DOT

Elevation : 6.4 | CPT Date : 10/13/93 14:30 | Sounding : CPT-26 Pg 1 / 1

Location : 96+40 18.0' R. | Cone Used : 302 | Job No. : MS 1826

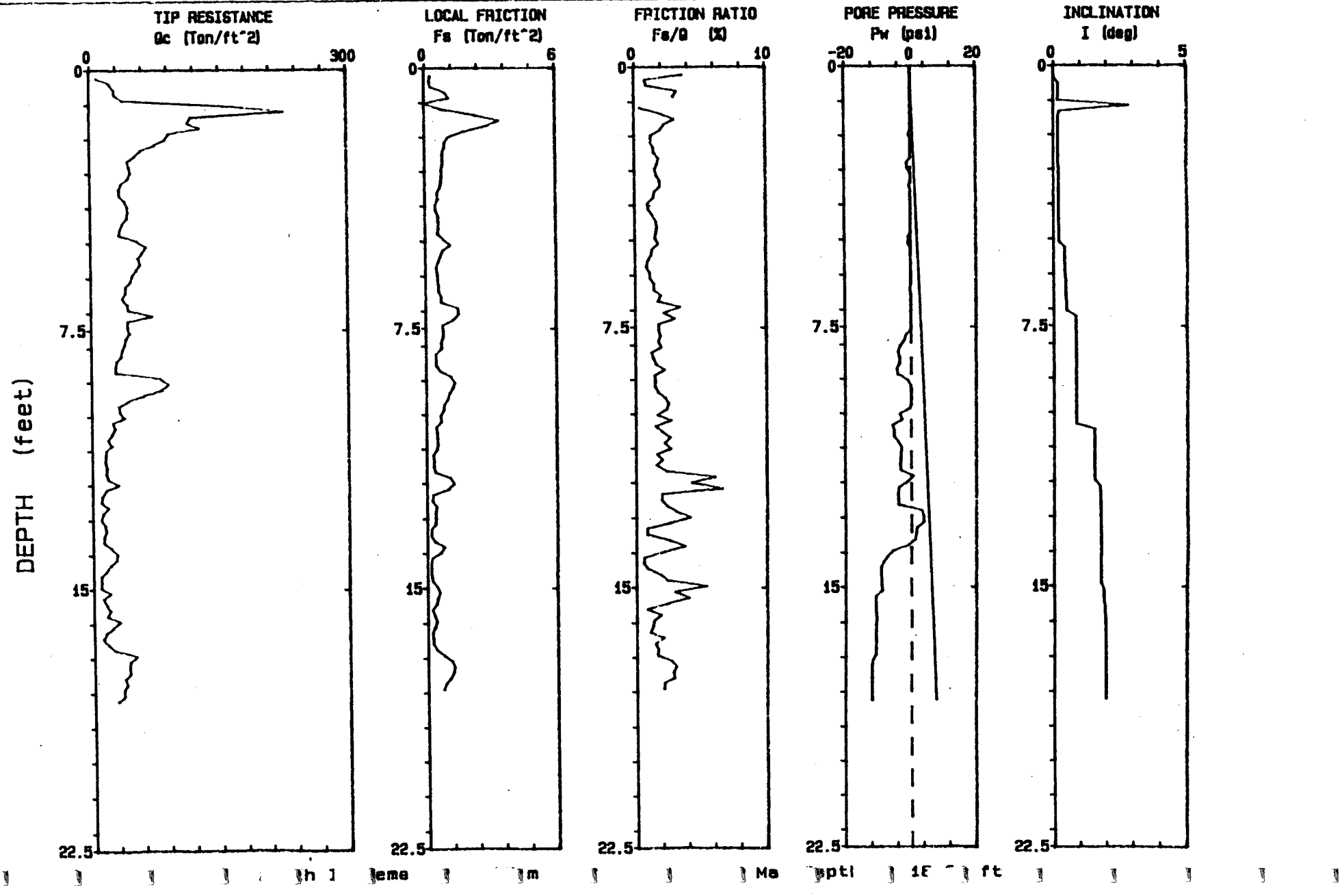

Washington DOT

Elevation : 5.7 | CPT Date : 10/14/93 8:10 5 | Sounding : CPT-27 Pg 1 / 2

Location : 102+34 C/L | Cone Used : 302 | Job No. : MS 1826

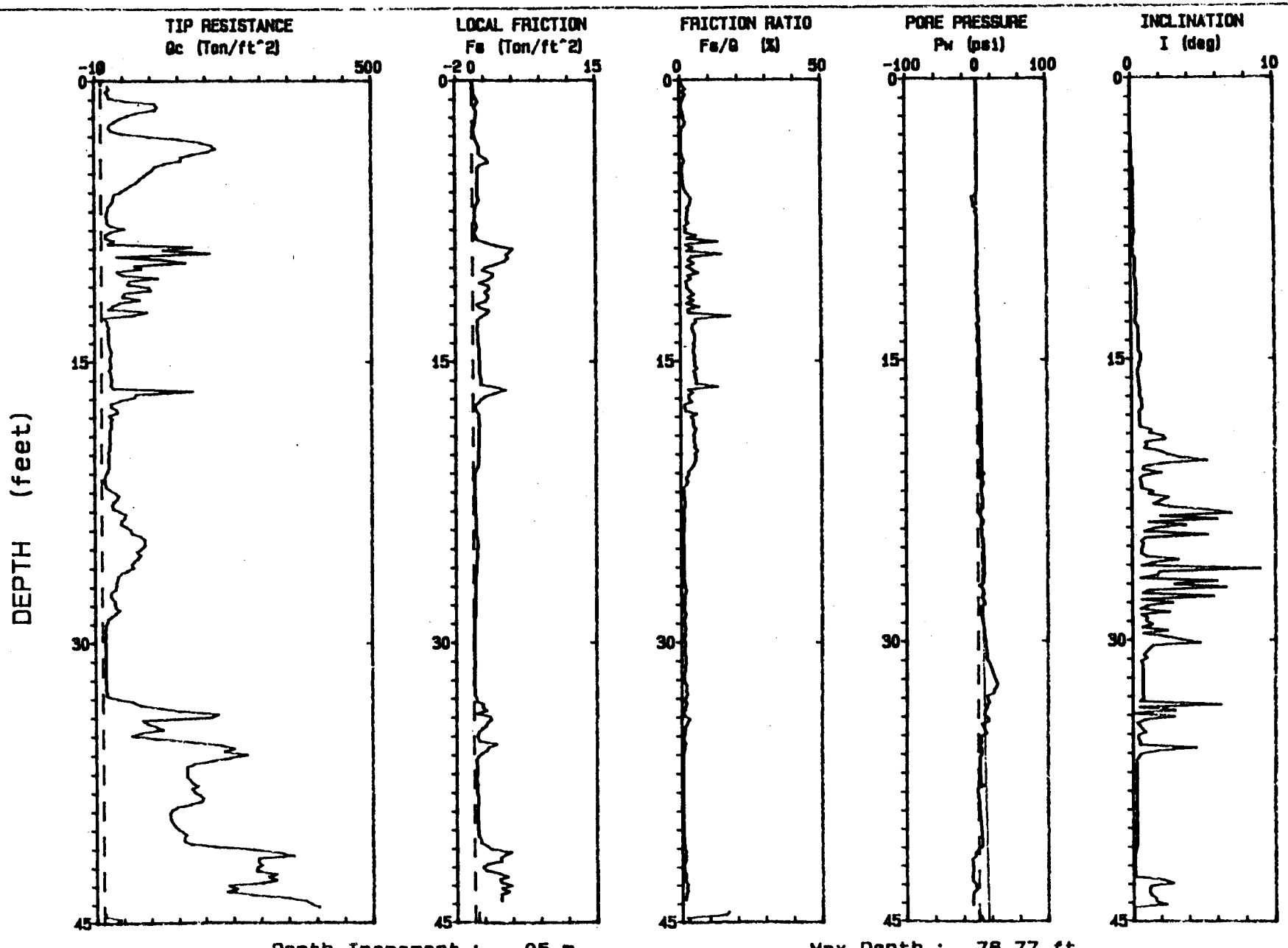

Depth Increment : .05 m

Max Depth : 78.77 ft

Washington DOT

Elevation : 5.7 | CPT Date : 10/14/93 8:10 5 | Sounding : CPT-27 Pg 2 / 2

Location : 102+34 C/L | Cone Used : 302 | Job No. : MS 1826

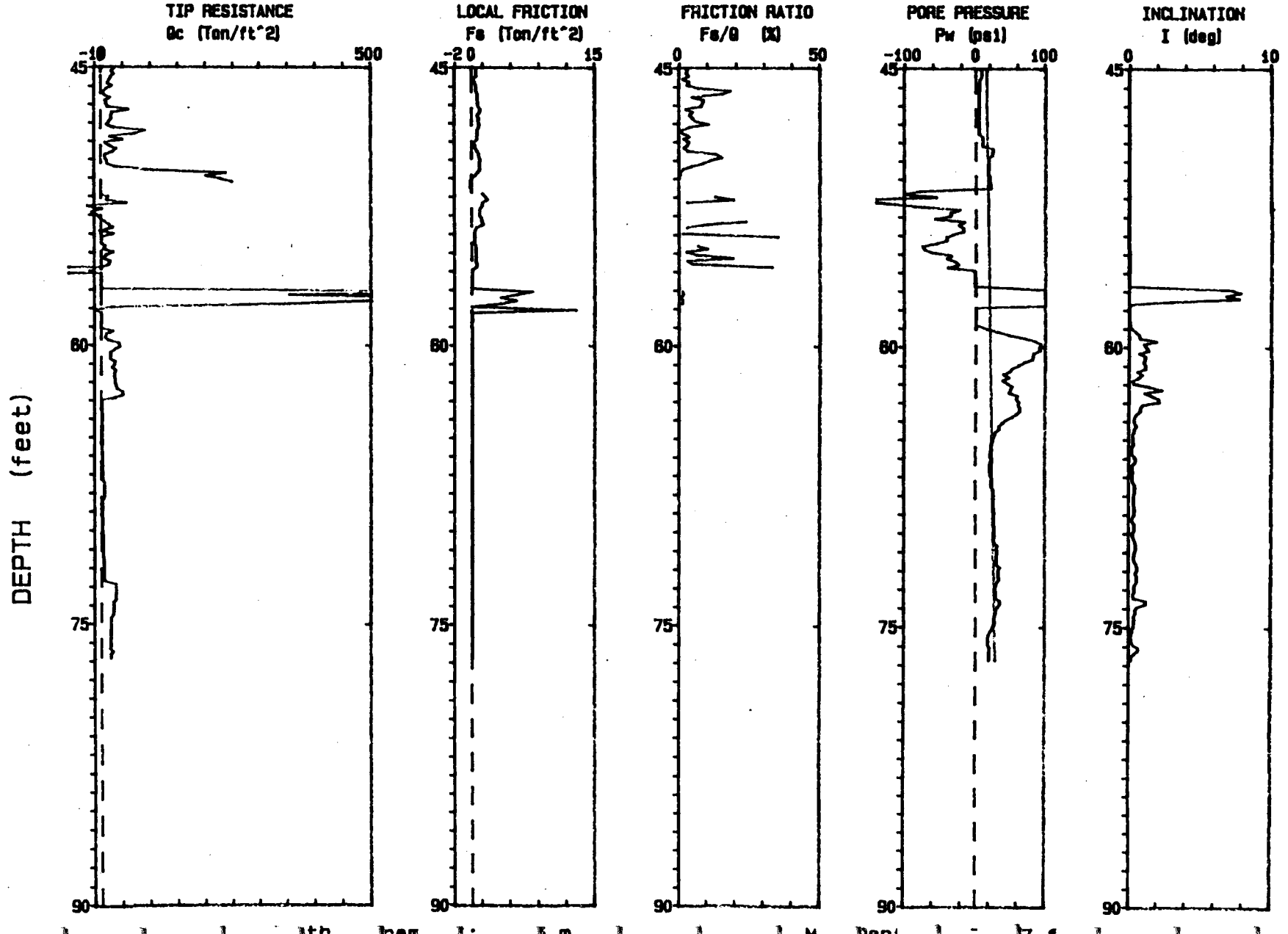

Washington DOT

Elevation : 6.6 | CPT Date : 10/19/93 15:30 | Sounding : CPT-28 Pg 1 / 1

Location : 59+75 24.0' L | Cone Used : . 302 | Job No. : MS 1826

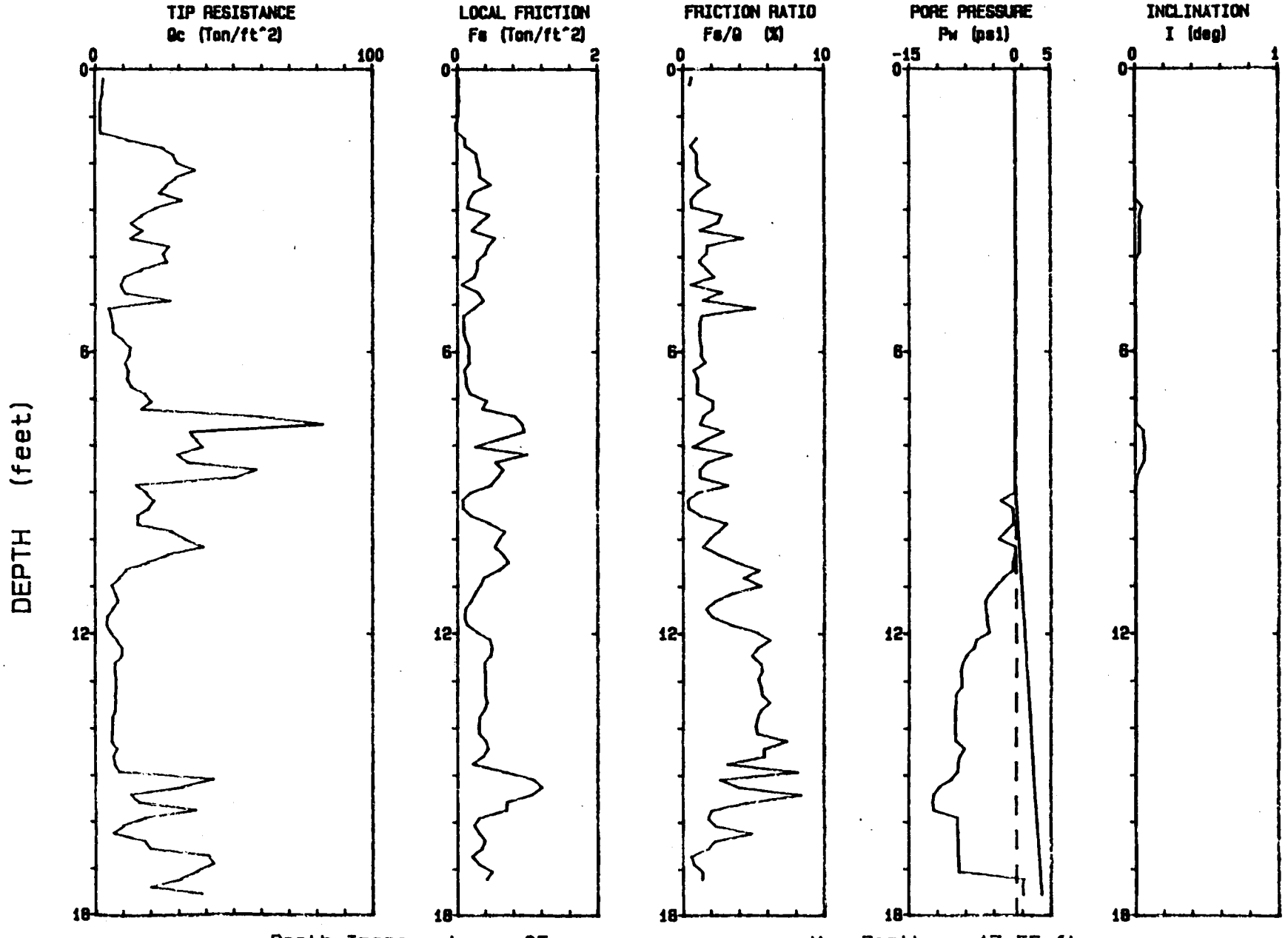

Depth Increment : .05 m

Max Depth : 17.55 ft

Washington DOT

Elevation : 5.3 | CPT Date : 10/20/93 9:25 | Sounding : CPT-29 Pg 1 / 1

Location : 74+17 31' L. | Cone Used : 302 | Job No. : MS 1826

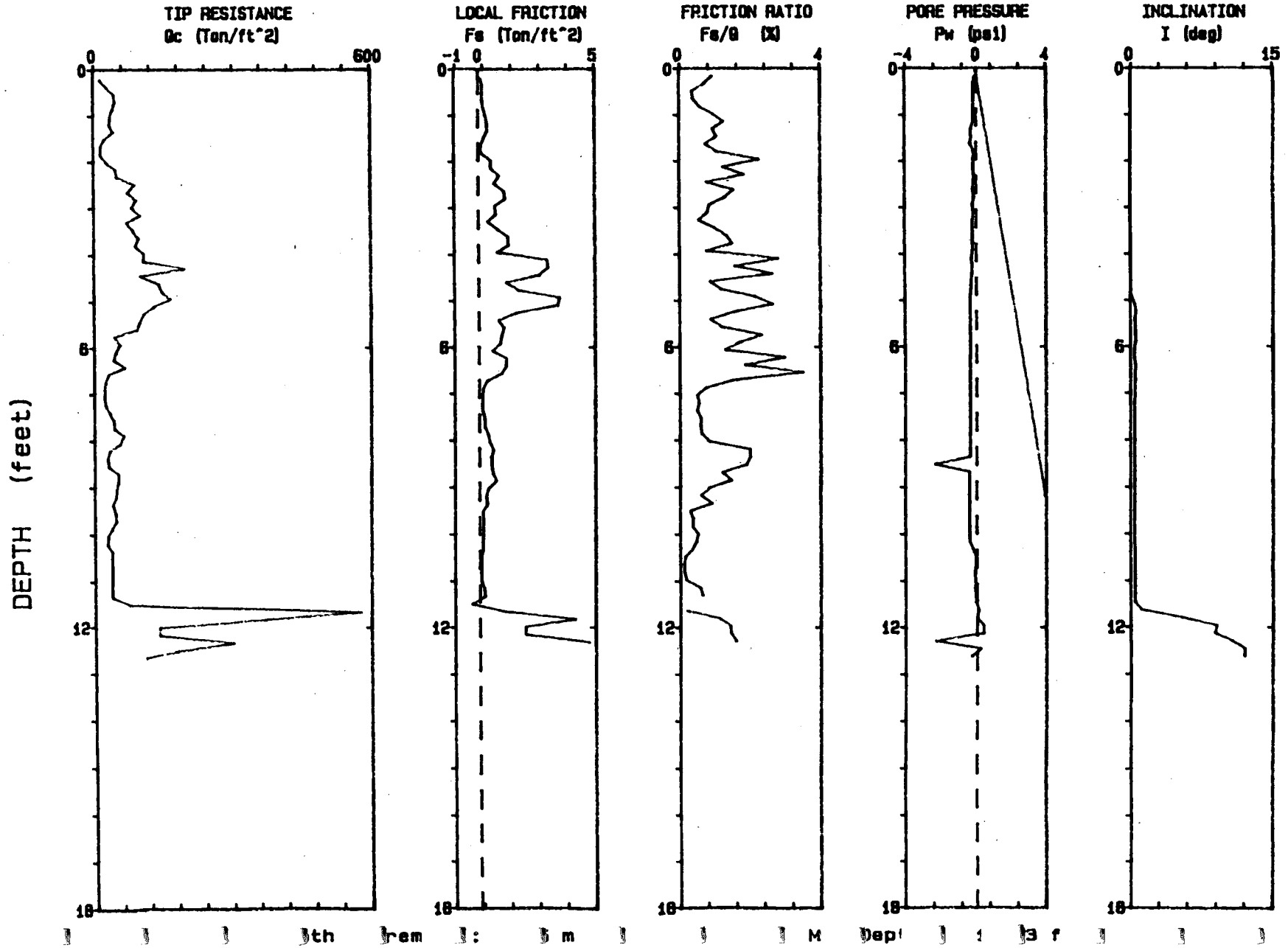

Washington DOT

Elevation : 6.6 CPT Date : 10/20/93 14:50 Sounding : CPT-30 Pg 1 / 1

Location : 61+62 23.7' R. Cone Used : 302 Job No. : MS 1826

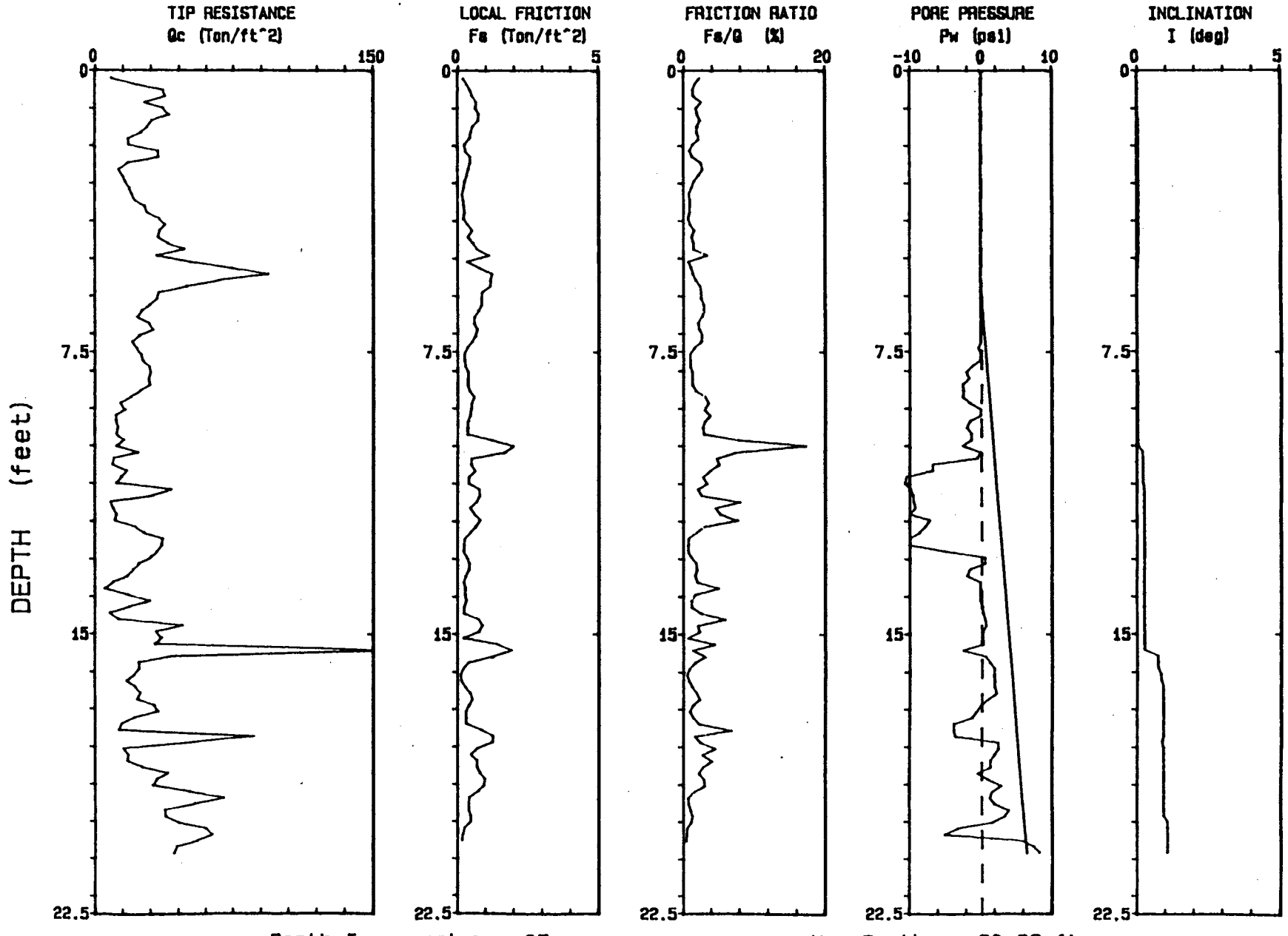

Depth Increment : .05 m

Max Depth : 20.83 ft

Washington DOT

Elevation : 6.4 | CPT Date : 10/21/93 7:55 | Sounding : CPT-31 Pg 1 / 1

Location : 93+14 17.5' R. | Cone Used : 302 | Job No. : MS 1826

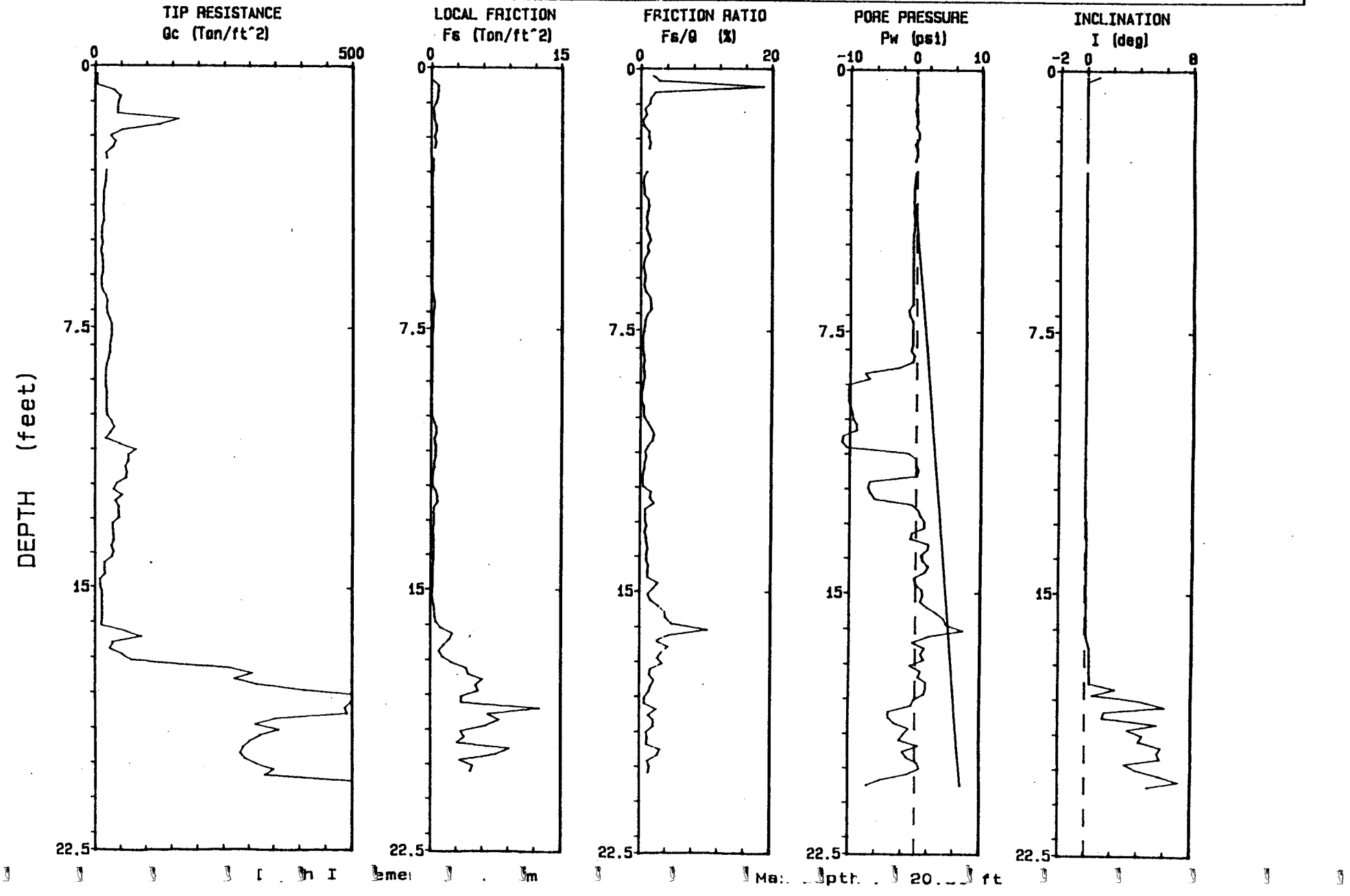

Appendix C

Supplementary Subsurface Investigation

Shear Wave Velocity Test Results

WSDOT Seismic Cone

Project: Alaska Way Viaduct
SR-99 C.S.

Hole No. CPT-1

Station: Offset:

Source: Beam

Offset = 0.64 ft Depth = ft

DEPTH OF GEOPHONE feet	meters	Time Diff millisec	VELOCITY ft/sec	m/sec
3.77	1.15			
7.05	2.15	6.62	491.82	149.91
10.33	3.15	6.73	486.13	148.17
13.62	4.15	7.69	426.01	129.85
16.90	5.15	9.07	361.40	110.16
20.18	6.15	9.03	363.10	110.68
23.46	7.15	8.03	408.39	124.48
26.74	8.15	7.66	428.16	130.51
30.02	9.15	6.91	474.67	144.68
33.30	10.15	6.69	490.30	149.45
36.58	11.15	7.25	452.45	137.91
39.86	12.15	7.18	456.87	139.26
43.14	13.15	7.29	449.99	137.16
46.42	14.15	7.14	459.45	140.04
49.70	15.15	5.47	599.73	182.80

WSDOT Seismic Cone

Project: Alaska Way Viaduct
SR-99 C.S. Job No. MS-1826

Hole No. CPT-2

Station: 105+04 Offset:

Source: Beam

Offset = 0.50 ft Depth = 0.00 ft

DEPTH OF GEOPHONE feet	meters	Time Diff millisec	VELOCITY ft/sec	m/sec
3.64	1.11			
6.92	2.11	6.80	480.10	146.34
10.20	3.11	10.00	327.50	99.82
13.48	4.11	5.50	595.97	181.65
16.76	5.11	6.10	537.54	163.84
20.05	6.11	6.90	475.30	144.87
23.33	7.11	7.10	461.96	140.81
26.61	8.11	7.60	431.60	131.55
29.89	9.11	8.20	400.03	121.93
33.17	10.11	8.50	385.93	117.63
36.45	11.11	7.00	468.64	142.84
39.73	12.11	6.90	475.44	144.92
43.01	13.11	4.50	729.01	222.21
46.29	14.11	4.40	745.59	227.26
49.57	15.11	3.70	886.65	270.26
52.85	16.11	3.10	1058.27	322.57
54.92	16.74	2.40	861.17	262.49

WSDOT Seismic Cone

Project: Alaska Way Viaduct SR-99 C.S. Job No. MS-1826

Hole No. CPT-3

Station: 90+00 Offset: 21 ft LT

Source: Auger

Offset = 3.83 ft Depth = 5.00 ft

DEPTH OF GEOPHONE feet	meters	Time Diff millisec	VELOCITY ft/sec	m/sec
4.13	1.26			
7.41	2.26	3.65	191.13	58.26
10.70	3.26	3.10	753.49	229.67
13.98	4.26	5.05	573.41	174.78
17.26	5.26	5.20	592.75	180.67
19.06	5.81	1.35	1283.15	391.11

WSDOT Seismic Cone

Project: Alaska Way Viaduct SR-99 C.S. Job No. MS-1826

Hole No. CPT-4A

Station: 99+00 Offset: 10 ft LT

Source: Auger

Offset = 5.83 ft Depth = 3.50 ft

DEPTH OF GEOPHONE feet	meters	Time Diff millisec	VELOCITY ft/sec	m/sec
4.13	1.26			
7.41	2.26	1.90	609.46	185.77
10.70	3.26	2.40	932.71	284.29
13.98	4.26	2.95	924.86	281.90
17.26	5.26	4.20	702.91	214.25
19.55	5.96	4.50	475.12	144.82

WSDOT Seismic Cone

Project: Alaska Way Viaduct SR-99 C.S. Job No. MS-1826

Hole No. CPT-5

Station: 78+00 Offset: 0.5 ft LT

Source: Auger

Offset = 5.00 ft Depth = 5.00 ft

DEPTH OF GEOPHONE feet	meters	Time Diff millisec	VELOCITY ft/sec	m/sec
2.17	0.66			
5.45	1.66	4.90	4.05	1.24
8.89	2.71	3.60	365.48	111.40
12.01	3.66	3.30	688.80	209.95
15.29	4.66	6.00	471.75	143.79
18.57	5.66	6.90	437.98	133.50
21.85	6.66	6.00	519.18	158.25
25.13	7.66	9.20	344.16	104.90
28.41	8.66	7.60	420.67	128.22
31.69	9.66	12.30	261.55	79.72
34.97	10.66	11.20	288.46	87.92
38.25	11.66	13.00	249.26	75.98
[illegible]	[illegible]	[illegible]	[illegible]	[illegible]
43.01	13.11	1.00	1138.17	346.92

WSDOT SEISMIC CONE

Engineer: DVJ
Date: October 19, 1993

Project: Alaska Way Viaduct
SR-99 C.S. **Job No.** MS-1826

Hole No. CPT-28

Station: 60+00 **Offset:** West Column Pier 58

Source: Beam

Offset = 0.33 ft

DEPTH OF GEOPHONE feet	meters	Time Diff millisec	VELOCITY ft/sec	m/sec
4.10	1.25			
7.38	2.25	6.66	492	150
10.66	3.25	5.93	553	169
13.94	4.25	6.73	487	149
17.22	5.25	6.15	533	163

WSDOT SEISMIC CONE

Engineer: DVJ
Date: October 20, 1993

Project: Alaska Way Viaduct
SR-99 C.S. **Job No.** MS-1826

Hole No. CPT-30

Station: 62+50 **Offset:** East Column Pier 61

Source: Beam

Offset = 0.25 ft

DEPTH OF GEOPHONE feet	meters	Time Diff millisec	VELOCITY ft/sec	m/sec
5.02	1.36			
8.30	2.36	4.74	692	211
11.58	3.36	5.25	625	190
14.86	4.36	5.72	573	175
18.14	5.36	6.43	510	156
21.42	6.36	5.72	574	175

WSDOT SEISMIC CONE

Engineer: DVJ
Date: October 20, 1993

Project: Alaska Way Viaduct
SR-99 C.S. **Job No.** MS-1826

Hole No. CPT-29

Station: 75+00 **Offset:** East Column Pier 80

Source: Beam

Offset = 0.21 ft

DEPTH OF GEOPHONE feet	meters	Time Diff millisec	VELOCITY ft/sec	m/sec
4.10	1.25			
7.38	2.25	5.47	599	183
10.66	3.25	6.71	489	149
12.76	3.89	5.32	395	120

WSDOT SEISMIC CONE

Engineer: DVJ
Date: October 21, 1993

Project: Alaska Way Viaduct
SR-99 C.S. **Job No.** MS-1826

Hole No. CPT-31

Station: 92+50 **Offset:** East Column Pier 108

Source: Beam

Offset = 0.25 ft

DEPTH OF GEOPHONE feet	meters	Time Diff millisec	VELOCITY ft/sec	m/sec
4.46	1.36			
7.74	2.36	3.07	1,068	325
11.02	3.36	7.35	446	136
14.30	4.36	6.03	544	166
17.59	5.36	6.84	480	146
19.95	6.08	5.10	463	141

WSDOT SEISMIC CONE

Engineer: DVJ
Date: October 6, 1993

Project: Alaska Way Viaduct
SR-99 C.S. **Job No.** MS-1826

Hole No. CPT-21

Station: 126+50 **Offset:** West Column Pier 165

Source: Beam

Offset = 0.29 ft

DEPTH OF GEOPHONE feet	meters	Time Diff millisec	VELOCITY ft/sec	m/sec
2.66	0.81			
5.94	1.81	4.85	675	206
9.22	2.81	4.38	748	228
12.50	3.81	6.28	522	159
15.78	4.81	6.49	505	154

WSDOT SEISMIC CONE

Engineer: DVJ
Date: October 7, 1993

Project: Alaska Way Viaduct

Hole No. CPT-22

Station: 113+00

Offset: East Column Pier 146

Source: Beam

Offset = 0.29 ft

DEPTH OF GEOPHONE feet	meters	Time Diff millisec	VELOCITY ft/sec	m/sec
2.66	0.81			
5.94	1.81	9.51	344	105
9.22	2.81	6.63	494	151
12.50	3.81	6.81	482	147
15.78	4.81	6.95	472	144
19.06	5.81	6.82	481	147

WSDOT SEISMIC CONE

Engineer: DVJ
Date: October 12, 1993

Project: Alaska Way Viaduct SR-99 C.S.

Job No. MS-1826

Hole No. CPT-24

Station: 102+00

Offset: West Column Pier 122

Source: Beam

Offset = 0.41 ft

DEPTH OF GEOPHONE feet	meters	Time Diff millisec	VELOCITY ft/sec	m/sec
3.28	1.00			
6.56	2.00	7.15	457	139
9.84	3.00	8.27	396	121
13.12	4.00	7.71	425	130
16.40	5.00	12.75	257	78
19.68	6.00	9.95	330	100
22.97	7.00	9.11	360	110
25.49	7.77	9.11	277	85
30.77	9.38	14.42	366	112
34.05	10.38	7.13	460	140
37.34	11.38	5.13	639	195
40.62	12.38	2.70	1,215	370
42.09	12.83	1.99	742	226

WSDOT SEISMIC CONE

Engineer: DVJ
Date: October 13, 1993

Project: Alaska Way Viaduct
SR-99 C.S. Job No. MS-1826

Hole No. CPT-25

Station: 118+00 Offset: West Column
Pier 153

Source: Beam

Offset = 0.29 ft

DEPTH OF GEOPHONE feet	meters	Time Diff millisec	VELOCITY ft/sec	m/sec
1.64	0.50			
4.92	1.50	5.13	636	194
8.20	2.50	4.92	666	203
11.48	3.50	3.83	856	261
14.76	4.50	4.83	679	207
18.04	5.50	5.54	592	180
21.33	6.50	5.19	632	193
24.61	7.50	7.23	454	138
27.89	8.50	6.31	520	158
31.17	9.50	5.96	550	168
34.45	10.50	6.57	499	152
37.73	11.50	7.41	443	135
41.01	12.50	8.01	410	125
44.29	13.50	6.57	499	152
47.57	14.50	7.49	438	134
50.85	15.50	6.28	522	159
54.13	16.50	7.24	453	138
57.41	17.50	6.75	486	148
60.69	18.50	6.56	500	152
63.98	19.50	6.60	497	152
67.26	20.50	5.43	604	184
69.88	21.30	2.24	1,172	357

DOT SEISMIC CONE

Engineer: DVJ
Date: October 13, 1993

Project: Alaska Way Viaduct
SR-99 C.S. Job No. MS-1826

Hole No. CPT-26

Station: 95+00 Offset: West Column
Pier 113

Source: Beam

Offset = 0.25 ft

DEPTH OF GEOPHONE feet	meters	Time Diff millisec	VELOCITY ft/sec	m/sec
1.48	0.45			
4.76	1.45	5.51	593	181
8.04	2.45	4.08	803	245
11.32	3.45	4.91	668	204
14.60	4.45	5.20	631	192
17.88	5.45	5.00	656	200

WSDOT SEISMIC CONE

Engineer: DVJ
Date: October 14, 1993

Project: Alaska Way Viaduct
SR-99 C.S. Job No. MS-1826

Hole No. CPT-27

Station: 102+00 Offset: West Column
Pier 122

Source: Beam

Offset = 0.29 ft

DEPTH OF GEOPHONE feet	meters	Time Diff millisec	VELOCITY ft/sec	m/sec
4.43	1.35			
7.71	2.35	6.35	516	157
10.99	3.35	10.65	308	94
14.27	4.35	9.43	348	106
17.55	5.35	12.51	262	80
20.83	6.35	11.36	289	88
24.11	7.35	11.70	280	85
27.39	8.35	8.13	404	123
30.68	9.35	10.07	326	99
33.96	10.35	7.02	467	142
37.24	11.35	3.55	924	282
40.52	12.35	3.34	982	299
43.80	13.35	2.54	1,292	394